SEPTEMBER, 1953
IN TWO SECTIONS—SECTION I

Journal of METALS

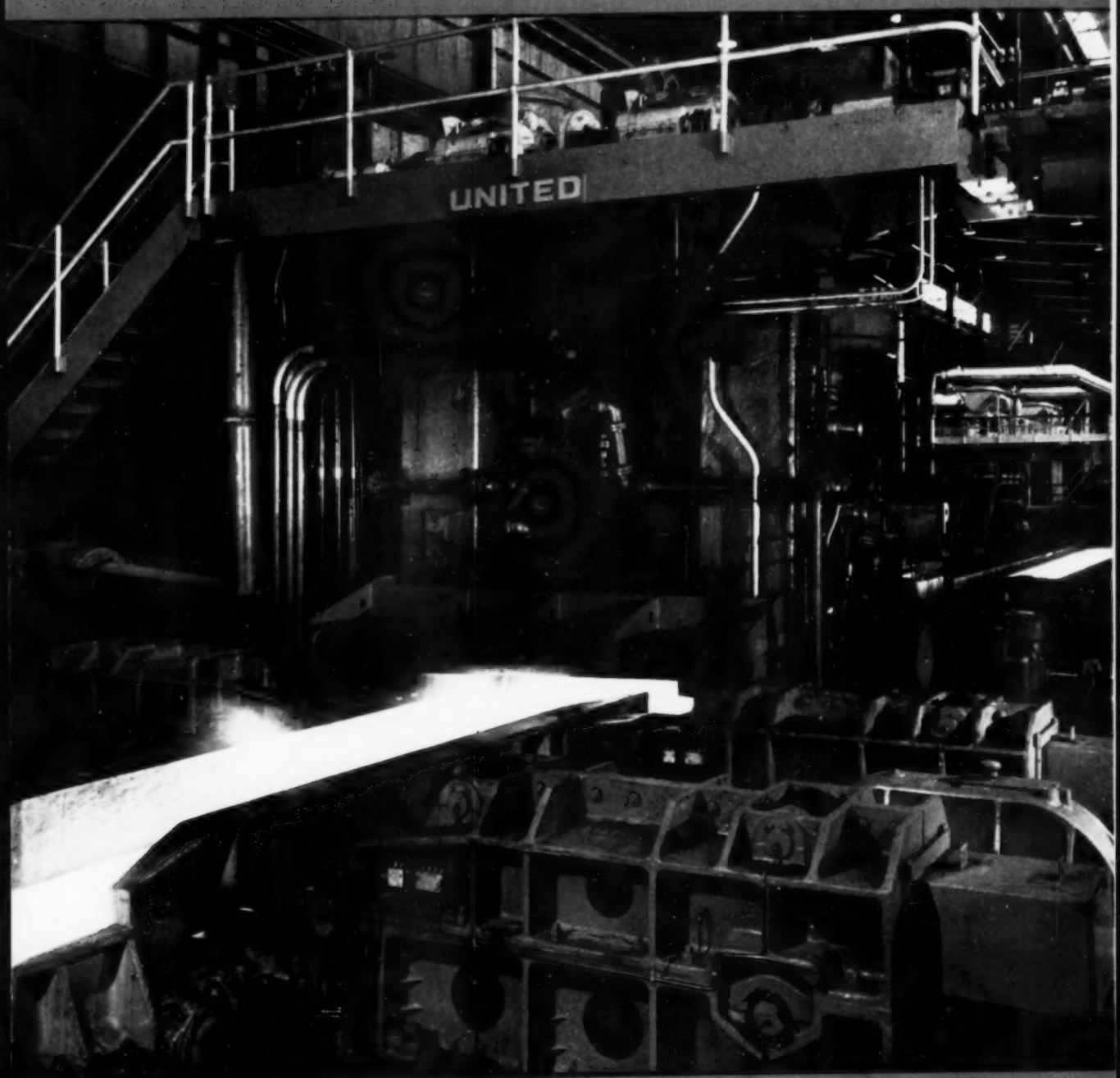

September JOURNAL OF METALS Highlights:

"Anode Casting Operations at Garfield Smelter Geared to High Production" - p. 1075
"Research in Progress" - p. 1081

Bailey

PIG CASTING MACHINES

Correctly designed for greater production and far longer service, these machines are produced in two models, a Foundry Type and a Blast Furnace Type. The exceptionally versatile Foundry Type is a completely self-contained unit —including the machine proper, motor gear unit, variable speed reducer and drive. Capacities: 3 to 50 tons. Sizes: 15 to 125 feet in multiples of 5 feet.

Stationary Wheel Design Eliminates 80% of Moving Parts of Conventional Machine

Both Foundry and Blast Furnace Types feature large diameter idler wheels, permanently mounted at intervals on the frame. An endless chain of moulds runs along those stationary, flanged wheels. Not only does this design eliminate moving parts, but it locates the wheels as far as possible from casting heat. The advantages to you: greatly increased service life and more efficient casting.

ENGINEERS

1221 BANKSVILLE ROAD PITTSBURGH 16, PA

Journal of METALS

VOL. 5, NO. 9 SEPTEMBER, 1953

IN TWO SECTIONS — SECTION 1

COVER

Pittsburgh Steel Co.'s new hot mill at Allenport, Pa., receives steel slabs from the company's Monessen works. In five passes back and forth on the reversing rougher, the slab is reduced from about 5 in. to ½ in., a reduction in thickness of about 90 pct. Vertical edging rolls maintain the steel at constant width.

NEWS

Employment Service	1050	Coming Events	1066
Books for Engineers	1054	Trends	1070
Meet the Authors	1056	Journal of Metals Reporter	1073
New Products	1059	Drift of Things	1074
Industrial Notes	1064	AIME News	1137

TECHNICAL FEATURES

Anode Casting Operations at Garfield Smelter Geared to High Production — N. R. Alston, M. J. Winkel — 1075

Automatic Controls Speed Refractories Output — 1078

Labor Legislation—As It Affects the Engineer — 1080

Research in Progress — 1081

IMD Fall Meeting Program — 1086

TRANSACTIONS

Oxygen Activity in Iron Oxide Slags — H. Larson, J. Chipman — 1089

Constitution of the FeO-Fe_2O_3-SiO_2 System at Slagmaking Temperatures — R. Schuhmann, Jr., R. G. Powell, E. J. Michal — 1097

Solutions of Metals in Fused Salts — D. D. Cubicciotti — 1106

Reaction of Silver with Aqueous Solutions of Cyanide and Oxygen — G. A. Deitz, J. Halpern — 1109

System Zirconium-Boron — F. W. Glaser, B. Post — 1117

A Study of Some Binary Hafnium Compounds — F. W. Glaser, D. Moskowitz, B. Post — 1119

Creep Behavior of Extruded Electrolytic Magnesium — C. S. Roberts — 1121

High Pressure Oxidation Rate of Metals—Copper in Oxygen — W. McKewan, W. Martin Fassell, Jr. — 1127

Plasticity of Columbium Single Crystals — R. Maddin, N. K. Chen — 1131

TECHNICAL NOTES

Some Low Temperature Properties of Titanium Alloy RC-130-B and Stainless Steel — W. W. Tyler, L. B. Nesbitt, A. C. Wilson, Jr. — 1104

This Special Issue of JOURNAL OF METALS is in two sections

Published to provide a continuing, authoritative, and up-to-date record of technological, engineering, and economic progress in all branches of the metals industry by the Metals Branch American Institute of Mining and Metallurgical Engineers, Inc. 29 West 39th Street, New York 18

ALVIN S. COHAN
Acting Manager of Publications
Editor, JOURNAL OF METALS

D. G. GARRETT M. A. MATZKIN
G. M. ZILL
Assistant Editors

GRACE PUGSLEY Production Manager
W. J. SEWING Asst. Prod. Mgr.

METALS BRANCH COUNCIL
K. C. McCutcheon — Chairman
E. O. Kirkendall — Secretary
M. Cohen — IMD Chairman
T. J. McLoughlin — ISD Chairman
R. R. McNaughton — EMD Chairman
W. A. Dean — R. D. Parks
T. D. Jones — D. S. Eppelsheimer

EDITORIAL ADVISORY COMMITTEE
J. S. Smart, Jr. — Chairman
W. A. Dean — Evan Just
J. C. Kinnear, Jr. — John Marsh
T. D. Jones — M. Tenenbaum

TECHNICAL PUBLICATIONS COMMITTEES
J. I. Laudermilk — AIME Chairman
W. C. Ellis — IMD Chairman
E. W. Pierce — ISD Chairman
J. Glasser — EMD Chairman
E. J. Kennedy, Jr. — Secretary

JAMES A. STANGARONE
Advertising Manager
FRED STANLEY
Eastern Representative

The AIME Publishes:
Journal of Metals
Mining Engineering
Journal of Petroleum Technology

Published the first day of each month by the American Institute of Mining and Metallurgical Engineers, Inc., 29 West 39th Street, New York 18, N. Y. Telephone: PEnnsylvania 6-9220. Subscription $8 per year for non-AIME members in United States and North, South and Central America; $10, foreign; $6 for AIME members, or $4 additional in combination with a subscription to "Mining Engineering" or "Journal of Petroleum Technology". Single copies, 75 cents; single copies foreign, $1.00; special issues, $1.50 . . . The AIME is not responsible for any statement made or opinion expressed in its publications. . . . Copyright 1953 by the American Institute of Mining and Metallurgical Engineers, Inc. . . . Registered cable address, AIME New York . . . Indexed in Engineering Index, Industrial Arts Index and Chemical Abstracts . . . Reentered as second-class matter Sept. 21, 1949, at the post office at New York, N. Y. under the Act of March 3, 1879. Additional entry established at Manchester, N. H.

IF

You Need Supplying Promptly With Custom-Built Alloy Metal Powders To Difficult or Hard-To-Get Specifications

THEN

Write To

POWDER METALLURGY LTD.

59-62, High Holborn, London, England.

WHO

Will Undoubtedly Be Able to Satisfy You.

— Personnel Service —

THE following employment items are made available to AIME members on a non-profit basis by the Engineering Societies Personnel Service, Inc., operating in cooperation with the Four Founder Societies. Local offices of the Personnel Service are at 8 W. 40th St., **New York 18;** 100 Farnsworth Ave., **Detroit;** 57 Post St., **San Francisco;** 84 E. Randolph St., **Chicago 1.** Applicants should address all mail to the proper key numbers in care of the New York office and include 6c in stamps for forwarding and returning application. The applicant agrees, if placed in a position by means of the Service, to pay the placement fee listed by the Service. AIME members may secure a weekly bulletin of positions available for $3.50 a quarter, $12 a year.

MEN AVAILABLE

Metallurgical Engineer, B.S., 33, single, desires a responsible part in an active industrial development program. Eight years' industrial experience in alloy development, production control, materials engineering, technical supervision, and sales development, with emphasis on the stainless and high alloy materials. Location immaterial. M-106.

Metallurgical Engineer, 34, Canadian, doctorate in physical metallurgy. Twelve years' experience in industry, research and foundry management—cast iron, malleable iron, copper, magnesium and aluminum alloy castings; experience in conducting and managing fundamental and applied research and development. Desires responsible management position, technical adviser or research manager. Location, Canada or USA. M-107.

Engineer seeks foreign position. Three years' experience as sales engineer in copper-base alloys. B.S. metallurgical engineering. B.F.T. from the American Institute for Foreign Trade. Knowledge Spanish. Naval aviator. Interested sales, administration and writing. Age 30, family. M-108.

Metallurgical Engineer, 38, married. Eleven years' experience nonferrous metallurgy lead, zinc, copper, bismuth, silver, gold. Locate U. S. or Canada. Available immediately. M-109.

POSITIONS OPEN

Assistant or Associate Professor of metallurgical engineering, to teach heat transfer and process metallurgy including thermodynamics. Advanced degree and experience essential. Position starts September 1954. Location, Pennsylvania. Y8993.

Metallurgical Engineer, young, who has had 2 to 5 years' experience in oil refineries for work as equipment inspector. Will consider recent graduate metallurgical engineer with an interest in oil refinery work. Salary open, depending on experience. Location, New Jersey. Y8956.

Technical Director with considerable administrative ability and metallurgical background to direct technical development program on precision metal parts. Salary, $15,000 to $20,000 a year. Location, New York. Y8907.

Sales Engineer, young, metallurgical or chemical, to work in New York City office on engineering sales or equipment for the metallurgical and chemical industries. Part of the time will be required to travel on sales and consultation work connected with discussions on design of plants and equipment. Salary about $6000 a year. Location, New York. Y8899.

Engineers for work in metals refining plant. (a) Assistant plant superintendent. Salary, $10,200 to $11,400 a year. (b) Chief metallur-

We need a young man with technical background, preferably powder metallurgy, to develop markets for interesting group of alloy powders.

Will travel extensively following training period.

Please write, outlining experience, background and salary requirements to Personnel Director, METAL HYDRIDES INCORPORATED, Beverly, Mass.

SYLVANIA'S ATOMIC ENERGY DIVISION

(Bayside-Hicksville, Long Island)

has openings for...

METALLURGISTS
METALLURGICAL ENGINEERS
POWDER WIRE DRAWING FABRICATION

or men with

GENERAL PHYSICAL METALLURGY EXPERIENCE

TO PARTICIPATE IN THE RAPIDLY EXPANDING APPLICATION OF ATOMIC ENERGY TO INDUSTRIAL USE

Send Resume to:
Mgr. of Personnel, Atomic Energy Div.
Sylvania Center, Bayside, L. I.

SYLVANIA
ELECTRIC PRODUCTS INC.
In New York's Finest Commuting Area

Physical Metallurgist, B.S. or M.S. in Metallurgy. Research and development work of Non-ferrous alloys. Salary open. Location vicinity of Boston.

Box G-21
JOURNAL OF METALS

gist. Salary, $10,800 to $13,200 a year. (c) Assistant metallurgist. Salary $6600 a year. (d) Chemist for analytical research on ores. Salary $6500 a year. (e) Microanalyst. Salary $6500 a year. (f) Chemical engineers, for liaison work between production and pilot plant. Salary $7200 a year. (g) Assistant chief engineer for production in plant. Salary, $8400 to $10,800 a year. (h) Analytical chemist, recent graduate or with a minimum of experience. Salary, $4800 a year. Location, Cuba. Y8889.

Professor in metallurgy, to teach undergraduate subjects in the field and conduct research of a development nature that would be sponsored by various local industries. Prefer Ph.D. degree. Location, Midwest. Y8883.

Salesmen, 2, 30 to 45, with at least two years of college courses in metallurgy, business administration, public speaking and human relations. Minimum of one years' experience in selling industrial products to manufacturing accounts. Company is a leading processor of steel and allied products. Car provided and all business expenses paid. Salaries, $5500 to $6500 a year to start plus bonuses and benefits. Company will negotiate placement fee. Location, New York, metropolitan area. Y8880.

Development Engineers, metallurgical or mechanical, 35. Must have had 5 years' experience on nonferrous fabricating field, preferably aluminum. Will be required to develop special technical knowledge relative to design and fabrication of aluminum and its products. One man to specialize in marine industry, one in petroleum chemical and process industries and one in machine and textile industry. Must have ability to work with personnel at management level. Salary, $7500 to $8500. Location, Chicago. C1124.

Production Engineer, 35 to 45, B.S. M.E. and/or Met with 1 to 3 years' experience in tool making; five or more years' supervisory work; tool, gage and die making and inspection; feeds and speeds study in connection with time study; familiarity with problems of metallurgy, jig and fixture design and the establishment of manufacturing tolerances; machine maintenance and machine rebuilding. Working knowledge of statistical quality control. Will direct the activities of a project engineer. Location, Connecticut. Y9000.

Sales Engineer, mechanical or metallurgical graduate, for sales promotion covering welding accessories. Salary, $4000 a year to start. Some traveling. Location, New York, N. Y. Y9004.

NOW there are TWO METALLOGRAPHS

New Research
METALLOGRAPH

FOR • BRIGHT FIELD
• POLARIZED LIGHT
• PHASE CONTRAST

Here is another remarkable AO *DESK-TYPE* Metallograph -- the new Model 2400P for phase, polarized light, and bright field photomicrography. It offers entirely new standards of convenience, speed, and accuracy in dealing not only with routine specimens, but also with anisotropic materials, non-metallic inclusions requiring polarized light, unetched specimens, and in determining differences of level within a specimen.

This newest Model 2400P permits instant change from bright field, to phase, to polarized light. Polarizer, rotating analyzer, and phase diffraction plate are all built-in. Rotatable full and quarter wave compensators are provided for examination of specimens which have low double refraction.

Mail coupon for complete information.

Only AO Desk-Type Metallographs Offer Such Convenience

ALL CONTROLS OPERABLE FROM SITTING POSITION . . .
From start to finish, every control, every operation, is at your fingertips.

FOCUS QUICKLY, AUTOMATICALLY, ACCURATELY. . .
Final focusing for photography is accomplished through visual system which is parfocal with photographic system.

UNBELIEVABLE SPEED AND PRECISION . . .
in changing magnification, adjusting lamp, making exposure.

OTHER FEATURES . . .
Graduated revolving stage, monocular or binocular bodies, revolving objective turret, two lamps — visual and photographic, exceptional arc lamp performance with both AC and DC current, ease of focus assured by "Autofocus" coarse adjustment control stop. Low-frequency shock absorbers, attachable to base of desk, are offered as optional equipment.

American Optical
INSTRUMENT DIVISION
BUFFALO 15, NEW YORK

Dept. W182.

Gentlemen:

Please send me your brochure on AO Metallographs.

Signed .....

Address .....

from iron...

Grefco's OLIVE HILL brick has proved its ability to pour out production through longer campaigns . . . has long been a favorite with steel men in blast furnace application.

to steel...

In the open hearth, Grefco's silica, RITEX chrome-magnesite basic brick... and STEELKLAD, Grefco's patented basic brick encased in a permanent steel shell have contributed *much* to modern steel production.

it's

GENERAL REFRACTORIES

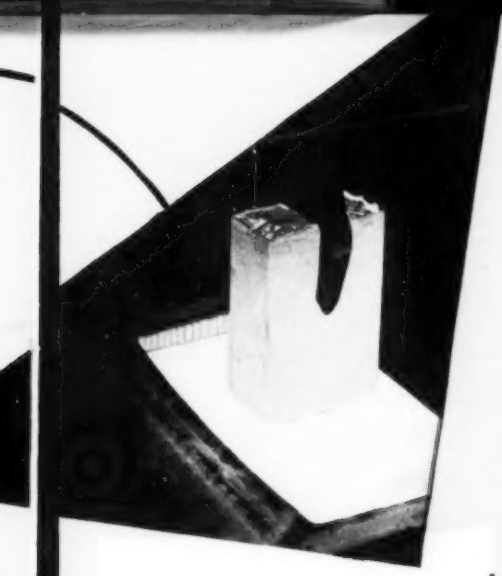

to supply!

Even the railroad cars in which the plate, sheet, strip or wire are shipped would not exist but for Grefco's truly *complete refractories service*. Call on Grefco yourself!

and ingot...

YOUGH silica brick, STEELKLAD and RITEX are superior refractories for lining soaking pits. From coast to coast and border to border, wherever there is a steel mill and soaking pit, chances are you'll find Grefco dependably on the job.

Grefco all the way!

GENERAL REFRACTORIES COMPANY

PHILADELPHIA

Books for Engineers

Sulphur. System No. 9, Section A2 and B1, of the eighth edition of Gmelin's Handbook of Inorganic Chemistry, Edited by the Gmelin Institute. *Verlag Chemie.* A2 450 pp., BI 372 pp., 1953.—The volume A2 treats, for the first time in modern scientific literature, the complete knowledge of the occurrence and technology of the sulphur compounds, of the colloidal chemistry of sulphur and the physiological phenomena caused by sulphur. Section B1 deals with sulphur hydrites and oxides. Formation of hydrogen sulphide from the elements, the equilibrium, and the composition of H_2S are fully discussed. Part A of System No. 9 will be concluded by Section A3 to appear in the fall 1953 and Part B will be completed by Section B2 in 1954.

ASTM Standards on Copper and Copper Alloys. *American Society for Testing Materials.* $5.00, 542 pp., 1953.—The book is a compilation of 115 specifications, test methods, and recommended practices pertaining to copper and copper alloy castings, sheet, strip, bars, shapes, wire, pipe and tube, filler metal, and covered steel electrical conductors. Specifications are given for several other nonferrous metals including; slab zinc, pig lead, nickel, phosphor copper, and silicon copper. Classified and numerical indexes are provided.

ORDER YOUR BOOKS THROUGH AIME—Address Irene K. Sharp, Book Department. Ten per cent discount given whenever possible. Order Government publications direct from the agency concerned.

Boron Steel, second edition. *American Society for Metals.* $1.00, 111 pp., 1953.—Contains four papers on general aspects, seven papers on actual experience, two on the effect of boron on steel, and three giving supplementary technical information on hardenability tests, H-steels, and their use. A data sheet presents approved specifications for the Jominy end-quench test.

Electrical Engineering, second edition, by Fred H. Pumphrey. *Prentice-Hall Inc.* $8.00, 404 pp., 1953.—This is a text aimed at students specializing in technical fields other than electrical engineering. The first 12 chapters review basic theory of electrical circuits, electromagnetism, electrical machinery, and measurements. The final chapters treat typical applications, controls, electrochemical processes, electron tubes, and various specialized applications of importance to civil, mechanical, and electrical engineers.

Engineering Drawing, by Frank Zozzora. *McGraw-Hill Book Co.* $5.00, 369 pp., 1953.—The book may serve as a text or reference work for the student or practicing engineer. It is arranged for easy study progress, beginning with basic elements and leading through geometrical constructions to sectioning, auxiliary views, intersections and developments, and various special depictions. Problems are carefully selected and illustrations well chosen.

Introduction to Engineering Economy, second edition, by Baldwin M. Woods and E. Paul De Garmo. *Macmillan Co.* $6.00, 519 pp., 1953.—For students, this book relates accounting, valuation, investment theory, statistical methods, and general economics to the management of engineering enterprises. While subject matter remains substantially the same as in the previous edition, material has been revised to conform with recent developments.

Low Temperature Physics, by Charles F. Squire. *McGraw-Hill Book Co.* $6.50, 244 pp., 1953.—The book is a study of the properties of matter at

First in the New Series of

ALLOYS OF IRON

Monographs

Edited by FRANK T. SISCO

ALUMINUM in IRON and STEEL

By SAMUEL L. CASE,
Battelle Memorial Institute,
and KENT R. VAN HORN,
Aluminum Company of America

The only comprehensive survey available

The major role of aluminum in modern ferrous metallurgy makes this volume particularly timely. It is the only critical, correlated summary of all important research work and published information on one of the most important elements used in steel manufacture. Thanks to the cooperation of hundreds of researchers, writers, translators, and editors, *Aluminum in Iron and Steel* brings you all important data published since 1890.

Reliable information, checked by experts

This monograph was reviewed in manuscript by men especially qualified to criticize all statements. Before publication it was given a final stamp of approval by the Iron Alloys Committee.

Time-saving, labor-saving data

This convenient, well-organized book spares you the time and labor necessary for research in over 340 journals in many languages. It saves you costly, time-consuming research that duplicates work already completed.

CONTENTS

Part I: Aluminum as a Deoxidizer in Iron and Steel

The Deoxidation of Steel by Aluminum. Oxide Inclusions in Steel Deoxidized with Aluminum. Sulphide and Nitride Inclusions in Steel Deoxidized with Aluminum. The Role of Aluminum in Austenitic Grain-Size Control. Effect of Aluminum on Notch Sensitivity and Related Properties of Steel. Effect of Aluminum on Aging of Steel. Some Other Consequences of the Use of Aluminum as a Deoxidizer.

Part II: Aluminum as an Alloying Element in Iron and Steel

The Constitution of Binary and Complex Iron-Aluminum Alloys. The Manufacture of the Simple and Complex Iron-Aluminum Alloys. Aluminum in Heat-Resisting Alloys. Aluminum in Permanent-Magnet Alloys. The Function of Aluminum in Nitriding Steels. The Aluminum Coating of Steel. Miscellaneous Uses of Aluminum as an Alloying Element in Iron and Steel.

1953 — 478 pages — 261 illus. — $8.50

Send for copy on 10-day approval today

JOHN WILEY & SONS, Inc.

440 Fourth Ave., New York 16, N. Y.

low temperature and their adherence to quantum laws. Extensive discussion is devoted to superfluid helium, superconductivity of metals, the complex magnetic and electric permeability of matter, and the thermal energy in the solid state. Current fields of research are also noted. Experimental methods and apparatus are treated to a limited extent.

1952 Book of ASTM Standards, Including Tentatives. *American Society for Testing Materials.* Part 1, Ferrous Metals, $12.00, 1602 pp.; Part 2, Nonferrous Metals, $10.00, 1359 pp.; Part 3, Cement, Concrete, Ceramics, Thermal Insulation, Road Materials, Waterproofing, and Soils, $12.00, 1666 pp.; Part 4, Paint, Naval Stores, Wood, Fire Tests, Sandwich Constructions, Building Constructions, $10.00, 1182 pp.; Part 5, Fuels, Petroleum, Aromatic Hydrocarbons, and Engine Antifreezes, $10.00, 1282 pp.; Part 6, Rubber, Plastics, and Electrical Insulation, $12.00, 1520 pp.; Part 7, Textiles, Soap, Water, Paper, Adhesives, and Shipping Containers, $10.00, 1364 pp. Total cost for seven parts, $76.00. This new combined edition covers more than 2000 specifications, tests, etc., and contains all the standards, adopted and tentative, as of the present date. Each volume contains its own index.

Physical Constants of Some Commercial Steels at Elevated Temperatures. *Butterworths Scientific Publications.* 38 pp., 1953.—Total and specific heats, coefficients of thermal expansion, electrical resistivities, thermal conductivities, densities, and mean thermal diffusivities are tabulated at 50° intervals from 50°C up to about 1200°C for pure iron and a selection of low and high alloy steels. Total heat-temperature curves and expansion-temperature curves are shown, and a summary of methods used in determining physical constants is included.

Plansee Proceedings, 1952, edited by F. Benesovsky. *Metallwerk Plansee, distributed in U. S. by Powder Metallurgy Bulletin.* $8.00, 316 pp., 1953—Papers presented at the first Plansee Seminar on powder metallurgy are grouped under three headings: General and physical metallurgy and physics of solids; problems of powder metallurgy in general; cemented carbides and other hard metals. Papers are in German or English with a summary in the language not used for the full text.

Textbook of the Materials of Engineering, by Herbert F. Moore and Mark B. Moore. *McGraw-Hill Book Co.* $6.00, 372 pp., 1953—The book is elementary in nature, devoted to common materials—metals, wood, concrete, building stone, ceramics, etc. Emphasis is placed on strength, toughness, and stiffness of stress-carrying material. Information on new materials is added in this new edition.

Manual on Industrial Water (Special Technical Publication No. 148) *American Society for Testing Materials,* $4.25, 336 pp., 1953.—This book discusses uses of water and problems of supply; composition, sampling, and analysis of industrial water; water-formed deposits; and the reaction and corrosion products of water. The appendix contains all ASTM water standards and test methods. A reference manual.

Uranium-Vanadium Deposits of the Thompsons Area, Grand County, Utah. With Emphasis on the Origin of Carnotite Ores by Wm. Lee Stokes. *University of Utah,* $1.00, 51 pp., 1951.—Of interest to students of fissionable materials, Bulletin 46 is by the author of the *Guidebook to the Geology of Utah—1948.*

Air Pollution Abatement Manual, Chapter 12—Bibliography, Appendix 2, compiled by George F. Jenkins and edited by C. A. Gosline, *Mfg. Chemists' Assn. Inc.,* 35¢, 20 pp., July, 1953.—This is the second semi-annual supplement. Loose-leaf forms enable these pages to be arranged with preceding references. The originally-issued Chapter 12 Bibliography is 50¢. A subscription to Appendices for a 3-year period is $1.50.

PROFESSIONAL SERVICES

Limited to AIME members, or to companies that have at least one AIME member on their staffs. Rates $40 per year per inch.

SCIENTISTS
CONSULTANTS
METALLURGISTS

Small Jobs Welcomed

SAM TOUR & CO., INC.

Laboratories and offices
44 Trinity Place, New York 6, N. Y.

Testing—Certifying
American Standards
Testing Bureau, Inc.

MAX STERN
Consulting Engineer

Expert for Scrap Recovery and Shipwrecking — Modernization of Plants and Yards for Ferrous and Nonferrous Metal Scrap

149 Broadway New York 6, N. Y.

This

NEW

information may solve your materials problems

Refractory Hard Metals

The new book by *Paul Schwarzkopf* and *Richard Kieffer* presents

4 NEW chapters in the chemistry of metals

You'll have much information that has only recently become known—some of it published here for the first time—on the preparation and properties of the compounds of carbon, nitrogen, boron, and silicon with the transition metals of the 4th to the 6th group in the periodic system.

Important HIGH TEMPERATURE data

You'll find this information of first importance for high temperature applications because the basically different structure of these high-melting compounds permit uses not possible with other materials. The book includes the first critical evaluation and comparison of today's possible materials for high temperature uses.

New BASIC knowledge

You'll have the basic scientific knowledge most needed today for solving materials problems—a critical treatment of both theory and experimental fact by experts, on materials that have already revolutionized machining techniques, are now being used in some of the new engineering developments, and offer still further important potentialities.

Let us send you a copy of this important book on approval. And you'll also want Schwarzkopf's POWDER METALLURGY for basic reference on the processing techniques, products, and theory of the powdered metals.

USE THIS COUPON

The Macmillan Co., 60 Fifth Ave., New York 11

Please send me the book(s) checked below. I will either remit the full price plus small delivery charge, or return the book(s) in 10 days. (Save: enclose check or money order and we pay delivery charge.)

☐ Refractory Hard Metals $10.00
☐ Powder Metallurgy $4.00

Signed .....

Address .....

(This offer good only within continental limits of U.S.A.)

Meet The Authors

M. J. Winkel (p. 1075), a Member of the Salt Lake Section, AIME, was born at Cleveland and is a graduate of Notre Dame University, 1935. Following graduation he was employed by the Stamford Rolling Mills, Springdale, Conn. for two years. He has been associated with the Anaconda Copper Mining Co. and Federated Metals Co. In 1939 Mr. Winkel joined the American Smelting & Refining Co. at Baltimore. He was transferred to the Garfield, Utah, plant as metallurgist and dept. head in charge of the anode casting dept., a position he presently holds. During World War II, Mr. Winkel was a lieutenant commander in the Navy.

N. R. Alston (p. 1075), is a metallurgist with the American Smelting & Refining Co., Garfield, Utah. After graduating from the University of Utah (1934, B.S.), Mr. Alston joined the Nevada Consolidated Copper Corp., McGill, Nev. He was promoted to metallurgical clerk and then smelter test engineer. At the beginning of World War II he was employed by the Permanente Metals Corp., San Jose, Calif. From August 1942 to 1945 he was in the Navy, lieutenant commander, USNR. After his discharge he joined AS&R.

E. J. Michal (p. 1097), received his B.S. from the University of Nevada and his S.M. and Sc.D. from the Massachusetts Institute of Technology. Born in Reno, Nev., Dr. Michal was a physicist in the Civil Service prior to joining the Navy. During his time in the Navy he was located in the Pacific area. Following his discharge in 1946, Dr. Michal was an instructor in metallurgy at Massachusetts Institute of Technology. In 1951 he joined the National Lead Co., South Amboy, N. J. A member of the AIME New York Local Section, he previously had a paper published in the July 1952 issue of JOURNAL OF METALS.

R. G. Powell (p. 1097), is a staff member of the div. of industrial cooperation, Massachusetts Institute of Technology. He was born at Sherbrooke, P. Q., Canada and graduated from the University of Laval, Quebec. Mr. Powell has gained varied experience in mines both in the United States and Canada. Prior to joining MIT he had been employed by the New Jersey Zinc Co., Austinville, Va. in the mill and also worked in the smelter at the Quebec Iron & Titanium Co., Quebec. While at MIT he has done research development work on foundry process. Mr. Powell is a hockey fan, but also enjoys playing tennis and prospecting.

R. G. POWELL

D. D. CUBICCIOTTI

Daniel D. Cubicciotti (p. 1106), a native Philadelphian, is now residing at Whittier, Calif. Dr. Cubicciotti attended the University of California, graduating in 1946 (Ph.D.). He returned to the East after graduation and was an instructor at New York University. In 1947 he joined the staff at the University of California. For three years he was associated with the Illinois Institute of Technology. Since 1951 Dr. Cubicciotti has been with North American Aviation, Inc., where he is now a research chemist in the atomic energy research dept.

Keep NATIONAL Carbon Brick on hand for MAINTENANCE

TRADE-MARK

KEEP THESE STANDARD SIZES ON HAND FOR EMERGENCY!

13½" x 6" x 3" series
9" x 6" x 3" series
2" x 4½" x 2½" series

☆

Write for Catalog Section S-6210

If you think of carbon only in terms of complete furnace linings, check these other important locations in and around the furnace where "National" carbon brick and shapes will also save time and money as a maintenance refractory:

- ✓ ***RUNOUT TROUGHS***
- ✓ ***CINDER NOTCH LINERS***
- ✓ ***CINDER NOTCH PLUGS***
- ✓ ***SPLASH PLATES***
- ✓ ***SKIMMER PLATES***

. . . and Many More!

The term "National" is a registered trade-mark of Union Carbide and Carbon Corporation

NATIONAL CARBON COMPANY

A Division of Union Carbide and Carbon Corporation, *30 East 42nd Street, New York 17, N. Y.*

District Sales Offices: Atlanta, Chicago, Dallas, Kansas City, New York, Pittsburgh, San Francisco

In Canada: National Carbon Limited, Montreal, Toronto, Winnipeg

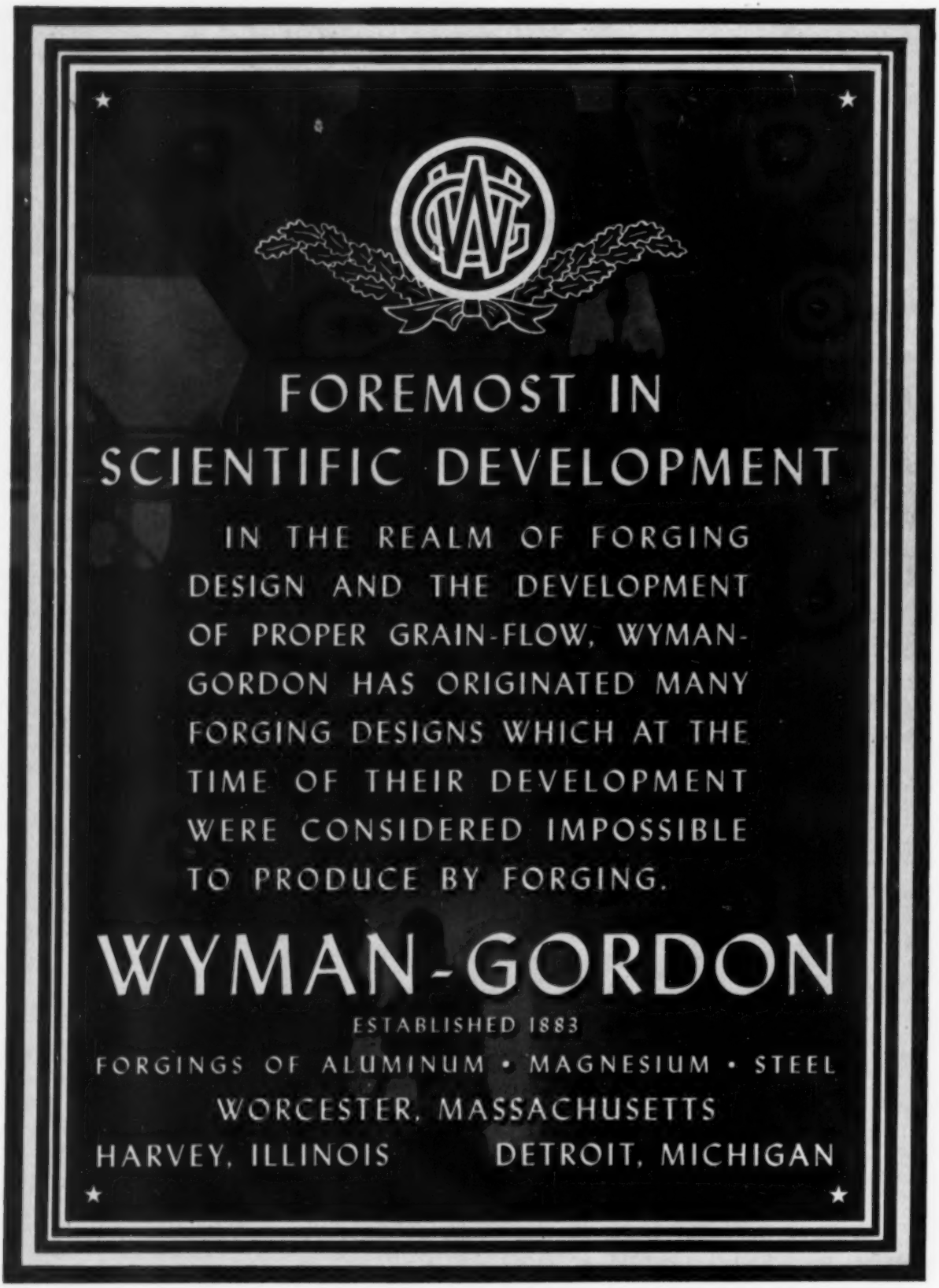
FOREMOST IN
SCIENTIFIC DEVELOPMENT
IN THE REALM OF FORGING DESIGN AND THE DEVELOPMENT OF PROPER GRAIN-FLOW, WYMAN-GORDON HAS ORIGINATED MANY FORGING DESIGNS WHICH AT THE TIME OF THEIR DEVELOPMENT WERE CONSIDERED IMPOSSIBLE TO PRODUCE BY FORGING.
WYMAN-GORDON
ESTABLISHED 1883
FORGINGS OF ALUMINUM • MAGNESIUM • STEEL
WORCESTER, MASSACHUSETTS
HARVEY, ILLINOIS
DETROIT, MICHIGAN

New Products

New Products **New Literature** **New Services**

For Further Information or Literature on any Product, Fill in the Coupon and Send to JOURNAL OF METALS

Students are Requested to Apply Directly to Manufacturers for Bulletins and Information

1—TITANIUM: Commercially pure titanium, precision rolled to very close tolerances and to thin gage and foil is now available from *American Silver Co., Inc.* Titanium is rolled in strip up to 8 in. wide and as thin as 0.0005 in. to tolerances as close as ±0.0001 in.

2—NONDESTRUCTIVE TEST: Magnatest FM 100 conductivity meter has been introduced by *Magnaflux Corp.* This instrument makes conductivity measurements quickly available for laboratory control or factory use. The FM 100 gives absolute conductivity measurements of nonferrous conducting materials directly from a large dial on the front of the unit. The need for wire like samples or cross-sectioning of parts is eliminated.

3—SPECIMEN SPINNER: A cylindrical specimen spinner that is used in place of the standard specimen

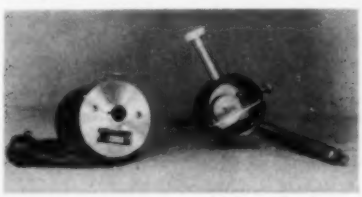

holder of the Norelco wide range goniometer for special X-ray analysis work has been announced by *North American Philips Co., Inc.* The holder is rotated at approximately 130 rpm.

4—EXTENSOMETER: A Microformer type extensometer designed to produce stress strain diagrams with high strain magnifications and low magnifications respectively, below and above elastic limit of materials is announced by *Baldwin-Lima-Hamilton Corp.*

5—TEMPERATURE TESTING: A hot-cold unit for high and low temperature available in capacities from 1 to 4 cu ft, operating at temperatures from 250° above zero to 130° below zero is available from *Sub-Zero Products Co.*

6—LUBRICANT: C-5 copper pigmented lubricant ideal for reducing wear on hot forging dies is offered by *Surveys, Inc.* It provides rapid heat dissipation on withdrawal, increases die life, and reduces wear.

7—HARDNESS TESTERS: Hand operated metal hardness testers that provide automatic load changing and magnified optical readings are available from *Opplem Co., Inc.* Automatic changing of loads is done

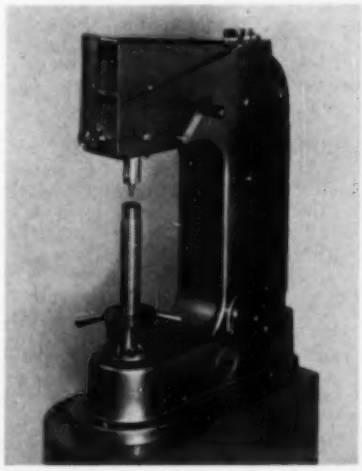

quickly by turning a dial which immediately switches the loads in the interior of the instrument. Speed of load application is regulated by a built in oil damper with an external control.

8—RADIATION SHIELD: A portable directional exposure shield for safe handling of strong sources of cobalt 60 for industrial radiography is announced by *Technical Operations Inc.* It can be used for thick or thin sections. The equipment functions to shield all radiation from a gamma source except a beam, which may be directed only at the area to be exposed.

9—METABLAST: A method of treating metals to produce surfaces of greater uniformity than possible with conventional surfacing techniques has been announced by *American Metaseal Mfg. Corp.* The process consists of shooting an abrasive that is suspended in liquid, in a controlled high pressure spray against a metal surface. Minute pits are produced that can be varied in coarseness or fineness, by using different grades of abrasive and changing the length, force, or direction of the spray.

10—AUTOMATIC REVERSAL: A packaged automatic reversal system for open hearths, regenerative soaking pits, and glass tanks has been introduced by *Askania Regulator Co.*

11—CU PASSIVATION: Passivation of copper and most copper alloys is now available in a simple chemical dip and rinse process. This process removes atmospheric oxides and simultaneously passivates the metal so that it will resist oxidation without surface coating for periods ranging from three to six months, depending on atmospheric conditions. *Rossaul Co.*

12—TORSION DEVICE: To produce pure torsion on a tension testing machine, *Baldwin-Lima-Hamilton Corp.* announces the Schaevitz torsion device. Test specimens up to ¾ in. sq and ranging from 2 to 12 in. long (+ 2 in. to be engaged by torque bars) can be twisted to a maximum angle of 24°. Maximum torque load is 60,000 in.-lb, obtained by applying a 12,000 lb tension load. The device is furnished with hardened socket liners for specimens ⅜, ½, ⅝, and ¾ in. sq or for round specimens with square ends of these sizes.

13—TEMPERATURE UNIT: A new molten steel temperature measuring unit comprising a molten steel recorder and an instrument called a balance detector, is said to give 50 pct faster readings and up to 1000 pct extension of life of immersion thermocouples. Utilization of the balance detector speeds up reading time to 10 to 15 sec. The unit signals the operator at the precise moment the maximum or true reading is obtained. *Minneapolis-Honeywell Regulator Co.*

Free Literature

20—HYDROSTATIC TESTING: Three typical machines are illustrated and described in bulletin published by *Steel City Testing Machines, Inc.* The bulletin explains the type of information that is necessary in advance to build this equipment to meet customer specifications.

21—MATERIALS HANDLING: Techniques of layout and conveyor handling of foundry materials are described in reprint offered by *Bifford-Wood Co.* The entire foundry operation is shown step by step.

22—EDGE POSITION: A bulletin on edge position control for every web guiding job has been released by *Askania Regulator Co.* Photos explain the system, types of models, and applications in various industries. These controls may be used in any web handling operation, with any material handled in webs.

24—MOTOR SERVICE: *General Electric Co.* has released a bulletin on a motor service plan for fractional and integral hp motors and generators.

25—ELECTRONIC CONTROLS: A new edition of *Cutting Production Costs With Electronic Controls* is available from *Photoswitch Inc.* Case studies show how standard packaged electronic controls have solved many problems.

26—ANHYDROUS AMMONIA: A manual printed for users of this chemical is obtainable from *Allied Chemical & Dye Corp.*, nitrogen div. Physical and chemical properties, specifications of anhydrous ammonia in cylinders, and other points are covered.

27—METAL FABRICATOR: New catalog describes and illustrates the *Wales-Strippit Corp.* sheet metal fabricator for punching, notching, and nibbling up to 165 strokes per min.

28—PACKAGE WATER CONDITIONER: This versatile and self-contained unit, designed to chlorinate, coagulate, clarify, filter, neutralize, de-alkalize, and soften raw water supplies is described in booklet issued by *Permutit Co.* Rating, capacities, sizes, and typical illustrations are included.

29—FUEL OIL BURNER: When gas is not available for starting up hot blast stoves, this *Hauck Mfg. Co.* fuel oil burner unit produces a luminous flame of long, cylindrical pattern that is easily adjustable in intensity and firing capacity. Catalog sheet 57 illustrates the equipment and gives specifications.

30—PORTABLE TOOLS: Catalog on portable electric power tools has been announced by *Thor Power Tool Co.* Accessories and attachments available for equipment are also included.

31—MINERAL DRESSING: Descriptions of representative Heavy-Media plants treating a variety of metallic and nonmetallic ores are included in publication issued by *American Cyanamid Co.* Bulletin entitled *Heavy Media Separation Processes for Mineral Concentration* contains a complete bibliograhy on Heavy-Media separation.

32—SPECIMEN POLISHING: Folder describes the advantages of diamond abrasives for polishing metallurgical specimens. Diamet-Hyprez is offered in three different particle sizes, all in 5 g and 18 g gun applicators. *Buehler Ltd.*

33—GEAR MOTORS: Function, design, and application of gear motors are described in publication announced by *General Electric Co.* Standard types of GE Tri-Clad gear motors with ratings from 1/6 up to 200 hp are discussed.

34—FASTENER SELECTOR: A slide chart calculator enables manufacturers of assemblies to select the right fastener for each job quickly and easily. The selector is 8½ in. wide and 5½ in. high. Tabulated information is given for extruded and drilled tubular rivets and cutlery rivets and other data are included. *Milford Rivet & Machine Co.*

35—BLAST CLEANING: Bulletin 100A describes blast cleaning hose machines produced by *Pangborn Corp.* Various blast cleaning accessories are pictured; direct pressure and section methods of applying abrasive are explained, as well as applications of both wet and soft abrasives.

36—MAGNETIC POWDERS. Technical data, permeability rating graphs, etc. on uses and applications of annealed carbonyl iron powders are included in catalog 354 issued by *Magnetic Powders, Inc.* Hydrogen reduced iron powders and magnetites are also discussed.

37—TESTING MACHINES: Folder illustrating current Amsler machines for test in tension, compression, torsion, shear, fatigue, bending, and ductility is available from *Adolph I. Buehler, Inc.*

38—INDUCTION HEATING: Catalog designed to illustrate some of the ways in which *Lepel High Frequency Laboratories, Inc.* induction heating equipment is helping the metals industries to perform metal heating jobs faster, better, and more economically, has been published.

39—CONE DRIVE GEARS: How double enveloping worm gearing has helped improve design, performance and service life of all types of equipment in recent years is illustrated in booklet available from *Michigan Tool Co.*

40 — SPECTROPHOTOMETRY: *Beckman Instruments* has issued a booklet entitled *What Every Executive Should Know About Spectrophotometry.* The whole story is presented and case histories included. Just exactly what a spectrophotometer is, how it works and what to look for in selecting an instrument is told.

41—LITHIUM: Guide book on lithium and its compounds is available from *Foote Mineral Co.* New ideas and applications of these chemicals and a complete coverage of the current commercial applications are contained in the book.

42—CHROMIC ACID: Of interest to platers is a process developed by *Barnstead Still & Sterilizer Co.*, whereby rinse water can be passed through ion exchange resins said to effect nearly 100 pct chrome recovery. In addition, as a byproduct of the process, the user obtains a supply of demineralized water which can be used to good advantage in rinse tanks and solutions.

43—WORK-O-MATIC: Material handling system is described in booklet released by *Union Metal Mfg. Co.* On the job photographs show material positioning with bin boxes and gravity fed hoppers, etc.

Journal of Metals
29 West 39th St.
New York 18, N. Y.

September

Please send me { More Information ☐ / Free Literature ☐ / Price Data ☐ } on items indicated.

1	2	3	4	5	6	7	8	9	10
11	12	13	14	15	16	17	18	19	20
21	22	23	24	25	26	27	28	29	30
31	32	33	34	35	36	37	38	39	40
41	42	43	44	45	46	47	48	49	50

Name_____ Title_____

Company_____

Street_____

City and Zone_____ State_____

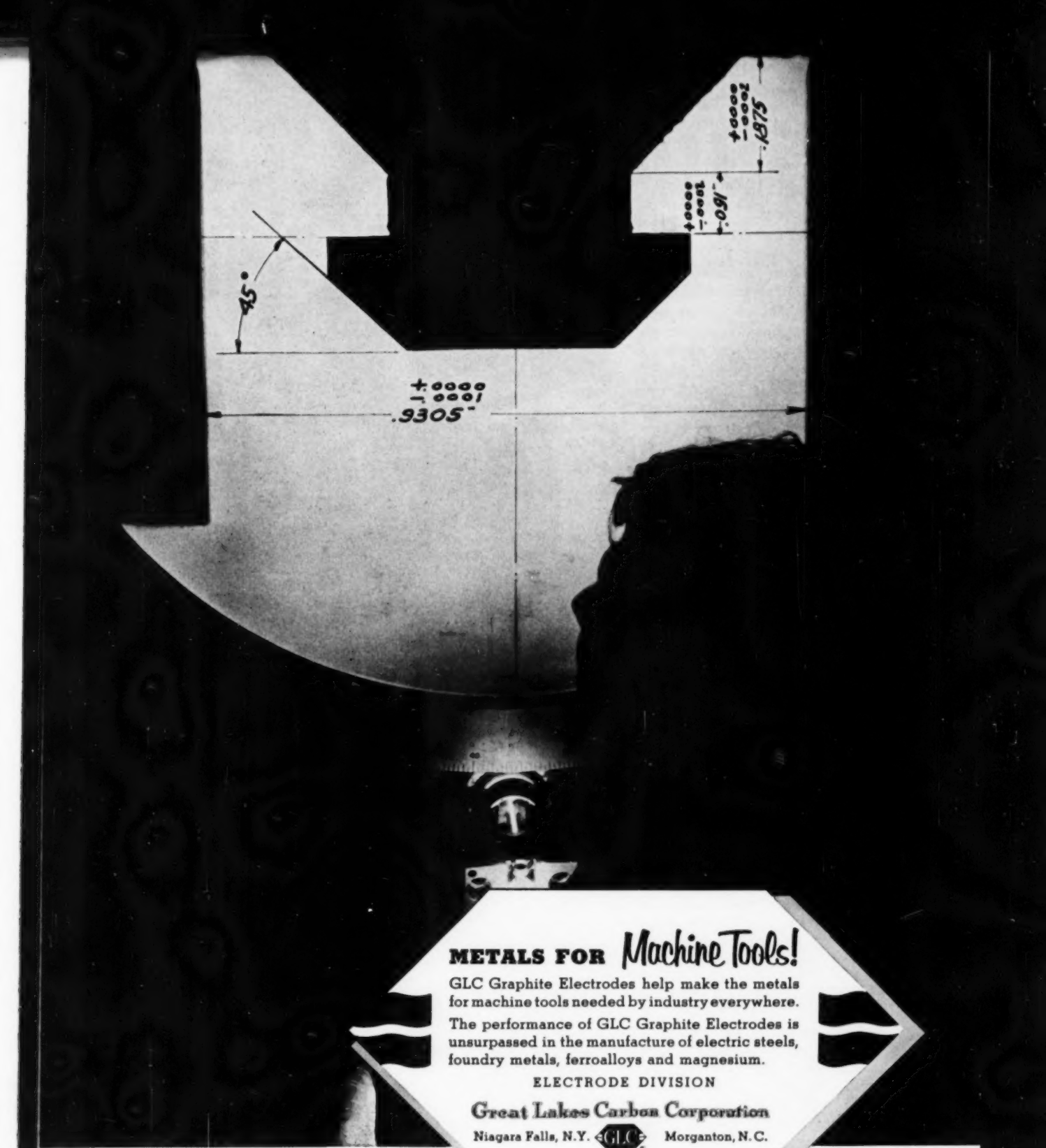

METALS FOR *Machine Tools!*

GLC Graphite Electrodes help make the metals for machine tools needed by industry everywhere.

The performance of GLC Graphite Electrodes is unsurpassed in the manufacture of electric steels, foundry metals, ferroalloys and magnesium.

ELECTRODE DIVISION

Great Lakes Carbon Corporation

Niagara Falls, N.Y. GLC Morganton, N.C.

Graphite Electrodes, Anodes, Molds and Specialties

Sales office: Niagara Falls, N. Y. · **Other offices:** New York, N. Y., Chicago, Ill., Pittsburgh, Pa.

Sales Agents: J. B. Hayes, Birmingham, Ala., George O'Hara, Long Beach, Cal., Great Northern Carbon & Chemical Co., Ltd., Montreal, Canada.

ALUMINUM IS *Why* EVERY WHEEL ADDS FORTY POUNDS OF PAYLOAD

In most states, the maximum weight of a trailer tractor and its load is fixed by law. So, in the trucking business, the object is to put the weight in the freight and not in the rig that hauls it.

Truckers do this by using a lot of aluminum in their tractors and trailers. Alcoa Aluminum Forged Disc Wheels combine the strength and durability of a forging with the lightness of aluminum. Weighing 30 to 50 pounds less than their steel counterparts, they can add 400, 700, perhaps 1,100 extra pounds of payload—depending on the number of wheels the rig has.

Alcoa Aluminum Forged Disc Wheels offer other important advantages besides weight savings. Tires run cooler because of aluminum's high-heat conductivity. Tires change easier because Alcoa Wheels are smooth and free from rust. Alcoa Wheels offer easier steering, longer tire life and smoother ride because they are precision forged and machined to run true.

Alcoa Aluminum

ALUMINUM COMPANY OF AMERICA

ALCOA IS *How*

It was Alcoa who first recognized the extra bonus of lightness that forgings could give truck wheels. And it was Alcoa Engineers, who designed the first forged wheel. In Alcoa Research Laboratories, special testing machines were built to punish and study the wheels under every conceivable condition of service life. Almost 50,000 Alcoa Forged Disc Wheels are giving extra payload to truckers all over the country . . . many wheels have run over ½ million miles and are still going strong. Aluminum Company of America, 879-J Alcoa Building, Pittsburgh 19, Pa.

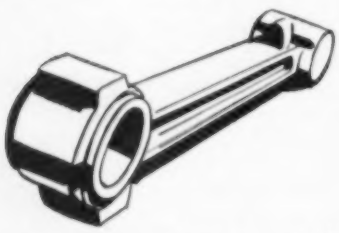

CONNECTING RODS for diesel engines, air compressors and outboard engines are forged of aluminum. They combine maximum strength with minimum weight and size.

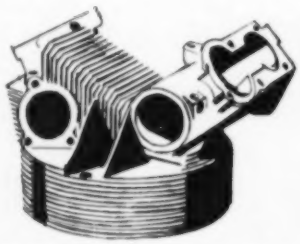

CYLINDER HEADS for aircraft have long been forged of aluminum by Alcoa. Aluminum heads increase power, reduce weight with no change in engine size.

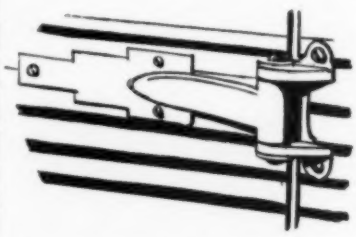

FORGED HINGES and other heavy-duty automotive hardware are forged of aluminum by Alcoa. Extra strong, extra light, corrosion resistant all the way through.

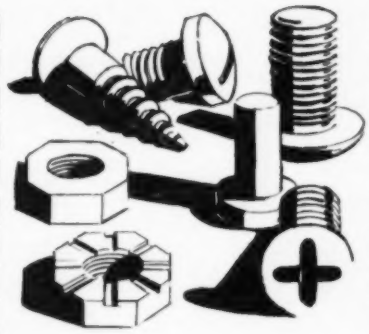

***FASTENERS** of Aluminum are made by Alcoa in every commercial size and shape. A must with aluminum assemblies, they also dress up wood and plastic products.

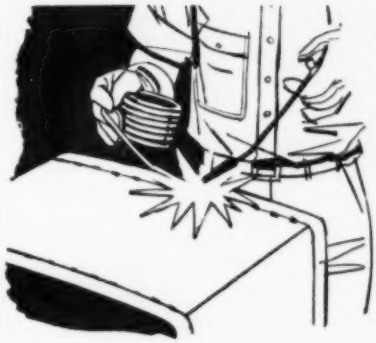

***FILLER METAL** of Alcoa Aluminum is available in many alloys for use in brazing, torch welding and arc welding. It is also packed suitably for automatic welding operations.

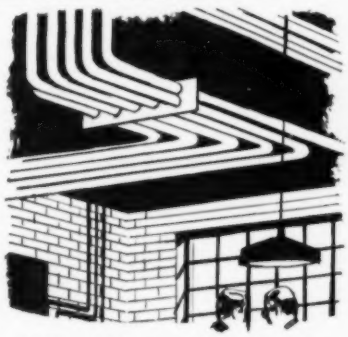

***RIGID CONDUIT** of Alcoa Aluminum is the lowest cost corrosion resistant metallic conduit available. Its nonmagnetic properties improve electrical efficiency—its light weight speeds installation.

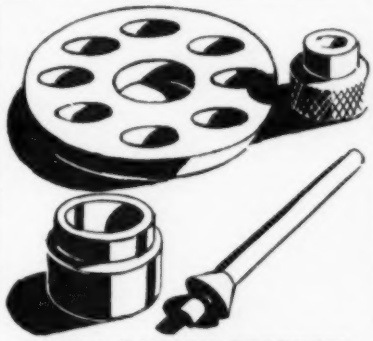

SCREW MACHINE PRODUCTS made of Alcoa Aluminum are light, lustrous and low cost. Alcoa's Edgewater, N. J. Plant is a screw machine job shop, turning out all types of fittings, special fasteners, etc., to customer specification.

***INDUSTRIAL BUILDING SHEET** of Alcoa Aluminum is light and easy to install. It never requires painting or maintenance—costs far less than you would think.

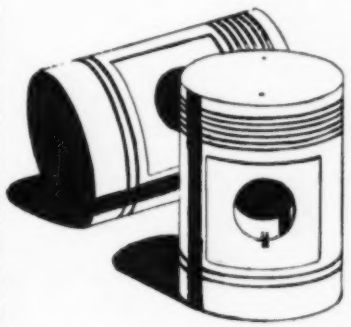

GIANT PISTONS and bearings weighing up to 800 pounds are cast of aluminum in permanent molds at Alcoa foundries! Tolerances and surface finish are exceptional.

Products marked* are available from your local Alcoa Distributor listed here

ALABAMA
Birmingham
Hinkle Supply Co.

CALIFORNIA
Los Angeles
Ducommun Metals & Supply Co.
Pacific Metals Co., Ltd.
San Francisco
Pacific Metals Co., Ltd.

COLORADO
Denver
Metal Goods Corp.

CONNECTICUT
Milford
Edgcomb Steel of New England, Inc.

FLORIDA
Hialeah
Florida Metals, Inc.
Jacksonville
Florida Metals, Inc.
Tampa
Florida Metals, Inc.

GEORGIA
Atlanta
J. M. Tull Metal & Supply Co., Inc.

ILLINOIS
Chicago
Central Steel & Wire Co.
Steel Sales Corp.

LOUISIANA
New Orleans
Metal Goods Corp.

MARYLAND
Baltimore
Whitehead Metal Products Co., Inc.

MASSACHUSETTS
Boston
Edgcomb Steel of New England, Inc.
Cambridge
Whitehead Metal Products Co., Inc.

MICHIGAN
Detroit
Central Steel & Wire Co.
Steel Sales Corp.

MINNESOTA
Minneapolis
Steel Sales Co. of Minn.

MISSOURI
Kansas City
Metal Goods Corp.
St. Louis
Metal Goods Corp.

NEW JERSEY
Harrison
Whitehead Metal Products Co., Inc.

NEW YORK
Buffalo
Brace-Mueller-Huntley, Inc.
Whitehead Metal Products Co., Inc.
New York
Whitehead Metal Products Co., Inc.
Rochester
Brace-Mueller-Huntley, Inc.
Syracuse
Brace-Mueller-Huntley, Inc.
Whitehead Metal Products Co., Inc.

NORTH CAROLINA
Charlotte
Edgcomb Steel Co.

OHIO
Cincinnati
Williams & Co., Inc.
Cleveland
Williams & Co., Inc.
Columbus
Williams & Co., Inc.
Toledo
Williams & Co., Inc.

OKLAHOMA
Tulsa
Metal Goods Corp.

OREGON
Portland
Pacific Metal Co.

PENNSYLVANIA
Philadelphia
Edgcomb Steel Co.
Whitehead Metal Products Co., Inc.
Pittsburgh
Williams & Co., Inc.

TEXAS
Dallas
Metal Goods Corp.
Houston
Metal Goods Corp.

UTAH
Salt Lake City
Pacific Metals Co., Ltd.

WASHINGTON
Seattle
Pacific Metal Co.

WISCONSIN
Milwaukee
Central Steel and Wire Co.
Steel Sales Corp.

Salem-Brosius has a

habit

that means profit to you!

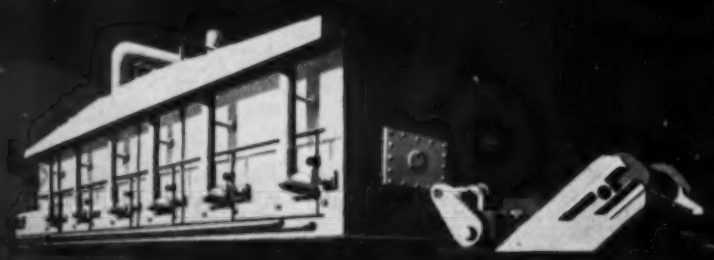

Controlled-atmosphere small-parts hardening furnace-segment of a Salem-Brosius harden, quench and draw line.

Salem-Brosius has the unfortunate habit of going to the extra trouble of engineering more quality into its furnaces than the application might indicate. Unfortunate for Salem-Brosius, but fortunate for you. Prices being equal, you, as a customer, can hardly lose from an extra measure of good design and sturdy construction that assures you of greater production, longer life, and easier operation.

Take the case of the Salem-Brosius controlled-atmosphere furnace illustrated here, which is employed with certain design variations for the hardening of such small items as cartridge cases, bolts, pins, aircraft parts, machine parts, and tools. You'll enjoy better production from these furnaces because they are not standard . . . each is extra-engineered to fit your specific application . . . each is quality-tailored for longer life and improved operations. Why not take advantage of our bad habit of extra quality. Send Salem-Brosius your next inquiry for this or any other type of heating or heat-treating furnace. You'll profit by doing so.

SALEM-BROSIUS, INC.

Industrial Notes . . .

• The steel industry consumed some 465,000 tons of new manganese during 1952, according to the Dept. of Commerce. The U.S. imported a record amount of manganese ore from 19 countries. Tonnage of contained manganese was 969,000 tons, also a record. Five leading sources were Cuba, Brazil, Union of South Africa, India, and the Gold Coast.

• Blast furnace production of pig iron and ferroalloys set a record of 38,313,549 net tons during the first half of 1953, surpassing the previous high period, the second half of 1951, by 2 million tons. Gain amounted to 8.4 million tons over the first half of 1952.

• Equipment for induction heating of shells prior to forging has been sold to Hoffman Machinery Co.'s Scranton div., by Westinghouse Electric Corp. It will be the largest installation of its kind in the U.S. and will be supplied with 960 cycle power for induction heating of 8 in. and 155 mm shells by four 1250-kw high frequency motor generators. High frequency circuit breakers will be used to protect the installation against short circuits in the main distribution bus.

• Packaged engineering control systems providing automatic control have been reported by Minneapolis-Honeywell Regulator Co. The units well be designed to take advantage of the uniformity among many process operations. Each unit is to be specially engineered for the specific process operation and will include recording and controlling instruments, measuring and control elements, and related accessories. Minneapolis-Honeywell engineers cite similarity of batch cooking operations in the textile, chemical, pharmaceutical, and food industries as an example of the feasibility of the idea. Packaged systems will enable a processor to select an instrumentation system on the basis of overall function.

• The Atomic Energy Commission approved Vanadium Corp. of America's plan to install a roaster for processing vanadium-uranium ores at its Naturita, Colo. mill. Ore to be processed will come from the company's properties and from independent producers. The roaster and auxiliary facilities should be in operation by the end of 1953. The company also exercised its option to buy the uranium-vanadium mill at Durango, Colo., previously operated under lease from the AEC.

• A machine for testing abrasive action on stern, tube, and strut bearings of navy ship propeller shafts has been developed at the U. S. Naval Engineering Experiment Station, Annapolis, Md. While

the components to be studied are lubricated by sea water, abrasive action is often caused by silt, sand, and other matter. The machine is said to reduce testing time for bearing materials from months to days.

• **The monstrous steel ball, some 225 ft in diam. starting to loom up over the West Milton, N. Y. countryside, is to house a land based prototype of an atomic power plant for submarines. Purpose of the structure is to protect the surrounding population from radioactive materials should all reactor controls fail simultaneously — highly unlikely. A ring of 26 steel columns will support the sphere which will rest in a saucer-like foundation made of reinforced concrete. When finished a prototype submarine hull will be placed inside and partially immersed in water. Inside the hull will be an atomic power plant representing one of two basic approaches to controlled atomic energy. Liquid sodium metal will be used to transfer heat from the reactor core to a *boiler*. Water in the boiler will be converted to steam which will drive the turbines that propel the sub.**

• Lithium Corp. of America, Inc. has liquidated its wholly owned subsidiary Metalloy Corp. Metalloy previously operated as the chemical and sales div. of the parent firm. Hereafter, all business will be conducted under the name of Lithium Corp. of America, Inc.

• *Board of directors of the Alan Wood Steel Co. authorized the installation of a new 4-stand tandem cold rolled strip mill, with necessary buildings and other equipment, at an estimated cost of $6 million. The new facilities are to be located at Ivy Rock, Pa., with completion expected in the first quarter of 1955. Initial estimated annual capacity will be 120,000 tons of cold rolled strip. Financial arrangements will come from internal sources, although a standby credit of $3 million has been arranged with a group of Philadelphia banks.*

• U. S. Steel Corp. executives officially broke ground for what has been termed one of the most modern research centers devoted to development of processes for making better steel. Plans call for three buildings with a total floor area of 132,000 sq ft. The structure will house equipment for study of steelmaking from the raw material stage to finished product. Some of the problems to be investigated are offsetting the deteriorating quality of available raw materials, how to conserve scarce strategic metals, and how to develop new and improved steels to meet military and civilian requirements.

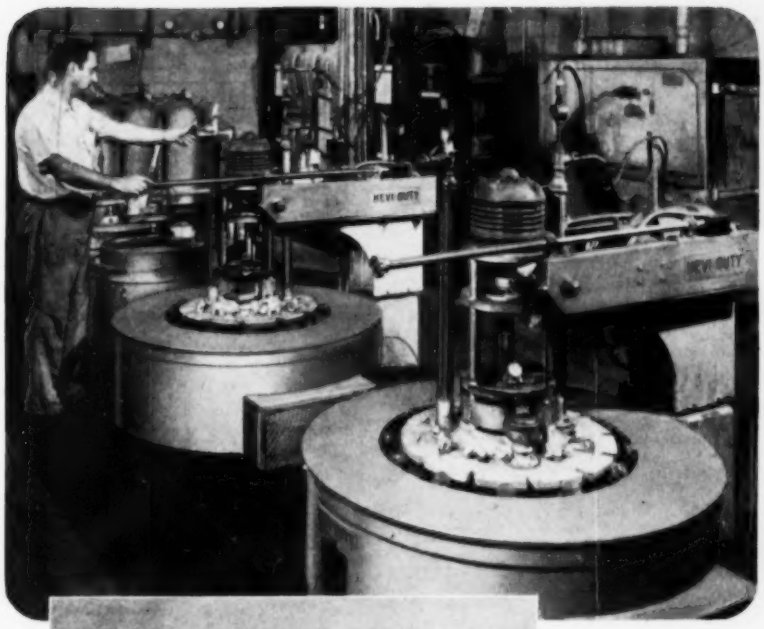

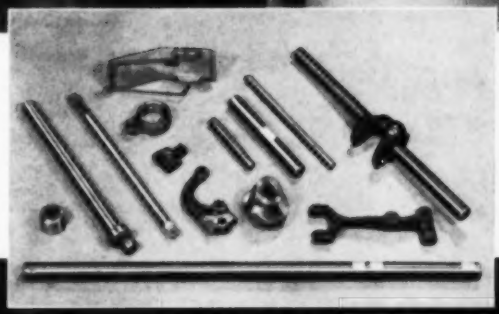

Typical parts heat treated in Hevi Duty furnaces at the Union Special Machine Co.

UNION SPECIAL
heat treats precision parts in
HEVI DUTY FURNACES

• Over 100 different heat treating operations are represented in one Union Special industrial sewing machine. All the carburizing, dry cyaniding and bright annealing of precision ground shafts, bearings, journals, castings and eccentrics is done in versatile Hevi Duty Vertical Retort Furnaces.

Walter Weinwurm, chief metallurgist at Union Special, says "Our Hevi Duty furnaces do an exceptionally good job of heat treating precision parts. The work comes out of the furnaces clean with no scale or oxidation."

Learn more about Hevi Duty vertical retort furnaces — write for your copy of bulletin HD-646 today.

HEVI DUTY®

HEVI DUTY ELECTRIC COMPANY
MILWAUKEE 1, WISCONSIN
Heat Treating Furnaces... Electric Exclusively
Dry Type Transformers *Constant Current Regulators*

Coming Events

Sept. 11, AIME, St. Louis Local Section, Lead Belt Meeting, tour St. Joseph mines and mills.

Sept. 13-16, Electrochemical Chemical Society, Inc., Ocean Terrace Hotel, Wrightsville Beach, N. C.

Sept. 14-17, Society of Automotive Engineers, tractor and production forum, Milwaukee.

Sept. 16-18, Porcelain Enamel Institute, annual shop practice forum, Columbus.

Sept. 17-18, National Foundry Assn., annual meeting, New York.

Sept. 18, AIME, National Open Hearth Steel Committee, Chicago Section, golf party, Olympia Fields Country Club, Chicago.

Sept. 21, ASME, Industrial Instruments and Regulators Div., and Instrument Society of America, exhibit and joint conference, Sherman Hotel, Chicago.

Sept. 21-23, Steel Founders' Society, fall meeting, Hot Springs, Va.

Sept. 21-24, American Mining Congress, Metal and Nonmetallic Mineral Mining Convention, Olympic Hotel, Seattle.

Sept. 28-30, National Electronic Conference, Chicago.

Sept. 28-30, ASME, Petroleum Mechanical Engineering Conference, Rice Hotel, Houston.

Sept. 28-Oct. 1, Assn. of Iron and Steel Engineers, annual convention, Wm. Penn Hotel, Pittsburgh.

Oct. 5-7, ASME, fall meeting, Hotel Sheraton, Rochester.

Oct. 6, AIME, National Open Hearth Steel Committee, Buffalo Section, Hamilton, Ont., Canada.

Oct. 7, AIME, National Open Hearth Steel Committee, Chicago Section, Phil Smidt's, Chicago.

Oct. 7-9, National Assn. of Consulting Engineers, south central region, Mayo Hotel, Tulsa, Okla.

Oct. 8-9, National Conference on Industrial Hydraulics, annual meeting, Hotel Sheraton, Chicago.

Oct. 9, AIME, St. Louis Local Section, St. Louis University, St. Louis, Mo.

Oct. 9, AIME, National Open Hearth Steel Committee, Eastern Section, fall meeting, Warwick Hotel, Philadelphia.

Oct. 15-17, AIME, National Open Hearth Steel Committee, Southwestern Section, fall meeting, Baker Hotel, Dallas, Texas.

Oct. 19-21, AIME, Institute of Metals Div., fall meeting, Hotel A' erton, Cleveland.

Oct. 19-23, American Society of Civil Engineers, annual meeting, Statler Hotel, New York.

Oct. 19-23, National Metal Congress and Exhibition, Cleveland.

Oct. 22, AIME, St. Louis Local Section, Engineers Club of St. Louis and ASCE, Engineers Club, St. Louis.

Oct. 27, Assn. of Consulting Chemists & Chemical Engineers, 25th anniversary annual meeting, Hotel Belmont Plaza, New York.

Oct. 28-Nov. 2, AIME, El Paso Fall meeting, El Paso.

Oct. 29-30, AIME Coal Div., **ASME** Fuels Div., Conrad Hilton Hotel, Chicago.

Oct. 29-31, National Council of State Board of Engineering Examiners, annual meeting, Plaza Hotel, San Antonio, Texas.

Oct. 30-31, AIME, National Open Hearth Steel Committee, Southern Ohio Section, Desh-ler-Wallick, Columbus.

Nov. 4-6, Time and Motion Study and Management Clinic, Sheraton Hotel, Chicago.

Nov. 5-6, Pittsburgh Diffraction Conference, Mellon Institute, Pittsburgh.

Nov. 5-7, Electron Microscope Society of America, annual meeting, Pocono Manor Inn, Pocono Manor, Pa.

Nov. 6, AIME, National Open Hearth Steel Committee, Pittsburgh Section, William Penn Hotel, Pittsburgh.

Nov. 13, AIME, St. Louis Section, coal meeting, York Hotel, St. Louis.

Nov. 29-Dec. 4, ASME, annual meeting, Statler Hotel, New York.

Nov. 30-Dec. 5, Exposition of Chemical Industries, Commercial Museum and Convention Hall, Philadelphia.

Dec. 1-4, National Assn. of Corrosion Engineers, conference, University of Oklahoma.

Dec. 2-4, AIME, Electric Furnace Steel Conference, Netherland-Plaza Hotel, Cincinnati.

Dec. 11, AIME, St. Louis Section, York Hotel, St. Louis.

Dec. 13-16, American Institute of Chemical Engineers, annual meeting, Hotel Jefferson, St. Louis.

Dec. 28-29, Annual Chemical Engineering Symposium, University of Michigan, Ann Arbor.

Feb. 15-18, 1954, AIME, annual meeting. Metals Branch, Hotel McAlpin; Mining and Petroleum Branches, Hotel Statler, New York.

TOPS FOR PRODUCTION OF HIGH GRADE STAINLESS, ALLOY AND RIMMING STEELS

Heroult

ELECTRIC MELTING FURNACES

EMBODYING the latest in mechanical and electrical equipment, these widely used furnaces are noted for their efficient performance and safety, and low operating cost and maintenance.

We welcome an opportunity to help you select and install the furnace best suited to your particular requirements.

AMERICAN BRIDGE DIVISION, UNITED STATES STEEL CORPORATION
GENERAL OFFICES: 525 WILLIAM PENN PLACE, PITTSBURGH, PA.

Contracting Offices in New York, Philadelphia, Chicago, San Francisco and other principal cities.
United States Steel Export Company, New York

Removable roof of new design now available for large furnaces.

USS

UNITED STATES STEEL

STEP AHEAD TO SELECTIVE SCANNING SPEEDS

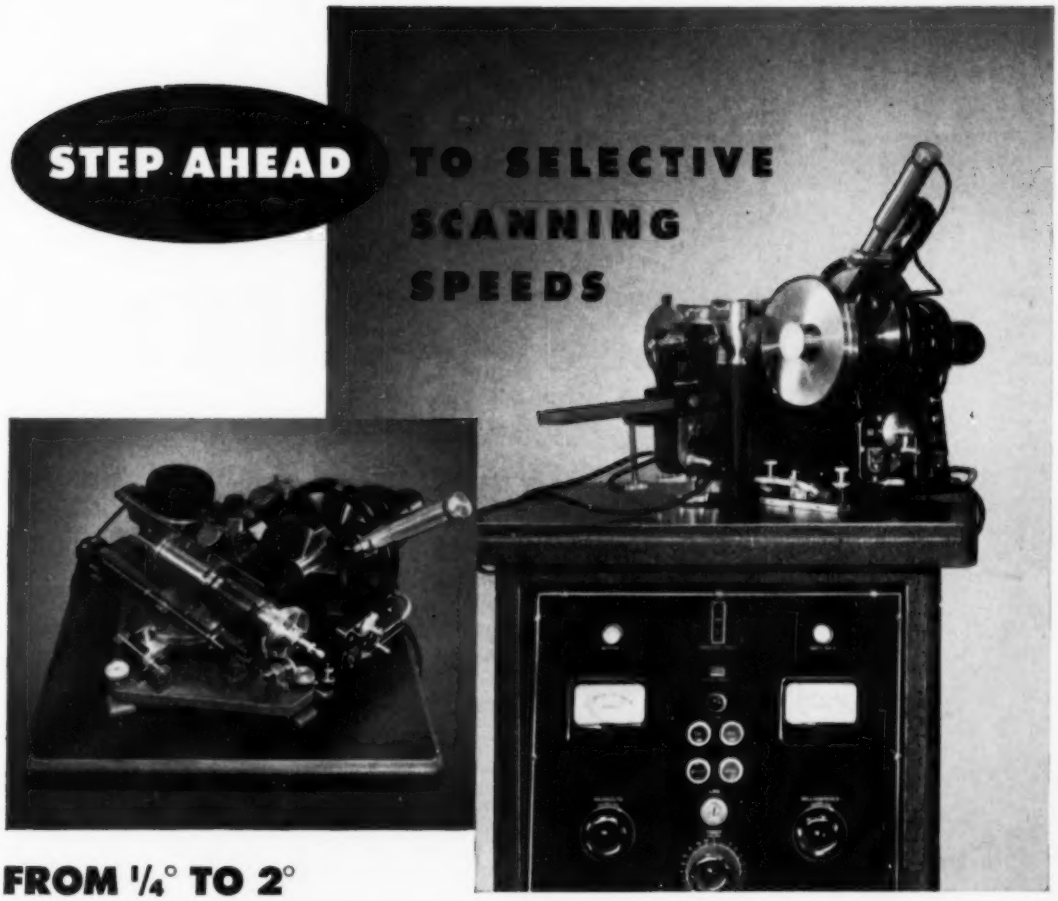

FROM ¼° TO 2°

PER MINUTE WITH UNEXCELLED RESOLUTION

★ Many users have found the facility of a wide selection of scanning speeds to be of extreme value in diffractometry. The operation of a synchronous motor drive, with change gears for speed variation, offers precise control which can be duplicated.

Scanning speeds up to 2° per minute can be obtained with exceptional resolution exceeding that attained from other apparatus under comparable operating conditions.

Work load of the NORELCO Diffractometer can actually be *doubled* by utilizing a second Wide-Range Goniometer in conjunction with the second line focus port of the NORELCO *four-window* X-ray tube.

A Norelco PRODUCT NORTH AMERICAN PHILIPS COMPANY, INC.

Serving Science and Industry

Dept. IG-9 • 750 South Fulton Avenue, Mount Vernon, N. Y.

In Canada: Rogers Majestic Electronics Ltd., 11-19 Brentcliffe Road, Leaside, Toronto 17, Ontario

Two great basic refractories...

for smelting, refining and melting furnaces

CHROMEX B

CHROMEX B is an extremely hard-burned, dense, chrome-magnesite refractory, notable for its stability of volume and high strength at high temperatures, and resistance to thermal spalling and to slagging and erosion.

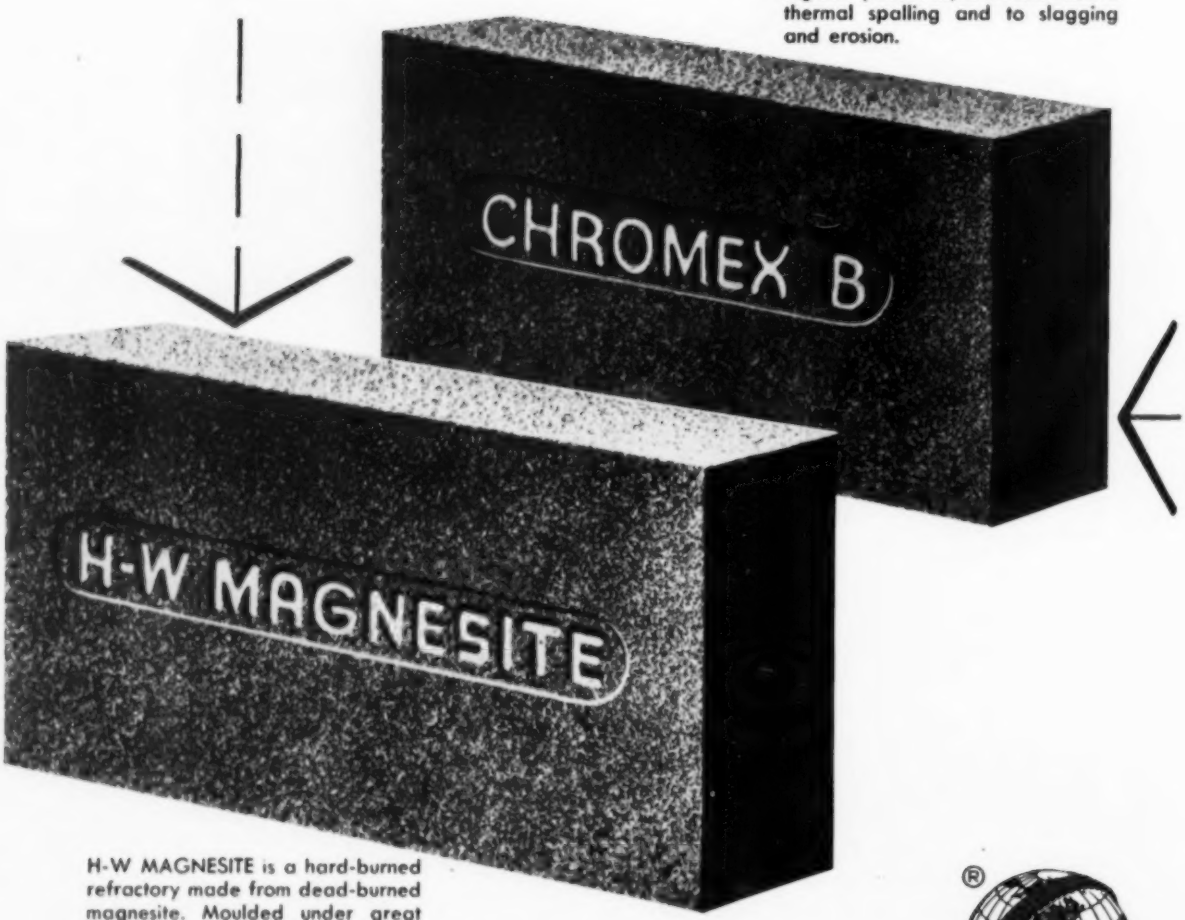

H-W MAGNESITE is a hard-burned refractory made from dead-burned magnesite. Moulded under great pressure and fired at high temperature. Recommended for use where a strongly basic lining is required.

®

Harbison-Walker

and H•W MAGNESITE

The excellent performance of basic refractories in applications where conditions are particularly severe has brought about increased interest in these products. Harbison-Walker has been a leader in the development and manufacture of basic refractories, and has long specialized in this class of products. The complexities of manufacture require a skilled, highly-trained organization, and Harbison-Walker is fortunate in having the personnel required to produce basic refractories of consistently high quality.

Two of the most widely used brands in the Harbison-Walker line of basic refractories are H-W Magnesite and Chromex B. Both find many applications in smelting, refining and melting furnaces. We will be glad to assist you in applying these refractories to best advantage.

HARBISON-WALKER BASIC REFRACTORIES

are used advantageously for

Aluminum Melting Furnaces • Copper Converters and Holding Furnaces • Copper Reverberatory Furnaces • Anode and Wire Bar Furnaces • Secondary Metal Melting Furnaces • Lead Softening and Reverberatory Furnaces • Open Hearth and Electric Furnaces • Nickel Furnaces

HARBISON-WALKER REFRACTORIES COMPANY

AND SUBSIDIARIES — GENERAL OFFICES: PITTSBURGH 22, PENNSYLVANIA

World's Largest Producer of Refractories

THE coal industry has come up with an idea that may bring coal and electric utilities substantial new business and at the same time, save the steel industry millions of dollars annually. After two years of research, Bituminous Coal Research, Inc., in conjunction with 14 electric utility firms says that the electric furnace should replace the open hearth for steel production. Bituminous Coal Research says that the results of investigations show that savings of up to $3.15 per ton in making low carbon steel from cold metal are possible. Key to the proposal is that conversion would raise national electricity production some 12 pct while increasing coal production about 25 million tons per year.

Electric and coal production increases assume total replacement of the 950 open hearth furnaces by 760 electric furnaces. However, Bituminous Coal Research points out that even 10 pct replacement in the near future would be of tremendous importance to the industries concerned. About 83 million tons or 89 pct of the steel made in the U. S. comes from open hearths. Most of this is low carbon.

Three plant sizes were included in the study—250,000 tons, 500,000 tons and 1,000,000 tons annual steel production. No plant more than eight years old was included in the investigation. Three steel industry representatives advised on the collection of data and preparation of the final report. Battelle Memorial Institute conducted the research for the electric companies and Bituminous Coal Research.

The report shows that capital cost for electric furnace installation is only 60 pct of that for open hearths; the cold melt steelmaking process using scrap and pig iron shows lower cost for the electric furnace, and electric furnaces show a greater annual return on invested capital. For the 50 pct hot metal/50 pct scrap process, annual return for the electric furnace is equal to or greater than the open hearth, according to the report.

Electric furnaces today are used mainly for the production of special alloy steels. The World War II expansion left a surplus of electric furnaces after the end of hostilities, leading some manufacturers to experiment with the production of low carbon steels. Improvements, such as the swing roof, high rates of energy input, and increase in furnace size took place at about the same time. The resulting important economies brought electric furnace steelmaking costs down to the level of the open hearth.

The report states that the electric furnace, in addition to capital investment savings and reduced cold melt practice production costs, offers flexibility. It can be placed in production or withdrawn almost at will. Electric furnaces can operate all but 15 days per year, while open hearths are usually down about 30 days. Rebuilding time for the electric furnace is shorter. The same amount of materials yields about 2 pct more in the electric furnace. Sulphur control is greater in the electric furnace. More accurate temperature control saves steel production time. Nitrogen control by the electric furnace is expected to match that of the open hearth. The report can be obtained at $10.00 per copy from Bituminous Coal Research, Inc., 2609 First National Bank Bldg., Pittsburgh, 22.

The converter aisle at the Copper Cliff, Ont., smelter of International Nickel Co. is the biggest of its kind in the world. A ladle containing 13 tons of molten nickel-copper-iron sulphide from a reverberatory furnace is emptied into one of the 19 huge converters. Converters are 35 ft long and 13 ft in diam, housed in a building 1435 ft long and more than 100 ft high.

◆◆◆◆◆◆

IT has been the practice in recent months to publicize the "tightness" of the long term money market. However, in 1952 some 31 companies were able to obtain such financing compared with 21 the previous year, according to the *Yearbook of Private Placement Financing*. Reserve Mining Co. received the largest loan with an issue of $148 million worth of 4.25 pct first mortgage bonds, due in 1980 and placed with nine institutional investors. Funds were for construction of beneficiation of taconite facilities on the Mesabi Range.

Another issue, second in size for the year, was placed for Reynolds Metals Co. with a large list of lenders. The loan amounted to $76.75 million first mortgage bonds, due in 1968, carrying interest rates up to 5 pct after the first year or two.

Youngstown Sheet & Tube Co. was the largest borrower among integrated steel companies, with a loan of $50 million first mortgage bonds, series C, bearing an interest rate of 3.75 pct due 1982. Kaiser Steel Corp. sold $27.5 million 4.75 pct first mortgage bonds, due in 1970, to a group of institutions, and Armco Steel Corp. placed $25 million 3 pct debentures, series C with a single institution.

Five nonintegrated steel producers received a total $30.3 million through private sources. Those obtaining the financial aid were Granite City Steel

Co.; Allegheny-Ludlum Steel Corp.; Continental Steel Corp.; Copperweld Steel Corp.; and Lukens Steel Co.

Kaiser Aluminum & Chemical Corp. drew down the second largest loan in the aluminum field, $29 million 4.50 pct 24 year first mortgage bonds. Total private financing in 1952 reached $5,032,803,000, compared with $5,085,238,000 in the previous year. Industrial corporations accounted for 65 pct of the total, against 70 pct in 1951. Information for the Yearbook is obtained principally from a study of the investment portfolios of more than 200 life insurance and other long term investment companies.

◆◆◆◆◆◆

SOLAR Aircraft Co.'s San Diego plant has placed in operation the nation's first conveyorized, mass production unit for applying high temperature ceramic coatings to alloy steel components. Coating time for critical jet engine parts is said to be cut in half. Solar is currently using the facility for Solaramic coating inner combustion chambers and transition lines for General Electric J47 turboject engines. However, the equipment can be adapted to coat other military or civilian items.

Solar's conveyorized coating dept. can handle 5000 combustion chambers and 5000 transition liners per month on single shift operation. Working force numbers 12 persons. First step in the operation is automatic sandblasting of parts to produce a roughened surface to assure good bond strength. After sandblasting, parts are sprayed with Solaramic coating. Spray operations are divided into three steps: Inside spraying, outside spraying, and touch-up and stenciling. Parts are hung on the conveyor line after inside spraying, and remain on the conveyor throughout the processing.

Gas-fired direct flow dryers operating at 150°F dry the coating. Firing takes place in the furnace at 1700°F. Entire cycle time from parts receipt to packing for shipping is 1 hr.

◆◆◆◆◆◆

"ALTHOUGH majority control of a company by its employee-retirement trust is an almost unique form of ownership, we feel it is particularly appropriate to our situation." Thus Earl P. Stevenson, president of Arthur D. Little, Inc., summarized his feelings toward the aquisition of controlling interest in the firm by employee's trust. The change in ownership was brought about by an offer from the employee's retirement trust to purchase the shares of common stock of individual holders. Among these were shares held in trust for the benefit of the Massachusetts Institute of Technology. However, there will be no change in management or method of operation.

"Arthur D. Little Inc., is a personal service organization, composed largely of professional personnel. Since our success as an organization depends in part upon the creativity of our staff, it is fitting that the staff should have a stake in the company's corporate success," Mr. Stevenson said.

The company established an employee's profit sharing trust some time ago, to which all employees belong. Arthur D. Little contributes a fixed proportion of its earnings to this trust, which invests for the benefit of employees who make the firm a career.

◆◆◆◆◆◆

PITTSBURGH Steel Co. made official entrance into a new market with the inauguration of a $28 million mill for production of steel sheets. The semi-continuous hot rolled sheet mill is the largest installation of its kind to be built in the Pittsburgh district in more than a decade. The mill, at Allenport, sent a 5 in. x 5 ft x 20 ft hot slab through four rollers in official opening ceremonies. At present, the mill can produce steel sheets at the rate of 1770 fpm. For now, monthly production will be limited to 50,000 net tons. Cold rolled steel sheets facilities are under construction adjacent to the hot mill, and are expected to go into operation later this year.

In addition to the hot rolling mill, the new installation includes a 500-ft continuous pickling line, a temper mill, and a shear line. Buildings cover an area of 350,000 sq ft.

Rodney Metals, Inc. 25-in. Sendzimer mill at the New Bedford, Mass., plant cold reduces carbon steel to as thin as 0.001 in., and stainless steel to 0.002 in., while maintaining accuracy within 3 pct across widths up to 25 in. The mill can also cold roll aluminum alloys to 0.006 in.

DUCTILE IRON GEARS provide *Superior Strength with Excellent Resistance to Wear*

Large Gears... such as these Ductile Iron girth gears drive large tube mills in the cement and mining industries. Put into service without heat treatment, they normally provide 92,000 to 100,000 psi ultimate tensile strength, 3 to 5% elongation, and 270-290 BHN on the tooth surface.

In addition to excellent castability, ready machinability and moderate cost, Ductile Iron offers properties that are vital in a gear material.

For along with high strength and measurable ductility, Ductile Iron "as cast" combines good resistance to wear and galling, with superior values for notched endurance limits.

Ductile Iron can be heat treated to provide tensile strengths of over 150,000 psi. It develops surface hardnesses of over 600 BHN after flame or induction hardening. Service data show also that annealed Ductile Iron develops impressive properties which result in peak performance.

Ductile Iron can provide a chilled, carbidic, abrasion-resistant surface supported by a tough ductile core. No other single material combines these properties. Still another advantage is its ability to damp out vibrations that otherwise might build up stresses to dangerous levels.

Send us details of your prospective uses, so that we may suggest a source of supply from some 100 authorized foundries now producing Ductile Iron under patent licenses. Request a list of available publications on Ductile Iron ... mail the coupon now.

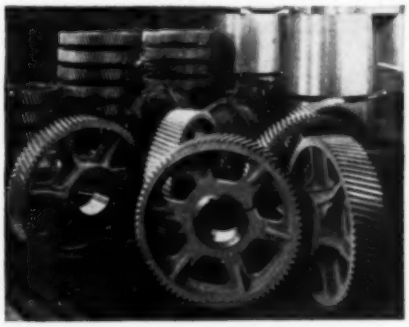

Medium Gears produced in heat treated Ductile Iron have replaced steel gear castings and forgings in papermaking and allied equipment. Annealed Ductile Iron can be machined at a rate of 2 to 3 times that of good quality gray iron of comparable hardness.

The International Nickel Company, Inc.
Dept. 20, 67 Wall Street, New York 5, N. Y.

Please send me a list of publications on: **DUCTILE IRON**

Name_____ **Title**_____

Company_____

Address_____

City_____ **State**_____

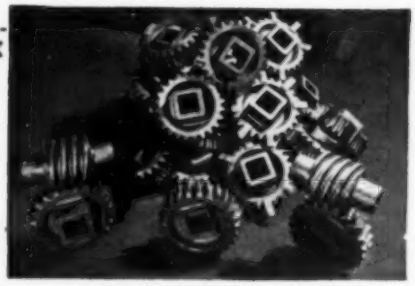

Small Gears... also worms ... exemplify an application of Ductile Iron in the railroad field.

THE INTERNATIONAL NICKEL COMPANY, INC.

67 WALL STREET
NEW YORK 5, N. Y.

Pact initiated between Cramet Inc., wholly-owned subsidiary of Crane Co., Chicago, and Defense Procurement Administration is expected to increase titanium sponge production 6000 tons annually. Under the contract Cramet will construct a $25 million plant at an undecided location. Production is scheduled for 1955, with full production a year later. Facilities for titanium alloy and titanium ingot production will be included. The contract calls for production of 30,000 tons of sponge over a five-year period. The Government has agreed to buy up to 6000 tons during that time. Similar contracts have been signed with Titanium Metals Corp. of America and E. I. du Pont de Nemours & Co., Inc., for production of 18,000 tons and 13,500 tons over the same period.

Electric furnaces produced 4.2 million net tons of ingots and steel for castings during the first six months of 1953, for a record tonnage rate. It represents an increase of 34.5 pct compared with a year ago. Total steel production increased 29 pct. About 52 pct of electric furnace output in the first five months was carbon steel. Total output represented about 7.3 pct of all steel made. For additional information on electric furnace steel see this month's Trends.

A record high cobalt supply is expected to offer a surplus for stockpiling. Defense Materials Procurement Agency expects more than 18 million lb in 1953 and an all-time high of more than 22 million in 1954. Calera Mining Co.'s refinery at Garfield, Utah is expected to turn out 1 million lb this year, and 3.3 million lb annually when normal operations are reached.

First plant of the denationalized British steel industry sold back to private interests went to original owners of the Templeborough Rolling Mills, British Ropes, Ltd., and William Cooke & Co. The British Iron & Steel Holding & Realization Agency said it received the equivalent of $20.30 per share of stock. British Ropes and William Cooke took 72,000 shares each.

National Lead Co. is taking over distribution of all production at the Government-owned Nicaro nickel plant in Cuba. National Lead has set up a Nickel Sales div., for technical assistance to nickel users. The company will work with the National Production Authority in allocating nickel production.

Bell Telephone Laboratories reports a new silicon alloy junction diode. Present plans call for use of the diode in the memory organ of a computer. Bell officials believe it may take the place of mechanical switches used to remember telephone numbers while a call is completed. Like transistors the diodes need a warm-up period. Unlike present germanium transistors they can operate under high temperatures. Production problems are being worked out.

H. K. Ferguson Co. terms the plant it is building at Henderson, Nev., for Titanium Metals Corp. of America, the world's first large scale titanium facility. When work is completed on the former World War II magnesium producer, production capacity will reach 3600 tons annually.

Drift of Things

AIME headquarters recently received a letter from a Student Associate in Texas who had received his B.S. degree in engineering in May. He was immediately drafted. He completed eight weeks of infantry basic training, and was then in AAA (artillery anti-aircraft). He stated that he had an MOS (military occupational specialty) of an infantryman and expected to be given an MOS of a cannoneer. He wrote, "What steps can I take, now while I am in basic, to get an MOS of an engineer? Also, I understand there is an S&PP [Scientific and Professional Personnel] program which no one here [Fort Bliss] seems to know anything about. Can you all give me any information? A radar course is offered here which lasts from 34 to 36 weeks. I am qualified but won't know if I am accepted until after my present eight weeks of training. If I don't find out now about any programs open to engineers, or how to become connected with engineering work, and am turned down in radar school, it would probably be too late to do anything after I get my orders for shipment, possibly to FECOM. I am hoping that you might give me some information as to what I might do during the remaining seven weeks of basic so that I might be a little more sure that my engineering education might be put to work, and so that I wouldn't forget everything before I am discharged and get an engineering job."

This letter was turned over to the Engineering Manpower Commission, of Engineers Joint Council, and he was advised, in part, as follows:

"As an engineering graduate with a B.S. degree in petroleum and natural gas engineering you are qualified for assignment to MOS #1393, Chemical Engineering assignment, in accordance with Dept. of Army Special Regulation #615-25-11 of Aug. 7, 1952. As an immediate step you should submit a formal application via the normal chain of command for consideration for the S&PP program, MOS #1393, in accordance with the above specified special regulation. What apparently happened during your interview for initial classification was that you were not recommended as an engineering graduate because you had not received your degree. There is no provision in the special regulations to cover this unusual contingency.

"The Engineering Manpower Commission is particularly interested in the efficiency with which the S&PP program, in all of its aspects, is working. We would appreciate, therefore, continuing information from you concerning the progress you make in your request for the proper MOS. In the event that your qualifications are not recognized, we desire to be informed so that we can bring your case to the attention of the proper authorities. Please do not hesitate, therefore, to continue this correspondence."

Following this letter, the young man followed the advice given and later was classified as Petroleum Laboratory Technician, MOS #1388. He indicated further difficulties, however, in his own case and in the experience of one of his companions, and EMC is giving him further advice and help. E.H.R.

EUGENE McAULIFFE, President of the Institute in 1942, has recently published a brochure entitled *When Can Their Glory Fade* devoted to General Custer and the Battle of the Little Big Horn, June 25, 1876. The author is a staunch admirer of the general, who was well known to his father. In the summer of 1876, Eugene was a boy of ten learning to operate a telegraph instrument in the railroad office at Fargo, Dakota Territory. His present contribution to the Custer anthology narrates some of the incidents of McAuliffe's early life in the area in which Custer made his last stand, and gives details of the events leading up to the massacre, which utterly annihilated 262 men. A page of the *Bismarck Tribune* giving the first detailed news of the fight is reproduced. Mr. McAuliffe says he never loved the Indian, as a race or as an individual. He urges that an equestrian statue of Custer be erected on the battlefield to honor "the greatest field soldier American arms ever produced." E.H.R.

THIS September issue marks the passing of summer, and the ¾ mark of the year. Many developments have taken place this past summer, with the truce in Korea (permanent, we hope) standing out as most notable occurrence since the beginning of hostilities in 1950. We happened to be on vacation at the time United Nations (American) troops landed in Korea, and the week we returned marked the beginning of our association with AIME. It was, incidently, also our last vacation!

Although foregoing our vacation this summer was partly voluntary, it may be that we caused the many members of Colorado Fuel & Iron Corp., who played the major role in preparing the October issue of JOURNAL OF METALS, to change some of their plans. The coming CF&I issue will represent the efforts of some 50 people, not including those who may have assisted behind the scenes. For JOURNAL OF METALS it will be the largest single undertaking to date.

In looking back over the summer, we would be amiss not to mention the Coronation of Queen Elizabeth II, and the conquering of Mt. Everest. One minor result of the Coronation was the appearance of a photograph of the Queen on the cover of the June issue of the *Canadian Mining & Metallurgical Bulletin*. To our knowledge this marked the first appearance of a "cover girl" on a technical magazine, and it was a welcome sight indeed. However, we have since been informed by Ed Robie that the August 1936 and July 1946 issues of MINING & METALLURGY featured "cover girls." Just shows that you can't beat AIME!

IN this issue, there is an article on the part AIME is playing, through Engineers Joint Council Labor Panel, concerning labor legislation. Too little has been written about the many important functions in which the Institute plays an important role. Much time and energy is expended by AIME members who serve on these *outside* committees. Although they do not seek any recognition, the work they do is definitely of interest to Institute members. The unsung members serving on internal and external committees are assisting the Institute in living up to its objectives as stated in its Certificate of Incorporation: The promotion of the arts and sciences connected with the economic production of useful minerals and metals, the welfare of those employed in these industries, the holding of social and technical meetings, the publication of information, the maintenance of a meeting place, and the upkeep of a library.

Alvin S. Cohan

Fig. 1—Tilting-type poling furnace has a capacity of 240 tons, and is oil fired. After blowing and skimming the molten copper, green poles are inserted to reduce oxygen content to below 0.12 pct.

Anode Casting Operations at Garfield Smelter Geared To High Production

by N. R. Alston and M. J. Winkel

AT the start of the immense open pit mining operation at Bingham, Utah, the American Smelting & Refining Co. contracted to treat at its Garfield smelter, copper concentrates produced from that ore. Prior to June 1950, all copper produced at Garfield was cast into blister bars for shipment to one of the three ASARCO refineries. It was necessary to remelt and recast the crude blister copper into anode shapes before electrolytic refining.

Plans were formulated early in 1948 for the erection of a plant at the Garfield smelter to cast anode shapes. This planning followed Kennecott Copper Corp.'s decision to construct an electrolytic refinery in Utah. Anode casting operations commenced in June 1950. Today, Garfield's anode dept. casts a greater tonnage than any other single plant in the world.

Present production of anode copper is approximately 23,000 tons per month. Fourteen thousand tons of anodes per month are currently allotted to the Kennecott Utah refinery and the balance of the anode production is shipped to AS&R refineries at Baltimore and Perth Amboy. To provide sufficient capacity for this high rate of production, the plant was designed to include a holding furnace, four poling furnaces, and two casting wheels, together with necessary service facilities. Two anode dept.

N. R. ALSTON and M. J. WINKEL are metallurgists with the American Smelting & Refining Co., Garfield, Utah.

craneways parallel the converter aisle. One of these services the poling furnaces, and the second the casting and loading depts.

Holding Furnace

The holding furnace, located in the converter aisle, is an intermediate reservoir for blister copper produced in the operation of six or seven of the smelter's eight Pierce-Smith converters. It has a capacity of 250 tons of liquid copper and is heated by natural gas. Originally the furnace was lined with burned magnesite brick, but during a recent repair, the end walls were replaced with chemically bonded magnesite. Present indications are that chemically bonded magnesite brick will have a longer life than burned magnesite in this furnace.

A self-propelled car conveys ladles of liquid copper from the holding furnace to the anode dept.'s 50-ton craneway. A similar car is used to transfer poling furnace slag and scrap copper from the anode dept. to the converter dept. Two 50-ton cranes service the poling furnaces and transfer cars.

The tilting-type poling furnaces are 13 ft in diam x 27 ft long, have a capacity of 240 tons each, and are lined with burned magnesite brick. Poling is done through a door in the center of the furnace, charging and firing through opposite ends. Although other smelter furnaces use natural gas as the primary fuel, poling furnaces are fired with oil. AS&R was unable to obtain the necessary permit for gas firing these furnaces because of shortages in gas supply for industrial use in the Salt Lake area. However, temperature control and operating conditions have been excellent with oil firing and it is doubtful that any appreciable performance improvement could be obtained by using natural gas, although gas would be less expensive and brickwork might have longer life.

The practice is to blow high pressure air into the copper bath in the poling furnace to accomplish oxidation of sulphur and lesser impurities. Blowing is continued at a metal temperature between 2000° and 2020°F, until sample ingots with a satisfactory *low set* indicate an oxygen content of approximately 0.7 pct. The small amount of slag produced is skimmed through the central poling door of the furnace into a ladle and returned to the converters.

Poling commences after completion of blowing and skimming. The oxygen content is reduced to less than 0.12 pct by submerging green poles in the molten copper. The butt end of a pole is placed in the furnace door by means of a cable rigged to a frame over the door and powered by a pneumatic hoist. The pole is so manipulated that the small end is elevated and the butt is forced into the bath. Garfield generally uses lodgepole pine or English spruce, 25 to 30 ft long and varying in diameter between 10 and 25 in. at the butt. About 15 poles are required for an average charge. Convenient pole storage is afforded by racks located on a floor at the level of the poling door.

At the end of the poling operation a temperature of 2070°F is desired. Metal temperatures are checked by use of a Brown Electronic Potentiometer, and ingot samples are taken periodically to check the progress of the poling. When the sample shows a slight crown and a fine grain set, the copper has been poled to the proper *pitch* and is ready for casting.

Anode Casting Wheels

Two Walker-type wheels are installed at the casting floor. They have 26 molds each and are 40 ft in diam. Reversible drives turn the wheels in either a clockwise or counter-clockwise direction. Inasmuch as two poling furnaces are tangent to each wheel, reversibility is necessary to afford maximum time for the copper to set and cool. Hydraulic drives which automatically stop the wheels at the correct positions for pouring were installed because of their smooth starting and stopping characteristics. Poling furnace controls are electrical whereas the spoon ladle is controlled by a hydraulic system. Wheel operating controls are located in enclosed pulpits adjacent to each furnace. These pulpits are positioned and elevated to permit good visibility by the operator of the metal flow into the mold.

Anodes

Suitable markings in the molds facilitate accurate pouring of 700 lb anodes. The anodes are approximately 1 9/16 in. thick, with lugs cast at the top end to support them in the electrolytic tanks. Careful control must be exercised throughout the operation to produce high quality anodes, uniform in thickness and free from surface defects. The maximum allowable variation in weight for individual anodes is ±5 pct.

As the wheel rotates, the anodes pass from the pouring position through a series of cooling water sprays. At a point approximately 180° from the pouring position, push-pins elevate one end of the anode in the mold. Take-off tongs lift the anode by its lugs and transfer it to one of three water-filled bosh tanks for further cooling. The tong assembly lifts the anode vertically from the mold, transfers it horizontally to the bosh tank, and lowers it into the tank. The assembly also has radial travel so that the tongs may be positioned over the proper bosh tank.

After the mold has passed the bosh tanks, a 10°, Baume mixture of alunite and water is sprayed on the mold by a Murphy gun and push-pins are sealed with a thick alunite mixture. Insert blocks which form the anode's Baltimore-type contact and tail lugs, are placed before casting and are removed after the copper has set under the water sprays. Finally, a gas flame is applied to heat and dry insert blocks just prior to completion of the wheel cycle. If moisture is present at the insert block when the anode is being poured, the block may become unseated, resulting in faulty lug formation.

Three pins support each mold on the wheel. One pin is at the back or bottom end and two are at the front or top corners. Each mold is checked for level before and periodically throughout the pour with a spirit level. This practice was adopted to insure that each anode would have a uniform thickness. Levelling is accomplished by inserting shims under collars on the two front corner pins.

Inspection

One of the two 25-ton cranes removes the anodes from the bosh tanks and transports them to an inspection area where they are checked for size and for imperfections such as blistered surfaces and defective lugs. Rough edges are trimmed by pneumatic chipping guns. Lift trucks are used for sorting and transporting anodes in this area. Shippable anodes are delivered to loading racks or box cars, and rejects are returned to the converter dept. for remelting. One anode out of ten is for sampling.

Cars for anode shipments are placed on two standard gage railroad tracks in the anode building. On one track, special rack cars are spotted for load-

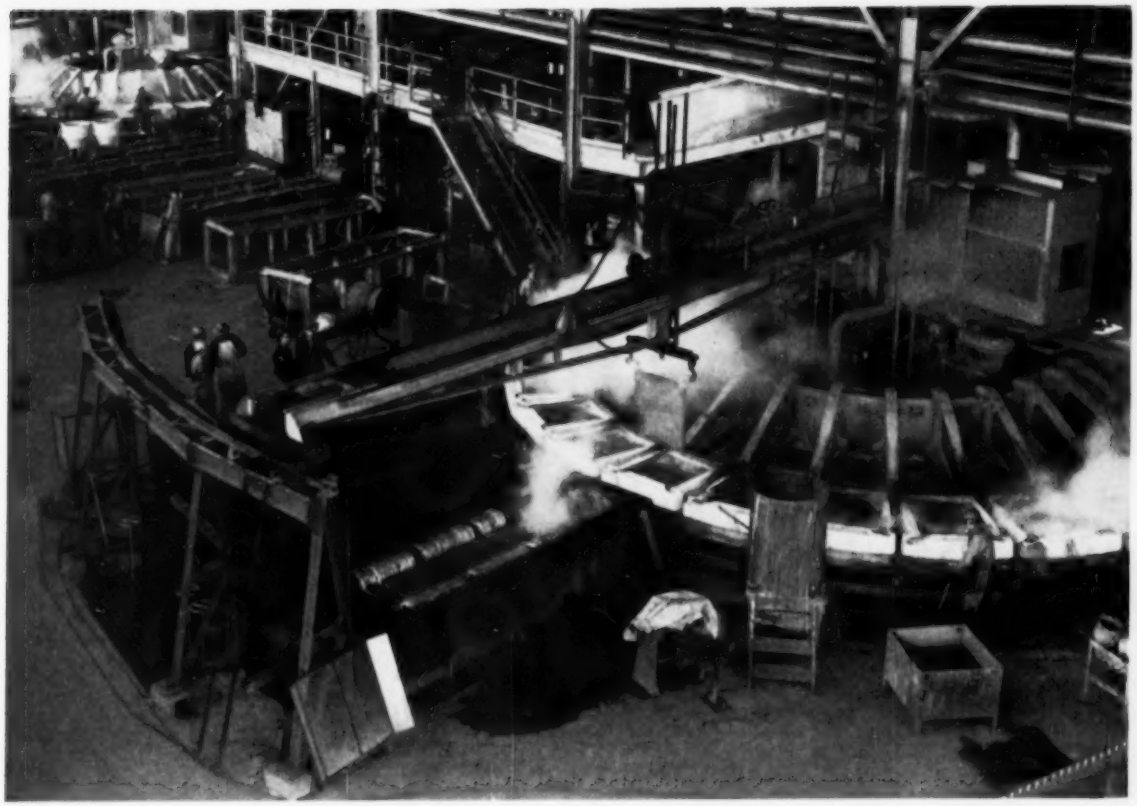

Fig. 2—Walker-type casting wheels have 26 molds each. Each anode poured weighs 700 lb ±5 pct. One wheel operating 24 hr per day can handle current production, and the second wheel is used when converter production rate is high.

ing the Utah refinery allotment. The 25-ton cranes transfer spaced anodes from loading cars to the rack cars. The anodes are spaced in notched racks on these cars to facilitate unloading and placing them directly in electrolytic tanks at the refinery. Anodes in excess of those allotted to the Utah refinery are loaded by lift trucks into box cars on the second track.

Lift trucks deliver sample anodes to the sampling area where they are placed on a large turntable. Each anode is marked for two sample holes, the locations of which are predetermined by a template. After marking, the anodes are rotated on the turntable under an electric drill for sampling. Drillings are collected and subsequently prepared for the laboratory by grinding in a Braun pulverizer. After the sampling has been completed, anodes are returned to their proper lots and shipped.

Molds

Molds used at Garfield are cast from poled copper in the anode dept. Sufficient copper for four molds is transferred from a poling furnace to a small tilting furnace. The liquid copper is poured from the tilting furnace into a mold form via a launder. When the required amount of copper has been poured into the form, the surface is skimmed clean by hand rabbling with a metal paddle, and then a water-cooled core is pressed into the surface by means of a mechanical screw arrangement. The core is removed after the copper has set and the mold is removed from the form. Mold life averages about 225 tons.

Because most of Utah's timber is located high in mountains where there is considerable winter snowfall, poles can be cut and delivered to the smelter only during the summer and early fall. Sufficient poles must be received and stored between the first of July and the middle of October to satisfy requirements for the balance of the year. It has been necessary to utilize a large area of the smelter yard for this pole storage and to supply locomotive crane service for stocking and reclaiming poles.

Design

The overall design has been satisfactory although, as with any new plant, there have been some minor problems and changes. There is sufficient installed capacity to give considerable flexibility in operation. Current production is cast on one wheel operating 24 hr per day. However, it has been necessary to schedule additional crews to operate both wheels simultaneously for short periods when converter production rate was unusually high.

Every effort has been made to reduce the requirements for physical labor and to provide good working conditions. Electric and pneumatic hoists, hydraulic tongs, overhead cranes, lift trucks, and other similar equipment are used whenever possible. Plant lighting and ventilation are good. A large lunchroom with adjoining wash facilities and a foreman's office have been built at one end of the anode building.

Automatic Controls Speed Refractories Output

PUSH button production is not just a conversation piece at the Windham, Ohio, plant of Harbison-Walker Refractories Co. The new refractories plant is the result of coordinated thinking of executive, operating, sales, engineering, research, mining, and traffic. Thus rock from the Sharon geological formation taken from a company-owned quarry six miles north of Windham, goes through an almost completely mechanized production cycle to emerge as one of two types of refractories produced simultaneously at the plant.

The company points to ten outstanding features which it feels make the Windham plant different: Methods of handling and storing raw materials; grain size control; precision of batch control; high pressure at which brick is formed; impact pressing; direct setting of brick from presses to tunnel kiln cars; uniformly high burning temperature; mechanized handling of brick by palletization and lift trucks; dust control; and laboratory testing program for continuous quality control.

Two types of silica refractories are manufactured at the new plant, Star brand of the conventional type and Vega brand of the super duty type. Raw material used in the plant is a silica conglomerate rock of the Sharon geological formation. All rock is crushed, with material to be used for Vega super duty silica brick washed and dried, while rock for Star brick is dried but not washed.

Crushed rock delivered to the plant is unloaded onto an apron feeder flowing to a bucket elevator for distribution to raw material bins. Rock from the bins is fed by electrically vibrated feeders to totally enclosed dry-pan grinding mills. Sizing screens divide the product of the pan into several fractions of different particle size. Sized material is distributed by chutes or conveyors to the various compartments of the ground material bins. A certain amount of material from the dry pans is fed to ball mills for fine grinding. Ball mills are controlled by electric *ears*, with bucket elevators delivering material to proper bins.

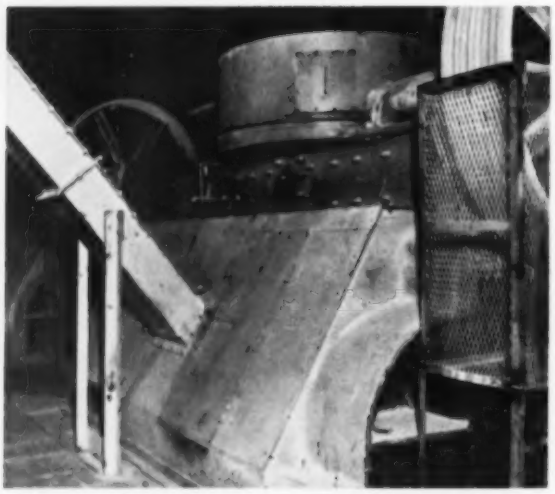

Rock from storage bins are automatically fed to totally enclosed dry-pan grinding mills. Sizing screens in the pan divide product into several fractions of different particle size.

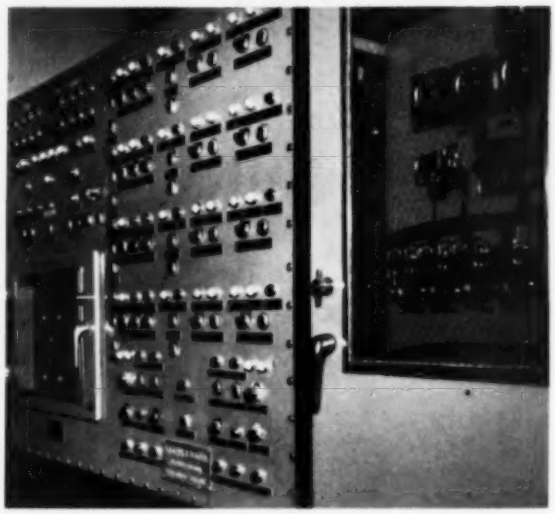

This control panel offers automatic batching and mixing of refractories material. System shuts down in event of interruption to any section and horn gives warning.

After grinding and classification the fractions must be re-assembled in proper proportions for forming into various sizes and shapes of brick. Preparation of the raw stock for forming into brick is done on an intermittent or batch basis, giving what Harbison-Walker feels is the greatest possible degree of control over composition and grain sizing. Materials are automatically discharged from the selected ground material bins in desired proportions by weight, batched, and delivered to the mixers. Simple adjustment of the control panel permits delivery from the bins to any of several mixers. If operation of any portion of the system is interrupted, the entire system automatically shuts down and a horn blast notifies the operator. Exact location of trouble is indicated on the control board.

Mixers

Mixers giving the batch its final processing in preparation for molding consist of totally enclosed stationary pans having rotating mullers and scrapers. Feed to the mixers is composed of ground and proportioned silica raw materials, water, and binders. Mixers are connected to the batching system so as to receive all materials in predetermined order. At the end of allotted mixing time, contents of the mixer are discharged into tram buckets. Filled buckets are delivered to the presses or special-shape molding stations.

Belt feeders automatically feed the power and impact presses. Mechanical pickers or standard pushers deliver pressed brick from the press. Press operators set standard sizes directly on the tunnel kiln cars. Larger and more involved brick shapes are set on pallets, which are placed on monorail supported rack cars. Various special shapes, many of extremely complicated design, are hand-molded.

Tunnel kiln cars containing undried brick are transferred by means of transfer cars and gasoline driven pushers to tunnel kiln car driers, and moved through the dryers in accordance with predetermined schedules. A kiln car dryer is in line with

each of the tunnel kilns. This makes possible rapid movement of a car from the dryer into the entrance end of the kiln with a minimum of temperature loss. Dryers are supplied with clean hot air from kiln cooling zones. Fans and ducts are arranged to insure movement of warm air throughout the complete cross-section of the kiln car load. Indicating and recording instruments are used to observe dryer temperature and humidity conditions.

Rack cars containing shapes to be dried are delivered to the rack car dryers, through which the cars are slowly and automatically pushed. After the dryers, bricks are reset on cars for tunnel kiln firing, or set directly in one of two round periodic kilns for firing. Hot air from tunnel kilns also heat rack car dryers.

Dust Control

Dust control, one of the most serious problems faced in designing a refractory plant has been given elaborate treatment at Windham. The dust control system is divided into two parts—one collecting from raw material processing equipment, and the other from grinding facilities. Either system can be operated independently. Every precaution is taken to prevent silicosis, a definite hazard in any plant processing free silica. All dust collection machinery is enclosed. Good housekeeping methods are constantly stressed.

Harbison-Walker was the first industrial organization licensed in the U. S. by the McIntyre Research Foundation to administer powdered aluminum prophylaxis as a preventative for silicosis. Weekly aluminum inhalation treatments are available to workers at Windham.

Windham Tunnel Kilns

The Harbison-Walker-designed tunnel kilns at Windham are 567 ft long, each holding 81 cars. The kilns have a load cross section of 6x5 ft. The kilns are equipped to burn heavy oil and the firing cycle can be controlled to fit required production. Each oil line has a parallel small steam line to heat oil to a temperature at which it will flow. Air at 700°F comes from the cooling zone of the kiln and is used through the burners as combustion air. Disruption of draft conditions and fuel-oil ratio is prevented by a double door and vestibule system.

Kiln insulation was designed to keep outside surface temperature of the kiln at 200°F or less. Thermocouple and radiomatic instruments measure kiln temperature, thus the operator can set up any desired firing curves within rather wide limits. Instrumentation also permits close adjustment of individual burners to maintain uniform heating conditions. Car trains in the kilns are under a constant push. As each car reaches the end of the tunnel kiln it is delivered to the unloading tracks adjacent to the stock sheds by transfer cars and gasoline driven pushers.

In the firing of silica brick, a permanent increase in dimension takes place altering the individual brick from green or mold size to fired size. This expansion is about 15 pct of volume. It results from the transformation of silica mineral quartz into crystalline forms of silica. Completion of the expansion to the optimum degree requires extended time as well as high temperature.

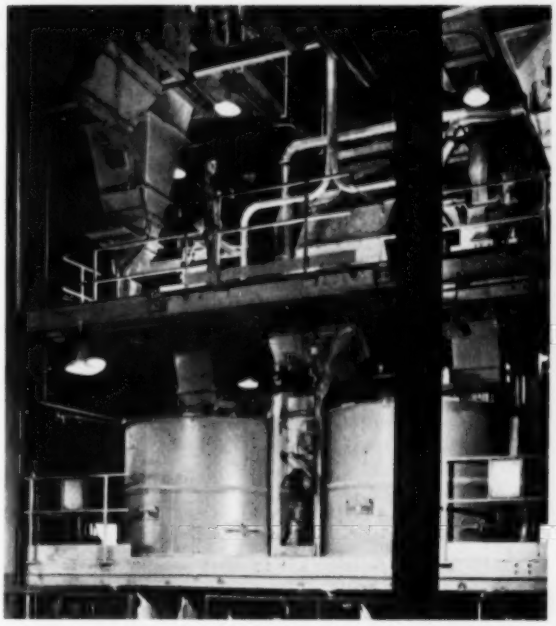

The two mixers give batch final processing before molding. Tramrail buckets, above mixers, deliver mixer contents to presses and special shape molding machines.

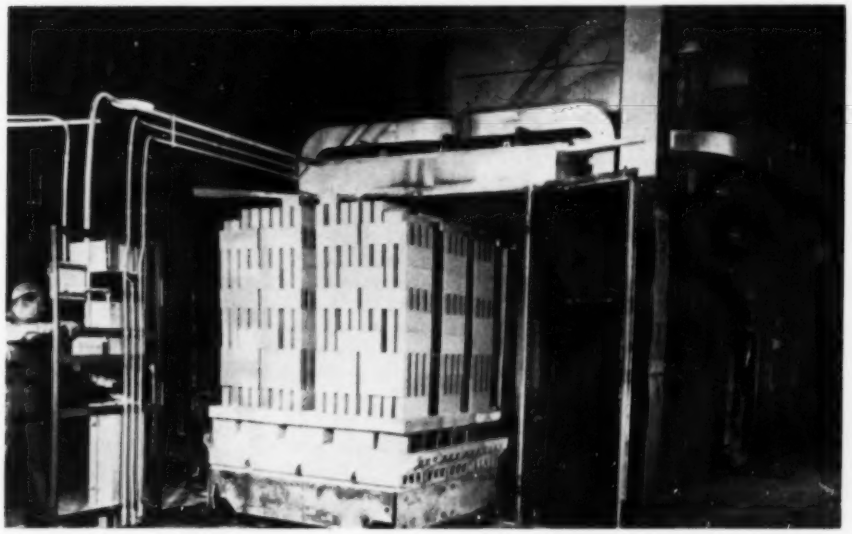

Loaded kiln car enters tunnel kiln. Cars entering kiln are under constant push. Unloading tracks are at the other end, adjacent to stock sheds.

Labor Legislation - - -

As It Affects the Engineer

According to the June 27 issue of *Business Week*, Rep. Kearns (R., Pa.) introduced a bill in Congress along lines suggested by the National Society of Professional Engineers, to amend the Taft-Hartley Act to permit scientific, technical, and professional groups to discuss wages, hours, and working conditions with management—with the protection and support of the federal law. The article reports that the bill is opposed by a loosely knit group of professional and technical unions, the Engineers & Scientists of America. This group wants Taft-Hartley amended to make it an unfair labor practice for employers to discuss collective bargaining matters with professional organizations.

One interested member of AIME reported to the Institute that he felt that he had the right to discuss wages, hours, and working conditions on his own initiative with the company he worked for. He was opposed to any group, professional or union, usurping this right. He also felt that if engineers are ever to obtain professional status, it will be on the basis of their individual ability and attainment rather than on bargaining agreements that might be pressured by a group.

To clarify this matter, AIME's representative on the Engineers Joint Council Labor Panel prepared the following outline of the national Labor Act as it affects professional engineers and the part the professional societies have played in modifying it in the interest of professional employees.

As it now stands, the Taft-Hartley Act allows professional employees: 1—To form their own collective bargaining groups; 2—to unite with some other group of their own choice; or 3—to reject collective bargaining entirely. It provides that the Labor Relations Board shall not decide that any unit is appropriate for purposes of collective bargaining if it includes both professional and nonprofessional employees unless a majority of such professional employees vote for inclusion in such a unit.

Under the original Wagner Act, no distinction was made btween professional (engineers, doctors, etc.) and other employees (carpenters, bricklayers, plumbers, etc.). A majority vote within a plant to establish a collective bargaining agency brought under the agency all employees, engineers included, whether they liked it or not, and they were governed by any instrument of bargaining executed between that agency and their employer. There was no recognized definition of a professional employee, which made it next to impossible for professional employees to form their own organization if they wanted to.

The ASCE was first to be aroused to the necessity for some action to protect the interests of a large group within their membership who came under the Act. It supported various means for maintaining the integrity of the engineer in matters of collective bargaining, and finally earned the sympathetic cooperation of other member societies of Engineers Joint Council, with the result that EJC appointed a Labor Legislation Panel in which ASEE and NSPE joined. As a result of the action of this group, following the election of a Republican Congress in 1946, a definition of a professional employee and the stipulation concerning their rights in matters of collective bargaining, as listed above, were written into the new Taft-Hartley Act.

Therefore, all engineers not bound to any organization which they have voted to recognize as their representative in matters of collective bargaining, have the right to discuss wages, hours, and working conditions on their own initiative with the company they work for.

The NSPE and EJC are concerned about an interpretation of the Taft-Hartley Act as it now stands, and as it affects technical associations. The matters in question bear on what has been termed Freedom of Association. Throughout the country there are groups of engineers banded together to discuss matters which logically come under the head of engineering and which may involve conditions of working and wages, but purely from an engineering viewpoint. The groups may be composed of representatives of management, possibly executives, as well as rank and file engineering employees. Now the present Labor Act defines a *labor organization* as "any organization of any kind, or any agency or employees representation committee or plan, in which employees participate and which exists for the purpose, in whole or in part, of dealing with employers concerning grievances, labor disputes, wages, rates of pay, hours of employment, or conditions of work." Under this definition the technical groups described could be called *labor organizations* and, as such, be subject to the regulation of the Act concerning matters of "unfair labor practices" and the like. If it be construed that any professional society exists for the purpose of dealing in part, with rates of pay, hours of employment, or conditions of work, it could be branded as a *labor organization* under the definition in the Labor Act.

The protection afforded such technical organizations, however, appears in the "Freedom of Speech" portion of the Act which says: "The expression of any view, argument, or opinion, or the dissemination thereof, whether in written, printed, graphic or visual form, shall not constitute or be evidence of an unfair practice under any of the provisions of this Act, if such expression contains no threat of reprisal or force or promise of benefit." Thus while under the Act the society could be branded as a *labor organization* by definition, it would be difficult to find it guilty of unfair labor practice under the "Freedom of Speech" provision.

The interests of the engineer cannot be taken care of by ignoring labor legislation. The AIME is not engaging in collective bargaining arrangements. Through the Labor Panel of EJC it is trying to preserve the right of the individual engineer, who has not elected to join a collective bargaining group, to discuss wages, hours, and working conditions on his own initiative with his company. Engineering groups have no desire to discuss matters of labor from the viewpoint of collective bargaining—only as a purely engineering concern.

The interest of AIME and EJC in matters of labor legislature is that which all engineers must have to preserve what independence of action the individual engineer desires.

Research In Progress

Progress of projects reported in the following abstracts will be discussed at the IMD Fall Meeting, Allerton Hotel, Cleveland, at 2 pm Tuesday, Oct. 20, 1953.

Heat Treatment of Titanium Alloys Generalized In Terms of Beta Prime

by Leonard D. Jaffe

CHANGES in properties of titanium alloys during isothermal transformation, during continuous cooling, and during tempering may be considered in terms of one curve: Hardness vs time. The low hardness (and brittleness) of β increases to a peak as β' forms, then decreases as β' decomposes to $\beta + \alpha$. For a first approximation, the effect of α' may be neglected.

LEONARD D. JAFFE is associated with the Watertown Arsenal, Watertown, Mass.

Solid State Bonding of Aluminum and Nickel

by S. Storchheim, J. L. Zambrow, and H. H. Hausner

THE solid state bonding of aluminum and nickel was studied as a function of temperature, pressure, and time at pressure. This was done by means of tensile tests and intermetallic penetration rates.

The initial results indicated that as the temperature for reaction was raised tensile strength increased, reached a maximum, declined and then levelled off. Plots of the log of penetration coefficient, P, versus the reciprocal of absolute temperature were straight lines.

As pressure was increased for tests at various temperatures, the tensile strength showed: Incipient bonding occurring at 400°C, increasing very sharply at 450° and 500°C; at 550°C, increasing slowly and to a lower maximum than for the 450° and 500°C temperatures and at 600°C, rising slowly from a relatively moderate maximum strength. The penetration coefficient was found to decrease as the pressure increased. This decrease was more rapid as the temperature of the reaction was raised.

Increased time at a pressure of 11 tsi for tests at various temperatures caused tensile strength to rise to a maximum and then slowly decline from this value. The greatest tensile strength was found to occur at 4 min for all the samples made at various temperatures.

Metallographic investigation showed, as polished, two intermetallic phases at the aluminum-nickel bond interface.

This work was done under Atomic Energy Commission contract AT-30-1-GEN-366.

S. STORCHHEIM, J. L. ZAMBROW, and H. H. HAUSNER are associated with the Atomic Energy Div., Sylvania Electric Products, Inc., Bayside, N. Y.

Grain Boundary Creep

by F. N. Rhines

THE shear displacement which occurs at grain boundaries during creep at elevated temperatures is found to occur in surges, the magnitude and frequency of which are dependent upon the temperature, stress and crystallographic relationships. Deformation is by slip simultaneously in a continuum of minute activated sites which are disposed along the grain boundary. The activated sites are localized regions of polygonization caused by the lattice bending that accompanies the propagation of slip from one crystal to its neighbor across the grain boundary. Slip in the activated sites reports as a shear along the grain boundary, because the total deformation in these sites is large compared to that in the adjacent partially work hardened metal and is confined to a thin plate of metal along the grain boundary. Otherwise the creep behavior at grain boundaries is not to be distinguished from that within the grains where, subsequently, kinking followed by polygonization and localized activated creep develops. Once activated sites have appeared, these continue to yield, work harden, re-polygonize and yield again in a cyclic manner. This process is

F. N. RHINES is associated with Carnegie Institute of Technology, Pittsburgh.

superimposed upon initial gross slip and work hardening and increases in importance as the number of activated sites grows. Thus, the decelerating creep rate of initial transient creep is first stemmed by the counteraction of activated creep, often to produce a temporary steady creep rate, and later is converted to an accelerating creep rate as the activated process becomes dominant.

The Spread in Orientations Among Microregions In Cast and Deformed Crystals

by W. C. Ellis

X-RAY evidence for crystal imperfections too small in size or orientation difference to reveal themselves by general radiation are obtained when the region is critically oriented for Bragg reflection of intense characteristic wave lengths. By changing the setting of the crystal a few degrees in successive exposures, a search for orientations clustering about the principal one for the crystal can be made. The data can be treated quantitatively in a manner similar to that for textures and a pole figure plotted.

W. C. ELLIS is a member of the Technical Staff, Bell Telephone Laboratories, Inc., Murray Hill, N. J.

Such imperfections have been observed in nearly perfect single crystals after a few percent extension at room temperature. They also occur in some cast crystals and a partial pole figure has been constructed showing the density of orientations about one particular [112] pole of a cast aluminum crystal. The observations are interpreted to be the result of nonhomogeneous flow in the stretched crystal and to minor thermal fluctuations during the freezing of the cast crystal.

Growth Structures Formed During the Solidification Of Metal Crystals

by C. Elbaum and B. Chalmers

IN order to expose the solid-liquid interface of a metal crystal during solidification or melting, an improved technique of decanting has been developed to separate the liquid portion of the metal from the adjacent solid. Microscopic examination of the interfaces prepared by this method has revealed a hitherto unreported structure. It has been found that the presence or absence of the structure depends on the crystallographic orientation of the specimen. In the case of lead, which has been studied in more detail than the other metals, the interface appears to consist of *steps*, formed by certain crystallographic planes, except when these planes make too great an angle with the interface, which then appears to be structureless.

B. CHALMERS is on the staff at Harvard University, Cambridge, Mass. C. ELBAUM is International Nickel Research Fellow, Dept. of Metallurgical Engineering, University of Toronto.

Thus far, this structure has been observed in all metals investigated in this research, namely, lead, tin, and zinc, each of which represents a different crystallographic system. The size of the steps, but not the general nature of the structure, depends on the speed of advance of the interface.

Curie Temperatures of Certain Ternary Sigma Alloys

by M. V. Nevitt and P. A. Beck

THE correlation between sigma composition and d-shell electron vacancy suggests that the sigma phase is an electron compound of a type different from the Hume-Rothery phases, and perhaps best described as an "electron vacancy compound." Consequently, its ferromagnetic properties, which are also related to the d-shell, are of considerable interest.

Many sigma alloys were found to become ferromagnetic at temperatures from about 50° to 200°K. The present work concerns the variation of Curie temperature with composition for two ternary sigma phases Fe-Cr-Mo and Co-Cr-Mo, which form rather broad fields, so that large variations in composition can be attained. The Curie points were determined by an induction method, employing a suitable cryostatic arrangement.

Curie temperatures for both (Fe, Cr, Mo)sigma and (Co, Cr, Mo)sigma appear to be independent of the chromium to molybdenum ratio, and to be a

function solely of the iron or cobalt content. This is reconcilable with the fact that the Curie temperature T_c of a ferromagnetic has been related to the saturation magnetic moment by the expression

$kT_c = \beta N I_o$ where:

β is the Bohr magneton
N is the Weiss molecular field constant
I_o is the saturation magnetic moment

Since chromium and molybdenum have similar electron distributions outside of filled shells, they might be expected to make equal contributions to the magnetic moment. However, molybdenum dilates the lattice of both Fe-Cr-Mo sigma and Co-Cr-Mo sigma and the magnitude of the exchange energy between near neighbors should be altered. In terms of the Neel criterion involving the interatomic spacing and the diameter of the unfilled *d*-shell, the addition of molybdenum should produce additional near neighbor positive Fe-Fe and Fe-Cr exchanges, but it should also introduce strongly negative Fe-Mo, Cr-Mo and Mo-Mo exchanges. The observed insensitivity of the Curie temperatures to the chromium to molybdenum ratio apparently signifies that the uncoupling tendency of molybdenum compensates the increase in positive exchange coupling due to lattice distention.

M. V. NEVITT and P. A. BECK are associated with the University of Illinois, Urbana, Ill.

The Effect of Grain Size on Ultrasonic Transmissibility

by Nicholas Grossman

MECHANICAL waves which have a frequency of over 20,000 cps are designated as ultrasonic waves. The velocity of propagation of these waves is a constant for an ideally elastic medium—at a given temperature and frequency. In polycrystalline metals the grain size and preferred grain orientation appear to have a definite influence on the transmissibility of the ultrasonic waves.

Experiments were performed on rolled alpha-brass rods of known chemical composition to determine the effects of grain size on transmissibility. Samples were prepared by heat treatment that yielded a series of specimens with average grain size from 0.015 mm to 0.150 mm (10:1). The Sperry Ultrasonic Reflectoscope was used in this investigation. Three different frequencies 2¼ mc, 5 mc, and 10 mc were used, and both the pulse technique (reflection) and the two crystal through transmission methods were studied.

It was found that as the ratio of the wave length to grain size decreased, the amount of ultrasonic energy reflected, or transmitted, was diminished—all other variables remaining unchanged. The range of wave length to grain size covered was from about 100:1 to 2½:1. It was observed that as the wave length to grain ratio approached 5:1 or less, the transmissibility became poor—under the experimental conditions outlined. No difference was detected between the pulse technique or transmission methods.

NICHOLAS GROSSMAN is associated with the Atomic Energy Div., Sylvania Electric Products, Inc., Bayside, N. Y.

Mechanism of Plastic Flow in Titanium At Low and High Temperatures

by F. D. Rosi and F. C. Perkins

THE present investigation was undertaken to examine the slip and twinning behavior in coarse-grained specimens of arc-melted iodide and sponge titanium at −196° and 500°C to determine the effect of temperature on the established mechanisms of plastic deformation at room temperature.

A. **Tests at −196°C**

1—Slip Behavior: Deformation by slip was observed to occur solely on prismatic planes of the type $\{10\bar{1}0\}$ in all specimens extended in liquid nitrogen despite several attempts to produce multiple slip by complex deformation. The effective slip direction was found to coincide with a type I digonal axis of indices $\{11\bar{2}0\}$.

2—Twin Behavior: Five twin types were observed in the specimens deformed in tension at −196°C. In order of frequency, these are: $\{11\bar{2}4\}$, $\{11\bar{2}2\}$, $\{11\bar{2}1\}$, $\{11\bar{2}3\}$ and $\{10\bar{1}2\}$. The occurrence of the predominant $\{11\bar{2}4\}$ type appeared to be orientation dependent, and that $\{11\bar{2}4\}$ plane operated on which the resolved shear stress was a maximum. The present results indicate that the same twin types occur at −196°C and at room temperature, but that a greater proportion of the deformation occurs by twinning at low temperatures, and the preponderance of twinning shifts from $\{11\bar{2}1\}$ to the $\{11\bar{2}4\}$ planes.

B. **Tests at 500°C**

1—Slip Behavior: Extensive slip on type I prismatic $\{10\bar{1}0\}$ planes occurred in all crystals extended at 500°C. In a few cases secondary slip on

F. D. ROSI and F. C. PERKINS are associated with the metallurgy laboratory, Atomic Energy Div., Sylvania Electric Products, Inc., Bayside, N. Y.

the type I, order 1 pyramidal planes were observed. Since this slip system was rarely encountered at room temperature, it would appear that its occurrence is facilitated by testing at elevated temperatures.

2—Twin Behavior: As yet no evidence of twinning was found in the specimens extended at 500°C.

This work is sponsored by the Aeronautical Research Laboratory, Wright Air Development Center, Contract AF 33 (616)-422.

Arsenic-Bismuth Phase Diagram

by G. A. Geach and R. A. Jeffrey

THE arsenic-bismuth diagram is a simple eutectic with the eutectic point very near to pure bismuth. By differential thermal analysis of specimens in sealed off, evacuated silica bulbs the liquidus has been determined, with an accuracy of ±0.25°C, as a smooth curve rising steeply from the melting point of bismuth and flattening out as the percentage of arsenic is increased. The melting point of arsenic was found to be 811° ±0.25°C. A dilatometer containing silicone oil used to determine the contraction on melting showed the eutectic temperature to be 270.3° ±0.05°C, and the melting point of pure bismuth to be 271.3° ±0.025°C. By metallographic examination the eutectic composition was shown to be 0.5 pct (atomic) arsenic.

Hardness measurements showed that the solid solubility of arsenic in bismuth ranges from 0.42 pct at the eutectic temperature to 0.2 pct at room temperature; since no hardening of arsenic by the solution in bismuth could be detected, this is not considered to exceed 0.05 pct at any temperature.

G. A. GEACH and R. A. JEFFREY are with Associated Electrical Industries, Ltd., Berkshire, England.

Deformation Bands in Titanium

by G. A. Geach and A. T. Churchman

THE appearance of deformation bands in polycrystalline or single crystal specimens of titanium or polycrystalline specimens of zirconium is accompanied by a load drop in the stress-strain curve reminiscent of the yield phenomena in iron. Immediate retesting shows no load drop; on ageing for up to 65 hr at 240°C very little strain age hardening takes place, but the discontinuity is again observed in the stress-strain curve. While this phenomenon is observed at room temperature with coarse polycrystalline specimens and single crystals, it is only found in finely polycrystalline specimens at higher temperatures.

Rotation of the lattice in the deformation band increases with extension even when this involves passing through the peak value of the resolved shear stress. If the resolved shear stress is greater in the band than outside it, slip only occurs in the band but will reappear in the matrix if the resolved shear stress in the band drops to that outside it again.

These observations may be related to an observation of Luders bands in polycrystalline titanium which has been recorded in the literature.

G. A. GEACH and A. T. CHURCHMAN are with the Associated Electrical Industries, Ltd., Berkshire, England.

Some Factors Governing the Micro-Hardness of Pure Metals

by G. A. Geach and J. Winton

A micro-hardness machine designed for loads of 1 to 50 g has been used to measure errors in hardness arising from vibration in the instrument and from imperfections of the diamond tip. Vibration from the very small 24-v dc electric motor originally used to operate the machine, which itself is quite massive, gave error equivalent to a 4 g increase in the load.

In a number of annealed metals increases of hardness with decreasing load corresponds to logarithmic indices of approximately 1.90. This increases to 2.0 upon cold working the metals.

It has been confirmed for micro-loads that a depth of material 10 times the impression depth is necessary for a correct hardness measurement when the particle under test is embedded in a matrix of different hardness. The width of the particle is not so important; good hardness measurements are obtained if the diagonal of the impression is less than three quarters of the width of the specimen.

G. A. GEACH and J. WINTON are connected with the Associated Electrical Industries, Ltd., Berkshire, England.

Crystallization of Silicon from Solution in Tin

by A. J. Goss

A STUDY is being made of the preparation of crystals of silicon from saturated solutions of silicon in other metals. The form and size of the crystals are being investigated as a function of temperature gradient and cooling rate of the solution; information on solubilities is also being obtained. Previous experiments with silicon dissolved in aluminum, in silver, and in zinc were made by v. Wartenberg,[1] and Keck and Broder[2] have obtained crystals from gallium and indium. Hitherto, no study of crystals prepared this way appears to have been made.

In this laboratory experiments to date have been made with saturated solutions of silicon in tin at temperatures up to 900°C. A seed is lowered into the solution and then the temperature of the solution is decreased. Oriented growth occurs on the surface of a single crystal silicon seed. In addition, small single crystals of silicon, several mm in length, are formed on nuclei adjacent to the seed. A low temperature gradient and a low rate of cooling are found to be the more satisfactory. X-ray examination shows the crystals to be single, with growth in the [110] direction and development of (111) faces.

References

[1] H. v. Wartenberg: *Z. Fur Anorg. Allg. Chem.* **265** 186 (1951).

[2] P. H. Keck and J. Broder: *Phys. Rev.* **90** 521 (1953).

A. J. GOSS is associated with the Bell Telephone Laboratories, Inc., Murray Hill, N. J.

Influence of Isotope Mass on the Physical Properties of Iron

by James O. McCaldin and Pol Duwez

IN metallic crystals the lattice frequencies,

$$\nu_i = \sqrt{\frac{ki}{m}},$$

and consequently the lattice energy levels, $\epsilon_i = (m + \frac{1}{2})\ \eta\nu_i$, vary inversely with the square root of isotope mass. Therefore thermodynamic functions which depend only on the ratio $\eta\nu/kT$, e. g. specific heat, should be homologous (that is, their plots versus temperature should be brought into coincidence by the appropriate change in temperature scale). This influence may extend to related physical properties, e. g. electrical resistance, as well.

Experiments are being carried out on two iron isotopes. Two hundred milligrams of both iron 54 and iron 57 were obtained from the isotope div. of the Atomic Energy Commission, Oak Ridge, Tenn. Measurements of the allotropic alpha-gamma transformation were made with a sensitivity of ± 1°C. Within this range of uncertainty no difference was found between the transformation temperatures of the two isotopes. This may be interpreted as evidence for the zero-point energy, $\frac{1}{2}\ \eta\nu$.

At present the electrical resistance and thermoelectricity of the two specimens in wire form are being examined. It is planned to include lattice parameter measurements later.

JAMES O. McCALDIN and POL DUWEZ are associated with the California Institute of Technology, Pasadena, Calif.

Solubility of Oxygen in Alpha Iron

by A. U. Seybolt

THE solubility of oxygen in alpha iron has been determined in the range of 700° to 900°C. The solubility values for these two temperatures were about 0.008 and 0.030 wt pct, respectively. The technique employed was to saturate thin strips of high purity iron by the addition of a controlled oxygen gas excess, thus forming a thin film of iron oxide on the surface. This film of iron oxide supplied oxygen to the sample by diffusion, the samples being held for sufficiently long periods of time at temperature to insure saturation. It was found that the data when plotted as log saturation solubility vs reciprocal absolute temperature fell fairly closely on a straight line, thus indicating that the Van't Hoff equation was obeyed. The heat of solution was about 16,000 cal.

A. U. SEYBOLT is associated with the General Electric Co., Schenectady, N. Y.

IMD Fall Meeting Program Completed For Metal Congress In October

Cleveland Meeting to Feature Symposium on Physical Metallurgy of Titanium and Its Alloys And Panel Discussion of Recrystallization

THE technical program of the Institute of Metals Div., AIME, at the National Metal Congress and Exposition, Oct. 19 to 21, 1953 at Cleveland, will feature an all day Titanium Symposium by world renowned experts in that field. The Research in Progress sessions, inaugurated in 1950 to bring to light research not far enough advanced to establish final results, have received a great deal of interest, and are being continued.

Another unique informal technical session similar to the one held in Chicago in 1950 is scheduled for Monday evening. A panel of experts will discuss recrystallization followed by participation by the audience. Each of the panel members will be assigned 15 min to present the main features of his topic. Liquid refreshments will be available after the formal discussion is completed. A charge of $1 will be made to cover the cost of the refreshments. These tickets should be purchased by Monday noon, although tickets will be available at the session.

Headquarters of the IMD during the Metal Show will be the Allerton Hotel, and all IMD technical sessions well be held there. Registration desks will be open on Sunday, October 18, from 3 to 9 pm; Monday from 8 am to 9 pm; Tuesday from 8 am to 5 pm; and Wednesday from 9 am to 4 pm. AIME Member registration fee is $2, and for nonmembers, $4. No admission will be charged for AIME Student Associates, but other students will pay $1. Reprints of most of the papers will be presented to registrants as long as the supply lasts.

The annual IMD Fall Dinner will be held at 7 pm Tuesday, October 20, in the Ballroom of the Allerton Hotel. Cleveland Local Section, AIME, will provide a complimentary cocktail party for all dinner guests at 6 pm in the Chester Room of the hotel, immediately preceding the dinner. Dress will be informal (business suits).

SUNDAY, OCTOBER 18

4:30 pm, Otis Room

IMD Publications Committee Meeting

8:00 pm, Otis Room

IMD Publications Committee Meeting

MONDAY, OCTOBER 19

9:30 am to 12:00 m, Ballroom

Plastic Deformation

Plasticity of Columbium Single Crystals: R. Maddin and N. K. Chen, Johns Hopkins University. JOURNAL OF METALS, September 1953.

Plastic Deformation of Iron Between 300° and 77.2°K: D. F. Gibbons, Royal Military College of Canada. JOURNAL OF METALS, September 1953.

Deformation of Ferrite Single Crystals: F. L. Vogel, Jr. and R. M. Brick, University of Pennsylvania. JOURNAL OF METALS, May 1953.

Plastic Stress-Strain Relations for 14S-T6 Subjected to Combined Tension and Torsion: Joseph Marin and H. A. B. Wiseman, Pennsylvania State College. JOURNAL OF METALS, September 1953.

9:30 am to 12:00 m, Mather Room

Metallography

Revealing the Subgrain Structure of Aluminum: M. S. Hunter and D. L. Robinson, Aluminum Co. of America. JOURNAL OF METALS, May 1953.

Grain Boundary Attack on Aluminum in Hydrochloric Acid and Sodium Hydroxide: E. C. W. Perryman, Aluminum Laboratories Ltd. JOURNAL OF METALS, July 1953.

Microscopical Examination of Tin Bronzes in the Alpha Range: E. C. W. Perryman, Aluminum Laboratories Ltd. JOURNAL OF METALS, July 1953.

Identification of the Precipitate Accompanying 885°F Embrittlement in Chromium Steels: R. M. Fisher, E. J. Dulis and K. G. Carroll, U. S. Steel Corp. JOURNAL OF METALS, May 1953.

Measurement of Particle Sizes in Opaque Bodies: R. L. Fullman, General Electric Co. JOURNAL OF METALS, March 1953.

Measurement of Approximately Cylindrical Particles of Opaque Samples: R. L. Fullman, General Electric Co. JOURNAL OF METALS, September 1953.

2:00 to 5:00 pm, Ballroom

Plastic Deformation

Plastic Deformation of Single Crystals of Copper: J. J. Becker, General Electric Research Laboratory, and J. N. Hobstetter, Bell Telephone Laboratories, Inc. JOURNAL OF METALS, September 1953.

Orientation Relationships in the Recrystallization of Deformed Copper Single Crystals: J. J. Becker, General Electric Research Laboratory, and J. N. Hobstetter, Bell Telephone Laboratories, Inc. JOURNAL OF METALS, September 1953.

Plastic Deformation of Rectangular Zinc Monocrystals: J. J. Gilman, Columbia University. JOURNAL OF METALS, September 1953.

Variation of Plastic Properties with Annealing Procedure in Zinc Single Crystals: Choh Hsien Li, Jack Washburn and E. R. Parker, University of California. JOURNAL OF METALS, September 1953.

Recovery in Single Crystals of Zinc: R. Drouard, Paris, Jack Washburn and E. R. Parker, University of California. JOURNAL OF METALS, September 1953.

Some Observations on the Work Hardening of Metals: E. H. Edwards, Jack Washburn, and E. R. Parker, University of California.

2:00 to 5:00 pm, Mather Room

Thermodynamics

Some Applications of the Thermodynamic Theory of Irreversible Processes to Physical Metallurgy: E. S. Machlin, Columbia University. JOURNAL OF METALS, March 1953.

Vapor Pressure of Silver Over Silver-Gold Solid Solutions: C. L. McCabe and H. M. Schadel, Jr., Carnegie Institute of Technology. C. E. Birchenall, Princeton University. JOURNAL OF METALS, May 1953.

Vapor Pressure of Silver: C. L. McCabe, Carnegie Institute of Technology and C. E. Birchenall, Princeton University. JOURNAL OF METALS, May 1953.

High Pressure Oxidation Rate of Metals-Copper in Metals: William McKewan, New Jersey Zinc Co. of Pa. and W. Martin Fassell, Jr., University of Utah. JOURNAL OF METALS, September 1953.

Self-Diffusion of Iron in Iron Oxides and The Wagner Theory of Oxidation: L. Himmel and R. F. Mehl, Carnegie Institute of Technology and C. E. Birchenall, Princeton University. JOURNAL OF METALS, June 1953.

Decay of Lattice Defects Frozen into an Alloy by Quenching: A. E. Roswell and A. S. Nowick, Yale University. JOURNAL OF METALS, September 1953.

2:00 to 5:00 pm, Chester Room

Constitutional Diagrams

Ternary System Ti-Ta-C: John G. McMullin, General Electric Research Laboratory and John T. Norton, Massachusetts Institute of Technology. JOURNAL OF METALS, September 1953.

Titanium-Rich Corners of the Ti-C-N, Ti-C-O and Ti-N-O Phase Diagrams: L. Stone and H. Margolin, New York University.

System Titanium-Chromium-Iron: R. J. Van Thyne, H. D. Kessler and M. Hansen, Armour Research Foundation of Illinois Institute of Technology. JOURNAL OF METALS, September 1953.

Vanadium-Uranium Constitutional Diagram: H. A. Saller and F. A. Rough, Battelle Memorial Institute. JOURNAL OF METALS, April 1953.

Order-Disorder Transformation in Cu-Au Alloys Near the Composition CuAu: J. B. Newkirk, General Electric Co. JOURNAL OF METALS, June 1953.

Analysis of Molten Zone Refining: N. W. Lord, Raytheon Mfg. Co.

4:30 pm, Otis Room

IMD Membership Committee Meeting

7:45 pm, Ballroom

Panel Discussion of Recrystallization

A considerable number of divergent views have arisen concerning the nature and the mechanism of recovery and recrystallization. To bring these viewpoints into sharp relief a panel discussion has been arranged on the physical nature and the driving forces of recrystallization.

B. L. Averbach, Moderator

Paul A. Beck:	*Do Metals Recrystallize?*
Cyril Stanley Smith:	*Interfacial Energy and Recrystallization*
B. L. Averbach:	*Recovery*
E. E. Stansbury:	*Stored Energy and Recrystallization*
D. Turnbull:	*Significance of Activation Energies*
J. E. Burke:	*Recrystallization as a Nucleation and Growth Process*
Robert Maddin:	*Textures and Recrystallization*

Each of the panel members will be assigned 15 min to present the main features of his topic. Cross-questioning by the panel members will be allowed during and after the formal talks. The meeting will then be open to questions from the floor and a beer party will follow. A charge of $1.00 will be made to cover the cost of the refreshments.

TUESDAY, OCTOBER 20

9:00 am to 12:00 m, Chester Room

Transformation

Silver-Cadmium Eutectoid: G. R. Speich, Westinghouse Electric Corp. and D. J. Mack, University of Wisconsin. JOURNAL OF METALS, April 1953.

Diffusionless Phase Change in the Indium Thallium System: M. W. Burkart and T. A. Read, Columbia University.

On the Theory of the Formation of Martensite: M. S. Wechsler, D. S. Lieberman and T. A. Read, Columbia University.

Rate of Propagation of Martensite: R. F. Bunshah and R. F. Mehl, Carnegie Institute of Technology. JOURNAL OF METALS, September 1953.

Rate of Formation of Isothermal Martensite in Fe-Ni-Mn Alloy: R. E. Cech and J. H. Hollomon, General Electric Co. JOURNAL OF METALS, May 1953.

Calculation of Martensite Nucleus Energy Using The Reaction-Path Model: J. C. Fisher and D. Turnbull, General Electric Co. JOURNAL OF METALS, July 1953.

Martensite Nucleation in Substitutional Iron Alloys: J. C. Fisher, General Electric Co. JOURNAL OF METALS, July 1953.

Stabilization of the Austenite-Martensite Reaction in a High Chromium Steel: S. C. Das Gupta and B. S. Lement, Massachusetts Institute of Technology. JOURNAL OF METALS, April 1953.

9:00 am to 12:00 m, Ballroom

Symposium on Physical Metallurgy of Titanium and its Alloys

M. A. Hunter and H. A. Jackson, Chairmen

Effect of Hydrogen on Mechanical Properties of Titanium: G. A. Lenning, C. M. Craighead, and R. I. Jaffee, Battelle Memorial Institute.

Initial Experience with a New Type Titanium Alloy: The All-Alpha: W. L. Finlay, R. W. Parcel, and R. C. Durstein, Rem-Cru Titanium Inc.

Isothermal Characteristics of Ti-Fe-V Alloys: W. P. Koster and J. F. Kahler, Metcut Research Associates, L. S. Busch, Mallory-Sharon Titanium Corp.

Research and Development Program at Wright Air Development Center: E. J. Hassell, Wright Air Development Center.

12:15 pm, Otis Room

IMD Executive Committee Luncheon Meeting

2:00 to 5:00 pm, Ballroom

Symposium on Physical Metallurgy of Titanium and its Alloys

M. A. Hunter and H. A. Jackson, Chairmen

Hardening and Embrittlement of Beta Stabilized Titanium Alloys: W. M. Parris, A. P. Young, A. J. Griest, Jr. and P. D. Frost, Battelle Memorial Institute.

Titanium-base Alloys for Elevated Temperature Applications: Harold Kessler and F. A. Crossley, Armour Research Foundation of Illinois Institute of Technology.

The Influence of Metallurgical Factors on the Mechanical Properties of Titanium Alloys: S. A. Heries, Titanium Metals Corp. of America.

Heat Treatment, Structure and Mechanical Properties of Titanium Manganese Alloys: F. C. Holden, H. R. Ogden and R. I. Jaffee, Battelle Memorial Institute.
Heat Treatment and Alloying of Titanium: L. D. Jaffe, Watertown Arsenal.

2:00 to 5:00 pm, Mather Room

Research in Progress

T. A. Read and David Turnbull, Chairmen

(Abstracts of papers to be presented at this session appear in this issue of JOURNAL OF METALS.)

Heat Treatment of Titanium Alloys Generalized in Terms of β′: L. D. Jaffe, Watertown Arsenal.
Solid State Bonding of Aluminum and Nickel: S. Storchheim, J. L. Zambrow and H. H. Hausner, Sylvania Electric Products, Inc., atomic energy div.
Grain Boundary Creep: F. N. Rhines, Carnegie Institute of Technology.
The Spread in Orientations Among Microregions in Cast and Deformed Crystals: W. C. Ellis, Bell Telephone Laboratories, Inc.
Growth Structures Formed During the Solidification of Metal Crystals: C. Elbaum, University of Toronto, and B. Chalmers, Harvard University.
Curie Temperatures of Certain Ternary Sigma Alloys: M. V. Nevitt and P. A. Beck, University of Illinois.
Effect of Grain Size on Ultrasonic Transmissibility: Nicholas Grossman, Sylvania Electric Products Inc.
Mechanism of Plastic Flow in Titanium at Low and High Temperatures: F. D. Rosi and F. C. Perkins, Sylvania Electric Products, Inc.
Arsenic-Bismuth Phase Diagram: G. A. Geach, R. A. Jeffrey, Associated Electrical Industries, Ltd.
Deformation Bands in Titanium: G. A. Geach, A. T. Churchman, Associated Electrical Industries, Ltd.
Some Factors Governing the Micro-Hardness of Pure Metals: G. A. Geach, J. Winton, Associated Electrical Industries, Ltd.
Crystallization of Silicon from Solution in Tin: A. J. Goss, Bell Telephone Laboratories, Inc.
The Influence of Isotope Mass on the Physical Properties of Iron: Pol Duwez, J. O. McCaldin, California Institute of Technology.
Solubility of Oxygen in Alpha Iron: A. U. Seybolt, General Electric Co.

2:00 to 5:00 pm, Chester Room

Creep

Inhomogeneity in Creep Deformation of Coarse Grained High Purity Aluminum: H. C. Chang and N. J. Grant, Massachusetts Institute of Technology. JOURNAL OF METALS, September 1953.
Kink Bend Formation in High Purity Aluminum During Creep at High Temperatures: A. M. Gervais, Societe Commentry-Fouchambault et Decazeville, J. T. Norton and N. J. Grant, Massachusetts Institute of Technology. JOURNAL OF METALS, September 1953.

ANNUAL DINNER

Tuesday, October 20

6:00 pm, Chester Room
Cocktail Party for Dinner Guests
Compliments Cleveland AIME Members and friends

7:00 pm, Ballroom
Annual Fall Dinner

Toastmaster: Morris Cohen, Chairman
Institute of Metals Div.

Welcome: Vernon Kalan, Chairman
Cleveland Section, AIME

Subgrain Formation in High Purity Aluminum During Creep at High Temperatures: A. M. Gervais, Societe Commentry-Fouchambault et Decazeville, J. T. Norton and N. J. Grant, Massachusetts Institute of Technology. JOURNAL OF METALS, September 1953.
Metallographic Observations of the Deformation of High-Purity Magnesium in Creep at 500°F: A. R. Chaudhuri, N. J. Grant and J. T. Norton, Massachusetts Institute of Technology. JOURNAL OF METALS, May 1953.
Creep Behavior of Extruded Electrolytic Magnesium: C. S. Roberts, Dow Chemical Co. JOURNAL OF METALS, September 1953.
Further Progress in the Development of Mg-Zr Alloys to Give Good Creep and Fatigue Properties Between 500° and 650°F: C. J. P. Ball, A. C. Jessup, P. A. Fisher, D. J. Whitehead and J. B. Wilson, Magnesium Elektron Ltd. JOURNAL OF METALS, July 1953.
Properties of Sand Cast Magnesium-Thorium-Zinc-Zirconium Alloys: K. E. Nelson, Dow Chemical Co.
Rationalization of Measured High Temperature Properties of Fe-Cr-Co-Ni Alloys: J. D. Nisbet and W. R. Hibbard, Jr., General Electric Co. JOURNAL OF METALS, September 1953.

6:00 pm, Chester Room

Cocktail Party

7:00 pm, Ballroom

Annual IMD Fall Dinner

WEDNESDAY, OCTOBER 21

2:00 to 5:00 pm, Ballroom

Plastic Deformation of Titanium, Molybdenum and Zirconium

Deformation Mechanisms in Alpha Titanium: E. A. Anderson, D. C. Jillson and S. R. Dunbar, New Jersey Zinc Co. of Pa. JOURNAL OF METALS, September 1953.
Cold Rolled Texture of Titanium: D. N. Williams and D. S. Eppelsheimer, University of Missouri.
Effects of Solid Solution Alloying on the Cold-Rolled Texture of Titanium: C. J. McHargue, University of Kentucky, S. E. Adair, Jr., Linde Air Products, and J. P. Hammond, University of Kentucky. JOURNAL OF METALS, September 1953.
Textures of Rolled and Annealed Iodide Zirconium: J. H. Keeler, W. R. Hibbard, Jr. and B. F. Decker, General Electric Co. JOURNAL OF METALS, July 1953.

2:00 to 5:00 pm, Chester Room

Physical Metallurgy

Effects of Macrostructure on the Performance of Alnico Permanent Magnets: D. G. Ebeling, General Electric Co. and A. A. Burr, Rensselaer Polytechnic Institute. JOURNAL OF METALS, April 1953.
Densification and Kinetics of Grain Growth During the Sintering of Chromium Carbide: H. J. Hamjian, Utica Drop Forge & Tool Corp. and W. G. Lidman, Sylvania Electric Products Inc. JOURNAL OF METALS, May 1953.
Influence of Aluminum and Silicon Deoxidation on the Strain Aging of Low-Carbon Steels: W. C. Leslie and R. L. Rickett, U. S. Steel Corp. JOURNAL OF METALS, August 1953.
Age Softening of Beta Brass: Harry Green, Horizons Inc. and Norman Brown, University of Pennsylvania. JOURNAL OF METALS, September 1953.
Anelastic Behavior of Pure Gold Wire: D. R. Mash and L. D. Hall, Stanford University. JOURNAL OF METALS, July 1953.
Some Properties of Columbium Containing Nitrogen: Choh-Yi Ang and Charles Wert, University of Illinois. JOURNAL OF METALS, August 1953.
Electrical Resistivity of Liquid Metals and of Dilute Liquid Metallic Solutions: E. Scala, Chase Brass & Copper Co. and W. D. Robertson, Yale University. JOURNAL OF METALS, September 1953.

Oxygen Activity in Iron Oxide Slags

by Hugo Larson and John Chipman

The ferrous and ferric oxide concentrations of slags, expressed as $j = Fe^{+++}/(Fe^{+++} + Fe^{++})$, have been established through gas-slag equilibrium at 1550°C in a range of oxygen pressure of 10^{-1} to 10^{-10} atm. The value of j is increased by basic additions (BaO, CaO, MgO, MnO) and decreased by acidic oxides (SiO_2 and TiO_2). Oxygen pressure is shown graphically as a function of composition for slags which are analogous to those at the slag-gas interface of the open hearth furnace.

THE progress which has been made in recent years in understanding the chemistry of metallurgical slags has been based largely on studies of slag-metal and slag-gas equilibria. There is a considerable body of knowledge which is applicable to reactions occurring at the slag-metal interface in open hearth steelmaking. There is little information concerning reactions of the slag with the furnace atmosphere and hence little basis for an understanding of the transfer of oxygen, sulphur, or hydrogen between gas and slag.

The oxygen pressure of the open hearth atmosphere is normally of the order of 10^{-1} to 10^{-3} atm which differs by several orders of magnitude from that of about 10^{-9} atm at the slag-metal interface. The chemical properties of the slag, for example, the ratio of ferric to ferrous iron and the ability of the slag to hold sulphur in solution, are greatly affected by changes in oxygen pressure.

This investigation was undertaken to enlarge our knowledge of the effect of oxygen pressure on steelmaking slags. Using air or controlled mixtures of CO and CO_2 a range of oxygen pressures from 10^{-1} to 10^{-7} was covered.

Review of the Literature

There are only a few references in the literature which pertain directly to this investigation. The most important is that of Darken and Gurry[1, 2] on the system iron-oxygen. This work included the determination of the phase diagram of the system and also a study of the field of homogeneous melts and their oxygen pressures. Their apparatus and procedure were very similar to that used in this study. Iron oxide was melted in a platinum crucible under an atmosphere of CO_2:CO, CO_2:H_2, H_2O, CO_2, air or O_2 depending upon the partial pressure of oxygen desired. After equilibrium was reached, the sample was quenched and analyzed for ferrous and ferric oxide. By appropriate calculations these authors were able to determine the oxygen and iron activities in the various slags, heats of formation of the oxides of iron, and heats of solution of iron and oxygen in the liquid slags.

In a subsequent paper[3] the same authors made a less thorough investigation of the effects of additions of lime and manganese oxide on the composition of iron oxide melts. Only a few experiments were made and those in a narrower range of temperature and oxygen pressure.

Darken[4] has investigated the fusion temperature of iron oxide in contact with silica under various atmospheres. He found that the temperature changes from 1120° to 1447°C as the gas composition changes from CO_2/CO equal to 20.8 to pure oxygen.

A comprehensive paper by White[5] predates the work of Darken and Gurry. The decomposition of ferric oxide into oxygen and lower oxides of iron was studied from 1000° to 1650°C and under oxygen pressures from 2 to 76 cm of mercury. The effect of

H. LARSON, Junior Member AIME, is Metallurgist, American Brake Shoe Co., Mahwah, N. J., and J. CHIPMAN, Member AIME, is Professor, Dept. of Metallurgy, Massachusetts Institute of Technology, Cambridge, Mass.

Discussion on this paper, TP 3586C, may be sent, 2 copies, to AIME by Nov. 1, 1953. Manuscript, April 11, 1953. Los Angeles Meeting, February 1953.

The Transactions papers appearing in the Journal of Metals during 1953 will subsequently appear in AIME Transactions Volume 197, and may be permanently referenced to that volume.

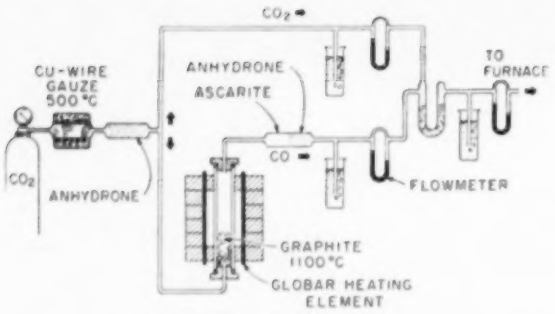

Fig. 1—Diagram of apparatus.

additions of lime and silica upon this reaction was also observed. The experimental procedure involved suspending a sample in a platinum crucible from one arm of an analytical balance. The proportions of ferrous and ferric oxides could be calculated by observing the weight loss caused by the reaction $Fe_2O_3 = 2FeO + \frac{1}{2} O_2$. Unfortunately iron dissolves in the crucible according to $FeO = Fe$ (in Pt) + $\frac{1}{2} O_2$ which causes a permanent weight loss to the system. The method used to correct for this reaction appears rather unsatisfactory. The results seem consistent in themselves, but in the pure iron-oxygen system they do not agree very well with those of Darken and Gurry. Moreover, the effect of additions of lime and silica differs from the results of this investigation.

Krings and Schackmann[6] have studied the same problem by a different procedure. They melted ferric oxide in an evacuated system and measured the oxygen pressure which resulted from its decomposition. Besides using pure ferric oxide they employed mixtures of lime and ferric oxide in the ratios 1:2, 1:1, and 2:1, and also silica and ferric oxide in a 1:1 ratio. The temperatures employed were 1550°, 1575°, and 1600°C. Their results for pure ferric oxide agree with those of Darken and Gurry better than do those of White. However, in the system lime:ferric oxide their results deviate considerably from those of both Darken and Gurry and of this investigation.

Analogous methods of slag-gas equilibria have been employed by Schuhmann and Ensio[7] and by Michal and Schuhmann[8] in studies of the thermodynamic properties of iron silicate slags.

The work of Fetters and Chipman[9] provided data at oxygen pressures corresponding to equilibrium with molten iron and served to fix the relation between slag composition and oxygen content of the metal. Their data, together with later studies of Taylor and Chipman[10] and Winkler and Chipman[11] and earlier work of Körber and Oelsen[12] provide a fairly comprehensive picture of the oxygen activity in slags which are in equilibrium with molten iron.

Experimental Method

The experimental procedure followed in these experiments is very similar to that described by Darken and Gurry.[2] The method of controlling the oxygen pressures is also similar to that used by Schuhmann and Ensio.[7]

Control of Oxygen Pressure: Air provides a constant oxygen pressure of 0.2 atm. Lower oxygen pressures were obtained through the reaction $CO + \frac{1}{2} O_2 = CO_2$, $K = p_{CO_2}/p_{CO} \cdot p_{O_2}^{1/2}$. Since the value of K is known, the oxygen partial pressure can be calculated from the CO_2/CO ratio. The most recent thermodynamic data for this reaction are available in tables published by the National Bureau of Standards[13] which are adequately represented by the expression[14]: $\text{Log } K = \frac{14.550}{T} - 4.405$.

The carbon dioxide:carbon monoxide atmosphere was prepared by starting with tank carbon dioxide containing approximately 0.09 pct oxygen, 0.07 pct water vapor, and 0.34 pct nitrogen. The carbon dioxide first passed through copper gauze maintained at 500°C to remove oxygen (Fig. 1) and then through anhydrone to remove water vapor. Since the gases were analyzed gravimetrically the presence of several tenths of a percent of nitrogen did not introduce any error in the measured CO_2/CO ratio. The gas stream then separated and one portion passed through a furnace containing graphite at 1100°C. The reaction $CO_2 + C = 2CO$ is virtually complete at this temperature; traces of carbon dioxide were absorbed in ascarite. Then both the carbon dioxide and the carbon monoxide passed through flowmeters, mixed, and passed on to the furnace containing the slag sample. The total flow amounted to between 200 and 300 cc per min.

The gas mixture was analyzed as follows: First the carbon dioxide was absorbed in a bulb containing ascarite and anhydrone, then the carbon monoxide was oxidized to carbon dioxide in a furnace containing copper oxide at 500°C, and finally the carbon dioxide so formed was absorbed in another absorption bulb containing ascarite and anhydrone. Assuming ideal behavior, the ratio of the partial pressures of carbon dioxide to carbon monoxide is equal to the ratio of the weight gains in the two absorption bulbs. The analytical train was flushed with purified nitrogen before and after taking a sample. Samples taken before and after passage through the furnace gave substantially identical results.

The gas from the graphite furnace was analyzed to determine if any hydrogen was being evolved either from hydrogen, hydrocarbons, or adsorbed water in the graphite. Less than one part of hydrogen was found per thousand parts of carbon monoxide.

Furnace: A schematic diagram of the furnace setup is shown in Fig. 2. The heating element was

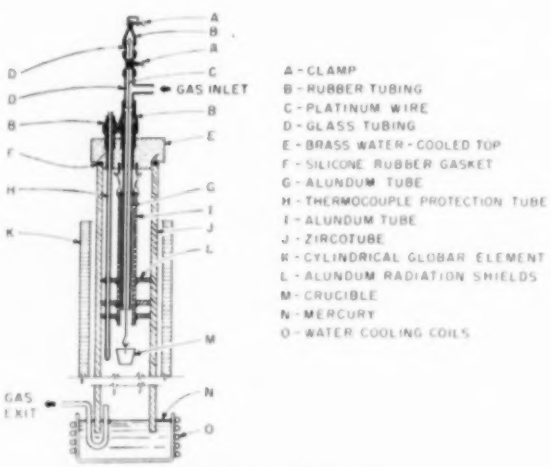

Fig. 2—Diagram of furnace.

a cylindrical globar element supplied by a motor-generator set. Inside the globar was a refractory zircotube whose dimensions were 1⅝ in. ID, ⅛ in. wall thickness and 30 in. in length. This tube was sealed at the top by a brass water-cooled head with a silicone rubber gasket. The lower seal was formed by a pool of mercury, also water cooled, which served as a means of quenching the samples.

The temperature was measured by a thermocouple inserted in a protection tube. With this arrangement it was possible to remove the thermocouple between readings, a procedure which decreased the rate of deterioration of the Pt-Pt-Rh thermocouple. The furnace temperature was controlled by another thermocouple inserted through the side of the furnace and connected through compensating lead wire to a Celectray controller. Furnace temperature was controlled to ±1°C. The temperature at the center of the furnace varied only 1°C over a length of 2 in. Since the platinum crucibles were only ½ in. in height, it was not difficult to position them properly.

The majority of these experiments were made with small platinum crucibles with a capacity of 1.3 cc. They held up very well as long as they were used in the more oxidizing atmospheres. In a reducing atmosphere the crucibles picked up appreciable amounts of iron which embrittled the platinum, and the crucibles broke when the sample was being removed. For these atmospheres smaller crucibles were made in a two-stage deep drawing process from 0.004 in. platinum foil. They were not as convenient, but they were more economical.

Procedure: The crucibles were suspended on a platinum wire, and when the slags had reached equilibrium they were quenched by being lowered rapidly until the crucible was floating in the mercury at the bottom of the refractory tube. The speed of cooling seemed important only for those slags which were melted in air. These have a tendency to pick up oxygen unless they are cooled with sufficient speed.

It was often possible to equilibrate several samples simultaneously. One advantage, of course, was that more data could be obtained in a given time. Second, since experimental conditions were the same for each sample, any discrepancies could be attributed to some factor which entered after the samples were removed from the furnace. Some of the more fluid slags could not be treated in this manner since some spilling inevitably occurred on quenching.

The sample weight varied with the type of crucible. In most of these experiments a 1 g sample was melted; in the smaller crucibles only 0.6 g was used.

In a number of preliminary experiments it was found that equilibrium was established within 1 hr. Nearly all runs were conducted for 1½ to 2 hr. It was usually possible to predict the approximate amounts of ferric and ferrous oxide which would be present in the equilibrated slags, and the appropriate amounts of the two oxides were added to the charge. This, of course, reduced the time necessary to attain equilibrium. An effort was made to have some slags in each series approach equilibrium from the oxidizing side and some from the reducing side. The attainment of equilibrium was indicated by agreement between samples obtained in this manner, see Fig. 3.

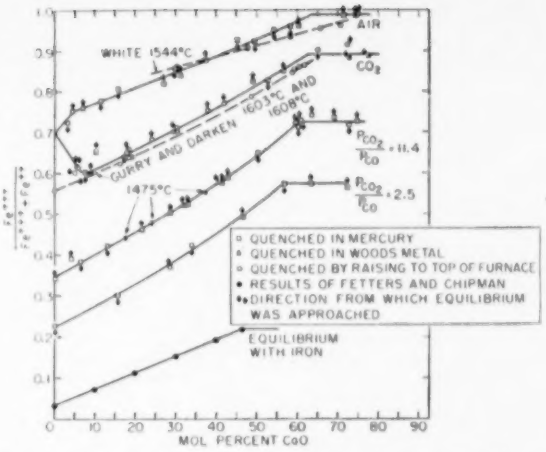

Fig. 3—Effect of atmosphere on lime-iron oxide slags at 1550°C.

Analytical Methods: Slag samples were dissolved in air-free hydrochloric acid saturated with CO_2. Usually one portion of a sample was used to determine total iron, and a second portion was titrated for ferrous or ferric oxide using $KMnO_4$ or $TiCl_3$ depending upon which oxide was present in smaller amount. At the outset, CaO was determined directly but this was done by difference in later experiments because the sum of the percentages of the iron oxides plus lime was in almost every case 100 ±0.25. Moreover in slags containing both lime and silica, the ratio of lime to silica was fixed by the composition of the three master slags, and both of these components could be determined by difference. In the iron oxide-magnesia slags, however, the magnesia content was seldom above 5 pct, and it was always determined directly.

The question arises as to whether the crushing or grinding of the slags prior to analysis oxidizes ferrous oxide to ferric oxide. Schuhmann and Ensio' report this difficulty in connection with their work on the system FeO-Fe_2O_3-SiO_2. They finally adopted a procedure of grinding to only 20 mesh, a fairly coarse size. It may be that their slags, all of which were in equilibrium with metallic iron, were particularly sensitive in this respect. In these experiments a different technique was used. The sample was crushed in a Plattner's diamond mortar to pass a 60 or 100 mesh screen. In order to reduce the tendency for the fines to oxidize by repeated crushing, the sample was crushed by a few taps with pestle and then screened. The oversize was then crushed lightly and screened again. This process was repeated six to ten times in order to crush the sample completely.

Several samples were made large enough to furnish material for several analyses. Separate portions were crushed to pass 40, 60, and 100 mesh screens. No tendency toward a higher ferric oxide content was observed in the more finely divided samples. Most of the samples were ground to pass a 60 mesh screen.

Most of the slags dissolved satisfactorily in hydrochloric acid, but those with high silica contents required the addition of a small amount of hydrofluoric acid. Even so several of the slags did not dissolve completely. The undissolved residue was fused with sodium bisulphate and analyzed for total iron. This was calculated to magnetite and the ap-

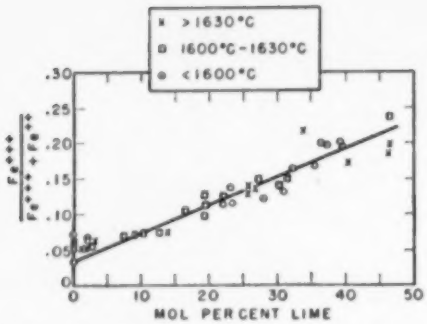

Fig. 4—$Fe^{+++}/(Fe^{+++} + Fe^{++})$ for lime-iron oxide slags in equilibrium with iron (Fetters and Chipman).

propriate amount was added to the percentages of ferrous and ferric oxide.

Lime-Iron Oxide Slags

Experimental Results: The ternary system CaO-FeO-Fe_2O_3 was studied at 1550°C under the following atmospheres: air, CO_2, $CO_2/CO = 11.4$ and $CO_2/CO = 2.50$. The corresponding oxygen pressures are 2×10^{-4}, 2.6×10^{-6}, 9.1×10^{-8}, and 4.4×10^{-7} atm. For each atmosphere lime additions were made from zero percent to lime saturation. Three slags were equilibrated at 1475°C under an atmosphere with a CO_2/CO ratio of 11.4. The slags were analyzed for FeO, Fe_2O_3, and CaO.*

* The analyses are given according to atmosphere in Table I. However, since the experimental data are completely shown in the figures, Tables I to III have been omitted. Copies of the tables may be obtained on request addressed to Professor John Chipman, Dept. of Metallurgy, MIT, Cambridge, Mass.

The analytical results expressed in weight percent were converted to mol percent, and the ratio of ferric iron to total iron was obtained. This ratio, $Fe^{+++}/(Fe^{+++} + Fe^{++})$, will hereafter be referred to by the symbol j. It is convenient to remember that j is always within 10 pct of the weight ratio, $Fe_2O_3/(Fe_2O_3 + FeO)$.

For each slag the value of j is plotted against the mol percent lime in Fig. 3. The increase of j with mol percent of added lime is roughly linear.

The experiments in a CO_2 atmosphere were the first to be performed. Most of these slag samples were quenched by being lowered to the bottom of the furnace. However, difficulty was anticipated if samples equilibrated in air were quenched in this manner. Without a more rapid quench the latter will pick up oxygen as they cool. Molten Wood's metal was the next quenching medium to be tried. Three samples were run, and the results are indicated by triangular points on Fig. 3. However, the platinum crucibles were ruined, and this method was abandoned. Mercury was next used, and the results seemed satisfactory both with respect to quenching efficiency and absence of attack on the crucibles. Mercury quenching was used for all subsequent experiments.

The discontinuity in the curves for air and CO_2 at small amounts of lime can be explained by the formation of solid magnetite. If pure iron oxide is heated to 1550°C in air or CO_2, solid magnetite is formed rather than liquid iron oxide. The melting point in air is about 1595°C and in CO_2 is about 1575°C. The composition of the solid magnetite was taken from Darken and Gurry.[9] In CO_2 magnetite has the stoichiometric composition Fe_3O_4; in air it has excess oxygen. A certain amount of lime must be added in order to flux the magnetite, approximately 4 mol pct for slags heated in air and 7 pct for those in CO_2. These phase relations can be understood more readily by referring to the ternary composition diagram in Fig. 7.

The discontinuities in the curves of Fig. 3 at high percentages of lime indicate saturation with CaO. After lime saturation is reached, further additions of lime do not change the composition of the liquid, and the j value of the liquid remains constant. The analyzed j value, i.e., j of material which was liquid at 1550°C plus excess solid lime, also remains constant since the solubility of iron oxide in lime is negligible.

The arrow beside each point indicates the direction from which equilibrium was approached. The fact that charges which were originally above and below the line fall on the same line indicates that sufficient time was allowed for equilibrium to be reached.

It was often possible to equilibrate several samples simultaneously. No attempt was made to indicate this on Fig. 3 since several different designations were already being used to indicate the method of quenching.

Comparison with Other Data: The only data of White's which can be compared with this investigation are those at 1544° with an air atmosphere. As shown in Fig. 3, the agreement is unsatisfactory.

Gurry and Darken's data at 1603° and 1608° under a CO_2 atmosphere are also shown. The dis-

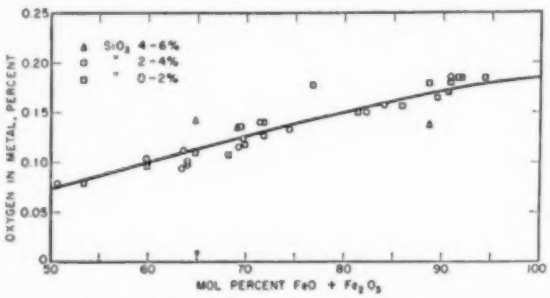

Fig. 5—Oxygen in liquid iron in equilibrium with CaO-FeO-Fe_2O_3 slags at 1550°C (Fetters and Chipman).

tance between the two lines is expected from the temperature coefficient they found for pure iron oxide melts.

Darken and Gurry found almost no temperature effect between 1550° and 1475° for pure iron oxide melted under a gas with a CO_2/CO ratio of 11.4. As indicated on Fig. 3, the addition of lime did not alter this temperature relationship.

Slags in Equilibrium with Iron: It was impossible to use an atmosphere more reducing than a CO_2/CO ratio of approximately 2.50. Iron is absorbed into the platinum crucibles according to the reaction FeO (slag) + CO = Fe (Pt) + CO_2, and in the extreme case melting of the crucibles occurs. However, data are available for slag-metal equilibria, and by appropriate calculations the data can be expressed in terms which permit extension of the present data to oxygen pressures corresponding to iron saturation.

The data of Fetters and Chipman[6] were used. They melted pure iron in an induction furnace and allowed the metal to come to equilibrium with various basic slags in the system CaO-SiO_2-FeO. Vari-

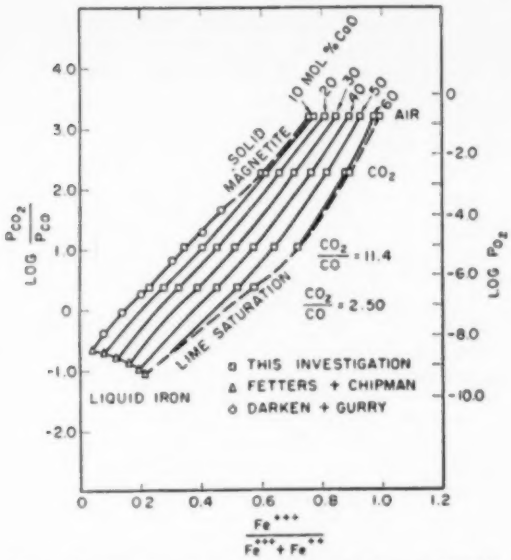

Fig. 6—Oxygen pressures in CaO-FeO-Fe_2O_3 slags at 1550°C.

ous amounts of magnesia were introduced from the magnesia crucible. From their data those slags were selected which had less than 6 pct SiO_2, the average being about 3 pct. The magnesia content varied from 5 to 12 pct with an average of about 7 pct. The j value of each slag was plotted against the mol percent of lime as shown in Fig. 4. Magnesia and silica, of course, exerted some effect, but no attempt was made to correct for them. The effect of magnesia is less than that of lime, and the magnesia and silica tend to neutralize each other. The temperature varied from 1550° to 1700°C, and the slags were divided into three groups according to temperature: less than 1600°C, 1600° to 1630°C, and greater than 1630°C. However, no temperature effect was observed; the points for the three groups are scattered at random. The j value for zero percent lime (0.034) was taken from Darken and Gurry.

The oxygen pressure or CO_2/CO ratio corresponding to each slag was calculated from the oxygen content of the metal in equilibrium with the slag. Since the data of Fetters and Chipman were obtained over a range of temperatures, it was necessary to convert their oxygen values to 1550°C. They found that the temperature coefficient of oxygen solubility in these slags was the same as under pure iron oxide slags. Therefore, it is possible to write

$$\%\ \underline{O}_{1550} = \frac{\%\ \underline{O}\ (\text{at } T)}{\%\ \underline{O}\ (\text{sat. at } T)} \times \%\ \underline{O}\ (\text{sat. at } 1550°)$$

After converting in this manner the data were plotted in Fig. 5 as % $\underline{O}$ vs $N_{FeO} + N_{Fe_2O_3}$.

The next problem is to determine what slag in the CaO-FeO-Fe_2O_3 will produce the same pct $\underline{O}$ as the impure slag for which data are available. As an example, suppose a slag has a composition of 20 pct CaO, 10 pct MgO + SiO_2, and 70 pct FeO + Fe_2O_3. There are three ways the impurities can be treated to convert this to a ternary system: 1—Ignore them and figure the composition on a silica and magnesia free basis; this gives 22 pct CaO + 78 pct FeO + Fe_2O_3. 2—Assume they act similarly to iron oxides; this gives 20 pct CaO and 80 pct FeO + Fe_2O_3. 3—Assume they act similarly to lime which gives 30 pct CaO and 70 pct FeO + Fe_2O_3. Since the oxygen in the metal is determined primarily by the iron oxide content, it seems most satisfactory to use method 3 and this has been done in constructing Fig. 5. On the other hand, lime has a much greater effect on j than does magnesia, and therefore in preparing Fig. 4, method 2 was adopted and the actual mol fraction of CaO was used.

The CO_2/CO ratio in equilibrium with oxygen-saturated iron at 1550°C according to Darken and Gurry is 0.200. The solubility is 0.185 pct and the oxygen activity is proportional to its concentration. It follows that the equilibrium constant for the reaction $\underline{O} + CO = CO_2$ is

$$K = \frac{p_{CO_2}}{p_{CO} \cdot [\%\ O]} = \frac{0.200}{0.185} = 1.08$$

This permits reading values of p_{CO_2}/p_{CO} from Fig. 5.

System CaO-FeO-Fe_2O_3: Oxygen pressures or CO_2/CO ratios throughout the liquid range of the ternary system may now be obtained by combining the data of Figs. 3, 4, and 5. The result is shown in Fig. 6 where log (CO_2/CO) and log p_{O_2} are plotted against j for slags of 0, 10, 20, 30, 40, 50, and 60 mol pct lime. The point on the zero lime curve at which solid magnetite appears was taken from the data of Darken and Gurry.[3] The same data are shown as a ternary plot in Fig. 7 as lines of constant oxygen pressure and the phase boundaries of the system at 1550°C.

Magnesia-Iron Oxide Slags

Experimental Results: Magnesia-iron oxide slags were melted at 1550°C in platinum and magnesia crucibles.† The magnesia crucibles were of two sizes, the larger 1⅛ in. high, ¾ in. OD, and slightly more than 1/16 in. in wall thickness; the smaller were ⅝ in. high, 15/32 in. OD, and slightly less than 1/16 in. in wall thickness. Thermal shock characteristics were excellent and slag penetration was slight. During the course of a 3 or 4 hr experiment the slag would become saturated with magnesia, and iron oxide would penetrate the crucible wall to a depth of approximately 1/32 of an inch.

When the larger magnesia crucibles were used, several distinct layers could be seen in the sample.

† Results are shown in Table II which also gives the analyses of the various slag layers referred to below. See footnote on p. 1092.

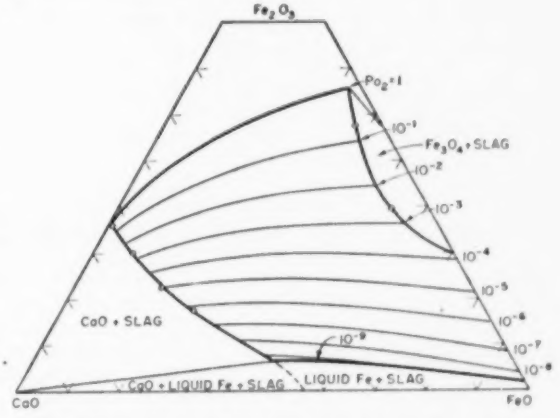

Fig. 7—Section of the ternary system at 1550°C showing oxygen pressures. Coordinates are mol fractions.

As shown in Fig. 8, they consisted of: 1—the portion of the crucible wall penetrated by iron oxide; 2—a layer which is probably a magnesia-wüstite solid solution; and 3—the portion of the sample which was liquid at temperature. The second and third layers broke away from the crucible wall quite easily. Portions of the crucible wall, which included zone 1, could be analyzed for the ratio of ferric to ferrous oxide. In several experiments it was possible to separate the two inner layers; either layer 3 could be ground away from layer 2 or vice versa.

As long as the solid solution layer (2) is completely removed from the slag layer (3), the latter sample will be representative of the material which

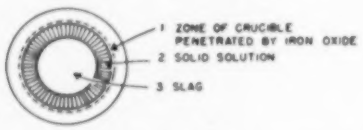

Fig. 8—Phases present after experiments in magnesia crucibles.

was liquid at 1550°C. However, the composition of the solid solution varies, and the composition of the sample taken from this layer depends upon how much of it was removed in the process of grinding away layer (2). Thus these values are only approximate averages.

The results of all experiments on magnesia slags are shown in Fig. 9 where the j value is plotted against mol percent MgO. The solubility of MgO is indicated by a vertical line at about 8.7 mol pct. This corresponds to the analyses of slags melted in the large magnesia crucibles; it is evident that slags from the smaller magnesia crucibles contained portions of zone 2. The solubility limit indicated also corresponds to intersections of the two branches of the series at CO_2/CO ratios 11.4 and 2.50.

Discussion: It is evident that MgO increases the value of j less strongly than does lime. This is in keeping with its generally weaker basic properties. At the high values of j associated with CO_2 atmospheres, the slags were solid or semisolid. It seems probable that magnetite occurred but the composition of this phase and its relation to other solid phases in the system remain unknown.

Referring again to Fig. 3, the conclusions regarding magnesia-iron oxide slags are summarized as follows: The liquid slag, zone 3, contains a maximum of about 8.7 mol pct MgO and its j value is higher than that of simple iron oxide slag. Zone 2 is a solid solution built up on the inner wall of the refractory; its j value is only slightly higher than that of the slag. Zone 1, the area of penetration, has a slightly lower j value.

Lime-Silica-Iron Oxide Slags

Experimental Results: Equilibrium in lime-silica-iron oxide slags was studied at 1550°C in a manner similar to that already described for lime-iron oxide slags. The same four atmospheres were used: air, CO_2, CO_2/CO = 11.4, and CO_2/CO = 2.50. Three master slags were prepared which had molar lime: silica ratios of 0.540, 1.306, and 2.235. Iron oxide was added as a mixture of ferrous and ferric oxide in proportions approximating the expected equilibrium composition. This, of course, decreased the time necessary to attain equilibrium.

The slags were analyzed for ferrous and ferric oxides and lime-plus-silica was determined by subtracting the sum of the iron oxides from 100. Occasional slags were analyzed completely and the lime: silica ratios agreed adequately with those of the master slags.

The experimental results‡ are presented in Figs. 10 to 13 as the ratio j against the mol percent of lime-plus-silica, the sum of these two at constant ratio being treated as a single component.

‡ Results are also listed in Table III. See footnote on p. 1092.

1—Lime:Silica Ratio 0.540. This system was studied from pure iron oxide to 100 pct lime plus silica. The results at low amounts of lime plus silica appear rather precise, but with larger amounts they show considerably more scatter.

These slags were the most difficult to analyze of those investigated. In several samples part of the iron oxide remained undissolved even with the addition of hydrofluoric acid. This insoluble portion was fused and analyzed for iron which was calculated as magnetite.

In Figs. 10 to 13 similar symbols along any one curve, except open circles, designate slags which were equilibrated simultaneously; open circles designate single samples. If one sample of a group deviates from the curve more than the others, the reason must be in either crushing or analysis. Any error in temperature, atmosphere, or quenching should produce a consistent error in all the slags in the group.

2—Lime:Silica Ratio 1.306. This system could

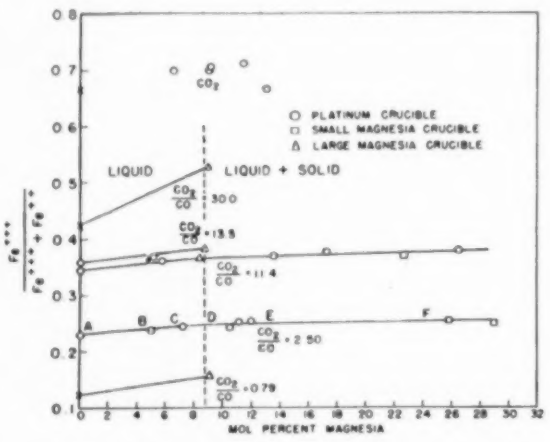

Fig. 9—Effect of atmosphere on magnesia-iron oxide slags at 1550°C.

also be studied from pure iron oxide to pure lime-plus-silica. Again the results at low concentrations of lime and silica are relatively consistent, while those at higher concentrations are not. The j value passes through a maximum, and the position of the maximum shifts toward pure iron oxide as the atmosphere becomes more reducing.

3—Lime:Silica Ratio 2.235. According to the FeO-CaO-SiO_2 phase diagram, the slags become saturated with dicalcium silicate when the lime-plus-silica is greater than approximately 50 pct. Charges were made to exceed this saturation value but there is no break in any of the curves. Samples

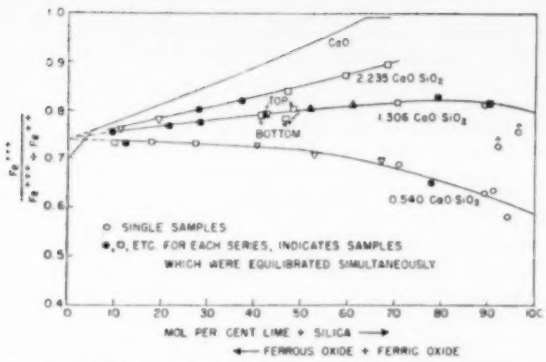

Fig. 10—Equilibria in lime-silica-iron oxide slags at 1550°C, air atmosphere.

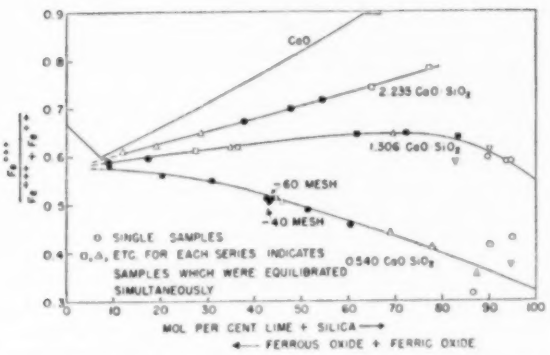

Fig. 11—Equilibria in lime-silica-iron oxide slags at 1550°C, CO_2 atmosphere.

286 and 287 are the top and bottom portions of a sample equilibrated under a CO_2/CO ratio of 2.50. If dicalcium silicate had precipitated, it should have segregated either at the top or the bottom of the crucible. Although some mixing probably occurred upon quenching, it was expected that the j ratio of the two layers would be the same even if the total amount of iron oxide differed. This is analogous to the situation which prevails when lime saturation is reached in lime-iron oxide slags. However, according to Fig. 13 neither the ratio nor the total amount of the two iron oxides were the same. Surprisingly both points fall equally well on the curve through the other points for that series. It seems likely that a solid phase is present which contains iron oxide in which the proportions of ferrous and ferric oxide are only slightly different from that in the liquid.

Bowen, Schairer, and Posnjak[15] have determined the phase diagram for the system $2CaO \cdot SiO_2$-$2FeO \cdot SiO_2$. At the dicalcium silicate end of the diagram solid solutions are present which contain up to 10 pct iron silicate. Although the effect of large amounts of ferric oxide is unknown, the possibility remains that some other solid phase than dicalcium silicate is present.

Under an air or CO_2 atmosphere at 1550°C pure iron oxide exists as solid magnetite. However, for each of the lime:silica ratios the addition of 10 mol pct lime plus silica was sufficient to produce a single liquid phase. No attempt was made to determine the actual boundary of the magnetite field.

The ability of a particular oxide or group of oxides to increase the ratio of ferric iron to total iron can be taken as a measure of the basicity of the oxides. Lime is a strong base and increases this ratio. Silica is a strong acid and has an almost equal ability to decrease the ratio. As indicated by Figs. 10 to 13, various combinations of lime and silica have intermediate effects. Of the slags studied those with a lime:silica ratio of 1.306 are the closest to neutrality as far as this criterion is concerned.

The System CaO-SiO_2-FeO-Fe_2O_3: Data are available for slags in equilibrium with iron which have the same lime:silica ratios as those used in the present investigation. The data of Fetters and Chipman[9] and of Taylor and Chipman[10] were used respectively for the more basic and the more acid slags. Graphical interpolation was used to determine the oxygen contents of metal (hence p_{O_2}) and j values for the slags along lines of constant lime-silica ratio.

The experimental data of this investigation and the data for slags in equilibrium with iron were plotted on curves similar to that of Fig. 4. Compositions at various oxygen pressures were determined, and these are plotted on the ternary composition triangle of Fig. 14. By interpolating between these curves it is possible to determine the oxygen pressure of any slag in the lime-silica-iron oxide system with a lime:silica ratio of 0.540 to 2.235 up to lime saturation.

Iron Oxide Slags with Other Additions

Iron oxide slags with additions of barium oxide, silica, manganese oxide, alumina, and titania were equilibrated under an atmosphere of CO_2/CO = 11.4 at a temperature of 1550°C. The experimental

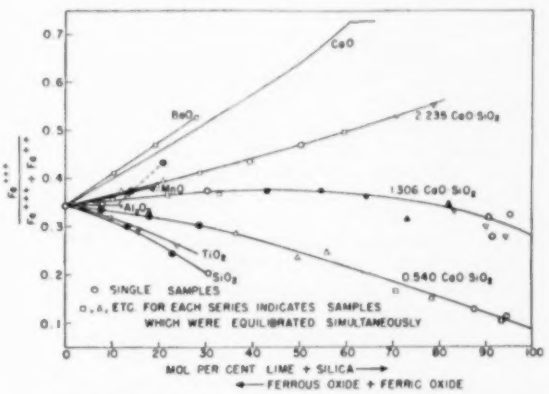

Fig. 12—Equilibria in iron oxide slags with various additions at 1550°C. CO_2/CO=11.4.

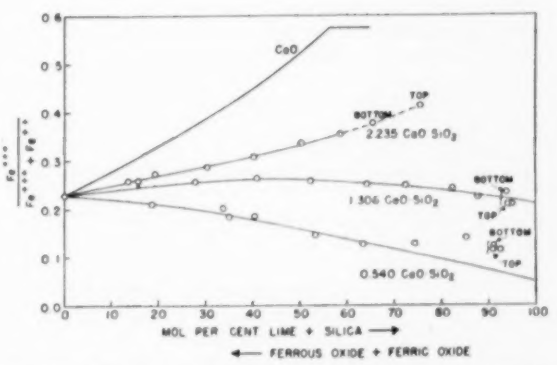

Fig. 13—Equilibria in lime-silica-iron oxide slags at 1550°C. CO_2/CO=2.50.

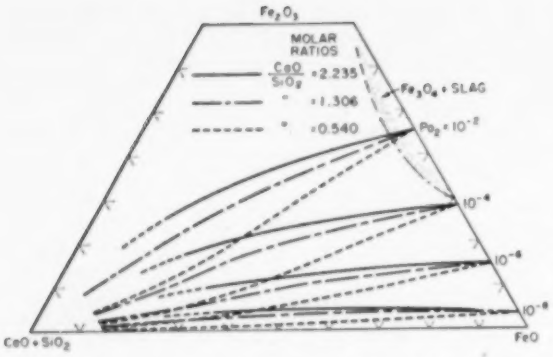

Fig. 14—Oxygen pressures in slags containing CaO, SiO_2, FeO, and Fe_2O_3.

results are plotted in Fig. 12 as j against mol percent added oxide.

The results for barium oxide, silica, and titania additions are such as would be expected from their usual chemical behavior. Barium oxide is somewhat more basic than lime. Titania and silica are both acidic with silica being somewhat stronger.

The effect of manganese oxide additions, however, is rather surprising. Gurry and Darken[3] report that manganese oxide is only slightly less basic than lime. This conclusion seems warranted from a comparison of their data for lime and manganese oxide additions at 1600°C under a CO_2 atmosphere. From the results of the present investigation, manganese oxide would be placed in a class with magnesia which has a much smaller effect than lime. Although only two samples with manganese oxide additions were obtained, their two points and the point for pure iron oxide lie on an easily defined curve. Also since these results were obtained immediately between the results for barium oxide and titania additions, both of which are apparently satisfactory, a major error in temperature or atmosphere control was improbable.

The results for alumina additions require some explanation. Since alumina is usually considered to have a weakly acidic effect, the first point at 8 mol pct Al_2O_3 appears reasonable. Actually it seems to be exactly neutral as far as its effect on the ratio of ferric to total iron is concerned. Moreover, this sample was equilibrated simultaneously with the sample containing 30 mol pct SiO_2, and the latter sample agrees with the others containing silica additions.

The other two alumina points define a line which deviates sharply from the line between the point for pure iron oxide and the first alumina point. This effect is not an analytical error. The samples having 8 and 14 mol pct Al_2O_3 were reanalyzed for total iron, and the figure obtained agrees very well with that from the first analysis. Also experiments before and after under the same atmosphere were satisfactory.

According to the phase diagram for the system FeO-Al_2O_3 determined by McIntosh, Rait, and Hay,[16] saturation with pure alumina occurs at about 27 pct Al_2O_3. Therefore, all of the present slags should lie well within the liquid region. However, both experimental and circumstantial evidence support the conclusion that the two high alumina slags are in a liquid-plus-solid region. The 20 mol pct Al_2O_3 sample was porous, had a rough uneven surface and fell out of the crucible in one piece. This might indicate that the sample had sintered rather than melted.

No diagram is available for the Fe_2O_3-Al_2O_3 system, but the two oxides are isomorphous in various naturally occurring minerals, particularly in spinels. Chromium trioxide, also similar in crystal structure and lattice constants, forms a continuous series of solid solutions with alumina. The compound hercynite, FeO · Al_2O_3, is formed in the FeO-Al_2O_3 system. Perhaps in the ternary system FeO-Fe_2O_3-Al_2O_3 this compound has a variable composition in which the ferric oxide replaces part of the alumina. The solid phase present may be either such a compound or a simple solid solution of Fe_2O_3 in Al_2O_3.

Summary

This paper covers a study of equilibrium between slags containing iron oxide and gases consisting of air or mixtures of CO_2 and CO. Together with earlier data on equilibrium between similar slags and molten iron, the results establish the value of $j = (Fe^{+++})/(Fe^{+++} + Fe^{++})$ over a range of oxygen pressures from 10^{-1} to 10^{-8} atm.

The value of j is strongly increased by additions of CaO and to a lesser degree by MgO. In slags containing CaO + SiO_2 the value of j is increased by additions in which the molar ratio (CaO)/(SiO_2) is 2.2 or 1.3 and decreased when the ratio is 0.54. For other additions the effect of basic oxides, e.g., BaO, is to increase j while acid oxides such as SiO_2 and TiO_2 have the opposite effect.

Oxygen activities at 1550°C are shown graphically for the ternary system CaO-FeO-Fe_2O_3 and for three pseudo-ternaries (CaO + SiO_2)-FeO-Fe_2O_3. The data cover slag compositions which are more or less similar to those at the slag-gas interface in the open hearth furnace.

Acknowledgments

The authors wish to thank D. L. Guernsey and his associates for the analytical work, and the Republic Steel Corp. for a fellowship grant which made the research possible.

References

[1] L. S. Darken and R. W. Gurry: *Journal* ACS (1945) **67**, p. 1398.
[2] L. S. Darken and R. W. Gurry: *Journal* ACS (1946) **68**, p. 798.
[3] R. W. Gurry and L. S. Darken: *Journal* ACS (1950) **72**, p. 3906.
[4] L. S. Darken: *Journal* ACS (1948) **70**, p. 2046.
[5] J. White: *Journal* Iron and Steel Inst., London. *Carnegie Scholarship Memoirs* (1938) **27**, p. 1.
[6] W. Krings and H. Schackmann: *Ztsch. Electrochemie* (1935) **41**, p. 479.
[7] R. Schuhmann and P. J. Ensio: *Trans.* AIME (1951) **191**, p. 401; JOURNAL OF METALS (May 1951).
[8] E. J. Michal and R. Schuhmann, Jr.: *Trans.* AIME (1952) **194**, p. 723; JOURNAL OF METALS (July 1952).
[9] K. L. Fetters and J. Chipman: *Trans.* AIME (1940) **140**, p. 170.
[10] C. R. Taylor and J. Chipman: *Trans.* AIME (1943) **154**, p. 228.
[11] T. B. Winkler and J. Chipman: *Trans.* AIME (1946) **167**, p. 111; METALS TECHNOLOGY (April 1946).
[12] F. Körber and W. Oelsen: *Mitt Kaiser Wilhelm Inst. Eisenforsch.* (1932) **14**, p. 181; (1933) **15**, p. 280.
[13] *Selected Values of Chemical Thermodynamic Properties.* National Bureau of Standards (1947).
[14] *Basic Open Hearth Steelmaking.* Revised Edition (1951) AIME.
[15] N. L. Bowen, J. F. Schairer, and E. Posnjak: *American Journal of Science* (1933) Series 5, **25**, p. 273.
[16] A. B. McIntosh, J. R. Rait, and R. Hay: *Journal* Royal Technical College, Glasgow (1937) **4**, p. 72.

Constitution of the FeO-Fe_2O_3-SiO_2 System At Slagmaking Temperatures

by R. Schuhmann, Jr., R. G. Powell, and E. J. Michal

Liquidus surfaces in the ternary system FeO-Fe_2O_3-SiO_2 were determined from 1250° to 1450°C by the procedure of equilibrating small samples in platinum crucibles, quenching, and microscopic examination. The experimental results were combined with previously published information to construct a ternary diagram for the system showing the entire temperature-composition range of stability of iron silicate slags. Metallurgical applications of the diagram, especially in copper smelting, are discussed briefly.

IRON oxides are almost unique among the common oxide constituents of metallurgical slags in that the iron occurs in two different states of oxidation, ferrous and ferric. Moreover, in liquid slags the degree of oxidation of the iron is readily changed by reactions of the slags with oxidizing agents or reducing agents. This behavior of iron oxides in slags accounts, for example, for the effective transfer of large quantities of oxygen through slag layers in open hearth steelmaking. In this process, oxygen supplied by reactions at the gas-slag interface is dissolved in the slag with the oxidation of ferrous iron to ferric. Ferric oxide is transported across the slag layer by convection, and at the slag-metal interface the oxygen reacts with liquid metal while the ferric iron is reduced back to the ferrous state. Another group of processes in which variation in degree of oxidation of iron has great practical importance is in copper smelting. In matte smelting and converting, such large proportions of the iron are oxidized to the ferric state that problems are encountered in preventing or controlling the formation of solid magnetite. The ferrous-ferric relationship also affects the attack of iron oxides on high-SiO_2 refractories, which appears to be most severe under reducing conditions for which ferrous iron predominates.

Darken and Gurry[1] determined the chemical properties and phase equilibria of pure iron oxide slags. Their data show that iron oxide melts can have compositions ranging almost all the way from FeO to Fe_2O_3. The melts of lowest oxygen contents, which exist in equilibrium with metallic iron, approach ferrous oxide in composition but still have a small percentage of ferric oxide. The melts of highest oxygen contents, which have oxygen dissociation pressures of 1 atm, are above magnetite in oxygen content, with over two-thirds of the iron in the ferric state.

The previously established phase diagrams for silicate slag systems all show FeO as the iron oxide component. However, Bowen and Schairer,[2] who determined the FeO-SiO_2 diagram and many of the other diagrams used by slag chemists, have been careful to point out that their systems always contained both ferrous and ferric iron. Thus, their data are for limiting mixtures with minimum contents of ferric iron, obtained by melting and equilibration in iron crucibles. Under these conditions, the Fe_2O_3 percentages found by analysis were small enough to justify simplification of the published phase diagrams by calculating the Fe_2O_3 to equivalent FeO and ignoring Fe_2O_3 as an additional component.

On the basis of experimental measurements of melting points of iron oxides on silica in the presence of various gas mixtures, Darken[3] worked out phase diagrams for the Fe-Si-O system which show the important phase equilibria in terms of temperature and gas composition. This study clarified many aspects of the application of the phase rule to the FeO-Fe_2O_3-SiO_2 system and was an important basing

R. SCHUHMANN, JR., Member AIME, is Associate Professor of Metallurgy, Massachusetts Institute of Technology, Cambridge, Mass., R. G. POWELL is a Staff Member of the Division of Industrial Cooperation, Massachusetts Institute of Technology, and E. J. MICHAL, Junior Member, AIME, is Research Metallurgist, National Lead Co., South Amboy, N. J.

Discussion on this paper, TP 3587D, may be sent, 2 copies, to AIME by Nov. 1, 1953. Manuscript, Jan. 13, 1953. New York Meeting, February 1952.

This paper is based on a thesis submitted by R. G. Powell in partial fulfillment of requirements for the degree of Master of Science to Massachusetts Institute of Technology.

point for the work described in the present paper.

The experimental work to be described in this paper consisted primarily in the determination of the liquidus surfaces in the FeO-Fe_2O_3-SiO_2 system, especially the three liquidus surfaces corresponding to equilibria with magnetite, wüstite, and silica (tridymite) respectively. By combining these new data with available data for other parts of the ternary system, a ternary diagram was developed which shows the entire temperature-composition range of stability of iron silicate slags containing both ferrous and ferric iron. Applications of this phase diagram are discussed briefly.

Experimental Methods

The experimental procedure was similar to that used by Bowen and Schairer[3] in studying the FeO-SiO_2 system and consisted in equilibration of known mixtures of FeO, Fe_2O_3, and SiO_2 at constant temperature, quenching to room temperature, and microscopic study of the quenched specimens to determine the phases present.

Materials: The primary starting materials were ferric oxide (Baker's chemically pure reagent), hydrogen-reduced iron powder (Mallinckrodt), precipitated silica, and Armco iron crucibles. From these materials, secondary stocks were prepared of fayalite slag (approximately $2FeO:SiO_2$ in composition), wüstite slag, and magnetite. These three secondary stocks with precipitated silica were mixed in appropriate quantities to obtain 10 to 20 g each of 76 experimental mixtures. Each of these experimental mixtures was homogenized by heating to 1450° to 1500°C in nitrogen in a platinum crucible, quenching, grinding to minus 65 mesh, and mixing. When complete fusion did not occur, this homogenization treatment was repeated two more times. The final mixtures were analyzed for FeO, Fe_2O_3, and SiO_2, and the subsequent equilibrations were conducted on small portions of these analyzed mixtures.

Apparatus: The equilibration experiments were made in a platinum-wound furnace provided with an automatic temperature controller. The furnace was of standard design, built around a vertical Alundum tube 24 in. long x 3 in. ID. Six closely spaced porcelain tubes, 42 in. long x ⅝ in. OD, passed through this furnace and provided for simultaneous and independent equilibration of six different samples at a time. A mercury bath sealed the lower ends of these porcelain tubes. Rubber stoppers were used on the upper ends. During the runs a stream of over 10 ml N_2 per min flowed through each tube. A positive pressure of 2 to 3 mm Hg was maintained in each tube by discharging the exit nitrogen under glycerine. The nitrogen fed to the tubes was purified in a train including ascarite, drierite, and anhydrone absorption tubes and a deoxidizing furnace containing hot copper gauze.

The experimental mixtures were held in homemade platinum crucibles, ⅜ in. high x ¼ in. in diameter and with a capacity of about 0.5 g of solids. Each crucible was suspended in a furnace tube by a fine platinum wire, brought out through a glass tube with a simple rubber-tubing and screw-clamp seal mounted in the rubber stopper at the upper end of the tube.

Temperatures were measured with a Pt, Pt-Rh thermocouple whose junction was located in one of the furnace tubes at the same level as the samples. Temperature explorations in the furnace tubes indicated that the reported temperatures represented actual sample equilibration temperatures to within about 3°C.

Procedure: The plan of experimentation involved the determination of five isothermal sections of the FeO-Fe_2O_3-SiO_2 system, at 1250°, 1300°, 1350°, 1400°, and 1450°C, respectively. At each of these temperatures a number of the experimental mixtures were brought to equilibrium, quenched, and studied microscopically. The studies were continued systematically at each temperature until sufficient data were available to locate the boundary curves of the melt field and to locate the lines separating the two-phase and three-phase fields.

First the furnace was brought to the desired temperature and flushed with nitrogen gas. Then the platinum crucibles were quickly introduced and suspended in the lower cold ends of the furnace tubes for at least 15 min of flushing with nitrogen to insure elimination of oxygen. After this flushing, the samples were pulled up into place in the hot zone of the furnace. Most of the points were checked by repetition of the equilibrations for different lengths of time. When the mixture fused or formed a substantial quantity of a liquid phase, equilibrium was attained quite rapidly and the runs were made for periods of 30, 60, and 90 min. Longer periods were used when the mixtures yielded little liquid phase. At the end of the run, the sample was quenched in the upper cold end of the furnace tube. This type of cooling did not prevent crystallization of the melt phase, especially at high iron contents, but no difficulty was experienced in differentiating primary crystals from the finer crystals and dendrites formed during cooling. Originally the samples were folded in platinum foil and quenched in mercury, but this technique proved troublesome with the most fluid melts and was little better than the simple cooling procedure in preventing partial crystallization of the liquid phase.

The quenched samples were broken out of the crucibles and crushed lightly. The large grains thus obtained were mounted in bakelite, and polished sections were prepared for microscopic examination. The sections were examined by reflected light using a standard metallurgical microscope. For the mixtures investigated, the phases present at the equilibration temperatures included liquid, wüstite, magnetite, and silica (tridymite). Primary tridymite and primary magnetite were readily recognized in the quenched samples both from their well-developed crystalline habits and from their reflectivities. The identification of the primary silica phase as tridymite was checked by refractive index measurements on loose grains, using the immersion technique. Wüstite grains quenched to a light gray, usually heterogeneous-looking structure. Some wüstite grains were rimmed with magnetite, others were peppered with small crystals of secondary magnetite, apparently formed during cooling. The quenching behavior of the melt phase varied considerably with composition. In some instances a dark gray glass was observed, but more commonly some sort of fine structure developed in the glass during the cooling. Many of the quenched melts were penetrated by very fine dendrites of magnetite. Some of the more silicious melts showed tiny rosettes of silica. A few typical structures are shown in Fig. 1.

Iron Absorption by Platinum Crucibles: The mixture analyses eventually used in plotting the equilibrium diagrams were the chemical analyses of the

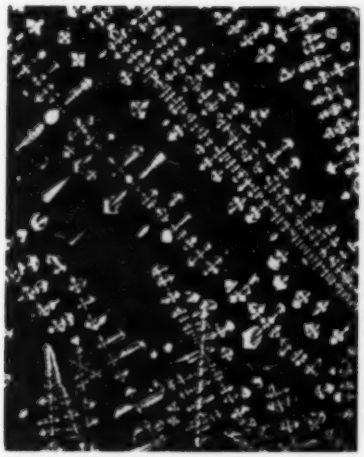

Fig. 1a—Quenched melt, showing magnetite dendrites formed in cooling. 47.0 pct FeO, 24.5 pct Fe_2O_3, and 28.5 pct SiO_2, equilibrated at 1350°C. X500. Area reduced approximately 50 pct for reproduction.

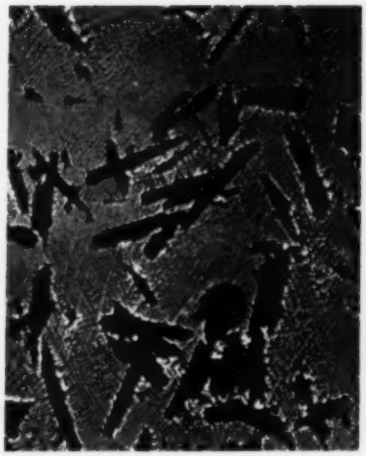

Fig. 1b—Primary tridymite plus melt, with dendrites formed during cooling. 45.0 pct FeO, 20.3 pct Fe_2O_3, and 34.7 pct SiO_2, equilibrated at 1350°C. X150. Area reduced approximately 50 pct for reproduction.

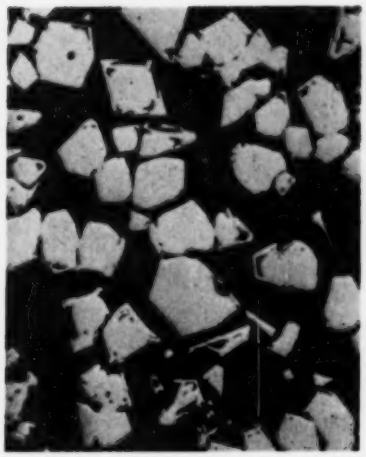

Fig. 1c—Primary magnetite and melt. 55.8 pct FeO, 29.1 pct Fe_2O_3, and 15.1 pct SiO_2, equilibrated at 1350°C. X150. Area reduced approximately 50 pct for reproduction.

Fig. 1d (left)—Primary tridymite, primary magnetite, and melt. 44.1 pct FeO, 26.4 pct Fe_2O_3, and 29.5 pct SiO_2, equilibrated at 1350°C. X150. Area reduced approximately 50 pct for reproduction.

Fig. 1e (right)—Primary wustite (partly decomposed) and melt, with wustite dendrites formed during cooling. 70.0 pct FeO, 23.3 pct Fe_2O_3, and 6.7 pct SiO_2, equilibrated at 1350°C. X150. Area reduced approximately 50 pct for reproduction.

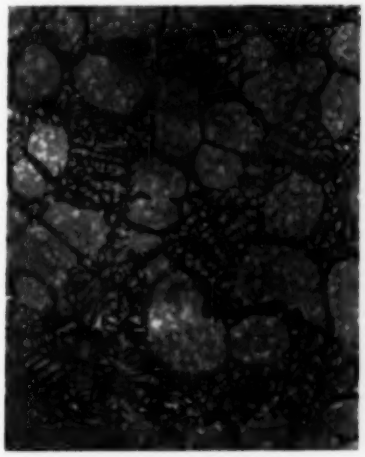

powdered experimental mixtures after the homogenization treatment but before equilibration. Accordingly, the principal sources of error in the final data were the changes in composition which occurred when the small samples were equilibrated in platinum crucibles. Analysis of the contents of each crucible after equilibration would have been desirable, of course, but this procedure was not adopted because it would have required a larger scale of experimentation with high platinum consumption and would have multiplied the analytical work.

The changes in composition during the equilibration runs were studied in a preliminary group of tests on five representative mixtures, and the results of these tests are summarized in Table I. Two series of tests were run for 1 hr at 1300° and 1400°C, respectively, with new platinum crucibles for each test. These crucibles and samples were weighed separately before use. After the equilibration tests, the crucibles were cleaned and reweighed. A third series of tests were then made with used crucibles, each crucible having been used once with the same mixture so that some opportunity was afforded for the crucibles to approach equilibrium with the various mixtures. In all cases, it can be seen that heating the mixtures in the nitrogen atmosphere and in the platinum crucible caused a decrease in the percentage of FeO, a comparable increase in the percentage of Fe_2O_3, and little change in the percentage of SiO_2. The increase in crucible weight is accounted for by transfer of iron from the mixture to the crucible in accordance with the reaction.

$$3FeO \text{ (in mixture)} \rightarrow Fe_2O_3 \text{ (in mixture)} + Fe \text{ (solid solution in Pt)}$$

To confirm this interpretation, the analyses of the various mixtures after equilibration were calculated from the weights and analyses of the original mixtures assuming that the increase in crucible weight represented iron transferred to the crucible in accordance with the chemical equation given above. These calculated analyses are given in parentheses in Table I, and are seen to check the actual analyses reasonably well when the various experimental difficulties in analyzing small samples and in cleaning the crucibles are considered. To eliminate the possibility that the composition changes might also reflect pickup of oxygen, a number of tests were made with weighed, empty Armco iron crucibles and with weighed rolls of copper gauze. These showed negligible weight increases in expo-

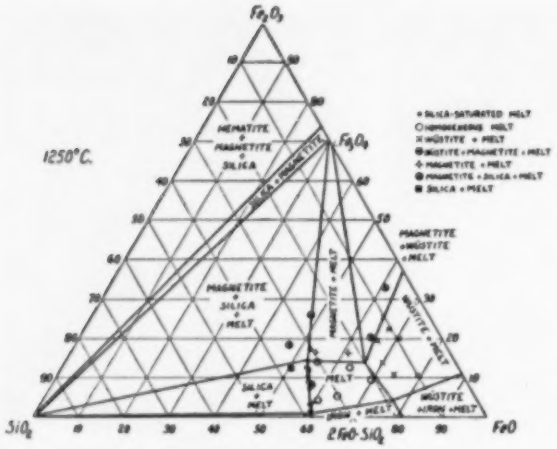

Fig. 2—1250°C isothermal section.

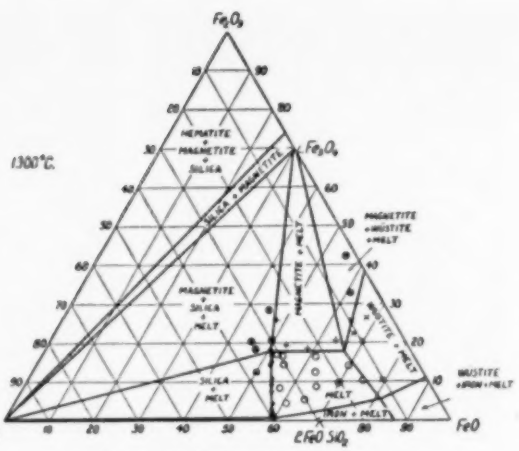

Fig. 3—1300°C isothermal section.

sures up to several hours.

On the basis of the results just discussed, it was decided to conduct all final equilibrations in crucibles which had been used at least once before with the same mixture. In the tests with once-used crucibles reported in Table I, the average change in composition was a decrease of about 2.2 pct FeO and a similar increase in the percentage of Fe_2O_3, and the maximum change was a 3.3 pct decrease in FeO and corresponding increase in Fe_2O_3. Accordingly, it is probable that the final results are subject to systematic errors of the order of +1 to +3 pct FeO and −1 to −3 pct Fe_2O_3.

Silica Liquidus: Experimental work on equilibria of silica-saturated iron silicate slags was reported in an earlier paper by two of the authors.[4] This earlier paper includes numerous analyses of iron silicate slags in equilibrium with solid silica at various temperatures, which afford determinations of points on the silica liquidus by a different and more refined technique than that of the work reported in the present paper. Also, in the work reported earlier, special pains were taken to determine the composition of slags saturated with respect to both solid silica and solid magnetite, and these data also were given major weighting in preparing the constitution diagrams to be discussed subsequently.

Results

The experimental results are plotted in the five isothermal sections, Figs. 2 to 6. For each composition studied by equilibration, quenching, and microscopic examination, the observed combination of phases is indicated by the different symbols as shown in the legend. In the 1250°, 1300°, and 1350°C isotherms, the compositions of silica-saturated liquids determined during gas-slag equilibrium studies in silica crucibles[4] are also plotted, and in this temperature range it can be seen that results of the two very different experimental methods are quite consistent. No new data were obtained in this investigation on the liquids in equilibrium with solid iron, since these compositions have already been studied thoroughly and are well established except

Table I. Composition Changes During Equilibration Tests in Platinum Crucibles

Mixture No.	Description of Equilibration Test	Sample Weight, Grams	Increase in Crucible Weight, Mg	Analyses,* Wt Pct FeO	Fe_2O_3	SiO_2
3		Original Analysis		63.60	12.59	23.81
	New crucible, 1 hr at 1300°C	0.502	8.1	58.29	17.68	24.03
				(58.4)	(17.4)	(24.2)
	New crucible, 1 hr at 1400°C	0.572	10.7	56.91	19.07	24.02
				(57.4)	(18.3)	(24.3)
	Used crucible,† 1 hr at 1400°C			61.07	14.78	24.15
4		Original Analysis		53.84	19.19	26.97
	New crucible, 1 hr at 1300°C	0.556	4.7	51.86	20.96	27.18
				(51.0)	(21.8)	(27.2)
	New crucible, 1 hr at 1400°C	0.550	7.5	50.70	22.18	27.12
				(49.3)	(23.4)	(27.3)
	Used crucible,† 1 hr at 1400°C			52.42	21.04	26.54
7		Original Analysis		55.81	29.11	15.08
	New crucible, 1 hr at 1300°C	0.605	6.6	52.67	31.77	15.46
				(52.1)	(32.6)	(15.3)
	New crucible, 1 hr at 1400°C	0.637	7.9	51.42	33.38	15.20
				(51.7)	(33.0)	(15.3)
	Used crucible,† 1 hr at 1400°C			54.70	30.22	15.08
10		Original Analysis		69.73	13.98	16.29
	New crucible, 1 hr at 1300°C	0.573	12.0	65.11	18.18	16.71
				(63.0)	(20.4)	(16.6)
	New crucible, 1 hr at 1400°C	0.457	10.1	61.45	22.04	16.51
				(62.4)	(20.9)	(16.7)
	Used crucible,† 1 hr at 1400°C			66.48	17.31	16.21
11		Original Analysis		57.54	8.35	34.11
	New crucible, 1 hr at 1300°C	0.504	5.7	54.30	11.29	34.41
				(53.8)	(11.7)	(34.5)
	New crucible, 1 hr at 1400°C	0.401	6.9	52.40	13.48	34.12
				(51.8)	(13.5)	(34.7)
	Used crucible,† 1 hr at 1400°C			55.16	10.70	34.14

* Analyses in parentheses were calculated from original mixture analysis, sample weight and weight increase of platinum assuming the reaction: 3FeO (sample) = Fe_2O_3 (sample) + Fe (crucible).
† Used once with same experimental mixture.

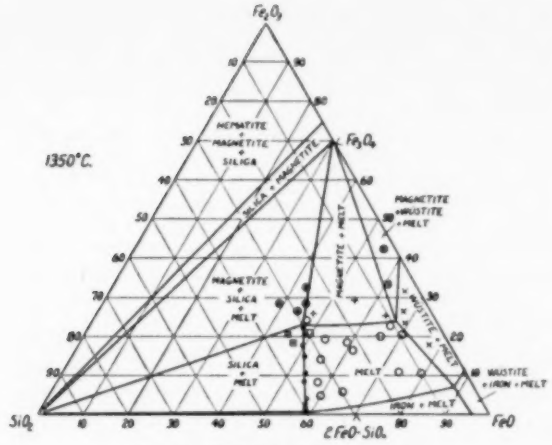

Fig. 4—1350°C isothermal section.

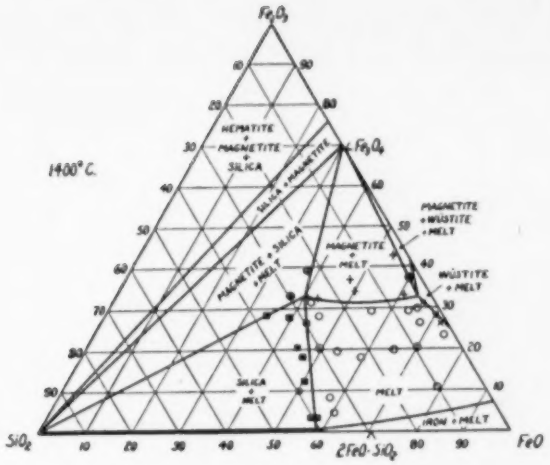

Fig. 5—1400°C isothermal section.

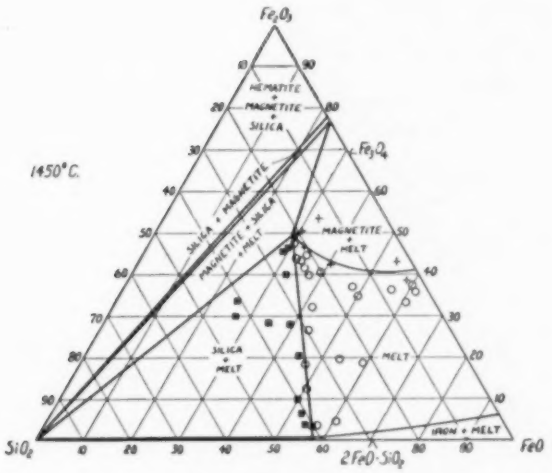

Fig. 6—1450°C isothermal section.

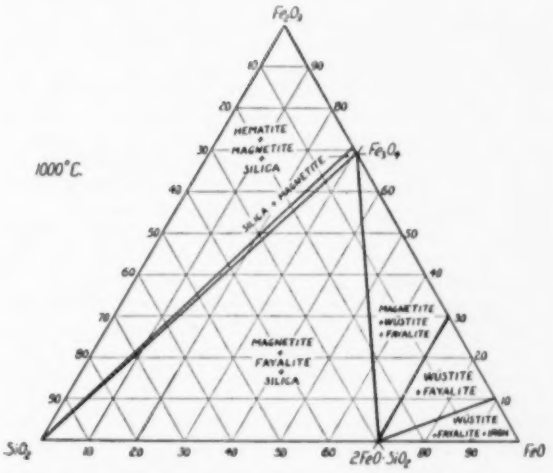

Fig. 7—1000°C isothermal section, based on binary systems.

for small uncertainties in Fe_2O_3 content.[2, 5] The points along the FeO-Fe_2O_3 edges of the isothermal sections are taken from the Fe-O diagram of Darken and Gurry.[3]

The final locations and shapes given to the melt field boundaries in Fig. 2 to 6 in some instances deviate a little from the curves of best fit with the experimental data. These deviations are the result of smoothing the data for the ternary system as a whole in accordance with the phase rule to eliminate minor discrepancies between the different sets of data on which diagrams are based.

In the figures and subsequent discussion, the solid silica phase is referred to simply as silica, although, strictly speaking, tridymite is the stable form of silica from 870° to 1470C°, and cristobalite is the stable form from 1470°C to the melting point. As pointed out by Darken,[2] changes in the crystalline form of silica have very minor effects on the equilibrium data under consideration.

Lower Temperature Isotherms: No equilibrium studies below 1250°C were made in the present investigation so that no new data were obtained directly measuring the fayalite liquidus. However, it

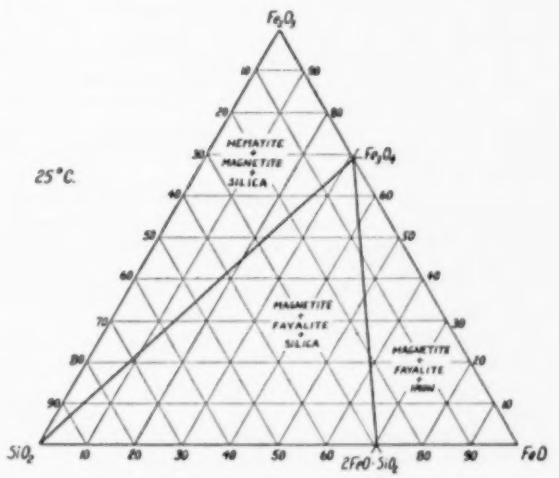

Fig. 8—25°C isothermal section, based on binary systems.

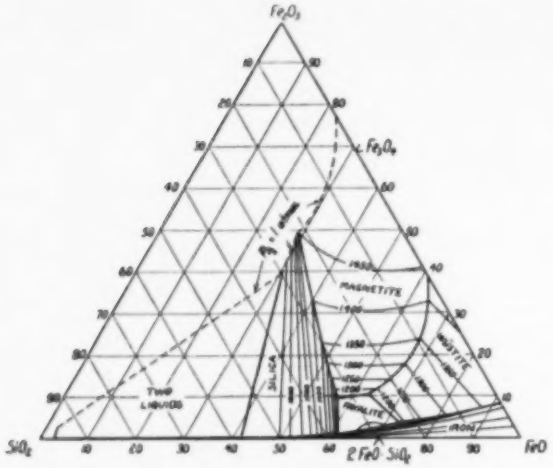

Fig. 9—Liquidus diagram for FeO-Fe_2O_3-SiO_2 system.

is now possible to locate the fayalite liquidus with reasonable confidence by combining the data of Bowen and Schairer on fayalite-iron-melt equilibria and Darken's determinations of invariant temperatures of the fayalite liquidus with extrapolations of composition data from the present investigation. The results of these constructions are shown in the complete liquidus diagram discussed later. Several successive isotherms would be necessary to describe the system completely in the temperature range of the fayalite liquidus (from 1208°C, the melting point of fayalite, down to 1118°C, the fayalite-magnetite-silica eutectic temperature).

Since no ternary compounds or ternary solid solutions have been found in the FeO-Fe_2O_3-SiO_2 system, the isothermal sections for temperatures below the ternary eutectic temperature are readily constructed from available knowledge of the binary systems. Between the invariant temperature 1118°C (magnetite, fayalite, silica, melt, and gas in equilibrium) and the invariant temperature 560°C (magnetite, wüstite, iron, gas in equilibrium), the system is represented by isotherms like Fig. 7. Fig. 8 shows the phases present in mixtures of various compositions below 560°C.

Liquidus Surfaces in FeO-Fe_2O_3-SiO_2 System: By combining the data of the present investigation with data published by various other investigators, the ternary diagram shown in Fig. 9 was constructed. This diagram shows all the liquidus surfaces in the FeO-Fe_2O_3-SiO_2 system and shows the complete temperature-composition field of stability of iron silicate slags at 1 atm. The basic data are outlined briefly below:

FeO-Fe_2O_3 edge: Complete data for the intersections of the iron, wüstite, and magnetite surfaces with the FeO-Fe_2O_3 edge were taken from the work of Darken and Gurry.[1]

Region of immiscible liquids: The limits of liquid immiscibility were measured by Greig.[4]

Silica liquidus: The silica liquidus is determined primarily by 1—the univariant curve for silica-iron-melt completely measured by Bowen and Schairer[2] and checked by Schuhmann and Ensio,[6] 2—the univariant curve for solid silica-liquid silica-liquid slag determined by Greig,[4] and 3—data of the present investigation in the range 1250° to 1450°C. The univariant curve silica-magnetite-melt is terminated at 1450°C where Darken found p_{O_2} equal to 1 atm.[5] The same univariant curve is extrapolated down to 1118°C, the temperature determined by Darken for the invariant equilibrium silica-magnetite-fayalite-melt.

Magnetite liquidus: This surface was determined in the present investigation from 1250° to 1450°C. The two terminal points of the bounding curve for p_{O_2} equal to 1 atm have been determined as already discussed, but the shape of this curve was estimated. The univariant curve magnetite-wüstite-melt was extrapolated to 1150°C, the temperature estimated by Darken for the invariant point magnetite-wüstite-fayalite-melt.

Iron liquidus: Bowen and Schairer's data on the "FeO-SiO_2" system, confirmed by Schuhmann and Ensio, locate the iron liquidus. However, to avoid an apparent violation of the phase rule, the Fe_2O_3 percentages given by Bowen and Schairer were lowered to be consistent with Darken and Gurry's measurement of the Fe_2O_3 content of molten iron oxide in contact with metallic iron at 1371°C.

Wüstite liquidus: Curves of intersection of the wüstite liquidus with the FeO-Fe_2O_3 edge and the iron liquidus were located as described above, and the rest of the surface was determined in the present investigation.

Fayalite liquidus: This surface is drawn to pass through the appropriate univariant curves and invariant points for which the methods of location were described above.

Table II summarizes temperatures and compositions for important fixed points in the ternary liquidus diagram.

Discussion

The liquidus diagram for the FeO-Fe_2O_3-SiO_2 system shows a number of relationships which are of practical importance in slagmaking and fluxing. All the iron silicate slags of lowest freezing points (e.g., 1200°C and below) have compositions close to that of the mineral fayalite (ferrous orthosilicate: $2FeO \cdot SiO_2$ or Fe_2SiO_4). The lowest temperature at which a stable iron silicate melt can exist is 1118°C, and the slag with this minimum freezing point has approximately the composition: 57 pct

Table II. Data on Fixed Points in FeO-Fe_2O_3-SiO_2 Liquidus at 1 Atmosphere

Phases in Equilibrium	Temperature, °C	Analysis of Liquid Phase, Wt Pct		
		FeO	Fe_2O_3	SiO_2
Magnetite, iron oxide melt, and O_2 at 1 atm	1583	22.6	77.4	0.0
Magnetite, silica, melt, and O_2 at 1 atm	1447	29	49	22
Magnetite, congruent melting point	1597	31.1	68.9	0.0
Magnetite, wüstite, and iron oxide melt	1424	61.0	39.0	0.0
Magnetite, wüstite, fayalite, and melt	1150	63.0	10.5	26.5
Magnetite, silica, fayalite, and melt	1118	57.0	9.5	33.5
Wüstite, γ-iron, and iron oxide melt	1371	91.8	8.2	0.0
Wüstite, fayalite, γ-iron, and melt	1180	72.8	3.8	23.4
Fayalite, incongruent melting point	1208	68.4	2.3	29.3
Fayalite, silica, γ-iron, and melt	1180	61.0	1.0	38.0
Solid silica, liquid silica, liquid iron, and liquid slag	1690	42 3	— —	58 97
Solid silica, liquid silica, liquid slag, and air (p_{O_2} = 0.21 atm)	1665	31.7 2.4	36.7 2.0	31.6 95.6

FeO, 9.5 pct Fe_2O_3, and 33.5 pct SiO_2. Ferric oxide in amounts up to 10 to 12 pct has little effect on the freezing point of fayalite slags, but increasing amounts of Fe_2O_3 beyond this point progressively raise the freezing point. When slags high in ferric iron are cooled from high temperatures, a substantial part of the ferric iron will have frozen out as magnetite by the time the temperature reaches about 1200°C. If the slag is then frozen and cooled slowly to room temperature, the remainder of the ferric iron also will appear finally as magnetite.

Stating the observations of the preceding paragraph in a different way, FeO is a good flux for SiO_2 whereas Fe_2O_3 and more particularly Fe_3O_4 are very poor fluxes for SiO_2. Thus, the higher iron oxides form silicate slags only if reducing agents are available to yield ferrous iron. In Fig. 9 the isotherms in the silica liquidus are substantially straight lines, and the extensions of all these lines come very close to the Fe_2O_3 corner of the diagram. That is, for slags saturated with silica, the ratio of SiO_2 to FeO is nearly independent of the Fe_2O_3 content of the slag. For example, at 1500°C, 57 parts by weight of FeO will flux a maximum of 43 parts of SiO_2 regardless of the amount of Fe_2O_3 present in addition. The relationship of the state of oxidation of iron to the fluxing of SiO_2 is also of obvious importance in understanding the behavior of silicious refractories in steelmaking, and has been discussed elsewhere by one of the authors.[7]

The magnetite liquidus surface covers a relatively large and centrally located portion of the composition triangle in Fig. 9, and thus it is not surprising that the nonferrous smelterman encounters problems which appear to be related to magnetite precipitation. Copper converting is conducted under relatively oxidizing conditions and with limited additions of silicious flux. A typical converter slag might analyze 45 to 50 pct total Fe, 25 pct SiO_2, and 15 to 20 pct Fe_3O_4. Recasting this analysis into terms of the percentages of FeO, Fe_2O_3, and SiO_2 and ignoring other slag constituents by adjusting (% FeO + % Fe_2O_3 + % SiO_2) to 100 pct, the composition is found to be equivalent to about 10 to 15 pct Fe_2O_3, 55 to 60 pct FeO, 25 to 30 pct SiO_2. On the ternary diagram (Fig. 9), such a composition falls in the region of the magnetite liquidus surface and in fact corresponds to saturation with magnetite at temperatures around 1200°C. Although the idea that copper converter slags are often saturated with magnetite is not new, it is significant that this apparent approach to saturation is confirmed quantitatively as an equilibrium condition in the phase diagram. In reverberatory slags, in general, lower contents of Fe_2O_3 and higher contents of SiO_2 are found than in converter slags, so that reverberatory slag compositions are represented in Fig. 9 by points below and to the left of the points representing compositions of converter slags. That is, reverberatory slag compositions apparently approach the conditions of silica saturation along the silica liquidus surface. Comparisons of published slag analyses with the phase diagram do not show clearly how closely silica saturation is actually approached in practice since no satisfactory basis is available for allowing for the effects of the CaO, Al_2O_3, MgO, and other minor slag constituents on the SiO_2 solubility.

Reference is sometimes made to the solubility of magnetite in slags. From the data summarized in Fig. 9 it is possible to evaluate at any given temperature the quantity of magnetite which can be

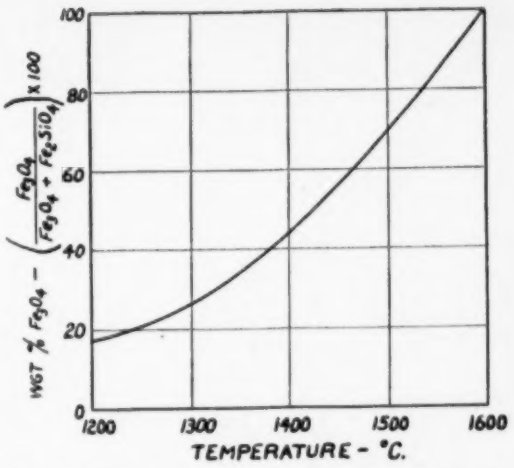

Fig. 10—Effect of temperature on magnetite solubility in fayalite slags.

dissolved in an iron silicate slag of given initial composition. To illustrate the variation of magnetite solubility with temperature, the ideal stoichiometric composition of fayalite, $2FeO \cdot SiO_2$, may be taken as a starting point. Fig. 10, based on the data of the magnetite liquidus in Fig. 9, shows the solubility of magnetite in fayalite slags as a function of temperature. The variations in Fe_3O_4 solubility with FeO-SiO_2 ratio in the initial slag are relatively small, so this plot probably is a good approximation of the magnetite solubility vs temperature relation for all types of iron silicate slags including copper converter slags. This graph shows that magnetite solubility increases rather rapidly with increasing temperature up to 1597°C, the melting point of Fe_3O_4 in the absence of silica. For example, from 1300° to 1250°C the solubility of magnetite drops from 25 pct down to 20 pct so that a slag saturated with magnetite at 1300°C would have to precipitate about 5 pct Fe_3O_4 in cooling only 50°C (90°F). To be even more specific, a ladle containing 10 tons of homogeneous magnetite-saturated slag at 1300°C would yield on cooling to 1250°C a mixture of 9.5 tons slag with 0.5 ton precipitated magnetite.

In some metallurgical processes, one of the important functions of the slag is to act as a carrier for oxygen. Oxygen dissolution in the slag involves oxidation of ferrous iron to ferric, and the reverse reaction occurs when the oxygen is given up. The dissolution of oxygen gas (e.g., in exposure of slag to air) may be written

$$4FeO \text{ (in liquid slag)} + O_2 \text{ (gas)} \rightarrow 2Fe_2O_3 \text{ (in liquid slag)}.$$

The solubility of oxygen in the slag at a given temperature might be defined as the maximum quantity of oxygen which can be dissolved without precipitating a new phase. Since oxidation by the above reaction not only increases the Fe_2O_3 content, but also reduces the FeO-SiO_2 ratio in the slag, the result of oxidation is that the point representing slag composition will move both upward and to the left on the composition triangle in Fig. 9. Thus, for some slags, the maximum oxygen dissolution is achieved when magnetite starts to form as a separate phase while in other slags the maximum oxygen dissolution is achieved when solid silica starts to form. Using the data in the ternary diagram, the sequence

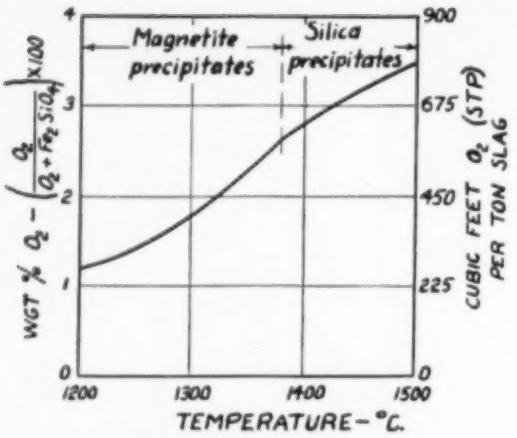

Fig. 11—Oxygen solubility in fayalite slags.

of changes during oxidation for any given initial slag composition can be easily followed. If the ideal stoichiometric composition $2FeO \cdot SiO_2$ is taken as a starting point, as was done previously in considering magnetite solubility, the oxygen solubility is given by Fig. 11. For this slag, the limit of oxygen dissolution at any temperature below 1380°C is reached when magnetite starts to precipitate. Above 1380°C, precipitation of silica limits the oxygen solubility.

The shape and location of the wüstite liquidus surface suggest the possibility that wüstite rather than magnetite might be the iron oxide phase forming in contact with iron silicate slags, especially for slags low in SiO_2 (less than 25 pct SiO_2) and at the same time low in Fe_2O_3. However, for the specific conditions of copper converting, thermodynamic calculations show that if conditions are sufficiently oxidizing to oxidize the sulphur of the matte to SO_2, magnetite will form automatically in preference to wüstite. This is another way of saying that the primary converting reaction will not proceed without formation of a high-Fe_2O_3 or high-magnetite slag.

Acknowledgment

The authors wish to express their appreciation to the American Iron and Steel Institute for their financial support of this work.

References

[1] L. S. Darken and R. W. Gurry: The System Iron-Oxygen. *Journal* ACS (1945) **67**, pp. 1398-1412; (1946) **68**, pp. 798-816.

[2] N. L. Bowen and J. F. Schairer: The System FeO-SiO_2. *American Journal of Science* (1932) **24**, pp. 177-213.

[3] L. S. Darken: Melting Points of Iron Oxides on Silica; Phase Relations in the System Fe-Si-O as a Function of Gas Composition and Temperature. *Journal* ACS (1948) **70**, pp. 2046-2053.

[4] E. J. Michal and R. Schuhmann, Jr.: Thermodynamics of Iron Silicate Slags: Slags Saturated with Solid Silica. *Trans.* AIME (1952) **194**, pp. 723-728; JOURNAL OF METALS (July 1952).

[5] R. Schuhmann, Jr. and P. J. Ensio: Thermodynamics of Iron Silicate Slags: Slags Saturated with Gamma Iron. *Trans.* AIME (1951) **191**, pp. 401-411; JOURNAL OF METALS (May 1951).

[6] J. W. Greig: On Liquid Immiscibility in the System FeO-Fe_2O_3-Al_2O_3-SiO_2. *American Journal of Science* (1927) **14**, pp. 473-484.

[7] R. Schuhmann, Jr.: Silica-Iron Oxide Systems. Amer. Iron and Steel Inst., Chicago Regional Meeting (1951).

Technical Note

Some Low Temperature Properties of Titanium Alloy RC-130-B And Stainless Steel

by W. W. Tyler, L. B. Nesbitt, and A. C. Wilson, Jr.

INVESTIGATIONS of thermal conductivity and impact strength of the titanium alloy RC-130-B and 316 stainless steel were undertaken because of interest in strong, nonmagnetic, commercially available alloys of low thermal conductivity for use in low temperature experiments. Measurements of electrical resistivity and thermoelectric power were also made for some of the samples studied.

The titanium alloy designated as RC-130-B is manufactured by Rem Cru Titanium Inc. It contains 0.14 pct C, 3.99 pct Al, and 4.7 pct Mn. A general discussion of properties of the two phase Ti-4Mn-4Al alloys is given by Finlay and Vordahl.[1] The alloy is machinable and has a yield strength greater than 130,000 lb per sq in. at 0.2 pct offset. The 316 stainless steel sample used for both conductivity and impact strength measurements was obtained from the Allegheny-Ludlum Steel Corp. and is designated as Allegheny metal 18-8M, Type 316, Grade 316. The sample had received 25 pct minimum final cold reduction and had a Brinell hardness rating of 255. Several impact tests were made on a sample of 316 stainless which had not received the 25 pct cold reduction. Also several data points are reported giving thermal conductivity and electrical resistivity for a sample of 304 stainless steel taken from stock.

Figs. 1 and 2 give thermal conductivity and electrical resistivity data for the titanium alloy and for

W. W. TYLER, L. B. NESBITT, and A. C. WILSON, Jr., formerly with Knolls Atomic Power Laboratory, are now associated with the Research Laboratory, General Electric Co., Schenectady.

TN 168E. Manuscript, March 25, 1953.

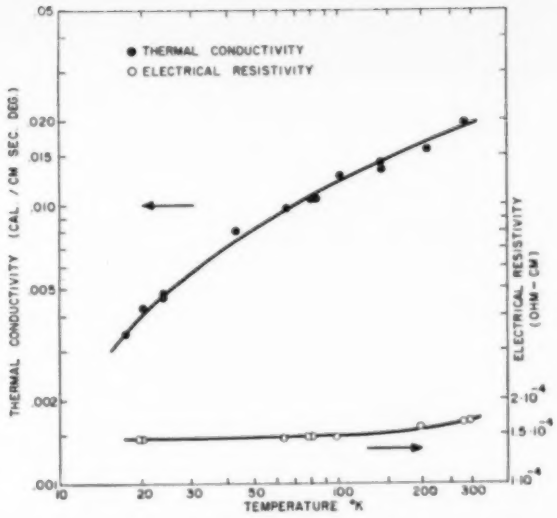

Fig. 1—Thermal conductivity and electrical resistivity of titanium alloy RC-130-B.

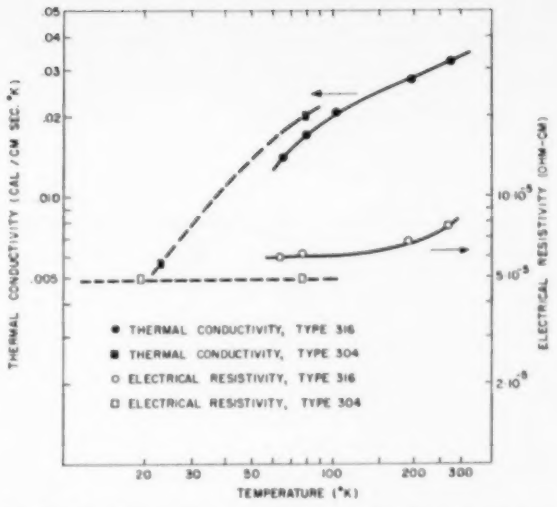
THERMAL CONDUCTIVITY (CAL / CM SEC °K)
ELECTRICAL RESISTIVITY (OHM-CM)
THERMAL CONDUCTIVITY, TYPE 316
THERMAL CONDUCTIVITY, TYPE 304
ELECTRICAL RESISTIVITY, TYPE 316
ELECTRICAL RESISTIVITY, TYPE 304
TEMPERATURE (°K)

Fig. 2—Thermal conductivity and electrical resistivity of stainless steel.

the stainless steel samples. Conductivity values for the stainless steel types 304 and 316 agree within our experimental error with the more extensive data on stainless steels obtained by Powers[2] and by Estermann and Zimmerman.[3] Fig. 3 shows the absolute thermoelectric power of the titanium alloy. This was derived from the thermoelectric power of a couple consisting of the titanium alloy and copper, using values of the absolute thermoelectric power of copper given by Borelius.[4] The absolute thermoelectric power for both the 316 and 304 stainless steels is of the order of a microvolt per degree or less throughout the temperature range and is consequently not given in detail.

The equipment and experimental techniques used in making the conductivity measurements have been reported in some detail[5] and will not be described here. The uncertainty in the magnitude of the thermal conductivity data estimated from knowledge of errors resulting from lead losses, thermal drift, and radiation losses is at most ±10 pct for the titanium alloy and less for the stainless steel. Values of electrical resistivity are correct within ±2 pct. Thermoelectric power data are probably accurate to within ±0.5 microvolt per degree.

As a measure of the behavior of the alloys under shock loading, Charpy impact tests were made on

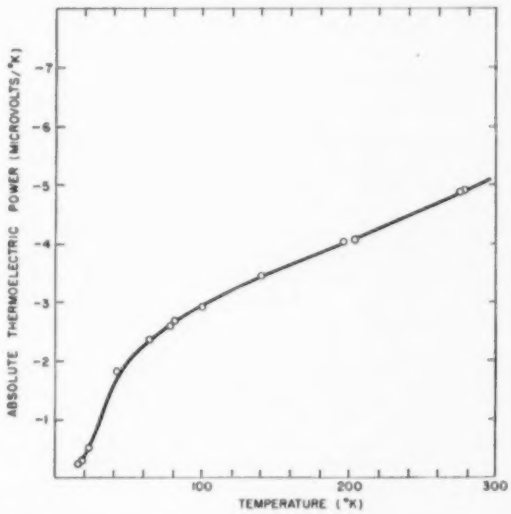

Fig. 3—Absolute thermoelectric power for the titanium alloy RC-130-B.

RC-130-B, cold drawn 316 stainless steel, and normal 316 stainless steel samples. The results are given in Table I. Tests were made at room temperature, liquid nitrogen temperature, and liquid hydrogen temperature. N_2 and H_2 temperatures were maintained for the 4 to 6 sec necessary to make the test by a reservoir of the liquid in a paper box surrounding the sample. The presence of the paper box introduced no appreciable error in the measurement.

Table I. Results of Charpy Impact Tests*

Sample	Room Temperature	N_2 Temperature	H_2 Temperature
RC-130-B			
½ size		6-7	6-7
Full size	12-18†		
316SS (25 pct reduction)			
½ size	41	42-44	42
Full size	101	87-100	91-89
316SS (Normal)			
½ size	66	84-85	76-74
Full size	189	159-175	178-179

* The numbers indicate energy absorbed during fracture of the sample in units of ft lb. For some of the materials, several tests were made and a range of values is indicated.
† Data provided by Rem Cru Titanium Inc.

References

[1] W. L. Finlay and M. B. Vordahl: *Metal Progress* (1952) **61**, p. 73.

[2] R. W. Powers: To be published.

[3] I. Estermann and J. E. Zimmerman: *Journal of Applied Physics* (1952) **23**, p. 578.

[4] G. Borelius: *Handbuck der Metallphysik* (1935) Vol. 1, pp. 181-485. Leipsig. Akad. Verlags Gesellschaft.

[5] W. W. Tyler and A. C. Wilson, Jr.: *Physical Review* (1953) **89**, p. 870.

Solutions of Metals in Fused Salts

by Daniel Cubicciotti

Measurements have been made of the solubilities of a number of metals in their fused halides and the effect of added salts on these solubilities. A structural model for the solution of metal in salt is presented to account for the experimental data.

IT has long been known that some metals are capable of being dispersed or dissolved in certain of their fused salts.[1] Davy[2] and Bunsen[3] were among the first to observe that in some fused salt electrolyses, a highly colored, strongly reducing salt phase appeared in the neighborhood of the cathode. Later workers found that the current efficiency of the electrolysis was markedly reduced when such a phase appeared. It was also found that the strongly reducing salt could be made by melting the metal and normal salt together. Chemical analysis showed that in such salts the metal ion to anion ratio was always larger than in the normal salt.

From such observations arose two different explanations of the nature of metal in salt solutions. When a solution of this type is quenched, it is possible to find small globules of metal in the salt. From this and other observations, Lorenz[4] and coworkers assumed the metal in salt solution to be a colloidal dispersion of metal in the fused salt and called it "metallnebel" or metal fog formation. They made a number of experiments to substantiate this point of view. Another school felt that when the metal dissolved it reduced the salt partially to a mixture or solution of normal salt and subsalt. Both of these ideas could explain the strong reducing character of the salt formed and the low current efficiency of the electrolysis. If either a metal colloid or a subsalt were formed at the cathode and diffused to the anode, it would be oxidized to the normal salt. Thus a cyclic process of oxidation and reduction could be set up conducting the current without giving rise to a net change in the system.

These facts led the author to investigate some of the properties of metal in salt solutions with the hope of elucidating their nature further. Among the metal-salt systems that form metal in salt solutions most markedly are the alkaline earth metal-halide systems and cerium, bismuth, and cadmium halides. Other systems of halides, oxides and sulphides form such solutions to a lesser degree. The first work undertaken was a study of the temperature-composition diagrams of some of the systems.[5] From such diagrams it would be possible to distinguish between a subhalide formation or a colloid. A subhalide should give rise to characteristic changes in the phase diagram, while a colloidal dispersion of metal in salt would not alter the freezing point of the salt.

The results obtained on a number of alkaline earth metal-halide systems were all quite similar. Fig. 1 shows the barium-barium chloride system. The other

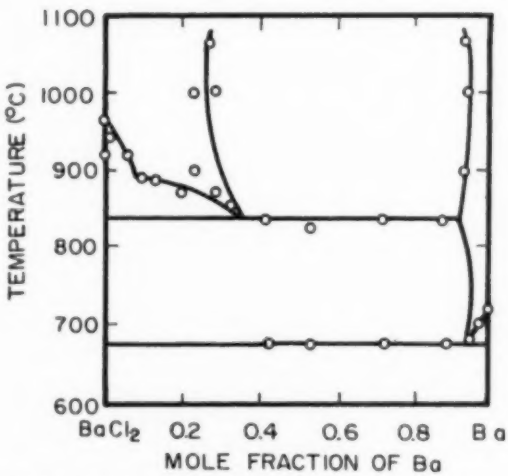

Fig. 1—The temperature-composition diagram for the barium-barium chloride system (from ref. 5).

D. CUBICCIOTTI is associated with the Atomic Energy Research Laboratory, North American Aviation, Inc., Downey, Calif.

Discussion on this paper, TP 3589D, may be sent, 2 copies, to AIME by Nov. 1, 1953. Manuscript, Feb. 24, 1953. Los Angeles Meeting, February 1953.

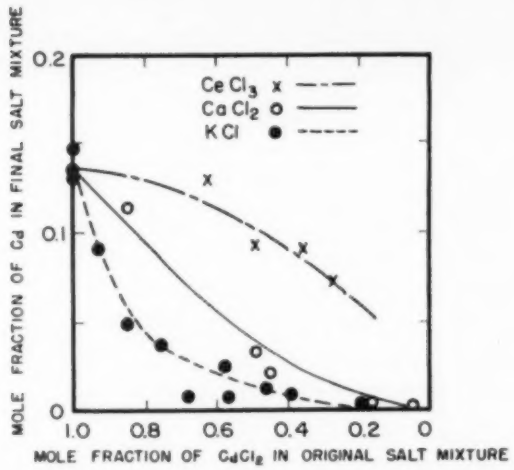

Fig. 2—The solubility of cadmium in mixtures of cadmium chloride with the chlorides of monovalent, divalent, and trivalent electropositive metals at 740° (from ref. 7).

systems were all of this type—a simple eutectic system with a region of liquid immiscibility. The phase diagrams of these systems show that no high temperature stable subhalide was formed. In addition, they show that the solution cannot be colloidal in nature because the freezing point of the salts were depressed as the metals were added. Thus the metal in salt solutions are simply true solutions in the normal sense.

From a comparison of the solubilities of the alkaline earth metals in their fused chlorides an interesting correlation can be made. Going down the periodic table from magnesium to barium, including the subgroup elements zinc and cadmium, it is seen that the solubility of the metal in the salt increases. In Table I these solubilities are compared with the reducing power of the metal (i.e., the free energy of formation of the normal salt) and the ionic radius of the metal ion. There is no correlation between the solubility and the reducing power of the metal; however, as the cationic radius of the metal increases so does its solubility in the fused chloride—for this group of the periodic table.[5] Another correlation can be made between the solubility and valence of cation or better cation to anion ratio in the normal salt. In Table II are given the solubilities of potassium, strontium, and cerium in their chlorides.[6] For these metals the cationic radii are essentially the same but the solubility increases as the ratio of number of cations to anions decreases.

The effect of added foreign salt on the solubility of

Table I. Solubilities of the Metals of Group II in Their Molten Chlorides. From Ref. 5

Metal	Solubility* in Chloride, Mol Pct	Temperature, °C	Radius of +2 Ion, A	$-\Delta F_{298}$ for Formation of Salt, Kcal per Mol
Mg	1.2	900	0.65	141.2
Ca	16	900	0.99	180.1
Sr	20	900	1.13	186.0
Ba	30	900	1.35	193.2
Zn	10^{-4}	500	0.74	88.5
Cd	16	650	0.97	82.7

* The solubilities for zinc and cadmium are not known above 500° and 650°C, respectively.

Table II. Solubilities of Metals in Their Salts at About 800°C. From Ref. 6

Metal	Solubility, Mol Pct	Cation Radius, A
K	1	1.33
Sr	20	1.13
Ce	33	1.15

a metal in its halide was another variable that could easily be investigated.[7] For this investigation the cadmium-chloride and bismuth-chloride systems were chosen because these metals would have little tendency to reduce the added salts. In Fig. 2 is shown the effect of several foreign chlorides on the solubility of cadmium in its chloride. It may be seen that any added salt reduced the solubility of the cadmium and further the larger the cation to anion ratio the more effective the added salt in reducing the solubility. The effect of different salts with the same cation to anion ratio is seen in Fig. 3. There it can be seen that the more electropositive the metal of the cation of the added salt, the more the solubility of the cadmium was reduced. The electropositive character of the metal of the added salt is given in Table III. The smaller the equilibrium constant the more electropositive the metal of the salt.

Table III. Equilibrium Constants for the Reactions of Salts with Cadmium at 740°C. From Ref. 7

Salt	Equilibrium Constant for Reaction $Cd + \frac{2}{n} X Cl_n = CdCl_2 + \frac{2}{n} X$
$CaCl_2$	$10^{-23.4}$
$MgCl_2$	$10^{-11.9}$
$MnCl_2$	$10^{-4.4}$
$ZnCl_2$	$10^{-1.9}$

Similar results were obtained in the bismuth-chloride system.[8] These are shown in Fig. 4. The solubility of the bismuth was decreased by the addition of any salt. The smaller the cation to anion ratio of the added salt, the less the solubility was depressed. For the same cation to anion ratio the

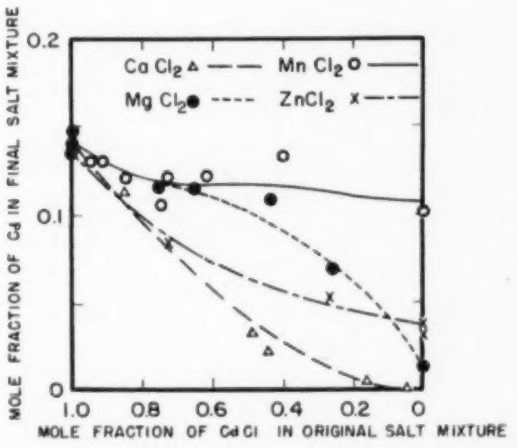

Fig. 3—The solubility of cadmium in mixtures of cadmium chloride with several divalent chlorides at 740° (from ref. 7).

more electropositive the metal of the added salt, the greater the decrease of the bismuth solubility.

The data so far obtained on the solubilities of metals in their fused chlorides can be summarized as follows: 1—For the metals of group II of the periodic table the solubility of the metals in their chlorides increases as the cation radius increases. 2—The solubility increases as the ratio of number of anions to cations increases (shown in the case of potassium, strontium, and cerium). 3—The solubility is decreased (for cadmium in cadmium chloride) on the addition of the chloride of an electropositive metal; the smaller the anion to cation ratio of the added salt, the more the solubility is decreased. 4—On the addition of chlorides (divalent chlorides to cadmium chloride) the solubility is decreased, and the more electropositive the metal of the added chloride, the greater the decrease in the solubility.

These experimental facts are in accord with the following picture of metal in salt solutions.* The chloride ions of the molten salt may be considered to be arranged approximately in a close-packed structure. They are packed in that way and determine the general structure of the system because they are the larger ions. The positive ions are situated in the octahedral holes left among the chloride ions. The cations of the dissolved metal go into any such unoccupied holes.

* From the model presented above little or no solubility of sodium in molten sodium chloride would be expected because the octahedral holes are all occupied in the normal salt. However, Dr. M. Bredig of the Oak Ridge National Laboratory has found this solubility to be about 11 mol pct. He has suggested to the author that the sodium ions may be small enough to fit into the unoccupied tetrahedral holes that occur in the close-packed structure.

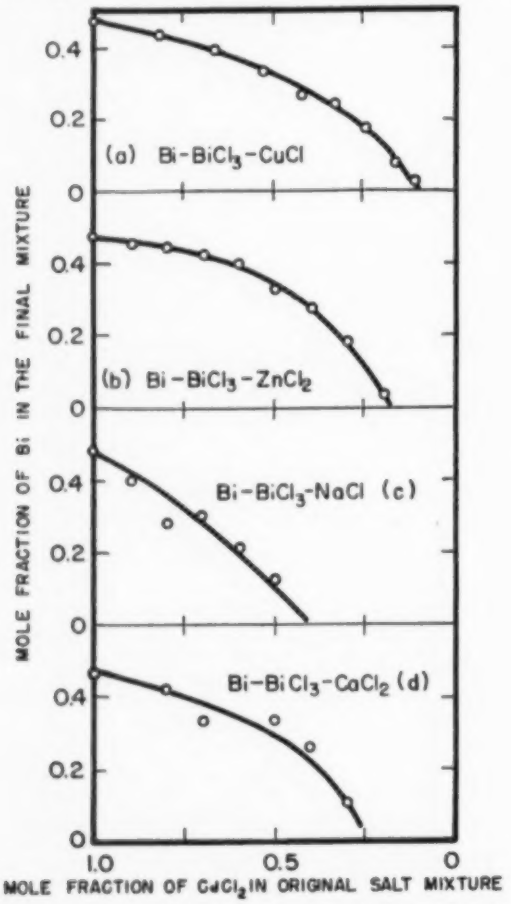

Fig. 4—Influence of added salt on the solubility of bismuth in its trichloride at 450° (from ref. 8).

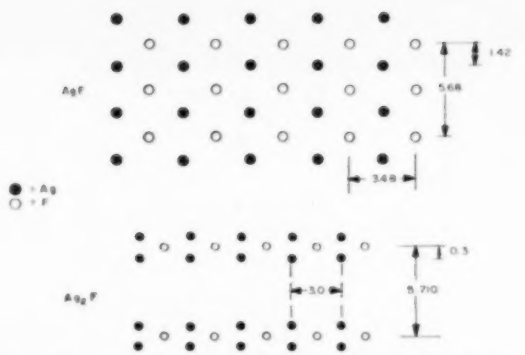

Fig. 5—Comparison of the structures of AgF and Ag_2F. Distances are in Angstrom (from refs. 9 and 10).

In a 1-1 salt there are as many cations as holes and so in the pure salt the holes are all filled. In a 2-1 or a 3-1 salt, one-half and two-thirds of the holes are empty. Therefore, the greater solubility of metal in a salt of large anion to cation ratio (item 2 above) is plausible since the concentration of holes in the salt depends upon the anion to cation ratio. The larger the cation the further the anions surrounding the hole are separated. Thus the metals with larger cations are more soluble (items 1 and 3 above).

The electrons transferred to the salt by the dissolved metal are in bands or zones of energy states belonging to the salt system as a whole. As the salt of a more electropositive metal is added the energy levels would be raised, making it more difficult for an electron from the metal to be transferred to the salt and in effect reducing the solubility of the metal (item 4 above).

In the silver-fluoride system in addition to the compound AgF there exists a substance of empirical formula Ag_2F in the solid. The structures of these two phases have been determined.[9,10] It is interesting to note that the two structures are very similar except that a series of fluoride vacancies exist in the Ag_2F structure. The two structures are shown schematically in Fig. 5. It can be seen that a layer of fluoride ions is missing in the Ag_2F structure. The addition of the fluoride ions to Ag_2F would be comparable to the addition of Ca to $CaCl_2$. This similarity to the picture proposed for metal in salt solutions may be entirely coincidental and not a confirmation of the proposal.

References

[1] A collection of references in this field was made by Cubicciotti, USAEC declassified document MDDC-1058, June 1946.

[2] H. Davy: *Trans.* Royal Soc., London (1807) **97**, p. 1.

[3] R. Bunsen and G. Kirchhoff: *Pogg. Ann.* (1861) **113**, p. 364.

[4] R. Lorenz and W. Eitel: *Pyrosole*. Leipzig. (1926).

[5] D. Cubicciotti and C. Thurmond: *Journal* ACS (1949) **71**, p. 2149.

[6] D. Cubicciotti: *Journal* ACS (1949) **71**, p. 4119.

[7] D. Cubicciotti: *Journal* ACS (1952) **74**, p. 1198.

[8] G. Cleary and D. Cubicciotti: *Journal* ACS (1952) **74**, p. 557.

[9] A. F. Wells: *Structural Inorganic Chemistry*. (1945) London. Oxford Press.

[10] Terrey and Diamond: *Journal* Chem. Soc., London (1928) **131**, p. 2829.

Reaction of Silver With Aqueous Solutions of Cyanide and Oxygen

by G. A. Deitz and J. Halpern

The kinetics of dissolution of silver in cyanide solutions under oxygen pressure have been investigated over a wide range of conditions with a view to establishing the reactions involved and the factors which influence the rate. The results indicate that the rate is determined principally by the transport of reactants in solution to the silver surface. The thermodynamic features of the reaction with particular reference to the influence of pH and CN^- are also discussed and summarized in the form of potential-pH diagrams.

METALLIC silver is readily attacked and dissolved by cyanide solutions in the presence of oxygen. This reaction has long been recognized and extensively applied[1] in the well-known cyanide process for the extraction of silver from its ores. While this process has been subjected in the past to a number of investigations[2,3] both of a practical and fundamental nature, some features relating to the chemistry of the reactions involved, the role of oxygen, the nature of the rate-controlling step, and the effects of pH and certain reagents such as lime, are still not fully understood. It was felt that this situation justified a further investigation of the reaction, made with a view to obtaining a better understanding of its kinetics and mechanism.

In the present investigation rate curves for the dissolution of silver were determined over an extensive range of carefully controlled reaction conditions. By carrying out the reactions in a pressure vessel, the partial pressure of oxygen, and hence its concentration, could be varied widely. The influence on the reaction of other variables including temperature, pH, and the concentrations of cyanide, peroxide, and other salts was also examined.

The results of these kinetic studies are presented and discussed in this paper, together with a summary of available thermodynamic information relating to the possible reactions which can accompany the attack on silver by aqueous solutions of cyanide and oxygen.

Chemistry and Thermodynamics of the Reaction

The chemistry of the reactions of gold and silver with aqueous cyanide solutions has been the subject of several recent reviews.[2,3] It has been proposed[4] that the following reaction occurs when silver dissolves in cyanide solutions in the presence of oxygen:

$$4Ag + 8CN^- + O_2 + 2H_2O \rightarrow 4Ag(CN)_2^- + 4OH^- \quad [1a]$$

An equation of this form, for the corresponding dissolution of gold, was first suggested by Elsner.[4] Bodlaender[5] proposed a similar overall reaction, but suggested that it took place in two steps,

$$2Ag + 4CN^- + O_2 + 2H_2O \rightarrow 2Ag(CN)_2^- + 2OH^- + H_2O_2 \quad [2a]$$

followed by

$$2Ag + 4CN^- + H_2O_2 \rightarrow 2Ag(CN)_2^- + 2OH^- \quad [3a]$$

On the other hand, Janin[6] suggested that the dissolution of gold can occur with the liberation of hydrogen, rather than by reduction of oxygen. The corresponding equation for the dissolution of silver is

$$2Ag + 4CN^- + 2H_2O \rightarrow 2Ag(CN)_2^- + 2OH^- + H_2 \quad [4a]$$

All these reactions represent oxidation-reduction processes and may be resolved into the corresponding separate oxidation and reduction components. The oxidation step involves the formation of the argentocyanide ion and is the same for all the reactions, i.e.,

$$Ag + 2CN^- \rightarrow Ag(CN)_2^- + e \quad [5]$$

However, reactions 1a, 2a, 3a, and 4a differ in the nature of the reduction steps which are, respectively,

$$O_2 + 2H_2O + 4e \rightarrow 4OH^- \quad [1b]$$
$$O_2 + 2H_2O + 2e \rightarrow H_2O_2 + 2OH^- \quad [2b]$$
$$H_2O_2 + 2e \rightarrow 2OH^- \quad [3b]$$
$$2H_2O + 2e \rightarrow 2OH^- + H_2 \quad [4b]$$

G. A. DEITZ is associated with Kaiser Aluminum and Chemical Corp., Trentwood Plant, Spokane, Wash., and J. HALPERN is Assistant Professor of Metallurgy, University of British Columbia, Vancouver, Canada.

Discussion on this paper, TP 3590D, may be sent, 2 copies, to AIME by Nov. 1, 1953. Manuscript, Feb. 13, 1953; revision, June 18, 1953. Los Angeles Meeting, February 1953.

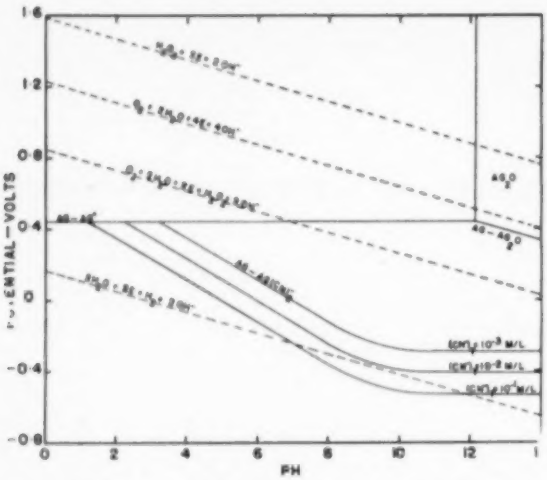

Fig. 1—Potential-pH diagrams for Ag-H_2O and Ag-H_2O-CN^-. Temperature, 25°C.

The potentials corresponding to these reactions are shown in Fig. 1 as functions of the pH and total CN^- concentration of the solution. The calculations were made and the results plotted according to the method of Pourbaix[7] whose diagram for the system Ag-H_2O,[8] has been extended to include the effect of CN^-. Only silver and its monovalent compounds have been considered. The potentials shown for the reduction of O_2 and H_2O correspond to pressures of 1 atm of O_2 and 10^{-6} atm of H_2, respectively, and to a concentration of H_2O_2 of 10^{-6} mol per liter. The potentials for the oxidation of Ag and the equilibrium between Ag^+ and Ag_2O correspond to dilute silver solutions, the total concentration of dissolved silver (including Ag^+ and $Ag(CN)_2^-$) being arbitrarily taken as 10^{-6} mol per liter in accordance with the convention of Pourbaix. Details of the calculations which are based on data of Latimer[9] are given in an appendix to this paper.

The diagram shows that in the absence of cyanide, the solubility of Ag^+ exceeds 10^{-6} mol per liter at pH values below 12.3. At higher pH an insoluble

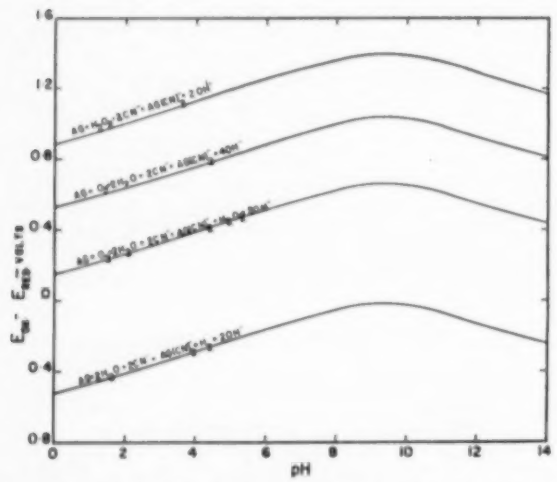

Fig. 2—Potentials for various dissolution reactions of silver in aqueous cyanide. Temperature, 25°C. $(CN^-)_T$, 10^{-2} mol per liter.

Ag_2O phase is formed. The equilibrium potential between Ag and Ag^+ is 0.446 v. Cyanide lowers the concentration of free Ag^+ ion (corresponding to a given total silver concentration of 10^{-6} mol per liter through formation of the argentocyanide complex

$$Ag^+ + 2CN^- \rightleftarrows Ag(CN)_2^- \qquad [6]$$

This results in the disappearance of the Ag_2O phase and in the lowering of the Ag–Ag^+ potential.

These results are further summarized in Fig. 2, where the differences between the potentials for the various reduction and oxidation reactions are plotted as functions of pH, under the conditions noted above for a total cyanide concentration (including CN^- and HCN) of 10^{-2} mol per liter. These plots show that Eqs. 1a, 2a, and 3a all correspond to positive potentials (i.e., to a decrease in the free energy, ΔF) and are therefore thermodynamically feasible. Reaction 4a corresponds to a negative potential and is therefore thermodynamically improbable under these conditions. A similar conclusion was reached by Barsky, Swainson, and Hedley[2] who determined the equilibrium constants for these re-

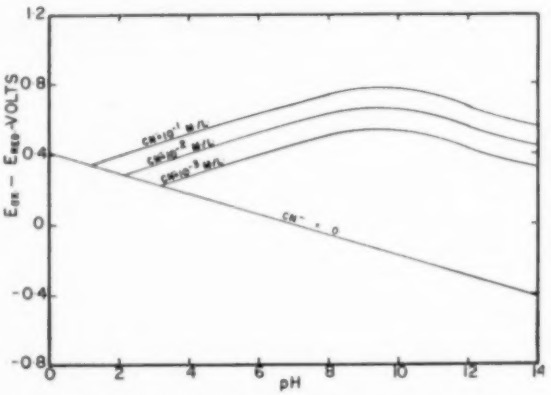

Fig. 3—Effect of pH and total cyanide concentration on the potential for the dissolution of silver with reduction of O_2 to H_2O_2. Temperature, 25°C. $(Ag^+)_T$, 10^{-6} mol.

actions. Experimental confirmation was obtained by McLaurin,[11] Christy,[12] and other investigators who have found that gold and silver do not dissolve in cyanide solutions in the absence of oxygen. Bodlaender[5] has shown that reaction 2a occurs by observing the formation of H_2O_2 in the solution. It has also been suggested[2,3] that reactions 1a and 3a participate in the dissolution process although the evidence for this is less conclusive.

Fig. 3 shows the plots of the potential for reaction 2a against pH for various cyanide concentrations, the total silver ion concentration remaining constant at 10^{-6} mol per liter. The potential is seen to increase with the total cyanide concentration, due to increased formation of $Ag(CN)_2^-$ ion in accordance with Eq 6. This also accounts for the rise in potential with pH, for any given total cyanide concentration, since there is a corresponding increase in the amount of free CN^- due to the ionization of HCN which is a weak acid, i.e.,

$$HCN + OH^- \rightleftarrows CN^- + H_2O \qquad [7]$$

This equilibrium lies effectively to the left at pH values below 4, and in this region cyanide (which exists largely as HCN) is without appreciable effect on the potential. On the other hand at pH values

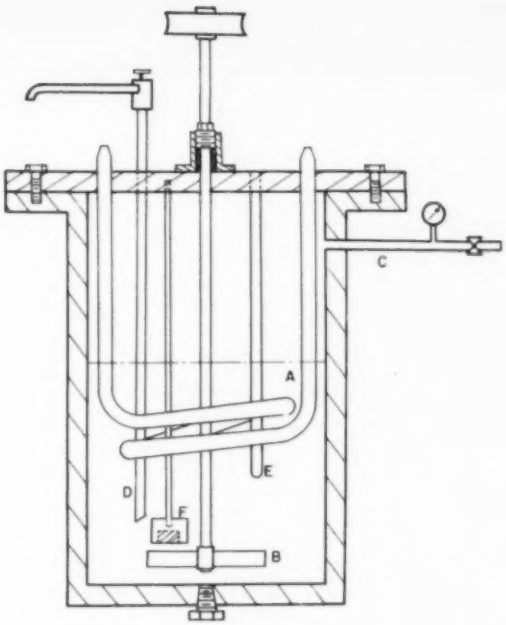

Fig. 4—Schematic diagram of stainless steel pressure vessel. A—Cooling coil. B—Stirrer. C—Gas inlet tube. D—Sampling tube. E—Thermometer well. F—Silver specimen in bakelite mount.

above 10, the equilibrium lies far to the right and increasing pH does not result in any further substantial increase in the amount of free CN^-. The decrease in overall potential for reaction 2a in this region, shown in Fig. 3, is due to a lowering in the potential for the reduction of oxygen.

Experimental

Materials: Reagent grade sodium cyanide and other chemicals used in making up the solutions, were supplied by Nichols Chemical Co. Oxygen was supplied in cylinders by Canadian Liquid Air Co. and used without further purification. Pure silver (99.99 pct) was melted in an induction furnace under an argon atmosphere and cast into ingots of 2 cm diameter. The ingots were cold-worked into rectangular bars, and sections of 2 cm length were annealed above the recrystallization temperature for 24 hr. The annealed sections were mounted in bakelite to insulate them electrically and to leave exposed only a desired surface cross section. The exposed surface of the silver was polished and etched prior to measurement of the dissolution rate.

Apparatus: The apparatus used in this study is described in Fig. 4, and was constructed entirely of stainless steel which was inert to the solutions used. The vessel measured 7 in. ID x 11 in. in height and was designed for pressures up to 10 atm. The bakelite mount containing the insulated silver specimen was held by a stainless steel rod, so that the silver surface was exposed to the solution about 5 mm above the stirrer which was 2 in. in diameter and rotated at 895 rpm. The autoclave was heated externally by a gas burner, and the temperature of the solution maintained to within ±0.5°C by a Wheelco controller coupled to a platinum resistance thermometer. A desired pressure of oxygen was maintained above the solution by means of a standard two-stage gas regulator mounted on the oxygen regulator. A 2.5 liter volume of solution was generally used.

Procedure: The course of the reaction was followed by withdrawing samples of the solution through the tube *D*, at measured time intervals and determining the concentration of dissolved silver by the mixed-color dithizone method[12] using a Beckman DU spectrophotometer. The samples were first rendered free of cyanide, which interferes with the colorimetric determination, by acidifying with HNO_3 and evaporating to dryness.

Cyanide concentrations were determined by titration with standard $AgNO_3$ using KI as indicator. The pH measurements were made with a Beckman H-2 pH meter. Other determinations were made by standard analytical procedures.

Table I. Reproducibility of Rate Measurements

$(NaCN)_T$, 0.0096 mol per liter. Temperature, 24°C. O_2 pressure, 3.4 atm.

Experiment No.	Dissolution Rate, Mg Ag per Sq Cm per Hr	Deviation from Mean Rate, Pct
1	4.50	−5.6
2	4.94	+3.6
3	4.66	−2.3
4	4.61	−3.4
5	5.15	+8.0
Mean	4.77	±4.6

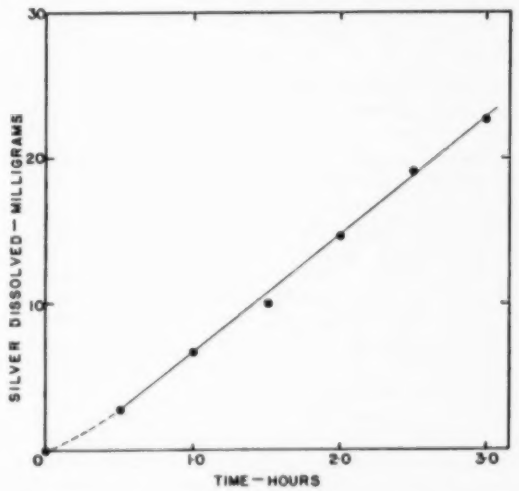

Fig. 5—Typical rate curve for the dissolution of silver. NaCN, 0.0096 mol. Temperature, 24°C. O_2, 3.4 atm.

Results

Rate Curves for the Reaction: A typical rate curve for the dissolution of silver is shown in Fig. 5. A short induction period, of the order of 15 min, was generally observed and is believed to be due to the slow dissolution of an oxide film initially present on the silver surface. Following this induction period, the rate plots were always linear, indicating a zero order reaction rate. Rates were calculated from the slope of this linear region.

The reproducibility of the rate measurements is illustrated in Table I. In a series of five experiments made under similar conditions, the measured rates ranged from 4.50 to 5.15 mg Ag per sq cm per hr. The average deviation of the rates from the mean value was ±4.6 pct. The maximum deviation was 8 pct.

KCN solutions were found to give dissolution

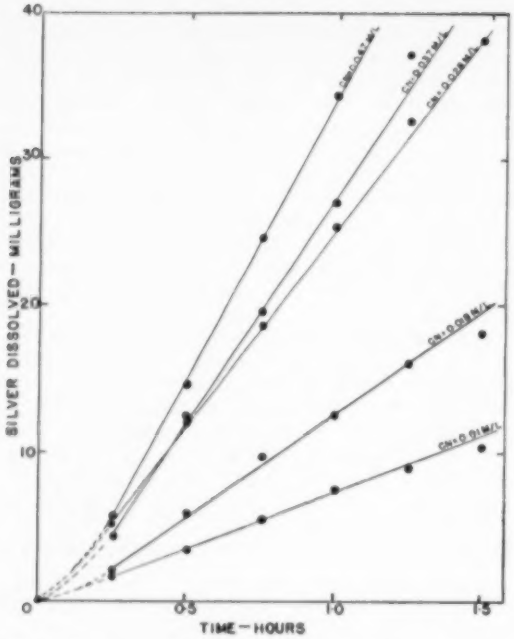

Fig. 6—Rate curves for the dissolution of silver at different NaCN concentrations. Temperature, 24°C. O_2, 7.5 atm.

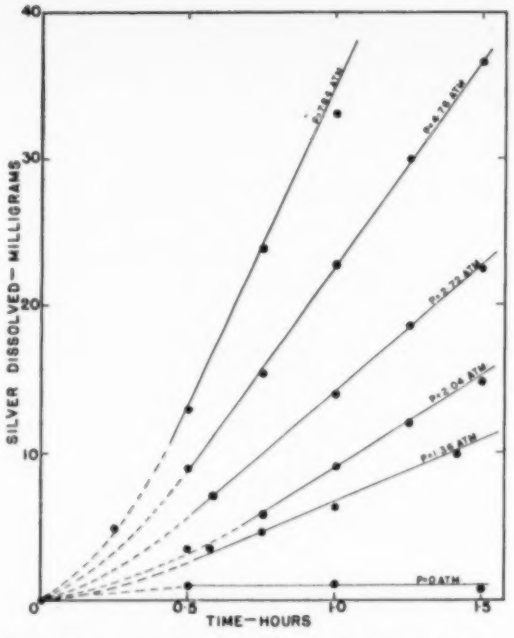

Fig. 8—Rate curves for the dissolution of silver at different O_2 pressures. Temperature, 24°C. NaCN, 0.055 mol.

rates identical with those for NaCN solutions of the same molar cyanide concentration.

Micrographic examination of the silver surface at the end of the experiments indicated that dissolution occurred uniformly on the surface. There was no evidence of etch pits or preferential grain boundary corrosion. The linearity of the rate curves indicates that the surface area of the silver remains effectively constant during the dissolution experiment, and that the dissolved silver is without effect on the reaction.

Effect of Cyanide and Oxygen Concentrations: Measurements of the rate of dissolution were made using solutions with NaCN concentrations ranging from zero to 0.065 mol per liter* at oxygen pressures of 3.40 and 7.48 atm. Some typical rate curves are shown in Fig. 6 and the rates of dissolution, at both oxygen pressures, are plotted against cyanide concentration in Fig. 7.

It is seen that at low NaCN concentrations the rate is proportional to the concentration of NaCN and is independent of the oxygen pressure. As the cyanide concentration is increased a point is reached where the rate levels off to a limiting value. The NaCN concentration at which this occurs is proportional to the oxygen pressure. The limiting rate also depends on the oxygen pressure.

To establish this dependence a series of experiments was made in which the limiting rate was measured at various oxygen partial pressures, ranging from 0 to 8 atm. The NaCN concentration was maintained constant at 0.055 mol per liter (i.e., corresponding to the limiting rate region). The rate curves are shown in Fig. 8 and the results summarized in Fig. 9 where the rate is plotted against

* The initial pH of the solutions varied with the concentration of NaCN due to hydrolysis of CN^- according to the following reaction: $CN^- + HOH \rightarrow HCN + OH^-$. The pH for any solution of given NaCN concentration can readily be calculated from the known ionization constant of HCN (Eq. 23, Appendix), which leads to the following approximate relation: pH = 11.699 + ½ log [NaCN].

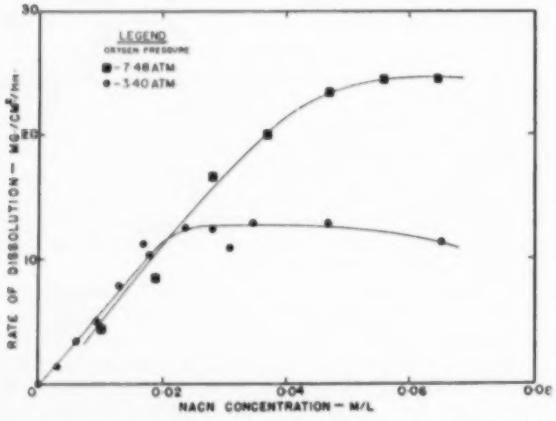

Fig. 7—Effect of cyanide concentration on the rate of dissolution of silver. Temperature, 24°C.

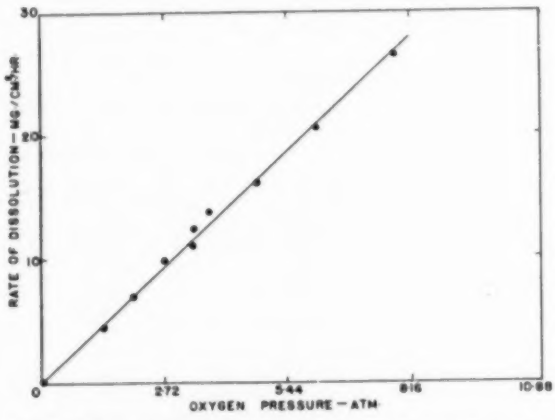

Fig. 9—Effect of oxygen on the rate of dissolution of silver. Temperature, 24°C. NaCN, 0.055 mol.

the oxygen pressure. It is seen that the limiting rate is directly proportional to the oxygen pressure. No appreciable dissolution occurs in the absence of oxygen.

These results suggest that at low NaCN concentrations, when oxygen is present in excess, the diffusion or transport of CN^- to the silver surface controls the rate of the reaction. This corresponds to the region in which the rate is independent of oxygen concentration but proportional to the concentration of cyanide. At higher cyanide concentrations the CN^- ions are transported to the surface more rapidly than the oxygen, and the diffusion of oxygen becomes rate controlling. This corresponds to the limiting region where the rate is independent of cyanide concentration but proportional to the concentration of oxygen. The small decrease in rate with further increase in the NaCN concentration in this region, evident in Fig. 7, may be attributed to a lowering of the solubility of oxygen.[17]

Similar conclusions regarding the existence of two regions corresponding to rate control by the transfer of oxygen and cyanide, respectively, have been reached by White[15] who studied the dissolution of gold in cyanide solutions.

The concentration of oxygen in air-saturated cyanide solutions has been determined,[2] and found to have a value close to 8.5 mg O_2 per liter. Assuming that this concentration is proportional to the partial pressure of oxygen above the solution, over the range of pressures investigated, it can be seen from the results in Figs. 7 and 9, that the transition from the region of rate control by cyanide transport to that by oxygen transport always occurs at a concentration ratio in the solution of 6.7 g of NaCN per g of O_2, or 4.4 mol NaCN per mol of O_2.

Effect of Temperature: Measurements of the rate of dissolution of silver in 0.037 mol NaCN solutions under 3.4 atm of O_2 were made at temperatures ranging from 24° to 110°C. The rate curves were all of the same linear form as described earlier. An Arrhenius plot showing the effect of temperature on the rate is given in Fig. 10. The activation energy for the dissolution process, calculated from the slope of this plot which is exactly linear over the entire temperature range, is 2400 cal per mol. Low activation energies of this order are generally considered to indicate a rate controlled by a diffusion process. This supports the conclusions noted earlier. Accurate measurements could not be made at temperatures exceeding 110°C because of excessive decomposition of the cyanide.

Effect of H_2O_2: Qualitative tests showed that peroxide was formed in the solution, and that its concentration increased with the amount of silver dissolved. This suggests that oxygen is reduced in accordance with Eq 2a and is in agreement with the results of Bodlaender,[5] who was able to account for about 70 pct of the theoretical amount of peroxide

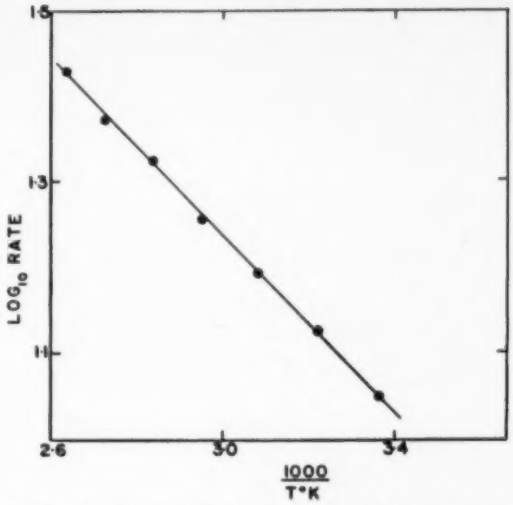

Fig. 10—Arrhenius plot showing the effect of temperature on the rate of dissolution of silver. NaCN, 0.037 mol. O_2, 3.4 atm.

that should be formed according to this equation. No attempt was made to determine quantitatively the amount of H_2O_2 formed in the present study.

However, experiments were conducted to determine the effect of peroxide on the rate of dissolution of silver, by adding different amounts of H_2O_2 to the solution. The results of these experiments are summarized in Table II.

It can be seen that small amounts of peroxide are entirely without effect on the rate. These results, together with the evidence for the build-up of H_2O_2 in the solutions, suggest that the predominant reaction in the dissolution of silver is that represented by Eq. 2a, involving the reduction of O_2 to H_2O_2, and that the further reduction of H_2O_2 to OH^-, represented by Eq. 3a, occurs only to a minor extent.

Effect of pH and Added Salts: Barsky, Swainson, and Hedley[2] found that the rate of dissolution of gold in cyanide solutions fell off with increasing pH and that this effect was particularly marked, when $Ca(OH)_2$ was used to raise the pH. Neutral calcium salts such as $CaSO_4$ and $CaCl_2$ were without effect. They were unable to provide an explanation for these results.

An investigation was undertaken to determine whether the dissolution of silver was similarly influenced by pH and salts. Varying amounts of KOH, $Ca(OH)_2$ and $Ba(OH)_2$ were added to standard NaCN solutions (0.057 mol per liter) and the rate of dissolution of silver in these solutions was measured. Rate curves for the KOH and $Ca(OH)_2$ series are shown in Figs. 11 and 12, and the results are summarized in Table III and Fig. 13. Addition of KOH, $Ca(OH)_2$, and $Ba(OH)_2$ all resulted in a falling off in the rate of dissolution. The effects of KOH and $Ca(OH)_2$ were similar to those observed by Barsky, Swainson, and Hedley[2] for the dissolution of gold. The effect of $Ba(OH)_2$ was intermediate between that of KOH and $Ca(OH)_2$.

It was observed that a white coating was formed on the surface of the silver specimens which had been exposed to reaction with the solutions containing $Ca(OH)_2$. The amount of material on the surface increased with the lime content of the solution. X-ray analysis showed that the coating consisted of calcium peroxide, CaO_2.[18]

Table II. Effect of H_2O_2 on the Rate of Dissolution of Silver

$(NaCN)_T$, 0.057 mol per liter. Temperature, 24°C. O_2 pressure, 4.8 atm.

(H_2O_2), Mol per Liter	Rate of Dissolution, Mg Ag per Sq Cm per Hr
0	16.04
1.8×10^{-4}	15.85
3.5×10^{-4}	16.30

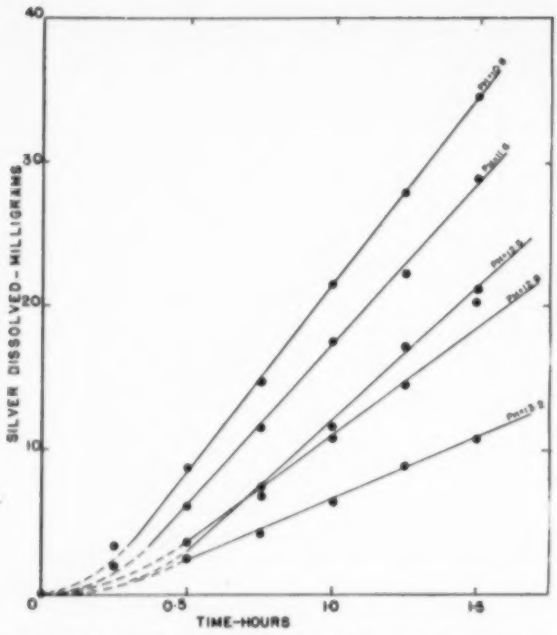

Fig. 11—Rate curves for the dissolution of silver in solutions containing different amounts of KOH. Temperature, 24°C. NaCN, 0.057 mol. O_2, 4.8 atm.

It is known that this salt, which is very slightly soluble, is formed when H_2O_2 is added to solutions of $Ca(OH)_2$. In these experiments the H_2O_2 arises from the reduction of O_2, as discussed earlier. The following reactions are involved:

$$2Ag + 4CN^- + O_2 + 2H_2O \rightarrow 2Ag(CN)_2^- + H_2O_2 + 2OH^- \quad [8]$$

$$H_2O_2 + Ca(OH)_2 \rightarrow CaO_2 + 2H_2O \quad [9]$$

The oxygen is reduced at the silver surface and the CaO_2 which is then formed appears to deposit on the surface. The resulting coating impedes the reaction and accounts for the observed lowering of the rate. This explanation receives further support from the fact that at high $Ca(OH)_2$ concentrations, the rate curve for the dissolution of silver was no longer linear, but showed a tendency to flatten out as the reaction proceeded. This is characteristic of rates which are determined by diffusion through a solid film whose thickness increases as the reaction proceeds.[15]

Eq. 9 shows that both Ca^{++} and OH^- ions are required for the formation of CaO_2. In agreement with the results of Barsky et al.,[5] neutral calcium salts, such as calcium acetate, were found to be without appreciable effect on the rate.

The formation of a similar surface coating was observed when the solutions contained $Ba(OH)_2$. In this case the coating was presumably BaO_2, although the data necessary for its identification by X-ray diffraction measurements were not available. The relative magnitude of the retarding effects of $Ca(OH)_2$ and $Ba(OH)_2$ on the rate is to be expected, since the solubility of BaO_2 exceeds that of CaO_2.[15]

The effect of KOH on the rate which is less marked than that of $Ca(OH)_2$ and $Ba(OH)_2$ cannot be similarly explained, since potassium peroxide is quite soluble. It appears more likely that the effect of KOH in retarding the reaction at high pH values is due to a lowered solubility of oxygen[17] and to a lowered potential for its reduction. (See Figs. 1 to 3.)

Discussion

Nature of the Reaction: The results obtained in this investigation indicate that the predominant reaction responsible for the dissolution of silver in aqueous solutions of cyanide and oxygen is

$$2Ag + 4CN^- + O_2 + 2H_2O \rightarrow 2Ag(CN)_2^- + H_2O_2 + 2OH^- \quad [10]$$

The following reactions do not appear to participate to any appreciable extent, although they would appear to be more probable on the basis of their thermodynamic properties which have been summarized earlier in this paper in the form of potential-pH-CN^- relations.

$$4Ag + 8CN^- + O_2 + 2H_2O \rightarrow 4Ag(CN)_2^- + 4OH^- \quad [11]$$

$$2Ag + 4CN^- + H_2O_2 \rightarrow 2Ag(CN)_2^- + 2OH^- \quad [12]$$

The following evidence supports these conclusions:

1—H_2O_2 was observed to accumulate in the solution as the reaction proceeded. This has also been confirmed quantitatively by Bodlaender.[5] When the solutions contained $Ca(OH)_2$ or $Ba(OH)_2$, the formation of a deposit of CaO_2 or BaO_2, respectively, on the silver surface was observed. These results suggest that the reduction of oxygen results in the formation of H_2O_2, in accordance with Eq. 10, and that the H_2O_2 thus formed is relatively stable with respect to further reduction.

2—Addition of H_2O_2 to the solution did not affect the rate. This suggests that reaction 12 does not occur to an appreciable extent.

3—The transition from the region where the rate is controlled by transport of CN^- to the region of control by transport of O_2, occurs at a ratio of con-

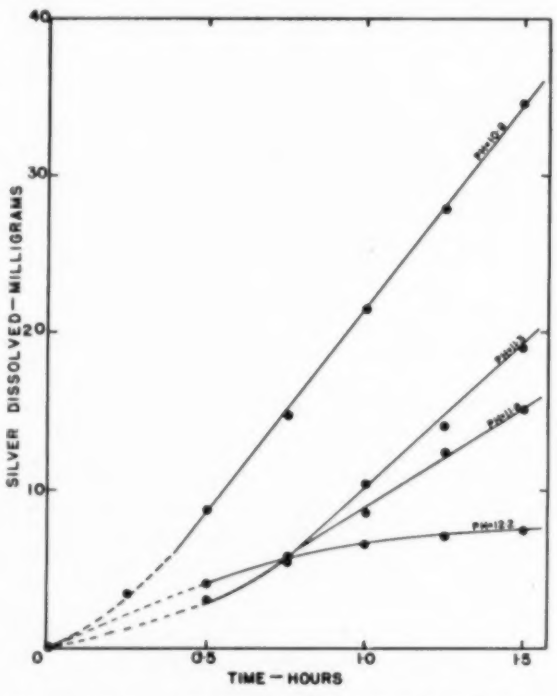

Fig. 12—Rate curves for the dissolution of silver in solutions containing different amounts of $Ca(OH)_2$. Temperature, 24°C. NaCN, 0.057 mol. O_2, 4.8 atm.

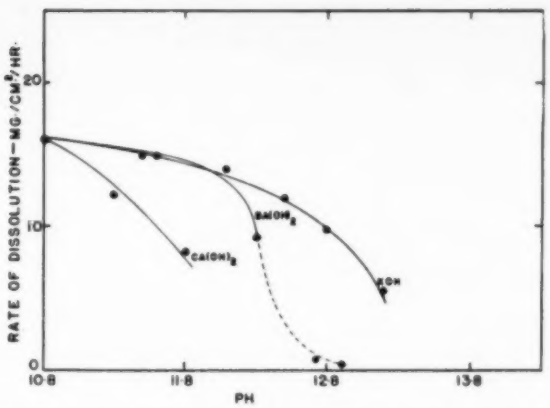

Fig. 13—Effect of KOH, $Ca(OH)_2$, and $Ba(OH)_2$ on the rate of dissolution of silver. Temperature, 24°C. NaCN, 0.057 mol. O_2, 4.8 atm.

centrations (NaCN): (O_2) of 4.4 mol per mol. This is close to the value of 4.0 which would be expected on the basis of Eq. 10 assuming that the diffusion coefficient of O_2 and NaCN are equal. The difference between the two values could be due to incomplete ionization of the cyanide, or to a slight difference between the two diffusion coefficients.

Eqs. 11 and 12 would correspond to a value of 8.0 for this ratio. Values of this order have been observed in similar studies on the dissolution of gold[9, 13] and it is possible that these reactions participate in the dissolution of gold, but not in the corresponding dissolution of silver.

The oxidation of silver by water, with liberation of hydrogen,

$$2Ag + 4CN^- + 2H_2O \rightarrow 2Ag(CN)_2^- + 2OH^- + H_2 \quad [13]$$

has been shown to be thermodynamically unfavorable at 25°C. Julian and Smart[18] suggested that this reaction became important at higher temperatures, but measurements of the rate of dissolution up to 110°C failed to support this conclusion. The Arrhenius plot was exactly linear over the entire temperature range indicating that nature of the reaction did not change with temperature. Participation in the dissolution process, of a reaction such as 13, which does not involve oxygen would be expected to result in a change in slopes of the Arrhenius plot. This was not observed.

Rate Control: Over the range of conditions investigated, the rate of dissolution was found to be controlled by the transport of the reactants to the silver surface. The results indicated that at low NaCN concentrations, when oxygen is present in excess, the transport of CN^- controls the rate. This corresponds to a region where the rate is independent of the oxygen concentration but is proportional to the cyanide concentration. At higher cyanide concentrations, when CN^- is transported to the surface more rapidly than oxygen, the transport of oxygen becomes rate determining. In this region the rate is essentially independent of cyanide concentration but is proportional to the concentration or pressure of oxygen.

Rate control by diffusion of oxygen persisted up to oxygen partial pressures of 8 atm. This is consistent with the conclusions of Salzberg et al.,[19] that metal dissolution reactions with a large potential difference between the metal and oxidant (as is the case for this reaction) are generally diffusion controlled.

In view of the fact that the rates of dissolution of silver, measured in this study, were controlled by a physical process (i.e., diffusion) the kinetic results obtained provide little information about the detailed mechanism of the chemical reaction itself.

Effect of $Ca(OH)_2$: The marked effect of $Ca(OH)_2$ in lowering the rate of dissolution of silver has been shown to result from the formation of a deposit of calcium peroxide, CaO_2, on the silver surface. $Ba(OH)_2$ was found to have a similar effect.

Acknowledgment

This research was supported by funds provided by the Atomic Energy Control Board and administered by the National Research Council of Canada.

Appendix

Calculation of Potential-pH Relations

General Procedure: Potential-pH relations were calculated according to the method of Pourbaix.[7] The equation for an oxidation-reduction reaction can be written in the general form

$$a_1A + a_2B + a_3H_2O + a_4H^+ + n\,e = 0 \quad [14]$$

where A and B are the oxidized and reduced forms of the reactant, respectively.

The potential, E, for this reaction at 25°C is then given by the following relation:

$$E(\text{volts}) = -\frac{1}{23060n}\Sigma a_i F^\circ_i + \frac{0.0591}{n}\Sigma a_i \log(i) \quad [15]$$

where a_i is the number of mols of each species, i, in Eq. 14; (i) is the corresponding activity (assumed to be the same as the concentration); and F°_i is the corresponding standard free energy of formation.

The subsequent calculations are based on this relation, the data being taken in all instances from Latimer.[9] Since the systems considered involve dilute solutions, the activity coefficients of the dissolved species have been taken as unity.

Potential-pH Relations for O_2 and H_2O Reduction Reactions:

(i) $O_2 + 2H_2O + 2e = H_2O_2 + 2OH^-$ (sample calculation)

i	a_i	(i)	F°_i
O_2 (g)	1	1 atm	0 cal per mol
H_2O (l)	2	1	56,690
H_2O_2 (aq)	1	10^{-4} mol per liter	31,470
OH^- (aq)	2	variable	37,595

Table III. Effect of pH and Added Salts on the Rate of Dissolution of Silver

$(NaCN)_T$, 0.057 mol per liter. Temperature, 24°C. O_2 pressure, 4.8 atm.

Added Salt, Mol per Liter	pH	Rate of Dissolution, Mg Ag per Sq Cm per Hr
None	10.8	16.0
KOH—0.0004	11.6	14.8
0.004	12.5	11.9
0.164	12.8	9.8
0.222	13.2	5.4
$Ba(OH)_2$—0.003	11.5	14.8
0.018	12.1	13.9
0.034	12.3	9.2
0.160	12.9	0.0
$Ca(OH)_2$—0.0029	11.3	12.2
0.0064	11.8	8.2
0.0210	12.2	Rate fell off with time
$Ca(C_2H_3O_2)_2$—0.063	10.8	15.8
0.126	10.8	15.6

Eq. 15 takes the form

$$E = \frac{-1}{23060n}(F^\circ_{O_2} + 2F^\circ_{H_2O} - F^\circ_{H_2O_2} - 2F^\circ_{OH^-}) + \frac{0.0591}{n}\log\frac{(O_2)(H_2O)^2}{(H_2O_2)(OH^-)^2} \quad [16]$$

$$= +0.679 - 0.0591\,pH - \frac{0.0591}{2}\log(H_2O_2) + \frac{0.0591}{2}\log(O_2)$$

$= 0.856 - 0.0591$ pH, when $(O_2) = 1$ atm and $(H_2O_2) = 10^{-6}$ mol per liter.

Similarly for:

(ii) $O_2 + 2H_2O + 4e = 4OH^-$; $E = 1.229 - 0.0591\,pH + \frac{0.0591}{4}\log(O_2)$

when $(O_2) = 1$ atm, $E = 1.229 - 0.0591$ pH [17]

(iii) $H_2O_2 + 2e = 2OH^-$; $E = 1.77 + \frac{0.0591}{2}\log(H_2O_2) - 0.0591\,pH$

when $(H_2O_2) = 10^{-6}$ mol per liter, $E = 1.59 - 0.0591$ pH [18]

(iv) $2H_2O + 2e = H_2 + 2OH^-$; $E = 0 - \frac{0.0591}{2}\log(H_2) - 0.0591\,pH$

when $(H_2) = 10^{-6}$ atm, $E = 0.174 - 0.0591$ pH [19]

Potential-pH Relations for the System, Ag-H_2O:

(i) $Ag^+ + e = Ag$; $E = 0.800 + 0.0591 \log (Ag^+)$
when $(Ag^+) = 10^{-6}$ mol per liter, $E = 0.446$ [20]

(ii) $Ag_2O + 2H^+ + 2e = 2Ag + H_2O$;
$E = 1.173 - 0.0591$ pH [21]

(iii) $Ag_2O + 2H^+ = 2Ag^+ + H_2O$
$\text{Log}\,(Ag^+) = 6.32 - pH$

when $(Ag^+) = 10^{-6}$ mol per liter, pH = 12.32

Relation Between Total Cyanide, CN^- and pH: In an aqueous solution of a cyanide salt, such as NaCN, the cyanide is present in two forms, as HCN and as free CN^-. Neglecting the cyanide tied up in complex ions, (i.e. as $Ag(CN)_2^-$),

$$(NaCN)_{Total} = (HCN) + (CN^-) \quad [22]$$

The following equilibrium relation applies in all aqueous solutions at 25°C:

$$\frac{(H^+)(CN^-)}{(HCN)} = 4x10^{-10} = \frac{(H^+)(CN^-)}{(NaCN)_T - (CN^-)} \quad [23]$$

This equation can be reduced to the form:

$$\log(CN^-) = \log(NaCN)_T + pH - 9.397 - \log(1 + 10^{pH-9.397}) \quad [24]$$

Relation Between (Ag^+), (CN^-), and $(Ag(CN)_2^-)$: The equilibrium

$$Ag^+ + 2CN^- \rightleftarrows Ag(CN)_2^- \quad [25]$$

is governed by the relation

$$\frac{(Ag^+)(CN^-)^2}{(Ag(CN)_2^-)} = 1.8x10^{-19} \quad [26]$$

$$\text{or } \log(Ag^+) = \log(Ag(CN)_2^-) - 2\log(CN^-) - 18.745 \quad [27]$$

According to this, when $(CN^-) < 4.3x10^{-10}$ mol per liter, $(Ag^+) > (Ag(CN)_2^-)$. In the construction of the potential-pH diagrams it has been assumed that in this region (i.e., at $(CN^-) < 4.3x10^{-10}$) the silver ions are predominantly in the form, Ag^+, and the small amount of $Ag(CN)_2^-$ has been neglected. This assumption introduces negligible error.

Similarly, when $(CN^-) > 4.3x10^{-10}$ mol per liter, Eq. 27 shows that $(Ag(CN)_2^-) > (Ag^+)$. In this region of cyanide concentrations, the dissolved silver is predominantly in the form of $Ag(CN)_2^-$ and the concentration of free Ag^+ ion has been neglected by comparison.

Potential-pH Relation for the System, Ag-$Ag(CN)_2^-$: Combining Eqs. 20 and 27 gives:

$$E = -0.308 + 0.0591 \log(Ag(CN)_2^-) - 0.118 \log(CN^-) \quad [28]$$

Assuming that $(Ag)_T = (Ag(CN)_2^-) = 10^{-6}$ mol per liter, this becomes

$$E = -0.663 - 0.118 \log(CN^-) \quad [29]$$

or substituting for (CN^-) from Eq. 24

$$E = -0.663 + 0.118\{\log(NaCN)_T + pH - 9.397 - \log(1 + 10^{pH-9.397})\} \quad [30]$$

As indicated above, this relation applies when $(CN^-) > 4.3x10^{-10}$ mol per liter.

References

[1] J. V. Dorr and F. L. Bosqui: *Cyanidation and Concentration of Gold and Silver Ores.* (1950) New York. McGraw-Hill Book Co.

[2] G. Barsky, S. J. Swainson, and N. Hedley: *Trans.* AIME (1934) **112**, pp. 660-667.

[3] *Chemistry of Cyanidation.* American Cyanamid Co., Mineral Dressing Notes, No. 17 (February 1950).

[4] L. Elsner: *Journal Prakt. Chem.* (1846) **37**, pp. 441-446.

[5] G. Bodlaender: *Ztsch. Angen. Chem.* (1896) pp. 583-587.

[6] Janin: *Mineral Industries* (1892) **1**, p. 239.

[7] M. Pourbaix: *Thermodynamics of Dilute Aqueous Solutions.* (1949) London. Edward Arnold and Co.

[8] P. Delahay, M. Pourbaix, and P. Van Rysselberghe: *Journal* Electrochem. Soc. (1951) **98**, pp. 65-67.

[9] W. M. Latimer: *The Oxidation States of the Elements and Their Potentials in Aqueous Solutions.* (1952) New York. Prentice-Hall.

[10] J. S. McLaurin: *Trans.* Chem. Soc. (1893) **63**, pp. 724-727.

[11] S. B. Christy: *Trans.* AIME (1896) **26**, p. 735; (1900) **30**, p. 864.

[12] E. B. Sandell: *Colorimetric Determination of Traces of Metals.* (1950) New York. Interscience Publishers.

[13] H. A. White: *Journal* Chem. Met. Min. S. Africa (1934) **35**, pp. 1-11.

[14] V. Katov and S. Raikhshtein: *Journal* Phys. Chem. USSR (1941) **15**, pp. 1057-1058.

[15] N. F. Mott: *Trans.* Faraday Soc. (1939) **35**, p. 1175; (1940) **36**, p. 472.

[16] N. V. Sidgwick: *The Chemical Elements and Their Compounds* (1950) Vol. I, p. 249. Oxford University Press.

[17] A. Seidell: *Solubilities of Inorganic and Metal Organic Compounds* (1940) New York. D. Van Nostrand Co.

[18] H. J. Julian and E. Smart: *Cyaniding Gold and Silver Ores* (1921) London. Griffin.

[19] H. W. Salzberg, H. Knoetgen, and A. M. Molless: *Journal* Electrochem. Soc. (1951) **98**, pp. 31-35.

System Zirconium-Boron

by Frank W. Glaser and Benjamin Post

Three borides of zirconium have been reported: ZrB,[1] ZrB_2,[2,3] and ZrB_{12}.[4] The phase relationships, ranges of stability, and some physical properties of these compounds are described.

THE zirconium borides differ considerably from one another, particularly with respect to their relative stabilities at high temperatures in the presence of carbon.[4,5] ZrB_2 is extremely stable at all temperatures (to the melting point) in contact with carbon. Both ZrB and ZrB_{12} tend to decompose at elevated temperatures when carbon is present in excess of about 0.5 pct. ZrB forms ZrB_2 and ZrC, and ZrB_{12} decomposes to form ZrB_2 and a boron-carbide phase. In the ZrB_{12} preparation, boron present in excess of that needed to form ZrB_2 reacts with carbon, if present, to form carbides, in preference to forming the higher boride. Similar instability of borides, other than diborides of the transition metals of the 4th and 5th groups of the periodic table, has been reported.[5,6] Special precautions had, therefore, to be taken to minimize carbon contamination in the preparation of ZrB and ZrB_{12}.

Reactions below 1400°C were carried out by heating powdered mixtures of zirconium hydride and boron in quartz tubes in a hydrogen atmosphere. For temperatures above 1400°C, reactions were carried out in graphite molds. Carbon contamination from the molds was minimized by employing extremely rapid heating rates to reduce carbon diffusion into the body of the specimen, and by subsequent "shaving" of sample surfaces that had been in contact with the graphite dies. A heating rate of about 2000°C per min was obtained by heating the dies (by direct conduction), using a current of 40,000 amp. Although this type of heating cycle apparently allowed little time for "homogenization," close approximations to equilibrium conditions were usually obtained as a result of the very strongly exothermic reactions between zirconium hydride and boron at elevated temperatures. Reproducibility of results in repeated runs under varying conditions was taken as a reasonable indication that equilibrium conditions had been effectively achieved.

Quenching was accomplished by rapidly immersing the entire die, containing the reaction products, in water. Specimens could also be cooled at controlled rates by adjustment of the rate of flow of water through the water-cooled copper electrodes in contact with the graphite dies.

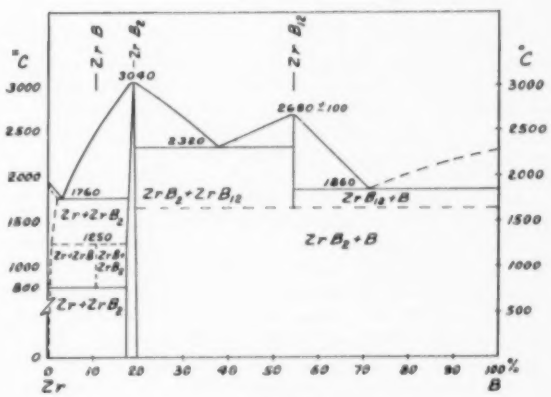

Fig. 1—Zr-B phase diagram.

F. W. GLASER, Member AIME, is associated with the American Electro Metal Corp., Yonkers, N. Y., and B. POST is associated with Polytechnic Institute of Brooklyn, Brooklyn.

Discussion on this paper, TP 3569E, may be sent, 2 copies, to AIME by Nov. 1, 1953. Manuscript, Jan. 3, 1953.

Table I. Description of Various Zr-B Compounds

Phase	Structure	Density Calculated	Density Measured	Electrical Resistivity, Microhm-cm at 20°C	Hardness, Rockwell A	Appearance
ZrB	Face-centered cubic (NaCl type). $a_o = 4.65 \pm 0.03$A	6.7	5.7	30-35	69-72	Gray to silvery-metallic luster and shows some ductility
ZrB_2	Primitive hexagonal alternating layers of Zr and B atoms. $a_o = 3.170 \pm 0.003$A $c_o = 3.533 \pm 0.003$A	6.09	6.10	9.2	87-89	Gray to silvery-metallic luster
ZrB_{12}	Face-centered cubic. $a_o = 7.408 \pm 0.002$A Zr atoms in face-centered positions and at centers of boron polyhedra consisting of 24 B-atoms	3.6	3.7	60-100	92-92.5	Black—no metallic luster

Analysis of the zirconium hydride starting material showed 98.2 pct Zr and 1.4 to 1.6 pct H. The boron powder was about 96.7 pct pure and contained, in addition, about 0.3 pct Fe and 0.08 pct C.

A series of mixtures of zirconium hydride and boron was prepared ranging in 2 pct steps, from 98 to 25 pct total zirconium content. For each composition several samples were used. In the regions of interest, samples were heated to temperatures differing by 50°C increments. Smaller intervals were employed in some critical regions. At low temperatures, 20° to 1400°C, temperature measurements were carried out with thermocouples. Above 1400°C, temperatures were measured using optical pyrometers that had been calibrated by melting metals or alloys of known melting points. Visual examination of cooled specimens indicated when specimens had melted.

Specimens were analyzed chemically after preparation. Phases present in the reaction mixtures were identified by X-ray diffraction methods supplemented by metallographic inspection. A Norelco Geiger counter spectrometer, using Cu $K\alpha$ radiation, was used in the X-ray investigation.

Results and Discussion

The results of this investigation are summarized in Fig. 1. Details of the α/β transformation of zirconium have been omitted for lack of experimental evidence. The melting points shown for zirconium[3] and boron[4] were taken from the literature. ZrB_2 was found to melt at 3040°C; this value is in good agreement with melting points previously reported.[7,8] X-ray evidence and chemical analyses indicated a narrow range of homogeneity for this compound. The dimensions of the unit cell are listed in Table I. These refer to the dimensions at stoichiometric composition; variation of parameters over the narrow range of composition was within the range of experimental error.

Pure ZrB_{12} samples could not be isolated; all specimens contained, at room temperature, 10 pct or more of ZrB_2 even after rapid quenching. There is, therefore, an uncertainty of approximately 100°C in the melting point reported for ZrB_{12} (2680°C). Estimates of the electrical resistivity of this phase were computed by extrapolating experimental values to 100 pct dense and essentially pure ZrB_{12}. The interesting crystal structure of ZrB_{12} has been described elsewhere.[4]

The ZrB phase has an extremely narrow range of stability and very rapid quenching is necessary in order to retain it at room temperature. There are indications that traces of carbon help to stabilize this phase somewhat.

The X-ray spectra of ZrN, ZrC, and ZrB are almost identical; in particular, the lattice constants of the latter two compounds are the same within experimental error. The X-ray data could, therefore, only indicate that one or more of these compounds was present; chemical analysis was necessary to exclude the possibility that the face-centered cubic phase was the carbide or nitride or some solid solution containing these compounds. Thus, specimens whose spectra indicated the presence of a considerable amount of the face-centered cubic phase, were found, on careful chemical analysis, to contain no detectable nitrogen and less than 0.3 pct C. Considerations of this sort, together with the zirconium and boron analyses, proved that the phase was ZrB.

In Table I a summary of some physical properties and structural data of ZrB, ZrB_2, and ZrB_{12} is given.

Summary

The phase diagram of the Zr-B system has been prepared. The phase relations among the three zirconium borides are shown. Only one of the three, namely, ZrB_2, exhibits good thermal and chemical stability. The preparation of the two other phases, ZrB and ZrB_{12}, is rather difficult, as has been described.

Acknowledgment

This work was supported by the Office of Naval Research and the authors would like to thank that agency for permission to publish this data.

References

[1] B. Post and F. W. Glaser: *Journal of Chemical Physics* (June 1952) **20**, p. 1050.

[2] J. T. Norton, H. Blumenthal, and S. J. Sindeband: *Trans.* AIME (1949) **185**, pp. 749-751; JOURNAL OF METALS (October 1949).

[3] R. Kiessling: *Acta Chem. Scand.* (1949) **3**, p. 90.

[4] B. Post and F. W. Glaser: *Trans.* AIME (1952) **194**, p. 631; JOURNAL OF METALS (June 1952).

[5] F. W. Glaser: *Trans.* AIME (1952) **194**, p. 391; JOURNAL OF METALS (April 1952).

[6] R. Steinitz: *Powder Met. Bull.* (1951) **6**, No. 1, pp. 54-56.

[7] F. W. Glaser: *Powder Met. Bull.* (1951) **6**, No. 1, pp. 51-54.

[8] R. F. Domagala, D. J. McPherson, and M. Hansen: *Trans.* AIME (1953) **197**, p. 279; JOURNAL OF METALS (February 1953).

[9] K. Moers: *Ztsch. anorg. allgem. Chem.* (1931) **198**, pp. 262-275.

A Study of Some Binary Hafnium Compounds

by Frank W. Glaser, David Moskowitz, and Benjamin Post

Lattice parameters of various hafnium compounds, two borides, a carbide and a nitride were determined. Some physical properties were measured and comparisons with the properties of the corresponing zirconium compounds were drawn.

ALTHOUGH borides of transition metals have been extensively investigated in recent years, there are few references in the literature to borides of hafnium. This is not surprising, in view of the extreme scarcity and great cost of the purified metal. Becker[1] reported the existence of a boride, carbide, and nitride of hafnium; he listed the formulas as HfB, HfC, and HfN. However, in his work no mention was made of chemical analyses of the reaction products. In this paper results of a study of various hafnium compounds, including borides, carbides, and nitrides, are reported. It was expected, of course, that these compounds would closely resemble their zirconium analogues, which have previously been extensively investigated.

Three borides of zirconium are known: ZrB,[2] ZrB_2,[3] and ZrB_{12}.[4] In addition, one carbide, ZrC,[5] and one nitride, ZrN,[5] have been reported. It should be noted that ZrB and ZrB_{12} are stable phases only in relatively high-temperature regions, unlike ZrB_2, which is stable from room temperature to its melting point.[6] It was felt that hafnium would yield corresponding borides, carbides, and nitrides with similar stability ranges.

Experimental Procedures and Results

A quantity of hafnium metal that was better than 97 pct pure, with zirconium as its major impurity, was furnished by the Argonne National Laboratories. The boron powder used was approximately 96.5 pct pure. In general, the procedure involved mixing the metal and boron powders in the desired proportions, and subsequently hot pressing them. The resulting specimens were analyzed chemically and phases present were identified by X-ray diffraction methods. A Philips Norelco Geiger counter spectrometer was used for identification of components and for measurement of lattice constants. Filtered copper radiation was used for all X-ray work.

Electrical resistivity and density measurements were carried out at room temperature.

The stable diboride, HfB_2, will be described first. Stoichiometric quantities of boron and metal were heated to approximately 2000°C during hot pressing. The reaction product was shown by X-ray diffraction methods to be isomorphous with ZrB_2 (space group D^1_{6h}; $P^6/_m\,mm$). Values of lattice constants of HfB_2 compared with those of ZrB_2 are shown in Table I.

Table I. Lattice Constants of HfB_2 and ZrB_2, A

Lattice	HfB_2	ZrB_2[3]
a	3.141 ± 0.002	3.170 ± 0.002
c	3.470 ± 0.002	3.533 ± 0.002
c/a	1.105	1.114

The calculated density of HfB_2 is 11.2 g per cc, compared with a measured (pycnometric) value of 10.5 g per cc. HfB_2 specimens prepared under a wide variety of conditions (including variations in initial Hf-B ratios) showed only insignificant variations in lattice constants, indicating a very narrow range of homogeneity. Like ZrB_2,[7] HfB_2 is an excellent electrical conductor. The resistivity at room temperature of hot-pressed samples, approximately 85 pct dense, is 12 microhm-cm. This compares favorably with the electrical resistivity of 10 mi-

F. W. GLASER, Junior Member AIME, and D. MOSKOWITZ are associated with the American Electro Metal Corp., Yonkers, N. Y., and B. POST is associated with Polytechnic Institute of Brooklyn, Brooklyn.

Discussion on this paper, TP 3570E, may be sent, 2 copies, to AIME by Nov. 1, 1953. Manuscript, Jan. 3, 1953.

crohm-cm reported by Becker,[1] indicating that his "hafnium boride" was probably HfB_2. The melting point of HfB_2 was measured with an optical pyrometer and found to be 3250° ± 100°C. The average coefficient of thermal expansion of HfB_2 from room temperature to 1000°C as measured under inert atmosphere was 5.3×10^{-6} per °C. Some physical properties of HfB_2 and ZrB_2 are listed for comparison in Table II.

When the starting mixture contained less than 66.7 atomic pct B, X-ray diffraction diagrams of the reaction products showed, in addition to the HfB_2 pattern, the pattern of a face-centered cubic phase. By analogy with similar zirconium and titanium phases,[2] this was identified as HfB. Strong patterns, due to this face-centered cubic phase, were obtained even in instances where chemical analysis showed the reaction products to contain less than 0.4 pct C and 0.15 pct N, precluding the possibility that the pattern was due either to HfC or HfN. Measurements of the lattice constant of this cubic phase showed $a_o = 4.62 \pm 0.02$A; the range of homogeneity could not be exactly established, but the variation in lattice dimensions of different samples indicated the possibility that it was rather wide.

A sample of HfC was prepared by hot-pressing a mixture of the elements at 2150°C. It was then checked for structure and composition by X-ray and chemical analysis. In addition, HfN was prepared by heating hafnium powder under a nitrogen atmosphere at 2000°C. Both these phases are cubic and isomorphous with the monoboride.

Table II. Some Physical Properties of HfB_2 and ZrB_2

	HfB_2	ZrB_2
Calculated density, g per cc	11.2	6.10
Measured density, g per cc	10.5	5.82
Melting point, °C	3250 ± 100	3040 ± 100
Resistivity, microhm-cm (85 pct dense samples)	12	13 to 15
Coefficient of thermal expansion per °C (20°-1000°C)	5.3×10^{-6}	5.5×10^{-6}

Values of a_o of HfB, HfC, and HfN, as determined in this investigation, are listed in Table III. Values of a_o of the corresponding zirconium compounds are listed for comparison. It is interesting, and perhaps surprising, to note that the lattice constants of the monoborides are smaller than those of the corresponding carbides, although the boron atom is larger than the carbon atom. McKenna[8] reported a_o for HfC as 4.4578 ± 0.0003A. That value appears to be much too low, and has, in fact, been criticized as "certainly incorrect."[9]

Efforts were also made to prepare the dodecaboride of hafnium. The conditions under which ZrB_{12} was prepared were duplicated,[4] but the only boride detectable in the X-ray diffraction pattern of the product was HfB_2. A wide variety of starting mixtures, reaction temperatures, and quenching procedures was tried, without yielding detectable amounts of HfB_{12}. It is evident that HfB_{12}, if it exists, has a surprisingly narrower range of stability than does the analogous zirconium compound.

Table III. Lattice Constants of Various Hafnium and Zirconium Compounds, A

HfB	4.62 ± 0.02	ZrB^{12}	4.65 ± 0.03
HfC	4.64 ± 0.02	ZrC[5]	4.685
HfN	4.52 ± 0.02	ZrN[5]	4.567

Table IV. Lattice Constants of Hafnium and Zirconium, A*

	Hafnium			Zirconium
	This Investigation	Nothling and Tolksdorf[10]	Van Arkel[11]	Van Arkel[11]
a	3.193 ± 0.002	3.33	3.206 ± 0.002	3.229 ± 0.002
c	5.052 ± 0.003	5.47	5.087 ± 0.005	5.133 ± 0.003
c/a	1.581	1.64	1.586	1.589

* While this paper was being prepared for publication, a redetermination of the lattice constants of hafnium by Duwez[12] came to our attention. He reported $a = 3.1952$A and $c = 5.0569$A, in very good agreement with the values obtained in this investigation.

Because of its purity compared with samples hitherto available, the hafnium metal used in this investigation was also subjected to X-ray diffraction analysis. Precision determinations of the lattice constants of the close-packed hexagonal unit cell revealed significant differences from the currently accepted values.[10, 11] These values, together with corresponding values for zirconium, are listed in Table IV. It is interesting to note that the presence of zirconium in hafnium would lead to an increase in the hafnium lattice parameter and might account for the larger unit cells reported by previous investigations.

Summary

A variety of hafnium compounds, including HfB, HfB_2, HfC, and HfN, have been investigated, using powder metallurgy techniques. X-ray diffraction methods were used to identify individual phases. Lattice parameters were determined and comparisons were made with the corresponding zirconium compounds. Measurements of some physical properties of HfB_2 were made. In addition, a redetermination of the lattice constants of hafnium metal has been made.

Acknowledgment

Thanks are due to the Office of Naval Research, under whose sponsorship this work was carried out, for permission to publish this data.

References

[1] I. K. Becker: *Hochschmelzende Hartstoffe und ihre Technische Anwendung.* (1933) Berlin. Verlag Chemie.
[2] B. Post and F. W. Glaser: *Journal of Chemical Physics* (1952) **20**, p. 1050.
[3] F. Norton, H. Blumenthal, and S. Sindeband: *Trans.* AIME (1949) **185**, p. 749; JOURNAL OF METALS (October 1949).
[4] B. Post and F. W. Glaser: *Trans.* AIME (1952) **194**, p. 631; JOURNAL OF METALS (June 1952).
[5] P. Duwez and F. Odell: *Journal* Electrochem. Soc. (1950) **97**, p. 299.
[6] F. W. Glaser and B. Post: The System Zr-B. This issue, p. 1117.
[7] K. Moers: *Ztsch. anorg. allgem. Chem.* (1931) **198**, p. 262.
[8] P. M. McKenna: *Industrial and Engineering Chemistry* (1936) **28**, p. 767.
[9] R. E. Rundle: *Acta Cryst.* (1948) **1**, p. 180.
[10] W. Nothling and S. Tolksdorf: *Ztsch. Krist.* (1925) **62**, p. 255.
[11] A. E. Van Arkel: *Ztsch. Physik Chem.* (1927) **130**, p. 100.
[12] P. Duwez: The Allotropic Transformation of Hafnium. *Journal of Applied Physics* (1951) **22**, p. 1174.

Creep Behavior of Extruded Electrolytic Magnesium

by C. S. Roberts

The creep mechanism and kinetics of fine-grained magnesium have been studied over the temperature range 200° to 600°F. As a result of a photographic study of microstructural changes, transient and steady-state creep components have been correlated with slip, subgrain formation, and cyclic deformation at the grain boundaries.

THE approach of this research has been the blend of a quantitative study of the creep strain of polycrystalline magnesium as a function of time, stress, and temperature with direct microstructural observations of the operative deformation processes. The validity of the conclusions is dependent on the condition that the microstructural changes seen on the polished surface qualitatively represent those occurring in the bulk of the metal. The work was intended as much to lay a background to a study of highly creep-resistant magnesium alloys as to provide a description of the behavior of the base metal itself.

The spectroscopic analysis of the electrolytic magnesium used in this study is as follows: Al, 0.009 pct; Ca, <0.01; Cu, 0.0011; Fe, 0.021; Mn, 0.012; Ni, 0.0004; Pb, 0.0012; Si, <0.001; Sn, <0.001; and Zn, <0.01. The impurity level is approximately that of commercial magnesium alloys. The original ingot was melted under Dow type 310 flux and cast as a 3 in. diam billet. It was extruded into 1¼x⅛ in. flat stock under the conditions: billet preheat 800°F (1 hr), container and die temperature 800°F, speed 3 ft per min, and area reduction ratio 45:1. The extrusion process was chosen in preference to rolling and recrystallization because it allowed easier grain size control from specimen to specimen.

The grains of the extruded metal were fairly equiaxial and uniform in the size range of 4 to 6 thousandths of an inch. The preferred orientation of basal planes about the transverse direction was determined by an X-ray diffraction surface reflection method. A beam of filtered copper radiation was directed at an angle of 17° to both the transverse direction and the surface yet perpendicular to the extrusion axis. Analysis of the (002) diffraction arcs in the resulting photographic patterns gave an approximate intensity distribution along the great circle which extends through the center of the basal plane pole figure and to the extrusion axis poles. Successive layers of metal were removed by macroetching between exposures.

The extruded texture is relatively sharp, but the most significant point is the position of the maximum basal plane pole density and its variation with depth below the surface. Fig. 1 shows that this maximum is rotated 15° from the normal at the surface toward the extrusion direction. Such an inclination has been reported for extruded 1 pct Mn and 8 pct Al-0.5 pct Zn alloys.[1] The inclination decreases until the maximum splits at about 0.025 in. depth into two elements of equal and opposite rotations from the ideal. The double texture persists to as great a depth as was experimentally convenient to examine. It probably continues to the very center of the extrusion. There is no great change in the sharpness of the individual elements of the texture with depth.

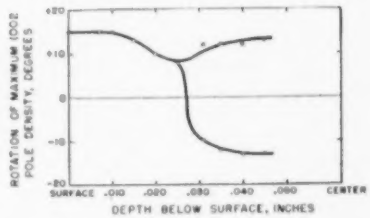

Fig. 1—Preferred orientation of extruded electrolytic magnesium. Positive angles toward extrusion direction.

A plate of metal about 0.015 in. thick at the surface of the extruded stock was produced by etching. A transmission diffraction pattern was made for the purpose of determining any preferred orientation of a direction in the basal planes. Relatively uniform {100} and {101} rings were produced. There is little tendency for parallelism of a given direction in the plane with the projection of the extrusion axis on it.

The creep specimens were machined from 6¼ in. lengths of the extruded stock. Creep was measured on the reduced section, ½x⅛x2¼ in. long. This section was electropolished on one side for the studies of microstructural changes during creep. An orthophosphoric acid-ethyl alcohol electrolyte was used under the conditions recommended by Jacquet.[2] Hand polishing was used for previous mechanical preparation. Electropolishing was continued until all mechanical twins had been removed. The electropolished surface was protected from oxidation during creep testing by a thin layer of silicone oil. All micrographs were taken at room temperature on conventional metallographic equipment and after removal of the oil film.

The creep tests were performed with machines which have been described in detail by Moore and McDonald.[3] Five testing temperatures, 200°, 300°, 400°, 500°, and 600° ±3°F were used. Difference in temperature between the two ends of the specimen reduced section was 2°F or less. The testing was done at constant load. Strain readings were taken as frequently as necessary to develop usable creep curves.

Tensile Creep vs Time, Stress, and Temperature

A definition of terms is necessary. Whenever successive sections of a creep strain-time curve show decreasing, constant, and increasing slope with time they will be termed primary, secondary, and tertiary

C. S. ROBERTS, Junior Member AIME, is associated with The Dow Chemical Co., Midland, Mich.

Discussion on this paper, TP 3596E, may be sent, 2 copies, to AIME by Dec. 1, 1953. Manuscript, March 16, 1953. Cleveland Meeting, October 1953.

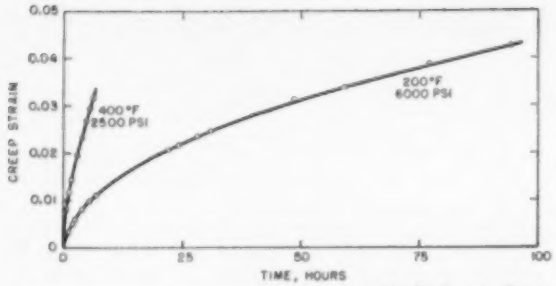

Fig. 2 (above)—Creep curves for extruded electrolytic magnesium when transient creep is the major process.

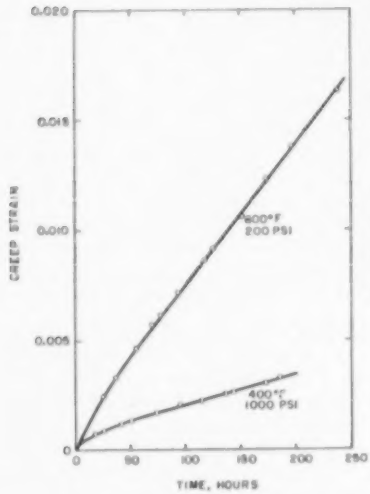

Fig. 3 (left)—Creep curves for extruded electrolytic magnesium when steady-state creep is the major process.

creep, respectively. The terms transient and steady-state creep will be applied in the conventional manner to the two separable elements which show finite decreasing and constant strain rates, respectively, from the beginning of the test. Primary creep may be used for a quantitative analysis of the transient component only when the steady-state creep is negligible. Secondary creep may be analyzed as steady-state creep only when the transient element is negligible.

Quantitative analyses of the linear coordinate plots of creep strain vs time for magnesium proved the existence of both transient and steady-state components. Transient creep was predominant for all stresses tested at the lowest temperature of test, 200°F. Steady-state creep becomes more predominant as the temperature increased and to a lesser extent as the stress decreased. There is negligible transient creep at the limit of low stresses at 600°F. The representative creep curves shown in Figs. 2 and 3 illustrate the change of curve shape over the experimental range of stress and temperature. Transient creep is predominant in the curves of Fig. 2. Fig. 3 illustrates the predominance of steady-state creep. Tertiary creep was never observed, although many tests were carried to a creep strain of 0.10.

In the first phase of this investigation creep curves were obtained from tests at the temperatures of 300°, 400°, 500°, and 600°F. Each test was continued until rectilinearity of the plot had demonstrated the existence of secondary creep. Secondary creep was never generated within the measurable strain range in the tests at 200°F. The first kinetic analyses were made with secondary creep rate, stress, and temperature as the variables. Attempts were made to fit isothermal rate data to the exponential, power, and hyperbolic sine functions of stress. With the use of tables constructed for the purpose[4] it was found that the latter function gave a poor fit of the data. Curvature of the semilog plot of stress vs secondary creep rate shown in Fig. 4 constitutes proof of the invalidity of the exponential relation. The plot of the data on log-log coordinates in Fig. 5 is a test of the power relation between stress and secondary creep rate. The rectilinearity of the isotherms proves the validity of the power function. A relatively sharp transition between two straight line segments in each isotherm is required to fit the data. Such transitions have been reported and discussed by Servi and Grant.[5, 6]

Transient Creep: The creep strain-time data for the higher stresses at 200°, 300°, 400°, and 500°F, where transient creep is very predominant, were plotted on log-log coordinates. Straight lines were obtained in agreement with the equation

$$\epsilon_t = \beta t^n$$

where ϵ_t is transient creep strain; β, a function of temperature and stress; t, the time in hours; and n, a constant.

Values of β and n, which are equal to the intercept at 1 hr and slopes of the straight line, respectively, are given in Table I. A remarkable constancy of n with an average value of 0.53 was found. The dependence of β on stress and temperature is shown in Fig. 6. Straight and reasonably parallel lines prove that β is of the form $B(T)\sigma^m$ where m, the average slope in Fig. 6, is 4.0. A straight line in the plot of β at 3000 psi vs the reciprocal of the absolute temperature, Fig. 7, shows $B(T)$ to be of the form $Ae^{-Q/RT}$. The β values plotted are the intercepts of the lines in Fig. 6, using extrapolation of the 500°F data. The temperature coefficient Q, is equal to 15,500 cal per gram atom. In the experimental range, the average slope in Fig. 6, is 4.0. A straight line in the the range of 200° to 500°F and 1250 to 10,000 psi may be represented by

$$\epsilon_t = 4.5\text{x}10^{-6}\, e^{\frac{-15,500}{RT}}\, \sigma^{4.0}\, t^{0.53}.$$

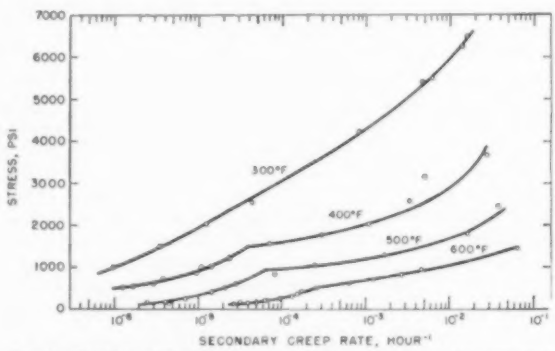

Fig. 4—Semilog plot of stress vs secondary creep rate for extruded electrolytic magnesium.

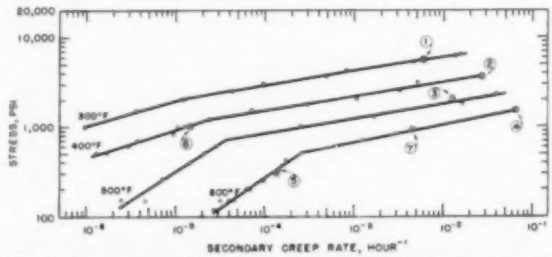

Fig. 5—Log-log plot of stress vs secondary creep rate for extruded electrolytic magnesium.

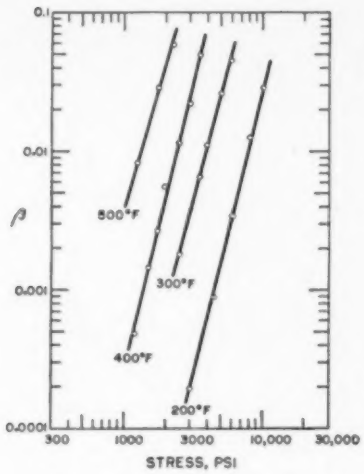

Fig. 6 (left)—Stress and temperature dependence of transient creep.

Fig. 7 (below)—Plot for determination of temperature coefficient Q, of transient creep.

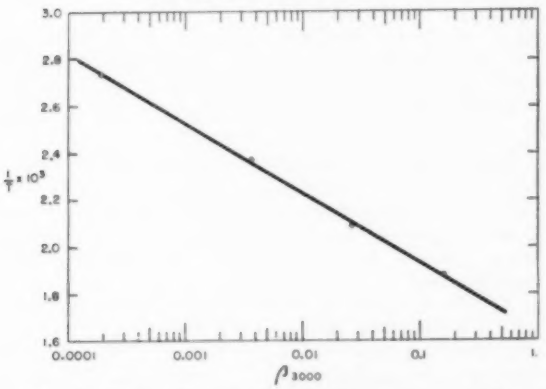

Steady-State Creep: Calculations were made of the transient creep rate $d\epsilon_t/dt$ which was occurring at the strain level of individual curves where the secondary creep rate was measured for the general kinetic analysis. Comparison of these rates with the measured secondary rates led to an understanding of the transitions shown in Fig. 5. The measured rates are predominantly the steady-state creep element on the high temperature-low stress side of a transition. Under conditions represented by the low temperature-high stress side of a transition, the measured rates are predominantly the transient creep element. Because of the markedly different stress dependence of the two rates, only in the near vicinity of the transition on the log-log plot are they of the same order of magnitude at the strain levels where the secondary rates were measured.

An analysis of the stress and temperature dependence of the steady-state creep element alone was made on the low stress segments of the isotherms of Fig. 5. The only conclusion that could be drawn was that the steady-state creep coefficient, k, was a power function of stress with the exponent b a function of temperature. The separable element of temperature dependence showed no simple form. That is, steady-state creep in polycrystalline electrolytic magnesium may be represented by

$$\epsilon_s = k\ (\sigma^{b(T)}, T)t\,.$$

Deformation Processes in Creep

Low-Temperature Type Deformation: Several electropolished specimens were deformed at high creep rates. Fig. 8 presents the microstructure of a specimen deformed at 200°F. The microstructures shown in Figs. 9 to 12 correspond to the test conditions labeled by the encircled numerals 1 to 4 in Fig. 5. With the exception of the one produced at 400°F, the structures may be directly compared at a total creep strain of about 0.04.

The slip lines are straight with a fineness and uniformity of spacing which decrease with increasing temperature. The formation of sharp subgrains is common to all temperatures. The sharpness of the subboundaries is clearly shown with vertical illumination in Fig. 10. At the lower strain level, oblique illumination is valuable in revealing their sharpness as in Fig. 11b. In general, however, oblique illumination was avoided because of the excessive shadows produced at the grain boundaries. The slight deviation of slip lines which pass through the subboundaries and the results of a few X-ray back-reflection studies showed that neighboring subgrains were only slightly disoriented with respect to each other. In all of these structures deformation at the grain boundaries is much less than that within the grains. However, the boundary deformation increases in magnitude and changes from a rough and broken-up to a smooth appearance as the temperature increases.

High-Temperature Type Deformation: The smooth variety of grain boundary deformation is a cyclic process of sliding and migration which is best studied under conditions when it is predominant. Figs. 13 to 14 which correspond to points 5 and 6 on the low-stress high-temperature segments in Fig. 5 present microstructures obtained when primary creep was nearly absent. The mechanical twins and vertical polishing scratches which unfortunately appear in Fig. 13 were present before testing because of insufficient electropolishing of this specimen only. All other specimens used in the research were free of twins and scratches after electropolishing. Subgrain formation has disappeared and slip lines are few in number. The ribbing of the displaced regions was the first clue to the cyclic nature of the process. Inspection of many grain boundaries revealed the following characteristics:

1—In almost all cases grain boundary sliding is such that the grain having the convex surface boundary contour subsides.

2—In all cases grain boundary migration is "downhill," i.e., into the subsided grain. Thus it is almost

Table I. Stress and Temperature Dependence of β, n, and m

Temperature, °F	Stress Psi	n	β	m
200	3,000	0.58	0.00019	
	4,500	0.58	0.00088	
	6,000	0.56	0.0034	
	8,000	0.50	0.0124	
	10,000	0.53	0.0285	
	Average	0.55		4.2
300	2,500	0.49	0.0018	
	3,500	0.50	0.0066	
	4,000	0.50	0.0110	
	5,000	0.54	0.0260	
	6,000	0.55	0.0450	
	Average	0.53		3.9
400	1,200	0.53	0.00048	
	1,500	0.49	0.00145	
	1,750	0.49	0.00265	
	2,000	0.51	0.0055	
	2,500	0.51	0.0113	
	3,000	0.49	0.0220	
	3,500	0.53	0.0500	
	Average	0.51		4.2
500	1,250	0.54	0.0082	
	1,750	0.54	0.0285	
	2,250	3.53	0.0580	
	Average	0.54		3.5
Average		0.53		4.0

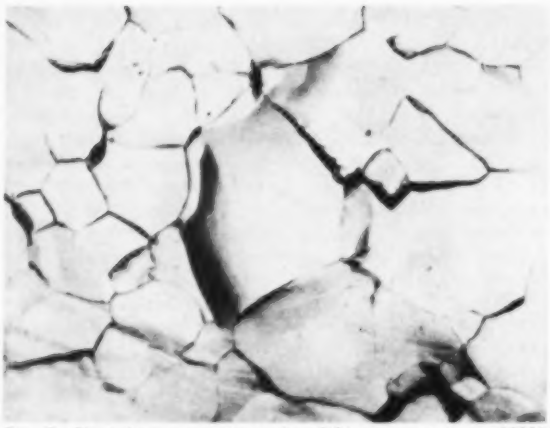

Fig. 8—Electrolytic magnesium after 0.04 creep strain at 200°F and 6000 psi. Stress axis vertical. X250.

Fig. 9—Electrolytic magnesium after 0.04 creep strain at 300°F and 5500 psi, conditions of point 1 in Fig. 5. Stress axis vertical. X250.

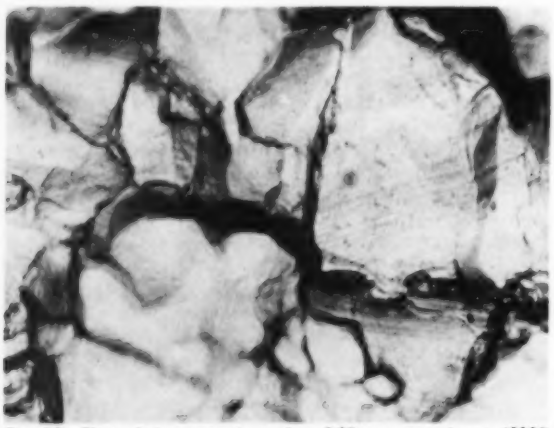

Fig. 10—Electrolytic magnesium after 0.08 creep strain at 400°F and 3675 psi, conditions of point 2 in Fig. 5. Stress axis vertical. X250.

always in the normal direction for grain growth (grain boundary energy induced process).

Grain growth is negligible if specimens are annealed at temperatures and for times equal to those necessary to produce boundary migration in the cyclic deformation process. It is reasonable to regard the process as one of accelerated grain growth accompanied by the generation of strain. The process can lead to the ultimate consumption of grains as is shown in Figs. 12 and 13. A series of photographs which also illustrates this point and which corresponds to point 7 in Fig. 5 has been presented.[7]

Discussion of Results

The cyclic grain boundary deformation process is perhaps the most striking one observed in this research. It has been observed and analyzed in the creep of polycrystalline aluminum by Servi and Grant[5, 6] and Chang and Grant.[8, 9] The latter investigators employed precise measurements of creep across the boundaries to obtain cyclic creep curves which correlated with the alternate elements of sliding and migration. The structure resulting from this process appears in the micrographs of aluminum by Hanson and Wheeler,[10] Wilms and Wood,[11] and McLean,[29] iron alloys by Jenkins and Mellor,[12] zinc by Cottrell and Aytekin[13] and Ramsey,[14] tin-antimony alloy by Betteridge and Franklin,[15] lead-thallium alloy by Gifkins,[16] magnesium by Suiter and Wood,[17] and tin by Puttick and King.[27]

Sliding appears to occur on boundaries nearest to 45° to the stress axis until stopped by the local interference at edges and vertices. The strain energy localized at the grain boundary regions then accelerates the activation of boundary migration. The migration evidently lowers the strain energy (local stress relief) and allows more sliding at the bound-

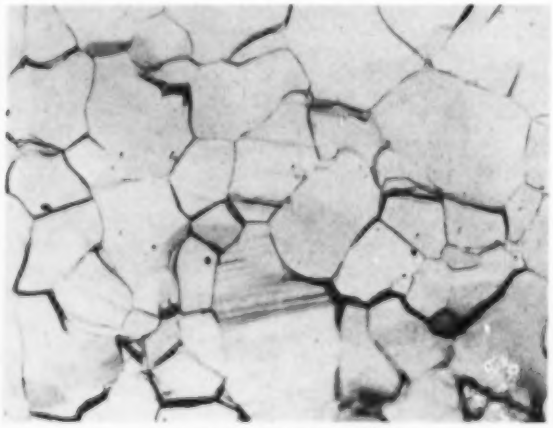

a—Vertical illumination. X250.

b—Oblique illumination. X250.

Fig. 11—Electrolytic magnesium after 0.04 creep strain at 500°F and 2000 psi, conditions of point 3 in Fig. 5. Stress axis vertical.

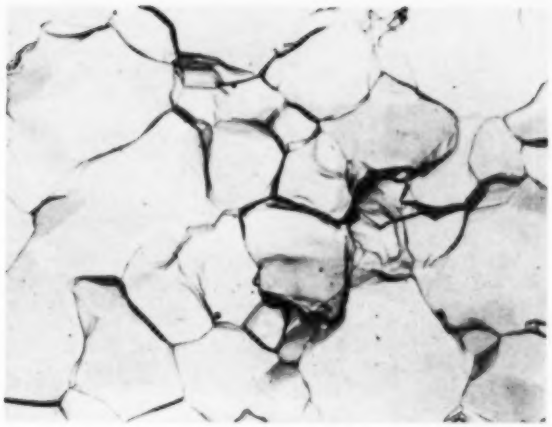

Fig. 12—Electrolytic magnesium after 0.041 creep strain at 600°F and 1500 psi, conditions of point 4 in Fig. 5. Stress axis vertical. X250.

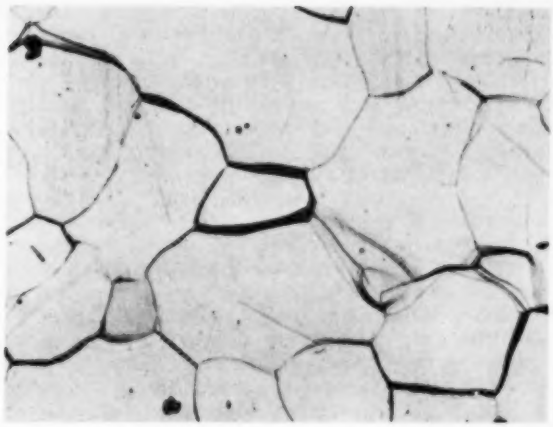

Fig. 13—Electrolytic magnesium after 0.02 creep strain at 600°F and 300 psi, conditions of point 5 in Fig. 5. Stress axis vertical. X250.

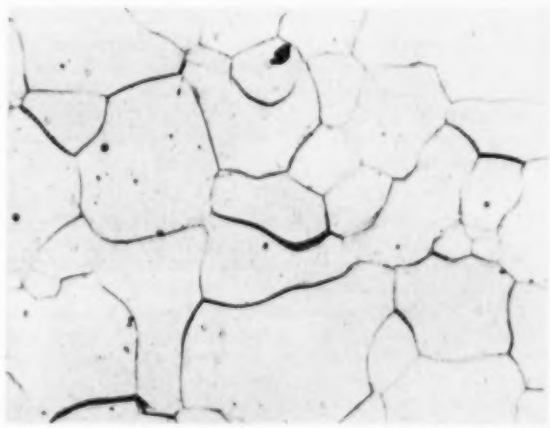

Fig. 14—Electrolytic magnesium after 0.01 creep strain at 400°F and 1000 psi, conditions of point 6 in Fig. 5. Stress axis vertical. X250.

ary. In other words, the process is guided by the tendency to lower both strain energy and surface energy. This was a conclusion reached in a previous study of aluminum.[9] The sparseness of slip lines in Figs. 13 and 14 indicates that in the limiting case of high temperature and low stress this process may be the sole mechanism of creep. The change of mass of the grain adds another degree of freedom not possessed by the deformation processes which lead only to change of grain shape.

The predominance of grain boundary deformation correlates with the predominance of steady-state creep. Perhaps the constancy of creep rate results from the existence of the cyclic self-recovery which boundary migration provides. The whole picture developed from these studies of creep rate and microstructural changes supports the concept of transient creep resulting from deformation within the grains and steady-state creep from grain boundary deformation. This viewpoint was first presented by Andrade[15, 19] and has since been supported by many investigators.[20, 11, 18, 10, 8, 6]

Although transient creep in magnesium obeys the power function of time, the exponent, 0.53, differs from the classical value 1/3. This is in contrast with the work on zinc by Cottrell and Aytekin[18] and that on aluminum by Servi and Grant[5] where agreement was found. This difference may be due to the testing conditions of constant load rather than constant stress. If this were the cause, it would hardly seem possible to obtain such consistent results, however. The exponential relation between transient creep and temperature has been found to hold over a range of 300°F (167°C) for extruded electrolytic magnesium. It has been proven for nickel over a 75°C range by Hazlett and Parker[21] and for zinc, aluminum, and magnesium over a 100°C range by Crussard.[28] The latter investigator reported Q for magnesium as ranging from 16,000 to 18,000 cal per gram atom, a good agreement with the result of this research. There is no evidence that Q can be identified as the activation energy of any simple rate-controlling process.

The occurrence of twinning was not found in any of the microstructural studies of extruded magnesium. This can be understood after an examination of the preferred orientation, Fig. 1. When basal planes lie at small angles to the tension axis, twinning is not to be expected. However, recent work on very coarse grained magnesium by Chaudhuri et al.[29] and the studies of zinc by Cottrell and Aytekin[18] and magnesium by Suiter and Wood[17] have shown that when orientation conditions allow it twinning plays an important part in creep behavior. Recent work on the rare-earth alloys of magnesium in this laboratory has elucidated the roles of twinning and also of non-basal slip in creep deformation. The results will be reported elsewhere.

The significance of subgrain formation in the creep deformation of aluminum, zinc and magnesium has been well established.[6, 11, 13–15, 17, 18, 24, 28] The similarity of this polycrystalline deformation process to kinking and polygonization phenomena in single crystals has been discussed by Washburn and Parker.[30] They illustrate how continuity at grain boundaries may be aided by the occurrence of subgrain formation. It has been concluded in some of the past investigations that the process is of importance only at high temperatures and low creep rates and further that there is an appreciable increase of subgrain size with increasing temperature. The present results show that subgrain formation in magnesium is most pronounced at high creep rates at all temperatures. As the creep rate decreases at a given temperature, it disappears before slip does. The cyclic boundary deformation serves as its successor. The microstruc-

tural studies show no appreciable change in subgrain size over the entire experimental range of temperature and creep rate.

The results show that with increasing temperature and decreasing stress, predominance in creep changes from the processes of slip and subgrain formation to that of grain boundary deformation. It seems possible that at very low stresses and at temperatures approaching the melting point, the viscous self-diffusion process postulated by Nabarro[25] and Herring[26] may become predominant. All these processes must overlap each other in operation. Nevertheless, transitions may be expected from one to the other as the major creep rate-controlling process.

Fortunately it is becoming more and more apparent as time passes that there is more similarity than difference in the creep mechanism and kinetics of polycrystalline metals. The agreement between studies of magnesium, aluminum, and zinc points out that although minor differences may be of technical importance, they can generally be integrated into a coherent picture of the fundamentals.

Conclusions

1—The creep strain of extruded polycrystalline electrolytic magnesium over the temperature range 200° to 600°F consists of both transient and steady-state elements. The two elements of creep strain may be represented as a function of time, stress and temperature by

$$\epsilon = 4.5\text{x}10^{9}\, e^{\frac{-18,000}{RT}}\, \sigma^{4.5}\, t^{0.32} + k\,(\sigma^{5.0(T)}, T)\, t.$$

2—A rather sharp transition occurs between two straight line segments of the isotherms in the log-log plot of stress vs observed secondary creep rate. This results from the markedly different stress and temperature dependence of the two creep components.

3—The transient component of creep results from the intragranular processes of basal slip and subgrain formation. It is of major importance at low temperatures and/or high stresses.

4—The steady-state element of creep results from a cyclic process of sliding and migration of the grain boundaries. It is predominant at high temperatures and/or low stresses.

5—Slip lines become coarser and less uniformly spaced as the creep temperature increases.

6—The size of subgrains formed in creep is independent of creep rate and temperature over the experimental range studied.

Acknowledgment

This work was sponsored by the Flight Research Laboratory, Wright Air Development Center, under Contract No. AF 33(038)-16655.

References

[1] R. L. Dietrich: Surface Orientation and Rolling of Magnesium Sheet. *Trans.* AIME (1949) **185**, p. 621; JOURNAL OF METALS (September 1949).

[2] P. A. Jacquet: *Electrolytic Polishing of Metallic Surfaces and Its Applications* (1948) p. 64. Saint-Germain-En-Laye. Editions Metaux.

[3] A. A. Moore and J. C. McDonald: Tensile and Creep Strengths of Some Magnesium-Base Alloys at Elevated Temperature. *Proc.* ASTM (1946) **46**, p. 970.

[4] P. G. McVetty: Creep of Metals at Elevated Temperatures. The Hyperbolic-Sine Relation Between Stress and Creep Rate. *Trans.* ASME (1943) **65**, p. 761.

[5] I. S. Servi and N. J. Grant: Creep and Stress Rupture Behavior of Aluminum As a Function of Purity. *Trans.* AIME (1951) **191**, p. 909; JOURNAL OF METALS (October 1951).

[6] I. S. Servi and N. J. Grant: Structure Observations of Aluminum Deformed in Creep at Elevated Temperatures. *Trans.* AIME (1951) **191**, p. 917; JOURNAL OF METALS (October 1951).

[7] C. S. Roberts: Discussion on ref. 8; *Trans.* AIME (1953) **197**, p. 732; JOURNAL OF METALS (May 1953).

[8] H. C. Chang and N. J. Grant: Observations of Creep of the Grain Boundary in High Purity Aluminum. *Trans.* AIME (1952) **194**, p. 619; JOURNAL OF METALS (June 1952).

[9] H. C. Chang and N. J. Grant: Grain Boundary Sliding and Migration and Intercrystalline Failure Under Creep Conditions. *Trans.* AIME (1953) **197**, p. 305; JOURNAL OF METALS (February 1953).

[10] D. Hanson and M. A. Wheeler: The Deformation of Metals Under Prolonged Loading. Part I—The Flow and Fracture of Aluminum. *Journal* Inst. Metals (1931) **45**, p. 229.

[11] G. R. Wilms and W. A. Wood: Mechanism of Creep in Metals. *Journal* Inst. Metals (1949) **75**, p. 693.

[12] C. H. M. Jenkins and G. A. Mellor: Investigation of the Behavior of Metals Under Deformation at High Temperatures. Part I — Structural Changes in Mild Steel and Commercial Irons During Creep. *Journal* Iron and Steel Inst. (1935) **132**, p. 179.

[13] A. H. Cottrell and V. Aytekin: The Flow of Zinc Under Constant Stress. *Journal* Inst. Metals (1950) **77**, p. 389.

[14] J. A. Ramsey: Some Observations on the Deformation of Polycrystalline Zinc. *Journal* Inst. Metals (1951) **80**, p. 167.

[15] W. Betteridge and A. W. Franklin: An Investigation of the Structural Changes Accompanying Creep in a Tin-Antimony Alloy. *Journal* Inst. Metals (1951) **80**, p. 147.

[16] R. C. Gifkins: Grain Movements During Creep. *Nature* (1952) **169**, p. 238.

[17] J. W. Suiter and W. A. Wood: Deformation of Magnesium at Various Rates and Temperatures. *Journal* Inst. Metals (1952) **81**, p. 181.

[18] E. N. daC. Andrade: On the Viscous Flow in Metals, and Allied Phenomena. *Proc.* Royal Soc. (1911) **84**, p. 1.

[19] E. N. daC. Andrade: The Flow in Metals Under Large Constant Stresses. *Proc.* Royal Soc. (1914) **90**, p. 329.

[20] E. Orowan: Creep of Metals. *Journal* West Scotland Iron and Steel Inst. (1947) **54**, p. 45.

[21] T. H. Hazlett and E. R. Parker: Nature of the Creep Curve. *Trans.* AIME (1953) **197**, p. 318; JOURNAL OF METALS (February 1953).

[22] C. Crussard: The Role of Grain Boundaries in the Deformation of Metals. Application to Creep and Fatigue. *Revue Métallurgie* (1946) **43**, p. 307.

[23] A. R. Chaudhuri, N. J. Grant, and J. T. Norton: Metallographic Observations of the Deformation of High-Purity Magnesium in Creep at 500°F. *Trans.* AIME (1953) **197**, p. 712; JOURNAL OF METALS (May 1953).

[24] J. A. Ramsey: The Subgrain Structure In Aluminum Deformed at Elevated Temperatures. *Journal* Inst. Metals (1952) **81**, p. 215.

[25] F. R. N. Nabarro: *Report of Conference on the Strength of Solids* (1948) p. 75. London. Physical Society.

[26] C. Herring: Diffusional Viscosity of a Polycrystalline Solid. *Journal of Applied Physics* (1950) **21**, p. 437.

[27] K. E. Puttick and R. King: Boundary Slip in Bicrystals of Tin. *Journal* Inst. Metals (1951-1952) **80**, p. 537.

[28] D. McLean: Crystal Fragmentation in Aluminum During Creep. *Journal* Inst. Metals (1952-1953) **81**, p. 287.

[29] D. McLean: Grain-Boundary Slip During Creep of Aluminum. *Journal* Inst. Metals (1952-1953) **81**, p. 293.

[30] J. Washburn and E. R. Parker: Kinking in Zinc Single-Crystal Tension Specimens. *Trans.* AIME (1952) **194**, p. 1076; JOURNAL OF METALS (October 1952).

High Pressure Oxidation Rate of Metals—Copper in Oxygen

by William McKewan and W. Martin Fassell, Jr.

The oxidation rates of copper have been determined at temperatures from 600° to 900°C in oxygen from 14.7 to 400 psi total oxygen pressure. The oxidation rate of copper is unchanged by oxygen pressures within the range studied. The observed data extend Feitknecht's conclusion concerning the pressure independence of copper from atmospheric pressure to 400 psi. All samples studied in the above-mentioned temperature and pressure range have both Cu_2O and CuO present in the oxide film.

NUMEROUS papers have been published on the oxidation of copper, some of which have noted the effect of oxygen pressure on the oxidation rate of copper. It must be noted, however, that no data on the oxidation rates of copper at pressure in excess of 1 atm have been reported in the literature. (Le Chatelier[1] reported that a black oxide of silver was formed at 300°C and 15 atm pressure.) This is likewise true for the other metals.

This investigation was initiated to obtain experimental oxidation rate constants for pure metals at elevated temperatures and high oxygen pressure. Copper was selected as the first metal since probably more reliable data are available on its oxidation rates and related physical and chemical properties than for any other metal or alloy.

As a general summary, the following conclusions appear well established for the oxidation of copper:

1—The oxide coating consists of Cu_2O with a superficial coating of CuO providing the ambient oxygen pressure exceeds the equilibrium pressure for the coexistence of Cu_2O and CuO.[2] The following sequence of phases is then $Cu/Cu_2O/CuO/O_2$ (gas). The Cu_2O consists of large crystals that have no relation to the orientation of the metal crystals, except for a very thin layer adjacent to the metal.[3] The CuO consists of very fine crystals randomly oriented. If the oxygen pressure is below the equilibrium pressure for the coexistence of Cu_2O and CuO, the coating consists of Cu_2O only.[2,4,5]

W. M. McKEWAN, Junior Member AIME, formerly graduate student in Metallurgy, University of Utah, is now with the New Jersey Zinc Co. (of Pa.), Palmerton, Pa., and W. M. FASSELL, Jr., Member AIME, is Assistant Professor, Dept. of Metallurgy, University of Utah, Salt Lake City.

Discussion on this paper, TP3595E, may be sent, 2 copies, to AIME by Dec. 1, 1953. Manuscript, Dec. 31, 1951; revision, Jan. 2, 1953. Cleveland Meeting, October 1953.

This paper is a report of work done under contract with the Atomic Energy Commission.

2—The rate-determining factor in the parabolic oxidation of copper is the diffusion of Cu^+ ions through the Cu_2O layer.[4,6,7] The Cu^+ ions are accompanied by electrons to maintain electrical neutrality. The mechanism of the reaction at the Cu_2O/CuO interface and the method of growth of the CuO is in some doubt.

3—On copper, there are three reported pressure effects: (a) At pressures below 0.3 mm Hg oxygen pressure, the oxidation rate increases directly with pressure.[2,4,5] Oxygen starvation at the surface may account for this effect. (b) At oxygen pressures from 0.3 to 63 mm, the oxidation rate increases as the 7th root of the oxygen pressure providing the temperature is such that only Cu_2O is present in the film. (c) At pressures from above the equilibrium pressure for the coexistence of Cu_2O and CuO (varies with temperature) to atmospheric pressure, the oxidation rate is independent of the oxygen pressure.[8]

Equipment

In order to determine the oxidation rates of metals in an oxidizing atmosphere at pressures up to 400 psi, the equipment is somewhat different than for low pressure work as is shown in Figs. 1 and 2. A Leeds and Northrup Micromax recording controller (*A*) is used to control the temperature of the Nichrome furnace winding in conjunction with a Micromax electric drive unit. The drive unit adjusts a 20 amp Variac (variable transformer) to control the power input into the Nichrome furnace winding.

Due to the "self heating" of the sample by oxidation, frequently encountered in oxidation rate studies, it is essential that the sample temperature be measured independently. This is done by means of a series of six chromel-alumel calibrated thermocouples located spirally around the oxidizing metal sample. Each thermocouple is partially shielded from the direct radiation of the furnace wall by

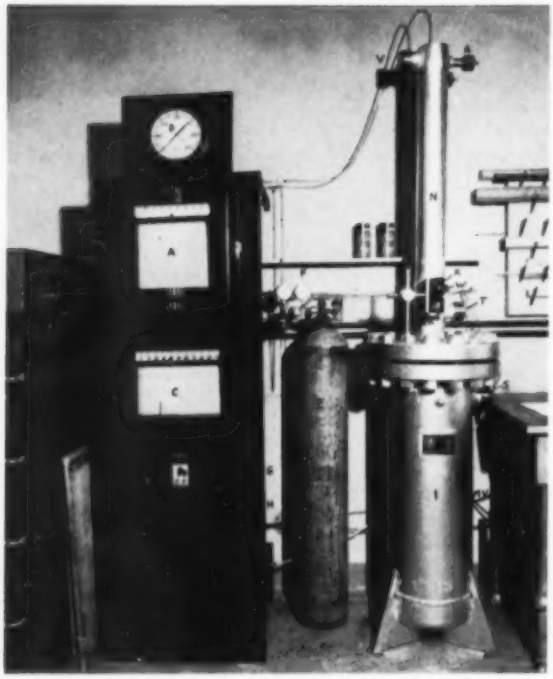

Fig. 1—Equipment for high pressure oxidation rate studies. See caption of Fig. 2 for explanation of letters.

means of an alundum shield (*J*). This arrangement gives apparent sample temperatures that are near the true temperature. The six sample thermocouples are connected to a Brown Electronic 12 point recorder (*C*).

The pressure in the furnace is measured by means of gage (*D*) (Master Gage Type 101, 0 to 600 psi, 3 pct accuracy with recalibration). For pressure measurements from 0 to 28 psi, a mercury absolute pressure gage is used for higher precision, not shown in Fig. 1. The oxygen from cylinder (*E*) is delivered via a high pressure reduction valve (*F*) (0 to 1000 psi) to the drying unit. The drying unit, not shown in Fig. 1, consists of an 18 in. length of 2 in. heavy wall pipe capped on the ends and packed with 2 lb of activated alumina (4-s mesh grade F-1, Alcoa). The dry oxygen is delivered from the drier to the furnace and pressure gage.

In order to remove the air in the furnace prior to the introduction of the oxidizing atmosphere, a Megavac vacuum pump (*MV*) is connected to the system. Valves (*G*) and (*H*) are used to release the pressure and connect the vacuum pump to the system, respectively.

The furnace shell consists of two sections. The lower section (*I*) contains the No. 18 Nichrome 7 heating element wound on a 2 in. ID x 36 in. alundum tube (Norton No. 12310), the alundum shielding tube 1 in. ID x 24 in. (Norton RA 98), the furnace insulation (*L*) (MgO, calcined chemical precipitate) and the thermocouple and power leads (*M*). The upper section (*N*) contains the quartz spring balance (*O*) (0 to 5 g capacity 12 mm diam x 65 mm length [Type B Houston Technical Laboratories]), and the gold suspension chain (*P*), wound around an 18-8 stainless steel drum (Q) used to lower the sample into the furnace. A No. 30 B and S Pt-20 pct Rh wire suspends the sample from the quartz spring. In order to keep the sample centered with respect to the cathetometer, the furnace tube, and the measuring thermocouples, the pitch of the threads on the drum is the same as that in the bonnet of the packing gland (*R*) so that there is no relative horizontal motion of the chain, quartz spring, and sample (*Z*).

The access opening (*T*), in the top section, is used for the placement and removal of samples on the Pt-Rh suspension wire. The sample is suspended on a small platinum hook coated with a thin layer of alundum cement, fired in situ. Access opening (*V*) is used for the initial placement and adjustment of the weighing and suspension components.

The microscope (*W*) and cathetometer (*X*), used to measure the rate of elongation of the quartz spring through the observation window (*Y*), are mounted rigidly to the furnace shell.

All power and thermocouple leads enter the lower section of the furnace through the multiple pressure packing gland (*S*).

Procedure

The copper metal samples used in this investigation are annealed commercial electrolytic sheet 0.018 in. thick x ½ in. x 1½ in.

The geometric surface area of each sample is calculated from micrometer measurements of the dimensions. A 0.125 in. hole is drilled near the top end for the suspension hook. Prior to oxidation, the sample is etched 5 min in 10 pct ammonium persulphate to remove any oxide film present, washed with distilled water and dried. After cleaning, the sample is weighed and placed on the hook through access opening (*T*).

With the sample in place, the cover plate is bolted on and the furnace evacuated. After the air is removed, oxygen is allowed to enter the furnace slowly to the desired pressure. The furnace is

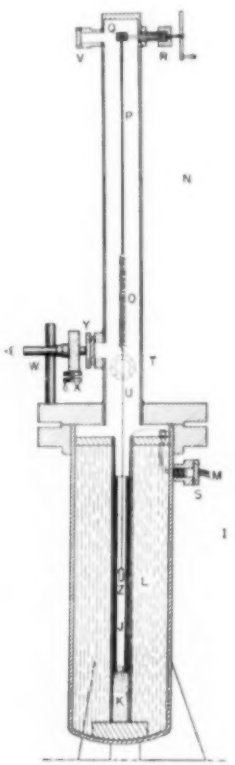

Fig. 2—High pressure oxidation furnace.

A—Recording controller
B—Electric control unit
C—12 point recorder
D—Pressure gage
E—Oxygen cylinder
F—High pressure reduction valve
G—Pressure valve
H—Vacuum pump valve
I—Lower section of furnace shell
J—Alundum shield
K—Grain alundum
L—Furnace insulation
M—Thermocouple and power leads
MV—Vacuum pump
N—Upper section of furnace
O—Spring balance
P—Suspension chain
Q—Stainless steel drum
R—Packing gland
S—Packing gland
T—Access opening
U—Pt-20 pct Rh suspension wire
V—Access opening
W—Microscope
X—Cathetometer
Y—Observation window
Z—Sample

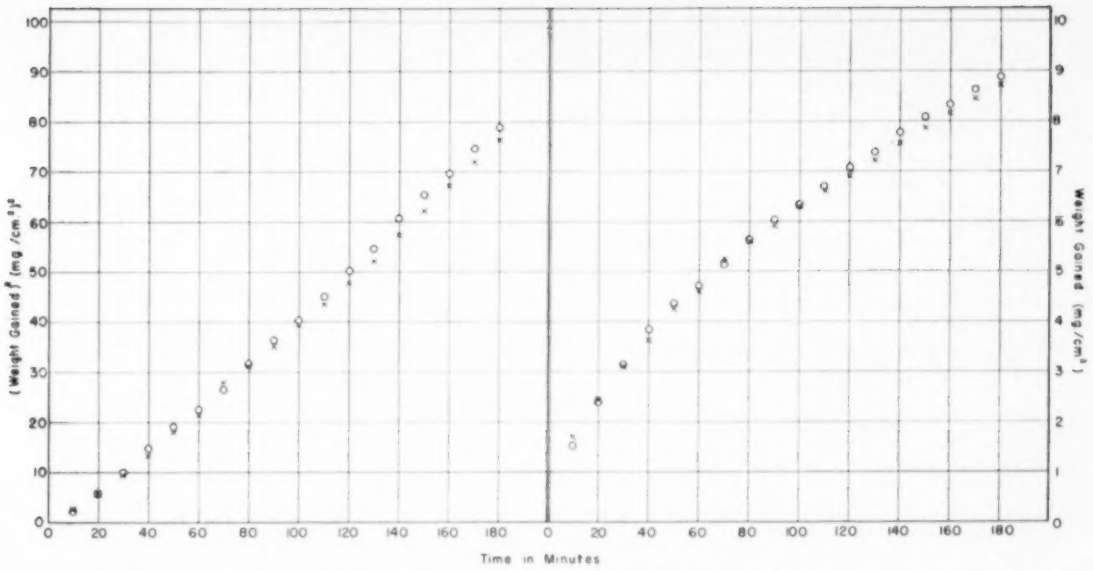

Fig. 3—Typical oxidation rate curves of pure copper. o No. 48 copper at 400 psi oxygen at 800°C. x No. 29 copper at 14.7 psi oxygen at 800°C.

brought to temperature and when thermal equilibrium is attained, usually in about 20 to 30 min, the sample is lowered into the hot section of the furnace and weighings are started immediately at 10 min intervals. The present equipment is capable of detecting weight changes of 0.04 mg.

Experimental Results

The results to be described are based upon the experimental observations of the oxidation of 63 copper samples in oxygen at 600°, 800°, and 900°C. The absolute oxygen pressure was varied from 14.7 to 400 psi. Typical curves showing the increase of weight with time for pure copper at 800°C are shown in Fig. 3. The direct plot of the weight gain vs time is satisfied approximately by the general equation of the parabolic law

$$w^2 = Kt + c.$$

The entire series of rate constants at 800°C obtained from the rate curves are plotted vs oxygen pressure in Fig. 4. The theoretical curve calculated from Wagner-Grunewald pressure dependence equation is included for comparison. Of course, it does not apply directly to the system investigated since Cu_2O and CuO are present. Fig. 4 indicates that the oxidation rate of pure copper in oxygen is independent of pressure above 1 atm total pressure. The rate constants obtained for each sample are listed in Table I.

Discussion of Results

The values of the rate constants obtained for copper agree reasonably well with those reported by Pilling and Bedworth.[5] They found the rate constants in oxygen at 1 atm pressure for copper at 600°, 800°, and 900°C to be 3.24, 86.9, and 349 x 10^{-10} g^2 cm^{-4} sec^{-1}, respectively, while the present work shows values of 3.28, 76, and 301 x 10^{-10} g^2 cm^{-4} sec^{-1} at the same temperatures and pressures.

These results clearly demonstrate that the conclusions reached by Feitknecht in 1929 and confirmed by Fröhlich[6] in 1936 on the pressure independence of oxygen on copper (maximum of 1 atm pressure) can be extended to 27.2 atm total pressure.

Aside from the experimental results previously mentioned, a few miscellaneous observations are worthy of note. In a run of 900°C, 14.7 psi O_2, oxidation rate measurements were continued for some time after the copper metal was completely oxidized. At the disappearance of copper, a sharp change in slope occurred on the w^2 vs t plot. The value of K for the gain in weight with copper metal present was 252 x 10^{-10} g^2 cm^{-4} sec^{-1} and for the oxidation of Cu_2O to CuO, K = 0.775 x 10^{-10} g^2 cm^{-4} sec^{-1}. The calculated value of K = 22.2 x 10^{-10} g^2 cm^{-4} sec^{-1} from Valensi's equation[7] does not agree with the experimental value.

The question of the mechanism at the Cu_2O/CuO interface and the method of growth of the CuO is of interest in the problem of oxidation of copper under conditions wherein both oxides coexist. Wagner[4] has shown experimentally that the rate is affected by oxygen pressure when only Cu_2O is present. In the present work and in that of Feitknecht and Fröhlich, CuO was present on the exterior of the sample. Hence, the CuO must be relatively impervious to oxygen and the effective concentration of oxygen at the Cu_2O/CuO interface remains unchanged at 27 atm oxygen pressure. Czerski[10] reported that CuO is nontransparent to oxygen and Seitz[11] states that the vapor pressure of oxygen has no effect on CuO as a semiconductor. It has been

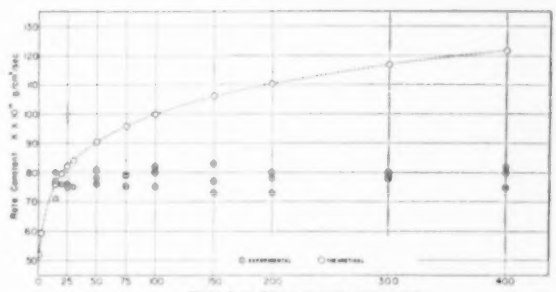

Fig. 4—Oxidation rate of copper vs oxygen pressure at 800°C.

shown experimentally[4,6,7] that the migration of Cu^+ ions alone is responsible for the growth of the Cu_2O film. The growth of CuO must occur by a similar process, since the CuO is apparently impervious to oxygen. The following mechanism of growth of the system $Cu/Cu_2O/CuO/O_2$ is proposed:

1. Formation of Cu^+ ions and electrons at the Cu/Cu_2O interface.
$$(Cu^+ + \epsilon)_{Metal} \rightarrow Cu^+_{Film} + \epsilon.$$
2. Migration of Cu^+ ions and electrons through the Cu_2O film.
3. Reaction of Cu^+ ions and electrons with CuO to form Cu_2O at the Cu_2O/CuO interface.
$$Cu^+ + \epsilon + CuO \rightarrow Cu_2O.$$
4. Migration of unreacted Cu^+ ions and electrons through the CuO film.*

* An alternate possibility may exist for steps 4 and 5. Since the CuO is a transition-type semiconductor,[12] an equilibrium concentration of oxygen vacancies could exist near the Cu_2O/CuO interface. The vacancies could then diffuse to the CuO/O_2 interface and be filled with oxygen. Then concentrations will be independent of the oxygen pressure at the CuO/O_2 interface. The net result would be essentially equivalent to steps 4 and 5.

5. Reaction of Cu^+ ions and electrons to form CuO.
$$Cu^+ + \epsilon + (O)_{Adsorbed} \rightarrow CuO.$$

It is not reasonable to expect the CuO to decompose to form Cu_2O and Cu since the CuO is thermodynamically stable. The oxidation process is a kinetic process and there is always a supply of Cu^+ ions and electrons as long as any metal remains which can easily react with the CuO. It is implied that there is a temperature dependent distribution of copper ions between steps three and four. Such a distribution of Cu^+ leads to a constant ratio of the thickness of the Cu_2O and CuO films at constant temperature and pressure. This is in agreement with the reported results of Valensi.[10]

When the metal is consumed, a different system is present. The following mechanism is proposed for the system $Cu_2O/CuO/O_2$:

1. Decomposition of Cu_2O at the Cu_2O/CuO interface to form CuO and Cu^+ ions and electrons.
$$Cu_2O \rightarrow CuO + Cu^+ + \epsilon.$$
2. Migration of Cu^+ ions and electrons through the CuO film.
3. Reaction of Cu^+ ions and electrons with oxygen to form CuO.
$$Cu^+ + \epsilon + (O)_{Adsorbed} \rightarrow CuO.$$

A gradient of Cu^+ ions and electrons will be established in the CuO film by the decomposition of the Cu_2O that will control the rate of oxidation. This process has been shown to be parabolic by Valensi[10] and in the present paper. However, this second process without metal present cannot be used to make predictions on the first process with metal present for the following reasons: The first process has metal present that stabilizes the Cu_2O in the presence of CuO. In the second process the metal is no longer present, and the Cu_2O is not stable in the presence of CuO and will decompose.

The CuO is disappearing at the Cu_2O/CuO interface and forming at the CuO/O_2 interface for the system $Cu/Cu_2O/CuO/O_2$. For the system $Cu_2O/CuO/O_2$, however, the CuO film is growing at both the Cu_2O/CuO interface and the CuO/O_2 interface.

In summary, the following pseudo equilibrium reaction at the Cu_2O/CuO interface can be considered:
$$Cu^+ + \epsilon + CuO \rightleftharpoons Cu_2O.$$
In the presence of copper metal the reaction goes to the right. When the metal is gone, the reaction goes to the left. Therefore, the rate of formation of CuO, in the absence of the copper metal, cannot determine the rate of formation of CuO when metal is present.

Table I. Oxidation Rate Constants for Copper at 600°, 800°, and 900°C, at Various Total Oxygen Pressures

Run No.	Temperature, °C	Oxygen Pressure, Psi	$K \times 10^{10}$ G^2 Cm^{-4} Sec^{-1}	Average K
51	600	14.7	3.42	3.28
52			2.93	
53			3.48	
54	600	300	3.34	3.17
55			3.05	
56			3.11	
27	800	14.7	79.8	76.0
28			71.4	
29			76.9	
25	800	20	75.8	
22	800	25	74.8	75.3
24			75.4	
47			75.8	
26	800	30	75.1	
16	800	50	76.3	78.3
31			77.5	
46			81.1	
15	800	75	74.8	77.4
30			78.7	
45			78.7	
17	800	100	79.8	78.4
33			82.2	
44			75.3	
18	800	150	77.4	78.0
37			83.7	
42			72.8	
19	800	200	73.0	77.3
38			80.3	
41			78.5	
20	800	300	79.5	79.2
39			78.2	
40			79.9	
48	800	400	74.7	78.7
49			79.7	
50			81.7	
85	900	14.7	315	301
86			295	
87			293	
88	900	300	279	275
89			258	
90			261	
91			301	

References

[1] H. Le Chatelier: *Ztsch. Physik Chem.* (1887) **1**, p. 516.

[2] W. Feitknecht: *Ztsch. Electrochemie* (1929) **35**, p. 142.

[3] R. F. Mehl, E. L. McCandless, and F. N. Rhines: *Nature* (1934) **134**, p. 1009.

[4] C. Wagner and K. Grünewald: *Ztsch. Physik Chem.* (1938) **B40**, p. 455.

[5] N. B. Pilling and R. E. Bedworth: *Journal* Inst. Metals (1923) **29**, p. 259.

[6] C. Wagner: *Ztsch. Physik Chem.* (1933) **B21**, p. 25; (1936) **B32**, p. 447.

[7] J. Bardeen, W. H. Bratten, and W. Shockley: *Journal of Chemical Physics* (1946) **14**, p. 714.

[8] K. W. Fröhlich: *Ztsch. Metallkunde* (1936) **28**, p. 368.

[9] G. Valensi: *Revue Metallurgie* (1948) **45**, No. 7, p. 205.

[10] L. Czerski: *Roezniki Chem.* (1937) **17**, p. 436.

[11] F. Seitz: *Modern Theory of Solids* (1940) p. 70. New York. McGraw-Hill Book Co.

[12] O. Kubaschewski and B. E. Hopkins: *Oxidation of Metals and Alloys* (1953) pp. 34-36. Academic Press.

[13] G. Valensi: *Comptes Rendus* (1936) **203**, p. 1354-1356.

Plasticity of Columbium Single Crystals

by R. Maddin and N. K. Chen

Columbium single crystals were deformed in tension and compression. Reorientation by X-rays and stereographic projections of slip traces indicate that plane of slip may be considered as {110}. The plastic behavior is shown to be quite similar to the deformation of molybdenum single crystals.

STUDIES on the crystallography of the deformation process in body-centered cubic metals have been renewed recently with investigations of α iron single crystals[1-3] and molybdenum single crystals.[4] It is now apparent that too many exceptions to the rationalization based upon the ratio of absolute testing temperature to absolute melting point by Andrade[5] exist to permit more serious discussion of this type of analysis. The considerations of resolved shear stress utilizing only planes of the type {110}, {112}, and {123}[3,6] permit analysis of the deformation only on the basis of those three types of planes.

The suggestions made by Elam[7] and by Greninger[8] in which the slip process is envisioned as a composite slip on two nonparallel {110} planes can be illustrated schematically in Fig. 1. It may be seen that an unresolved trace on any plane containing a <111> direction may be accomplished by varying the number of atoms participating in the composite process. By further varying the number of atoms in each plane but keeping the ratio of participating atoms constant, jogs could be obtained in the traces and hence wavy slip lines could be produced.

Vogel and Brick[1] studied the behavior of α iron single crystals in which they suggest that the plane of glide is "non-crystallographic" and may be predicted from the intersection between the great circle joining the slip direction and specimen axis with the great circle whose zone axis is the slip direction. In a more recent investigation on iron single crystals, Steijn and Brick[9] suggest that the slip mechanism may be considered as made up of a type of composite slip occurring on {110} and {112} planes.

Evidence for a possible composite nature of the slip process has been presented for the case of molybdenum in the form of analysis of asterism and specimen axis rotation.[4] Definite proof of a composite slip process must, however, await good electron microscopic resolution of the individual traces making up the unresolved optical trace used in determining the acting slip plane.

The present investigation was undertaken to study the behavior of columbium single crystals not only in tension but also in compression since the specimen axis migration should indicate the plane or planes of glide in the same manner that the specimen axis migration in tension indicates the direction of glide.

The orientations of eleven crystals investigated are shown in Fig. 2. Specific orientations are missing (those in the vicinity of [111] and [001]) and consequently the effect of orientation on the crystallography of deformation could not be considered.

Experimental Procedure

The ⅛-in. rods (7 in. long) were subjected to an axial tension in vacuo while at temperatures in the vicinity of 2000°C for 2 to 4 hr. This treatment resulted in large cylindrical grains (about ½ in. long) occupying the entire cross section. A number of these rods were used for the tension studies by observing the behavior of the individual grains. For the compression studies, single crystals approximately ¼ in. long by ⅛ in. in diameter were cut from the rods; the ends were ground parallel. All specimens were polished electrolytically in a solution of 15 cc HF(48 pct) and 85 cc H_2SO_4 (concentrated) using a platinum cathode, a current density of 0.04 amp per sq cm and a temperature between 25° and 60°C.[10] Orientations were obtained using a Laue back-reflection method (3 cm film to specimen distance) with a ½ mm collimator 9 cm long. For the compression specimens, a reference mark was scratched on one of the compression sur-

R. MADDIN, Member AIME, is Associate Professor of Metallurgy, and N. K. CHEN, Junior Member AIME, is Assitant Professor of Metallurgy, The Johns Hopkins University, Baltimore.

Discussion on this paper, TP 3606E, may be sent, 2 copies, to AIME by Dec. 1, 1953. Manuscript, Jan. 2, 1953; revision, April 20, 1953. Cleveland Meeting, October 1953.

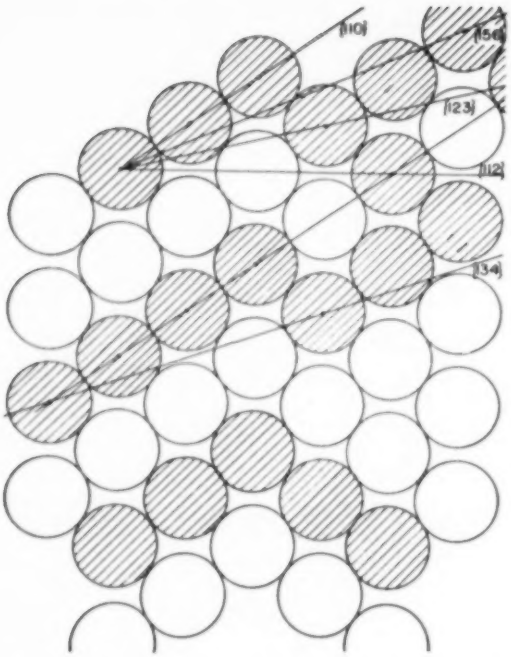

Fig. 1—Illustration showing the integrated trace produced by using different numbers of atoms in nonparallel {110} planes.

faces on each of the crystals. This reference scratch was aligned with a scratch on a specially constructed crystal holder which contained a steel indicator in line with the reference scratch on the surface of the holder. The assembly was used for all X-ray analysis and also for metallographic observations. The tensile specimens contained a reference mark on the surface just below one of the grip ends. All X-ray exposures were made with careful regard to the position of the reference marks so that subsequent metallographic observations (always made with respect to the reoriented specimen) could be coordinated with the photograms.

Compression was performed in a specially constructed apparatus operated by a hydraulic compression machine. A clip gage made of phosphor bronze to which were glued two SR-4 type A-1 strain gages was calibrated and used to measure strain. The compression plates were liberally greased. The same hydraulic machine was used for the tension studies.

Results

Tension: The specimen axis migrations for all crystals investigated in tension are shown in Figs. 3 to 5. Since all the tension specimens were rods composed of large grains, it is not known with certainty that the stress was simple tension. Nevertheless, analysis was referred to specimen axis rotation (stress axis) assuming a simple tension. Whenever surface conditions were satisfactory, i.e., no mistake could be made in differentiating slip traces from spurious markings, stereographic analysis of the traces was used.

The pole rotations for specimens Cb-2, 4, and 11 are shown in Fig. 3. Stereographic analysis of the traces on Cb-2 indicated a "noncrystallographic" glide plane deviating about 5° from the predicted plane (Fig. 3) using the method of Vogel and Brick.[1] Although the axis migration for 2 and 11 are too small for accurate interpretation, there is indication that these crystals behaved in an expected manner, i.e., the axis rotated toward the direction of slip, *D*. A lack of pronounced asterism prevented analysis by this method.[4] The larger amount of asterism shown in Fig. 6a for specimen Cb-4 after a greater amount of extension permitted analysis. The participation of more than one slip system is evident from the splitting of the Laue reflections shown in Fig. 6a, if it is assumed that the asterism is crystallographic in origin. The ends of the major asterism were plotted on the same projection and indicated an axis shift from position 4-0 to 4-1. In an effort to determine more accurately the axis about which the asterism occurred, Laue back-reflection photograms were made every 2° about the specimen axis in the vicinity of the critical position. The photogram (Fig. 6b) demonstrates a [112] axis as that about which the asterism occurred. The determination of the plane by the slip trace method indicated a noncrystallographic plane. A further extension until necking produced an axis shift to position 4-2. Based upon axis shift and asterism analysis, it would appear that slip systems IV*D* and II*A* have operated in the deformation of Cb-4.

The behavior of crystals Cb-6 and 7 is shown in Fig. 4. The extension of Cb-7 (about 5 pct) produced an axis shift along a great circle towards

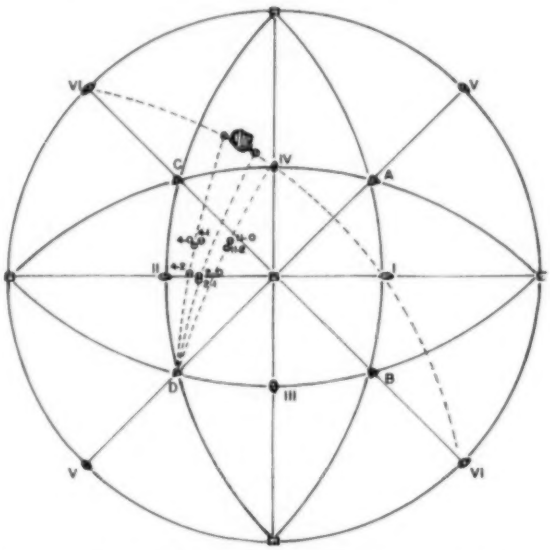

Fig. 3—Specimen axis migration for crystals Cb-2, 4, and 11 (tension). Stereographic determination of slip plane (Cb-2) from traces is shown as hatched area. Predicted planes are shown at intersection of the two dotted great circles.

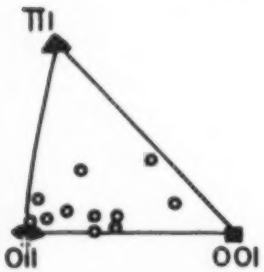

Fig. 2—Initial orientations of all crystals investigated.

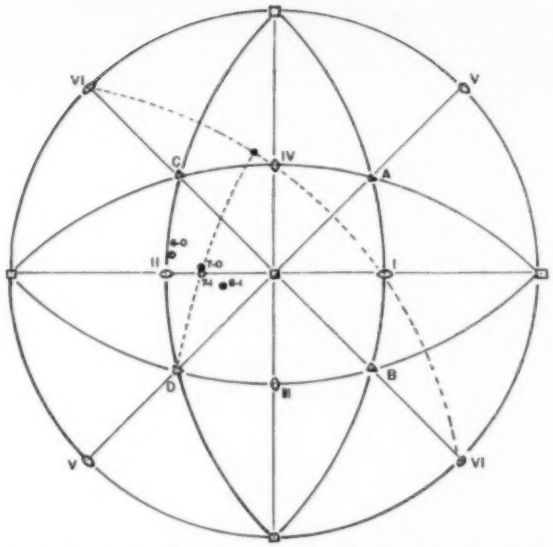

Fig. 4—Specimen axis migration of crystals Cb-6 and 7 (tension). The predicted plane for crystal Cb-7 is shown as the intersection of the two dotted great circles.

direction *D* and analysis of the traces showed plane IV as the plane of glide. The predicted plane based upon resolved shear stress is shown as the intersection of the two dotted great circles. Asterism was complex but not enough developed to permit accurate analysis.

Crystal Cb-6 was pulled until necking occurred. The pole rotation was determined by plotting only the points of maximum intensity on very extensively blurred streaks. The unexpected behavior cannot be explained on the basis of slip on only one plane of high resolved shear stress since the initial orientation is at a position where the resolved shear stress is almost the same on four different {110} planes (III, IV, V, VI). The behavior of Cb-6 should be compared with the behavior of Cb-9 which has a similar orientation.

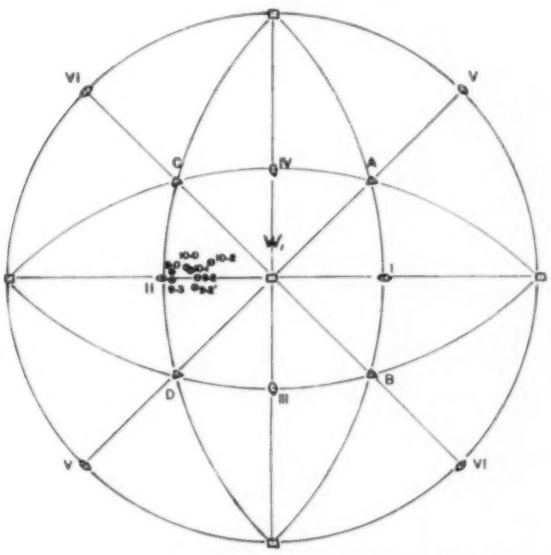

Fig. 5—Specimen axis migration of crystals Cb-9 and 10 (tension).

Since the orientation of crystal Cb-9 was quite close to that of Cb-6, a more careful technique was adopted. Two flat surfaces at 90° angles were polished on the specimen held in sealing wax. After etching in concentrated HF, the specimen was electropolished. Laue back-reflection photograms were made of each surface to indicate the removal of material affected by the polishing.

The specimen was extended about 2 pct and examined with microscope and X-ray. No slip lines and little or no axis shift were observed. The specimen was extended again to a total elongation of about 6 pct. Although slip lines were visible, great difficulty was encountered in attempting analysis from the traces. X-ray photograms made at different positions around the specimen axis testified to the complex behavior of this crystal. Referring to

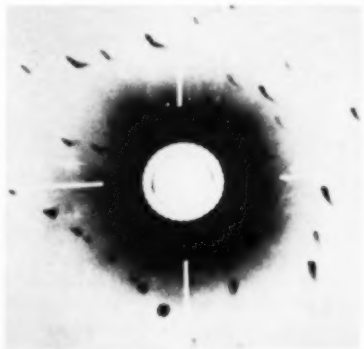

Fig. 6—X-ray photograms of crystal Cb-4.

a (left)—This shows two asterisms. The larger of the two is plotted as positions 4-0 and 4-1.

b (right)—Photogram used for determining the axis of asterism.

Fig. 5, the initial orientation of the crystal is plotted as 9-0 and the position of the axis after 6 pct elongation by 9-2. (Note the similarity to Cb-7.) The axis shift indicates a rotation towards *B*, a possible slip direction. The system II-*B*, however, is one of very low shear stress. Consequently, it is believed that the action may be of a composite nature involving the planes III, IV, V, and VI. After extension again to about 16 pct, the position of the axis was at 9-3. The slip lines were extremely complex showing not only a very wavy nature but also the pronounced development of markings similar to deformation bands or rumpling.

The behavior of Cb-10 with an initial orientation almost the same as Cb-9 but farther along the symmetry curve II-W_1, was not quite so complex. After about 6 pct elongation, the axis shift, 10-0 to 10-1 in Fig. 5, might likewise be explained on the participation of planes IV, V, and VI. However, after 16 pct elongation the axis shift indicated a possible

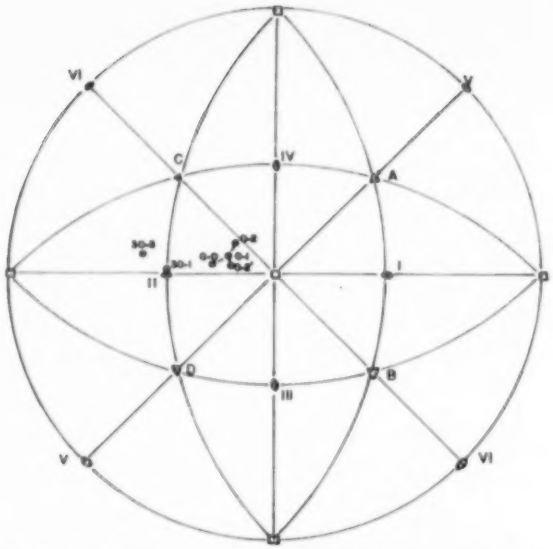

Fig. 7—Specimen axis migration for crystals Cb-0 and Cb-30 (compression).

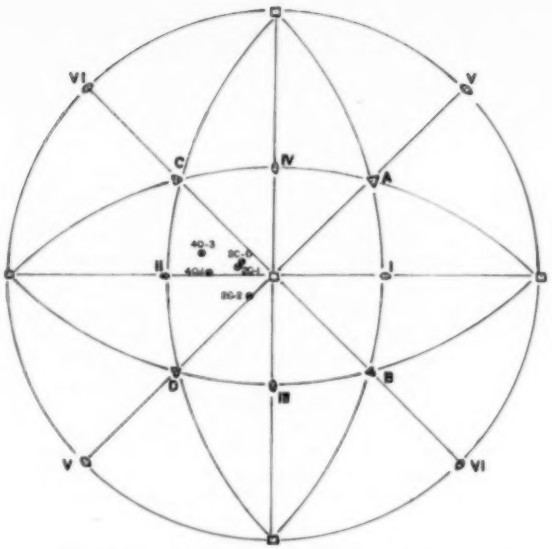

Fig. 8—Specimen axis migration for crystals Cb-2c and Cb-40 (compression).

participation of (II-*A*). The small deviation along the great circle to (*B*) may perhaps be attributed to the continual participation of IV and V in direction *B*, but on a small scale. However, the position of 10-2, being at the outer limit of the accuracy of orientation determination, cannot be classed as rigorously indicating the later activity of (II-*A*).

Compression: The axis migration of the specimens studied in compression are shown in Figs. 7 and 8. Crystal Cb-30 whose initial orientation is very close to II showed complex behavior similar to specimens Cb-6, 9, and 10 in tension. It appears very likely that more than one and perhaps all the planes concerned (III, IV, V, and VI) contributed to the deformation of Cb-30.

Crystal Cb-0 was compressed 5.97 pct. Analysis of the traces indicated IV as a plane of glide. From the axis migration to position 0-1 (Fig. 7), it appears more than likely that another plane contributed to the deformation since enough rotation was observed to show a decided deviation from the "prescribed" course toward IV. After compression to 11 pct, asterism was pronounced and showed indication of a dual nature (Fig. 9). The tails of both the asterisms shown in Fig. 9 were plotted stereographically as positions 0-2 and 0-2' in Fig. 7. It is believed here that planes IV and III have participated in the plastic deformation of Cb-0.

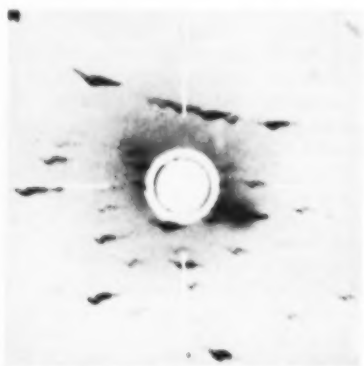

Fig. 9—X-ray photogram showing two asterisms. The ends of the asterisms are plotted in Fig. 7 as positions 0-1, 0-2, 0-2'.

The appearance of slip traces on Cb-0 after the first compression is shown in Fig. 10a to d. The traces are, for the most part, straight and prove to be caused by the ($\bar{1}$01) plane, (IV). The forked bands are presumably deformation bands whose boundaries agree with no low indices, high atomic density plane. In certain cases, the bands are seen to consist of small but straight lines reminiscent of bands of secondary slip in aluminum.

The behavior of crystals Cb-2c and 40 are shown in Fig. 8. Specimen Cb-2c was treated in the same manner as Cb-0. It was compressed 2.91 pct and observed by microscope. Analysis of the traces indicated three glide planes to have been operative; these were VI, II, and III. A micrograph of three sets of traces is shown in Fig. 11. It is possible that the slip direction is the same for all three of these planes. If the amount of glide on each of these planes in the same slip direction is the same, the movement of the axis along a great circle to II would be expected. However, as may be seen in Fig. 8, the pole movement 2c-0 to 2c-1 is not exactly along this great circle indicating an uneven amount of glide on the {110} planes concerned. After 14.5 pct compression, however, it is apparent that the glide on plane III predominates as shown by the movement of 2c-1 to 2c-2.

Crystal Cb-40 behaved in a somewhat complex manner, probably owing to its initial orientation on a symmetry curve. Nevertheless, the pole movement from 40-1 to 40-3 (Fig. 8) indicates a participation of both IV and VI (the resolved shear stress on both these planes are somewhat similar).

Stress-Strain Curves: A stress-strain curve for crystal Cb-30 is shown in Fig. 12. No attempt has been made to calculate a critical resolved shear stress since it is not known with certainty on what plane to resolve the stress.

a—Position at the reference mark.

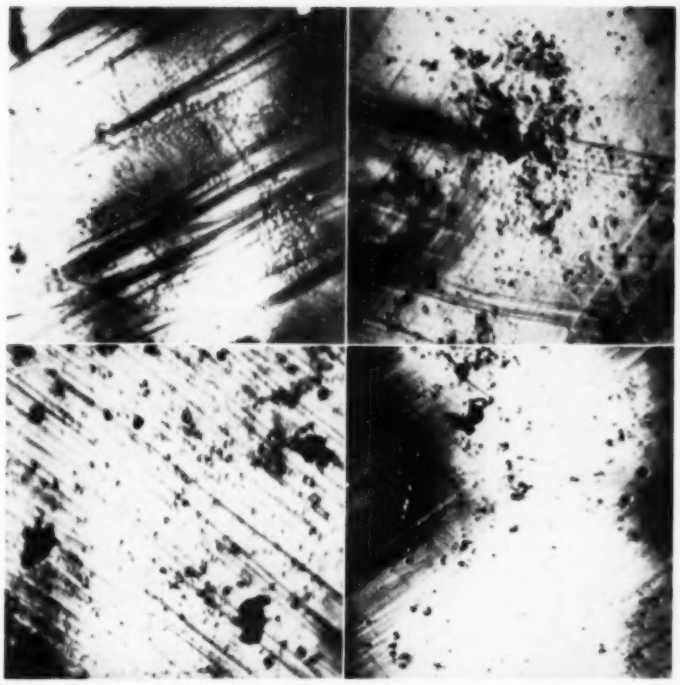

b—Rotated 58 degrees from position (a)

c—Rotated 160 degrees from position (a)

d—Rotated 20 degrees from position (a)

Fig. 10—Slip lines and deformation bands in crystal Cb-0 (compression). X500.

Fig. 11—Three sets of slip lines in specimen Cb-2c (compression). X500.

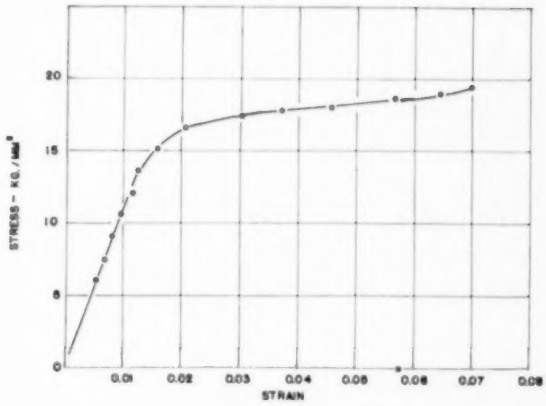

Fig. 12—Stress-strain curve for crystal Cb-30 (compression).

Results from Berg-Barrett Method: In an attempt to consider more carefully the extent of disorientation existing in the surface layers of the specimen after deformation, the Berg-Barrett microscopy[11, 12] was used. Cu $K\alpha$ radiation, 30kv, was reflected from a bent quartz crystal monochromator and focused on the specimen supported on a two circle goniometer. Reflections were obtained for certain specimen positions and recorded on spectroscopic VO plate held parallel to the focused beam almost tangent to the specimen surface yielding the reflection. Exposures of from 30 min to 4 hr were necessary to obtain suitable records. In Fig. 13a and b there is shown the striated and banded structure observed by this technique. The amount of disorientation as a result of 5.47 and 11 pct compression (Cb-2c) can be seen, at least qualitatively in these X-ray micrograms.

Throughout these compression studies, the amount of distortion (asterism) produced per amount of deformation was far greater in the case

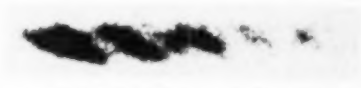

a—Cb-0 after first compression. X70.

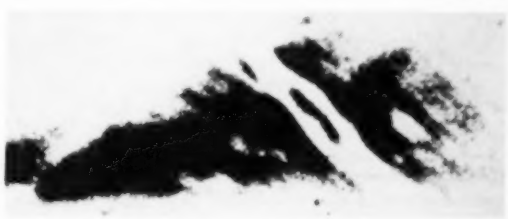

b—Cb-0 after second compression. X110.

Fig. 13—Berg-Barrett micrograms of crystal Cb-0 made using a bent quartz crystal monochromator; 30 Kv, Cu $K\alpha$ radiation, V-O plate.

of compression than in tension. For example, after 16 pct compression, the asterism is so great as not to permit orientation determinations whereas the same amount of extension produces much less disorientation.

Discussion of Results

Determination of glide planes from observation of the traces on the surface might be questionable when these traces are wavy, branched, and forked. Such is normally the case with traces observed on plastically deformed body-centered cubic crystals. Nevertheless, a direction is generally assigned to a wavy trace and with many such observations, a determination of the apparent glide plane is made.

With compression of columbium, however, the deformation markings are of a different character. Two types can be noted: those lines which are straight and narrow wherever observed and those bands of relatively large width which are branched, forked, and wavy. Stereographic plots of the straight narrow lines show {110} to be the glide plane whereas similar plots of the bands yield no confirmation of any low indices plane. However, it is sometimes possible to observe very small straight, narrow segments composing the bands; these, too, apparently are caused by {110} planes.

Perhaps a more sensitive indication of the glide plane would be found in analysis of the asterism resulting from deformation. As in the case of molybdenum,[4] a <112> axis is shown to be the axis about which asterism occurs. In the case here reported (Fig. 6b), it is readily seen that this axis is [121] in which case the plane of glide is $(\bar{1}01)$ (IV) and the direction $[1\bar{1}1]$ if it can be assumed that plastic deformation in the body-centered cubic crystals produces a Taylor type rotation, i.e., rotation of the plane of glide about an axis in the plane and normal to the direction of glide. There appears to be sufficient observations to support this assumption in the body-centered cubic crystals.[10,11] Had other types of planes acted as glide planes, other axes should be observed as the axes about which rotation occurs, e.g., for a {112} a <110> would operate. However, these have not been observed to date.

The optical analogy between diffraction of X-rays by bent atomic planes and the reflection of light by curved mirrors provides the basis of a method for interpreting asterism from deformed single crystals at least qualitatively in terms of the direction of rotation of the atomic planes.[12] Thus, if the ends of the asterism are plotted stereographically, the direction of displacement of these asterisms interpreted as positions of the longitudinal axis of the specimen indicates the direction of glide in tension and the plane of glide in compression. For example, the extent of asterism for Cb-4 in Fig. 3 indicates the participation of slip plane II in the first extension. Later rotation, however, shows the operation of plane IV. It would appear that the correct interpretation might be that both planes operated. In the compression case, Cb-0 (Fig. 7), a more apparent activity presents itself. Here, the rotation independent of asterism is not directly conclusive of any particular plane of glide, whereas the extent of asterism clearly demonstrates the collateral operation of IV and its conjugate III.

The use of X-ray microscopy lends further support to the idea that slip in the body-centered cubic crystals occurs in a complex manner. Although the resolution derived by this method is not greater than what is generally attainable with light microscopy, effects of surface conditions can be eliminated. Thus if there existed a sudden change in direction of slip traces which could not readily be observed because of surface conditions, X-ray microscopy might be expected to show this. Examples of this effect have been found in extended molybdenum single crystals.[16] Examples in Fig. 13 show relatively straight striae and bands where optical microscopy reveals branched and wavy bands.

The problem of resolving the traces into their possible composite nature would best be solved with aid of the electron microscope provided the actual number of atoms participating in the process is sufficiently large (the ratio remaining constant). Attempts are now being made using extended molybdenum single crystals.

A second possibility of presenting good evidence in favor of composite slip would be to develop a sensitive load measuring device in order to distinguish the small differences in load resolved along actual and "pseudo" planes. Careful resolved shear stress measurements would indicate the plane or planes along which glide has occurred. These experiments are now being contemplated using single crystals of various body-centered cubic metals.

Acknowledgment

The authors wish to acknowledge with appreciation the many helpful discussions of Dr. C. H. Mathewson and for application of the idea of composite slip to the present analysis. This work was supported by the Office of Naval Research under Contract No. Nonr 248(14).

References

[1] F. L. Vogel and R. M. Brick: Deformation of Ferrite Single Crystals. Technical Report No. 1; July 1, 1952, Contract AF 33-(038)15889, Univ. of Pa., Philadelphia.

[2] A. J. Opinsky and R. Smoluchowski: Crystallographic Aspect of Slip in Body-Centered Cubic Crystals. *Symposium.* Carnegie Inst. Tech., May 1950.

[3] A. J. Opinsky and R. Smoluchowski: The Crystallographic Aspect of Slip in Body-Centered Cubic Single Crystals. *Journal of Applied Physics* (1950) **22**, p. 1488.

[4] N. K. Chen and R. Maddin: Plasticity of Molybdenum Single Crystals. *Trans.* AIME (1951) **191**, p. 937; JOURNAL OF METALS (October 1951).

[5] E. N. daC Andrade: Report of a Conference on Internal Strains in Solids. *Proc.* Physical Soc., London (1940) **52**, p. 1.

[6] N. Farhenhorst and E. Schmid: *Ztsch. Physik* (1932) **78**, p. 383.

[7] C. F. Elam: *The Distortion of Metals* (1935) Oxford. Clarendon Press.

[8] A. B. Greninger: Discussion to C. S. Barrett, G. Ansel, and R. F. Mehl: Slip, Twinning and Cleavage in Iron and Silicon Ferrite. *Trans.* ASM (1937) **25**, p. 702.

[9] R. P. Steijn and R. M. Brick: Flow and Fracture of Single Crystals of High Purity Ferrites. Technical Report No. 2; January 1, 1953, Contract No. AF 33 (038)15889, Univ. of Pa., Philadelphia.

[10] G. W. Wensch: Private communication.

[11] W. Berg: Load History of Deformed Crystals. *Ztsch. Krst.* (1934) **89**, p. 286.

[12] C. S. Barrett: A New Microscopy and its Potentialities. *Trans.* AIME (1945) **161**, p. 15.

[13] E. N. daC. Andrade and L. C. Tsien: Glide of Single Crystals of Sodium and Potassium. *Proc.* Royal Soc., London (1937) **A163**, p. 1.

[14] C. S. Barrett: *Structure of Metals.* 2nd Edition (1952) p. 375. New York. McGraw-Hill Book Co.

[15] *Ibid:* pp. 414-420.

[16] N. K. Chen and R. Maddin: Glide in Extended Molybdenum Single Crystals. Unpublished.

AIME OFFICERS:
President—Andrew Fletcher
Vice-Presidents—T. B. Counselman, L. E. Elkins, O. B. J. Fraser, J. L. Gillson, A. B. Kinzel, J. B. Morrow
President-Elect—L. F. Reinartz
Treasurer and Controller—G. I. Brigden
AIME STAFF:
Secretary—E. H. Robie
Ass't. Secretaries—J. B. Alford, H. N. Appleton, E. J. Kennedy, Jr., Ernest Kirkendall, R. E. O'Brien
Ass't. Treasurer—P. J. Apol

aime NEWS

Report on Employment, Education, and Income Of Engineers Available From Bureau of Labor Statistics

Now available on request to the Bureau of Labor Statistics, Washington 25, D. C., is a 48-page mimeographed report on *Employment, Education, and Income of Engineers, 1949-50 — A Survey of Engineering Society Members of Full Professional Grade.* The survey was made by Engineers Joint Council on behalf of the Dept. of Defense. It covers returns from 55,000 engineers who hold full professional grades of membership in national engineering societies, or more than half of society members of full professional grade. Of the returns, about 40 pct came from mechanical engineers, 25 pct from civils, 15 pct from electricals, 12 pct mining and metallurgical, and 7 pct chemical. The groups with the lowest median age, 42 years, were the chemical and mining and metallurgical engineers. For the mechanicals the median was 43 years, for the electricals 46, and for the civils 47. There were only 56 women in the 55,000 considered in the survey.

Of the total in all fields, 3.7 pct held doctor's degrees (4.3 for mining and metallurgical engineers; 16.4 pct held master's degrees (16.5 pct for mining and metallurgical); 59.5 pct held bachelor's degrees (61.9 mining and metallurgical); and 20.3 pct held no degree (17.3 pct for mining and metallurgical).

Median incomes of those reporting ranged as follows:

Self employed, employer, or owner of business, $14,700; self employed, independent consultant, $10,700; private industry, $8400; educational institutions, $7100; government, $6600.

Among mining and metallurgical engineers, 81.7 pct were in private industry; 6.2 pct worked for governmental agencies; 5.2 pct were educators; 3.7 pct were independent consultants; 1.8 pct were employers or owners; and 1.3 pct worked for foundations.

Median incomes of various kinds of engineers, 35 years of age and over, 44,000 engineers reporting: Chemical, $9000; mechanical, $8400; mining, metallurgical, electrical, $8000; civil, $7100.

Median annual income of mining and metallurgical engineers, by age groups and highest degree earned are listed in table shown below.

Many other data are given in the complete report.

	35 to 39	40 to 44	45 to 49	50 to 54	55 to 59	60 to 64	65 to 69	70 Up
Ph.D.	$8800	$8500	$9300	$9400	———	———	———	———
M.S.	7000	8200	8500	9100	$10,100	$10,800	———	———
B.S.	6600	7600	8500	9200	10,300	11,000	$10,200	$8300
None	6000	6500	7700	9000	9400	8300	10,000	———

EMC Advises Engineers Facing Military Service

Engineering Manpower Commission has prepared the following statement which should be of interest to young men recently, or about to be, inducted into military service, or their parents.

U.S. Army Scientific and Professional Personnel Program

The U. S. Army Scientific and Professional Personnel Program should be of special interest to recent engineering graduates who will shortly be inducted into the armed forces. It was designed to channel as many such persons as possible into Army billets which will insure the maximum utilization of their engineering or scientific training and experience. This should promote their own continued professional development and the advancement of the Army's technical programs. The program is described in detail in Dept. of the Army Special Regulation #615-25-11, dated 7 August 1952.

The regulations provide for the identification, classification, assignment, and utilization of those persons who are qualified to perform scientific and professional level duties in research and development, instruction, and related work of professional or scientific nature.

Commanders of reception centers and other installations conducting initial reception processing are responsible for the proper indentification and indoctrination of scientific and professional personnel and for their transfer to appropriate basic training.

The regulations concerning the selection of Scientific and Professional Personnel are far too complex for adequate reproduction here. The regulations differ for each major scientific and professional field. In some cases, only a B.S. degree is required. In others, a Bachelor's degree plus a certain amount of experience or an advance degree are required.

Personnel qualified as Scientific and Professional Personnel are assigned a Military Occupational Specialty number (MOS) which reflects their specialty and is intended

ANNUAL MEETING PAPER DEADLINE

Sept. 15, 1953 is the deadline for all Institute of Metals Div. papers for the 1954 New York Annual Meeting and the deadline for all Iron and Steel Div., and Extractive Metallurgy Div. papers to be prepublished.

to be used as a guide in their assignment to billets in which their training and experience will be utilized. All the major engineering and scientific fields are covered by the regulation although, as has been said previously, the qualifications differ somewhat.

Copies of the basic regulation are available from the Dept. of the Army, Washington 25, D. C.

The Engineering Manpower Commission of Engineers Joint Council is interested in the efficiency of the Scientific and Professional Personnel program. It feels that the dissemination of information regarding the existence of the program is vital to its success and would appreciate information regarding engineers and scientists qualified under the program who are not being utilized in their fields of special qualification.

Phelps Dodge Corp. Is Host to Arizona Section

Phelps Dodge Corp. played host to a one-day meeting of the smelting div., Arizona Section, at the New Cornelia Branch at Ajo. Forty two registrants toured the smelter and were served luncheon at the copper loading dock. Three papers were presented at the afternoon session. They were: *Metallurgy of the Ajo Smelter*, by F. W. Denny; *Design and Operation of Ajo Reverberatory Furnace*, by W. C. Hunter; and *Ajo Anode Practice*, by A. H. Lyons. All are with Phelps Dodge. A cocktail party and dinner that evening were attended by 103 persons.

North Pacific Section To Hold September Meeting

The North Pacific Section, AIME, will hold their regular September meeting Saturday, Sept. 19, 1953, at 6:30 pm at the Engineer's Club, Arctic Club Bldg., 306 Cherry, Seattle, Wash., with President Fletcher speaking. Visiting members are cordially invited but should make reservations with Glenn E. Sigler, P.O. Box 1605, Tacoma, Wash., by September 16.

South American Local Section Holds Meeting

Two former Presidents of AIME attended the recent luncheon and meeting of the Lima, Peru Local Section. Donald B. Gillies, President during 1939 and Donald H. McLaughlin, President during 1950, attended. Frank E. Noe, metallurgist with the Bureau of Mines, addressed the more than 60 members on the subject of *The U. S. Bureau of Mines and Its International Activities.*

Columbia Section Holds Joint Meeting

Members of the Columbia Section, AIME joined with members of the ASM and AChS at a recent joint dinner meeting. Subject of the meeting was *Corrosion in Action.* A movie by International Nickel Co. was shown and a panel answered questions put forth by the gathering. The metals particularly discussed were titanium, magnesium, zinc, stainless steel, and aluminum. Approximately 70 members were present.

Science Fair Held in Spokane

Spokane area professional societies participated in a science fair held for students from various high schools in that area. F. R. Morral, Kaiser Aluminum & Chemical Corp., was co-chairman. Prize divisions were established for astronomy, geology, chemistry, electricity, magnetism, and others. Judges were members of the professional societies, which aided in the presentation of the fair.

AIME Honors H. N. Appleton

H. Newell Appleton, Assistant Secretary, manager of institute activities, and convention manager of the AIME, was honored at the July meeting of the Executive and Finance Committees on completion of 25 years of service. Newell, as he is known to hundreds of members, has long been more responsible than any one else for the smooth running of the Institute's Annual Meetings, and for many other Branch and Divisional meetings as well, including the Conferences.

Buffalo Section, NOHC To Convene in Ontario

The Buffalo Section of the National Open Hearth Steel Committee, AIME, will hold its annual fall meeting at the Royal Connaught Hotel, Hamilton, Ont., on October 6. One of the highlights of the program will be a visit to the No. 3 open hearth shop of the Steel Co. of Canada. There will be a luncheon and a technical session on open hearth will be held in the afternoon. The annual dinner will be held at 7 pm.

SPEEDS AND SIMPLIFIES HARDNESS TESTS

New, Low-Cost Standard and Superficial Testers Offer Magnified Optical Readings; Automatic Load Changing

Here they are—the first hardness testers to provide magnified optical readings. Only the new *Galileo* Hardness Testers project their measurements on a screen, with ball and diamond Rockwell scales easily visible at high magnifications; Brinell numbers easily obtained through readings on the screen. And only *Galileo* enables you to change loads quickly and automatically by simply turning a dial. All loads are obtained by exact, precision-made weights, insuring absolute constancy in calibration.

Exceptionally rugged and sensitive, the instruments are enclosed in dust-proof, grease-proof metal cases for trouble-free operation. Designed for Rockwell measurements on any type of metal within the range of 30 to 1000 Brinell units. They can also be used for Brinell tests, special loads and for Vickers measurements. Built-in oil damper with external control enables operator to regulate speed with which load is applied. The Standard Tester provides loads of 31,2—60—62,5—100—150—187,5—kgm; the Superficial Tester provides loads *starting at 5 kgm.* Diamond cone and steel ball penetrators. Maximum throat opening 7½". Wide range of accessories. Reasonably priced.

For details on the Hardness Testers and other *Galileo* instruments of modern functional design, write to the address below—Dept. M.

Imported and serviced by
OPPLEM COMPANY, INC.
Established 1890
352 Fourth Ave., New York 10, N. Y.

GALILEO
OPTICAL INSTRUMENTS

Personals

Manly B. Brown has been elected vice-president in charge of marketing for Great Lakes Carbon Corp., Chicago.

Norman M. Sted was appointed manager of sales for the Cleveland district, American Steel & Wire Co., div. U. S. Steel Corp.

G. Letendre has recently been elected a vice-president of the Canadian Institute of Mining and Metallurgy. Dr. Letendre is director, dept. of mines and metallurgy, University of Laval, Quebec.

Ralph M. Hunter has been named staff coordinator of all electrochemical activities for the Dow Chemical Co. Dr. Hunter will retain active charge of the Midland electrochemical laboratory.

W. D. Robertson has been promoted to the rank of associate professor, dept. of metallurgy, Yale University, New Haven, Conn.

G. A. Baker, vice-president of the Duriron Co., Dayton has been elected president of the Alloy Casting Institute.

William J. McCaughey, professor Emeritus of mineralogy at Ohio State University, was awarded the honorary degree of Doctor of Science by that institution. Dr. McCaughey has been a Member of AIME since 1918.

George B. Clark has been promoted to professor by the University of Illinois. **John W. Marx** has been made associate professor.

D. N. FREY

Donald Nelson Frey has been presented the first annual Award of Achievement for the Young Engineer by the Engineering Society of Detroit. Dr. Frey is manager, metallurgical dept., scientific laboratory, Ford Motor Co., Ann Arbor, Mich.

L. H. Oppenheim has been named a vice-president of the Henry J. Kaiser Co. Mr. Oppenheim will continue to serve as assistant general manager of Kaiser Engineers, a div. of the parent firm.

C. I. Bradford has been appointed vice-president and director of operations, and **W. E. Gregg** has been appointed assistant director of operations, Rem-Cru Titanium, Inc., Midland, Pa.

Robert F. Mehl, head of the metallurgical engineering dept. and director of the metals research laboratory, Carnegie Institute of Technology, has been appointed dean of graduate studies.

W. B. MATHER

W. B. Mather, chairman of the minerals technology dept., Southwest Research Institute, San Antonio recently returned from a trip to Brazil. He had been there studying the pegmatites of Brazil.

C. W. Cravens is superintendent of open hearth, Republic Steel Corp., Cleveland.

Nathaniel Howell Furman of Princeton University has been selected to receive the 1953 Palladium Medal of the Electrochemical Society. Professor Furman is Russell Wellman Professor of chemistry and chairman of the dept. of chemistry at Princeton.

Joseph D. Doherty has been appointed consulting engineer for the Island Creek Coal Sales Co. Mr. Doherty had been associated with the U. S. Bureau of Mines.

James A. Rolls is employed as a chemical engineer, technical supervisor, B. F. Goodrich Chemical Co., Institute, W. Va.

George P. Swift was elected president of the American Electroplaters Society. Dr. Swift is a consultant in Watertown, Mass. He was a Director for AIME between 1949 and 1952. **R. A. Schaefer,** director of research, Cleveland Graphite Bronze Co., Cleveland, was named first vice-president.

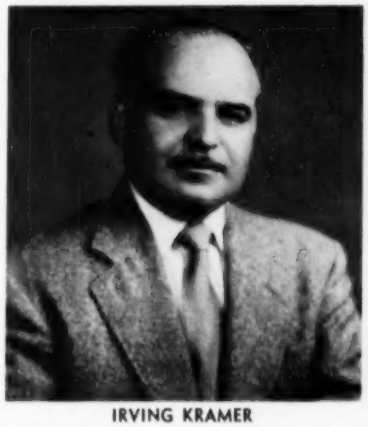

IRVING KRAMER

Irving Kramer has been named vice-president of the Mercast Corp., New York, where he will be in charge of research and development. Dr. Kramer had been assistant to the president, Horizons Titanium Corp. He will remain on the board of Horizons Zirconium Corp.

Joseph Stein has joined Sam Tour & Co., Inc., New York, as supervisor of the firm's nondestructive testing div.

I. Melville Stein has been elected president of Leeds & Northrup Co. Mr. Stein, formerly executive vice-president, succeeds **Charles S. Redding,** who becomes chairman of the board.

John W. Higgins, chairman of the board and treasurer, Worcester Pressed Steel Co., has been awarded an honorary degree as Doctor of Engineering by Worcester Polytechnic Institute.

Richard F. Puffer was named assistant general sales manager, American Brass Co. **Allen W. Rockwell** has been made manager of the Waterbury branch, and **R. R. Vance** will succeed Mr. Rockwell as works manager of the Waterbury branch.

Elwood G. Haney recently accepted a position with the Aluminum Research Laboratories, New Kensington, Pa. Mr. Haney is a research engineer in the physical metallurgy div.

Paul I. Swoger has been named midwestern sales manager for American Metallurgical Co.

H. Richard Gault has been appointed to serve as executive secretary of the div. of earth sciences, American Geological Institute.

George H. McBride was appointed assistant div. manager of Westinghouse Electric Corp.'s switchgear div., Pittsburgh.

James D. Nisbet, formerly manager of the materials and process section,

General Electric research laboratory, has been appointed director of research and development for Universal-Cyclops Steel Corp., Bridgeville, Pa.

Don A. Lawless, has joined the metallurgy dept. of the Sam Tour & Co., Inc., as assistant director. Mr. Lawless had been employed at Kaiser Aluminum & Chemical Corp.

James W. Perry, Madeline Berry, and **Allen Kent** have joined the staff at Battelle Memorial Institute, Columbus.

Thomas E. Lloyd, sales manager, Salem-Brosius, Inc., Pittsburgh, has been named director of sales.

James J. Dalton was named div. superintendent, cold roll div., American Steel & Wire, Cuyahoga works.

Lawrence D. Schmidt was appointed director of research for Semet-Solvay and Wilputte Coke Oven div., Allied Chemical & Dye Corp.

J. W. Campbell has been named assistant works manager of the Colorado Fuel & Iron Corp.'s Wickwire-Spencer plant in Buffalo. Since 1950 he has been wire mill superintendent of the Buffalo plant. Mr. Campbell has been with CF&I for 27 years.

William F. Born, Jr., is sales and consulting engineer with D. K. MacLennan Co., Los Angeles. He had been associated with Precision Engineered Products, Pacific Palisades, Calif.

Sydney Nashner has been appointed technical assistant to the president, Sherritt Gordon Mines Ltd., Toronto, Ont. He was formerly associated with the Chemical Construction Corp.

Gustav Egloff, director of research for Universal Oil Products Co., has been elected an honorary fellow of the Royal Society of Edinburgh. Dr. Egloff has been a Member of AIME since 1922.

Robert M. Parke has been named manager of the material and processes section of the metallurgy research dept., General Electric Co. research laboratory.

Obituaries

Oden Cass Garst (Member 1944) died suddenly on May 25, 1953. Mr. Garst was born at Trenton, Mo., in 1911 and graduated from the Missouri School of Mines. Mr. Garst was employed as a chemist for various firms in the midwest prior to joining the Bureau of Mines at Boulder City, Nev., as junior chemical engineer. He was later made assistant chemical engineer, metallurgical pilot plant operation. In 1942 Mr. Garst was promoted to associate chemical engineer and a short time later became chemical engineer. He was transferred to College Park, Md., where he became engineer in charge of waste metals projects. During World War II Mr. Garst was in Europe for the War Dept. and was then transferred to Japan. At the time of his death, he was residing in Rolla, Mo.

NECROLOGY

Date Elected	Name	Date of Death
1905	Julian Boyd	Mar. 8, 1953
1951	Grenville H. Grimwod	Unknown
1900	Donald F. Irvin	July 1, 1953
1921	Marvin Lee	July 7, 1953
1942	K. R. Paykull	June 18, 1953
1949	Kimball M. Williams	Unknown

NOW... *Enlarged and improved facilities* AT JAco TO SERVE YOU BETTER

JAco GROWS—BUT YOU BENEFIT

With our new and expanded manufacturing, sales and laboratory facilities, we can now bring you finer instruments and better service than at any time in our 50 years of experience. More than ever before JAco stands ready to provide you with assistance that will help you do your job more easily. Whether you come in person, or inquire by telephone or letter, it's always "open house" at our new plant. So why not consult us about *your* spectrographic problem *today*.

ALL THESE EXPANDED DEPARTMENTS UNDER ONE ROOF

Manufacturing Facilities — more than 12,000 square feet of space now available.
Sales Department — larger quarters, more trained personnel, enlarged field service facilities.
Customer Service Laboratory — a new test analyses service for you.

Write outlining your instrument problems today

Spectrographs—Source Units—Microphotometers—Spectrographic Laboratory Accessories—X-Ray Equipment—Geophysical Instruments—Refractometers—Polarimeters—Microscopes

JAco JARRELL-ASH COMPANY

26 FARWELL STREET, NEWTONVILLE, MASS.

SALES OFFICES

DETROIT 13680 Capitol Ave. | EL CERRITO, CAL. 1344 Devonshire Drive | CHATTANOOGA 1431 Broad Street | QUEENS VILL., N. Y. 80-56 220th Street

Proposed for Membership
— Metals Branch AIME —

Total AIME membership on June 30, 1953 was 19,010; in addition 1543 Student Associates were enrolled.

ADMISSIONS COMMITTEE

O. B. J. Fraser, Chairman; Philip D. Wilson, Vice-Chairman; F. A. Ayer, A. C. Brinker, R. H. Dickson, Max Gensamer, Ivan A. Given, Fred W. Hanson, T. D. Jones, G. W. Lutjen, E. A. Prentis, Sidney Rolle, J. T. Sherman, F. T. Sisco, R. L. Ziegfeld.

The Institute desires to extend its privileges to every person to whom it can be of service, but does not desire as members persons who are unqualified. Institute members are urged to review this list as soon as possible and immediately to inform the Secretary's office if names of people are found who are known to be unqualified for AIME membership.

In the following list C/S means change of status; R, reinstatement; M, Member; J, Junior Member; A, Associate Member; S, Student Associate.

California
Altadena—Clements, Donald S. (M) (R. C/S—A-M)

Illinois
Alton—Harney, Alfred A. (A)
Chicago—Merutka, John P. (J)

Massachusetts
Auburndale—Scott, Joseph R. (A)
Cambridge—Rosenfield, Alan R. (S)
Sharon—Gilbert, Leamon G. (M)

Michigan
Inkster—Morgan, Eric R. (M) (R. C/S—S-M)

Minnesota
Minneapolis—Adams, Salisbury (A)

Missouri
Glendale—Cobaugh, George D. (A)

New York
Kenmore—Cameron, Robert F. (A)
Hewlett—Alden, Sidney C. (A)
New York—Ruth, John P. (M)
New York—Scott, William H. (A)
Rego Park—Storchheim, Samuel (J)

Ohio
Cleveland—Bucur, Eugene J. (J)
Cleveland—Mataich, Peter F. (J)
Cleveland—Thellmann, Edward L. (J)
Cleveland Heights—Green, Harry M. (J)
Euclid—Straughn, Virgil E. (J)
Lakewood—Callendine, William A. (M)
Youngstown—Cahill, Jones M. (A)

Oregon
Portland—Anderson, Richard E. (J)

Pennsylvania
Bridgeville—Erdman, William W. (A)
Doylestown—Weik, Allen R. (A)
McKeesport—Peckman, Arnold L. (A)
Midland—Harkins, Thomas G. (A)
Narberth—Fitzgerald, Alex E. (A)
Narberth—Kingsbury, Stuart S. (M) (R. M)
Phila. Naval Base—Fabriani, Ferrucio (M) (C/S—S-M)
Pittsburgh—Braun, Ottwin L. (A)
Pittsburgh—Dean, Eugene R. (M)
Pittsburgh—Duncan, James W. (A)
Pittsburgh—Ellman, Louis (A)
Pittsburgh—Langley, Raymond M. (A)
Pittsburgh—Montgomery, Leroy (A)
Pittsburgh—Robinson, Lawrence R. (A)
Pittsburgh—Sack, John L. (A)
Wexford—Scott, Harold B. (M)

Tennessee
Knoxville—Morgan, William D. (M)
Mascot—Steuerwald, John B. (J)

Utah
Salt Lake City—Back, Alexander E. (M)
Salt Lake City—Williams, John F. (M)
Salt Lake City—Wilson, Dean G. (J)

Africa
No. Rhodesia—Timmermans, Owen E. B. (M)

Austria
Leoben—Cuscoleca, Otwin (A)
Leoben—Roesner, Kurt F. (A)

Canada
Nova Scotia—Cornell, H. I. (A)

Chile
Potrerillos—Wendt, Walter J. (M)

Germany
Berlin—Kohlmeyer, Ernst J. (R. M)

For the story of FERROCARBO in quality steelmaking, mail the coupon today—or phone or write the FERROCARBO distributor nearest you. You'll learn why steel deoxidized with FERROCARBO is "plus steel."

KERCHNER, MARSHALL & CO.
PITTSBURGH • Cleveland • Buffalo
Philadelphia • Birmingham • Los Angeles

MILLER & COMPANY
CHICAGO • St. Louis • Cincinnati

WILLIAMS & WILSON
TORONTO • Montreal • Windsor

THE CARBORUNDUM COMPANY, Dept. JM 84-31
Niagara Falls, New York

Gentlemen:

I would like to have the FERROCARBO story—no obligation on my part.

NAME AND TITLE

COMPANY

STREET AND NUMBER CITY ZONE STATE

FERROCARBO

TRADE MARK

by CARBORUNDUM

"Carborundum" and "Ferrocarbo" are trademarks which are registered in the U. S. by The Carborundum Company, Niagara Falls, New York, and in Canada by Canadian Carborundum Company, Ltd., Niagara Falls, Ontario.

Packed in Bags and Shipped on Pallets

Each bag holds 25 lb. of contained vanadium, so additions can be made without weighing. Bags prevent contamination and are shipped on pallets for easy and economical handling.

Use this New, Easy Method

. . . FOR ADDITIONS OF VANADIUM

You can handle additions of vanadium conveniently and economically with ELECTROMET ferrovanadium packed in bags.

Check these advantages:

- ***Convenient Packaging***—The alloy is packed in strong five-ply, paper bags. These bags have a wide blue band across the middle, as well as blue edges and bottom, for positive identification. The bags prevent contamination and preclude any chance of mix up with other alloys.
- ***No Weighing***—Each bag (25 lb. of contained vanadium) can be added without weighing.
- ***Handling Costs Reduced***—Pallet shipments are available at no extra charge. Each pallet holds about 4,000 lb. of ferrovanadium—2,200 lb. of contained vanadium. Pallets can be conveniently unloaded and handled in your plant by lift truck or overhead crane. Handling costs are reduced and inventory-taking is simplified. And you don't have to return the pallets.
- ***High-Quality Material for Every Need***—ELECTROMET ferrovanadium is uniform in analysis, closely graded, correctly sized, and physically clean. It is furnished in four grades:

	Vanadium	Silicon max.	Carbon max.
High-Speed Grade	50 to 55%	1.50%	0.20%
Special Grade	50 to 55%	2%	0.50%
Open-Hearth Grade	50 to 55%	8%	3%
Foundry Grade	50 to 55%	approx. 10%	3%

* **Immediate Delivery**—Vanadium is readily available and can frequently be used in engineering steels to replace part, if not all, of certain scarcer alloys.

* **Engineering Service**—Our staff of experienced metallurgical engineers is always ready to furnish technical assistance in the use of vanadium. Phone, wire, or write one of ELECTROMET's offices for additional information.

The term "Electromet" is a registered trade-mark of Union Carbide and Carbon Corporation.

ELECTRO METALLURGICAL COMPANY

A Division of Union Carbide and Carbon Corporation

30 East 42nd Street UCC New York 17, N. Y.

OFFICES: Birmingham • Chicago • Cleveland • Detroit
Houston • Los Angeles • New York • Pittsburgh • San Francisco

In Canada: Electro Metallurgical Company of Canada, Limited, Welland, Ontario

Electromet

TRADE-MARK

Ferro-Alloys and Metals